Perturbative and Nonperturbative Aspects of the Phenomenology of Composite Higgs Models

---

Dissertation

zur

Erlangung der naturwissenschaftlichen Doktorwürde
(Dr. sc. nat.)

vorgelegt der

Mathematisch-naturwissenschaftlichen Fakultät

der

Universität Zürich

von

Marc Gillioz

von

Nendaz VS

Promotionskomitee

Prof. Dr. Daniel Wyler *(Vorsitz & Leitung)*

Prof. Dr. Thomas Gehrmann

Prof. Dr. Ulrich Straumann

Zürich, 2012

Abstract

The discovery of the Higgs boson announced by CERN on July 4th 2012 was expected by the particle physics community since a long time. Indirect evidence that a Higgs boson must be present in the mass range of 100–200 GeV was provided by electroweak precision data collected at LEP already ten years ago. Yet, the existence of a fundamental scalar in nature poses a strong problem regarding the behaviour of the theory at high energy. The relative smallness of the Higgs mass compared to the scale at which new physics must appear is known as the hierarchy problem. So far, only two solutions to this problem can be formulated in terms of a local field theory in $3 + 1$ dimensions, namely supersymmetry and strong dynamics. The second option and the phenomenological consequences thereof are considered in this thesis. In this case, the Higgs boson arises as a composite state of new fermions confined by the strong interaction. Models with a new, strongly-coupled sector are also the natural four-dimensional effective description of theories based on extra-dimensions.

In this work, the requirements for building a realistic composite Higgs model are studied. In the simplest models, the natural scale at which new physics appears is close to the electroweak scale and should therefore be testable at the LHC. Vector resonances, new fermions coupling mostly to the top quark and anomalous Higgs couplings are the main signature of these models. Alternatively, models in which the light resonances are absent or hidden and for which the Higgs couplings mimic the Standard Model ones require the presence of larger symmetries. As a side effect, these models can contain additional massive, stable particles which are the equivalent of baryons in quantum chromodynamics. These particles arise in the low-energy effective description of the model as topological solitons, called skyrmions. The skyrmion's properties are studied first in a general framework and then in specific realisations of composite Higgs models. Despite being naturally very massive and weakly-interacting, which seems to indicate potential dark matter candidates, the stable skyrmion states are often electrically charged and incompatible with the early-universe cosmology.

Zusammenfassung

Die Entdeckung des Higgs-Teilchens, angekündigt vom CERN am 4. Juli 2012, wurde von der Teilchenphysik Gemeinschaft seit langer Zeit erwartet. Durch Präzisionsmessungen am LEP Experiment wurden schon vor zehn Jahren indirekte Anzeichen für ein leichtes Higgs-Boson im Massenbereich 100–200 GeV gesammelt. Die Existenz eines fundamentalen Skalar-Teilchens wirft jedoch ein Problem für das Verhalten der Theorie bei hoher Energie auf. Die relative Kleinheit der Masse des Higgs-Teilchens im Vergleich zum vorausssichtlichen Energiebereich neuer Physik ist bekannt als das Hierarchieproblem. Bis jetzt wurden nur zwei Lösungen des Problemes als lokale Quantenfeldtheorien in $3 + 1$ Dimensionen beschrieben, und zwar die Supersymmetrie und Theorien mit einer starken Wechselwirkung. Letztere Möglichkeit und deren Auswirkungen für die Phänomenologie der Teilchenphysik werden in dieser Arbeit betrachtet. In diesem Fall entsteht das Higgs-Boson als gebundener Zustand aus neuen Fermionen, die von der starken Wechselwirkung eingesperrt sind. Modelle mit neuen, stark wechselwirkendenden Teilchen sind übrigens die natürliche effektive vierdimensionale Beschreibung einer Theorie mit zusätzlichen räumlichen Dimensionen.

Die Voraussetzungen eines realistisches Modell des zusammengesetztes Higgs-Teilchens werden untersucht. In den einfachsten Modellen ist der natürliche Energiebereich der neuen Physik in der Nähe der typischen Energie der elektroschwachen Wechselwirkung, und sollte damit am LHC prüfbar sein. Die experimentelle Besonderheiten solcher Modelle sind Vektorresonanzen, neue Fermionen mit erhebliche Wechselwirkungen mit dem Top-Quark und ungewöhnliche Interaktionen des Higgs-Teilchens. Für Modelle in denen leichte Resonanzen abwesend oder unsichtbar sind und in denen die Higgs-Wechselwirkungen das Standardmodell nachahmen, werden weitere Symmetrien gefordert. Als Nebenwirkung enthalten solche Modelle zusätzliche massereiche, stabile Teilchen, die den Baryonen in der Quantenchromodynamik entsprechen. Diese Teilchen treten in der effektiven niederenergetischen Theorie als topologische Solitonen auf und werden Skyrmionen genannt. Die Eigenschaften der Skyrmionen werden zuerst in einem allgemeinen Rahmen beschrieben, dann in bestimmten Modellen eines zusammengesetztes Higgs-Teilchens. Obwohl sie sehr massereich und schwach wechselwirkend sind, und demzufolge mögliche Kandidaten für die dunkle Materie, entstehen die Skyrmionen meist als elektrisch geladene Teilchen, und sind deshalb unverträglich mit der Kosmologie des Universums.

Résumé

La découverte du boson the Higgs annoncée au CERN le 4 juillet 2012 était attendue par la communauté de physique des particules. Des preuves indirectes de l'existence d'un boson de Higgs dans le domaine de masse compris entre 100 et 200 GeV ont été fournies par les mesures de précision effectuées au LEP il y a dix ans déjà. Pourtant, la présence d'un champ scalaire soulève un problème concernant le comportement de la théorie à haute énergie. La petitesse de la masse du boson de Higgs comparée aux énergies auxquelles de nouveaux phénomène physiques doivent apparaître est connue sous le nom de problème de la hiérarchie. Jusqu'à maintenant, seulement deux solutions à ce problème ont pu être formulées en termes de théories des champs locales en $3+1$ dimensions, à savoir la supersymmétrie et les théories comportant une interaction forte. La deuxième possibilité et les conséquences qui en découlent pour la phénoménologie sont étudiées dans cette thèse. Dans ce cas, le boson de Higgs est une particule composite, faite de fermions confinés par une interaction forte. Les modèles comprenant un secteur soumis à une interaction de ce type sont par ailleurs la description naturelle en quatre dimensions de théories basées sur des dimensions spatiales supplémentaires.

Les conditions à la construction d'un modèle réaliste de boson de Higgs composite sont examinées. Dans les modèles les plus simples, l'énergie à laquelle de nouveaux phénomènes physiques sont attendus est proche de l'énergie typique des interactions éléctrofaibles, et donc dans le domaine testable par le LHC. La signature expérimentale de ces modèles est faite de résonances de boson vecteurs, de nouveaux fermions interagissant principalement avec le quark top et d'interactions anormales du boson de Higgs. Les modèles dans lesquels les résonances légères sont absentes ou invisibles et où les interactions du boson de Higgs imitent celles du Modèle Standard sont construits sur la base de plus grandes symmétries. Un effet secondaire de ces modèles est la présence de nouvelles particules massives et stables, qui sont l'équivalent des baryons dans la théorie de la chromodynamique quantique. Ces particules apparaissent dans la description effective du modèle à basse énergie en tant que solitons topologiques, dénomés skyrmions. Les propriétés des skyrmions sont étudiées d'abord dans un cadre général, puis dans des modèles spécifiques de boson de Higgs composite. Même s'ils sont naturellement massifs et interagissent faiblement, ce qui semble faire d'eux des candidats à la matière noire, les skyrmions stables sont généralement chargés éléctriquements et donc incompatibles avec la cosmologie de l'univers primordial.

Contents

1 Introduction

2012 will certainly remain as a key year in the history of particle physics. After its prediction nearly fifty years ago, the Higgs boson, only missing element of the Standard Model of particle physics, was discovered together by the ATLAS and CMS experiments at CERN. This event marks certainly the end of an era, but is above all the beginning of a new one. Extracting all information about the way the Higgs boson couples to matter and to gauge fields will probably take another couple of years. In the meantime, the LHC will still be looking for new discoveries, possibly modifying the present paradigm of particle physics.

As indicated in its title, the present PhD thesis is focused on the assumption that the Higgs is a composite state instead of an elementary particle. The approach chosen here is however not to study a particular model and analyse its consequences for the phenomenology at collider experiments, but rather to address the physical problems inherent to the Standard Model in an effective way, trying to proceed as much as possible in a model-independent way. The Standard Model is therefore introduced in chapter 2, not in its usual definition as a renormalisable theory, but rather such that its shortcomings are made evident. As it stands, this Standard Model requires the presence of a Higgs particle. More precisely, it is such a particle which unitarises the scattering of gauge bosons and allows the model to be valid up to arbitrarily high energies. The success of the Standard Model was made particularly evident after the collider experiments conducted in the last twenty years, among which the LEP electron-positron collider at CERN, which provided very precise tests of the Standard Model accuracy in the electroweak sector. More recently, the Tevatron proton-antiproton collider at Fermilab permitted the discovery of the next-to-last fundamental particle in the

model, the top quark, and confirmed our understanding of the strong interactions via quantum chromodynamics (QCD). Finally, the LHC proton-proton collider presently running at CERN is providing its first physics results, so far in accordance with the Standard Model. The discovery of the Higgs boson on the 4th of July of this year is without doubt the climax of particle physics in the last four decades. Ironically, the date of the Higgs discovery coincides with the submission of this PhD thesis, which was nevertheless entirely written beforehand.

It is known however that the Standard Model is not the ultimate theory of nature. Despite its great successes, a few elements indicate that new physics must be present. One of those indicators comes from the observation of neutrino oscillations, requiring them to have a mass, even the tiniest one. Other arguments coming from cosmology show that the spectrum of particles provided by the Standard Model cannot explain the fate of the universe as currently understood. The energy scale at which new physics phenomena should occur is unknown, but indirect evidence seem to indicate that it could be as low as the TeV scale, a scale which the LHC will probing in the next few years. The dream of all theoretical particle physicists is of course to complete the Standard Model in order to correct its few inaccuracies, without spoiling its impressive precision in verified processes. This task is however much more difficult than expected naively. A very delicate problem arising in this quest is known as the *hierarchy problem*, relating inevitably the last measured parameter of the Standard Model, the Higgs boson mass, to the scale at which the new physics should appear. Quantum corrections to the Higgs boson mass are indeed very sensitive to new physics, so that the two scales should be identical from naturalness arguments. The direct measurements of the Higgs boson mass obtained by LHC experiments show that the Higgs is as light as 125 GeV, while no new physics is observed around this scale. Unless an extraordinary cancellation of quantum phenomena happens, the hierarchy between the new physics scale and the Higgs boson mass should be explained by new symmetry arguments.

There are two natural solutions to the hierarchy problem. The first is *supersymmetry*, relating bosons and fermions through a fundamental symmetry of space-time, and offering a simple reason why a fundamental scalar particle can be light. The second possibility is *strong dynamics*, in which naturally light scalar degrees of freedom can arise as Goldstone bosons from the spontaneous breaking of a symmetry. Note that both possibilities are actually advocated by the modern development of string theory and quantum gravitation, which requires on the one hand supersymmetry as a fundamental ingredient, and on the other hand extra-dimensions, whose dynamics correspond in an effective four-dimensional description to a strongly-coupled quantum field theory. As indicated above, only the second of these two possibilities is going to be considered in this thesis. The longitudinal polarisations of massive gauge bosons in the Standard Model are hence assumed

to be Goldstone bosons arising from some new, strongly-interacting sector. It will be shown in chapter 3 that in addition to the latter, the presence of a light Higgs boson is favoured by indirect precision measurements in the electroweak sector. One of the reason to leave supersymmetry apart is that it has been studied extensively in the last 20 years, as were the *technicolor* models of a strong but Higgsless electroweak symmetry breaking. On the contrary, recent developments in the physics of extra-dimensions and in the field of strongly-coupled theories have open a door towards a new category of models in which a Higgs boson is present, although not elementary, and which can be grouped under the appellation of *composite Higgs models*.

After reviewing in chapters 2 and 3 the theory arguments outlined above and leading to the discovery of composite Higgs models, a few specific aspects of theses models are discussed in detail. In the framework of the minimal model satisfying all theoretical requirements, a study of the agreement with precision data from LEP and with direct experimental constraints from the LHC is performed in section 3.3, together with an analysis of the Higgs boson production, alone and in pairs. The results presented there are taken from the original research projects of the author, published in refs. [1, 2].

After the usual, perturbative approach to composite Higgs models, the second part of this thesis, presented in chapter 4, makes use of nonperturbative techniques to gain information about the low-energy spectrum of these models. The Skyrme model is first introduced, in which topological solitons represent the baryons in an effective description of QCD. The methodology leading to the construction of the so-called *skyrmions* is reviewed in detail. In a second step, modifications of the Skyrme model are discussed, following the research work of ref. [3]. The model is finally used to study the presence in composite Higgs models of massive, stable skyrmions, which like the Higgs boson are singlets under the strongly-interacting force. An important issue related to the electric charge of skyrmions is presented in section 4.4, following ref. [4], and a complete example is eventually provided in section 4.5, including the discussion of the consequences of skyrmions for cosmology. This last part is taken from the research paper [5]. The numerical methods used in the nonperturbative approach are presented in an appendix.

2

The Standard Model and the Need to Go Beyond

All fundamental laws of nature can be described within the framework of quantum field theory, with the notable exception of gravity. We are going to describe first in this work the theory used to unify the electromagnetic the weak and the strong interaction, known as the *Standard Model* [6, 7, 8]. We will however follow an effective approach rather than a historical one. Most of the material presented in this chapter is inspired by standard textbooks [9, 10, 11, 12, 13, 14], lectures [15, 16] and reviews [17, 18, 19, 20].

2.1 The Standard Model: gauge symmetries and fermion content

A quantum field theory can defined by an action, written as an integral over space of a Lagrangian density. It is useful nevertheless to take a different approach, in which the theory is constructed from symmetry principles, and where the Lagrangian density takes then the most general form respecting this principles. In the following, we are going to define the Standard Model completely, first presenting its gauge symmetry and the resulting non-trivial vacuum structure, then adding fermions to the theory, which have to transform under given representations of the gauge group.

2.1.1 Gauge symmetries, instantons and θ-vacuum

We introduce first the strong, weak and electromagnetic "forces" in the Standard Model as gauge fields. The Lagrangian is constructed so as to

preserve the fundamental local symmetries of the group

$$SU(3)_C \times SU(2)_W \times U(1)_Y. \tag{2.1}$$

The gauge bosons corresponding to the $SU(3)_C$ gauge group are the gluons G^a_μ ($a = 1, \ldots, 8$), and the index C refers to the usual denomination of *colour* gauge group. The study of processes involving the gluon field is hence denoted *quantum chromodynamics* (QCD). The gauge groups $SU(2)_W$ and $U(1)_Y$ are usually considered together (for reason to be clear in the next section), and form the branch of the Standard Model called the *electroweak* physics.[1] The electroweak gauge bosons are W^i_μ ($i = 1, 2, 3$) and B_μ. More precisely, $SU(2)_W$ is the *weak* force, while $U(1)_Y$ does not have a conventional name, but is associated with *hypercharge*, to appear below.

The Lagrangian for the gauge fields takes then the form[2]

$$\mathcal{L}_{\text{gauge}} = -\frac{1}{4} G^a_{\mu\nu} G^{\mu\nu\, a} - \frac{1}{4} W^i_{\mu\nu} W^{\mu\nu\, i} - \frac{1}{4} B_{\mu\nu} B^{\mu\nu}. \tag{2.2}$$

The field strength tensors are given by

$$G^a_{\mu\nu} = \partial_\mu G^a_\nu - \partial_\nu G^a_\mu + g_S \; f^{abc} \; G^b_\mu \; G^c_\nu, \tag{2.3}$$

$$W^i_{\mu\nu} = \partial_\mu W^i_\nu - \partial_\nu W^i_\mu + g \; \varepsilon^{ijk} \; W^j_\mu \; W^k_\nu, \tag{2.4}$$

$$B_{\mu\nu} = \partial_\mu B_\nu - \partial_\nu B_\mu, \tag{2.5}$$

where f^{abc} and ε^{ijk} are the structure constants of $SU(3)$ and $SU(2)$ respectively, and g_S, g are the gauge coupling associated with each of the two gauge groups. In addition, we will denote by g' the gauge coupling associated to the $U(1)_Y$ gauge group (appearing only once we introduce fermions in the theory). Under a $SU(3)_C$ gauge transformation, the gluon field transforms as

$$G_\mu \equiv G^a_\mu \frac{\lambda^a}{2} \to U G_\mu U^\dagger + \frac{i}{g_S} U \partial_\mu U^\dagger, \qquad U(x) \in SU(3) \tag{2.6}$$

where λ^a are the Gell-Mann matrices, i.e. $\frac{1}{2}\lambda^a$ are generators of $SU(3)$ normalised in the usual way. The field strength tensor transforms then in the adjoint representation as

$$G_{\mu\nu} \equiv G^a_{\mu\nu} \frac{\lambda^a}{2} \to U G_{\mu\nu} U^\dagger, \tag{2.7}$$

so that the Lagrangian (2.2) is invariant under any gauge transformation. Similar transformation rules apply to the $SU(2)_W$ and $U(1)_Y$ gauge group.

[1] The notation $SU(2)_L$ is often used instead of $SU(2)_W$. Our convention is chosen so as to avoid any confusion when discussing multiple copies of the Standard Model gauge group, as will be the case in chapter 3.

[2] The summation over repeated indices is always understood, unless stated otherwise. Lorentz indices, denoted by greek letters, are raised and lowered by the use of the metric: $B^\mu = g^{\mu\nu} B_\nu$.

In a gauge theory, there is in general the possibility to write an extra gauge-invariant term in the Lagrangian, in addition to the kinetic terms of eq. (2.2). Let us first consider a $SU(N)$ Yang-Mills theory in general [21], and the results will generalise to the Standard Model afterwards. In terms of a field strength tensor $F^a_{\mu\nu} = \partial_\mu A^a_\nu - \partial_\nu A^a_\mu + g f^{abc} A^b_\mu A^c_\nu$, the most general gauge-invariant Lagrangian is

$$\mathcal{L}_{YM} = -\frac{1}{4} F^a_{\mu\nu} F^{\mu\nu\, a} + \frac{\theta\, g^2}{32\pi^2} F^a_{\mu\nu} \widetilde{F}^{\mu\nu\, a}, \tag{2.8}$$

where θ is an arbitrary coefficient and the dual of the field strength tensor is defined using the totally antisymmetric tensor ε as

$$\widetilde{F}^{\mu\nu\, a} = \frac{1}{2} \varepsilon^{\mu\nu\rho\sigma} F^a_{\rho\sigma}, \tag{2.9}$$

The second term in (2.8) is usually called θ-term, and obviously violates parity and time-reversing symmetries since they involve three spatial derivatives and one time derivative, thus incidentally violating CP-symmetry as well. However, the θ-term does not contribute to the equations of motion and has therefore no physical meaning in the classical version of the theory. This is a consequence of the fact that it can be written as a total divergence, $F^a_{\mu\nu} \widetilde{F}^{\mu\nu\, a} = \partial_\mu K^\mu$ with[3]

$$K^\mu = 2\, \varepsilon^{\mu\nu\rho\sigma} \left(A^a_\nu \partial_\rho A^a_\sigma + \frac{g}{3} f^{abc} A^a_\nu A^b_\rho A^c_\sigma \right). \tag{2.10}$$

The latter is nothing but the Chern-Simons three-form $\omega_3(A)$ (up to a factor of 2), satisfying in the language of differential forms $\mathrm{d}\omega_3(A) = F \wedge F$. The θ-term is therefore a surface term and is absent of the classical equations of motion. Moreover, when considering field configurations of finite energy, the field strength tensor $F^a_{\mu\nu}$ has to go to zero faster than r^{-2} at the boundaries of space-time, which is naively reproduced by a gauge field decreasing faster than r^{-1}. The θ-term contribution to the action is then given by K^μ evaluated over the space-time boundaries, where it is vanishing following the naive convergence argument. There exist nevertheless, in $SU(N)$ Yang-Mills theories, pure gauge configurations which are equivalent to the vacuum, i.e. satisfying $F_{\mu\nu} = 0$, but for which the gauge field A_μ decreases only as r^{-1} at infinity. Such a configuration can for example be realised as

$$A_\mu = -\frac{i}{g} U^\dagger \partial_\mu U, \quad \text{with} \quad U = \frac{r^2 - d^2}{r^2 + d^2}\, \mathbb{1}_N + 2i \frac{r\, d}{r^2 + d^2}\, \hat{x}_i\, \overline{\sigma}^i, \tag{2.11}$$

with $r^2 = x_i^2$, $\hat{x}_i = x_i / r$, d is an arbitrary length and $\overline{\sigma}^i$ represents any embedding of the Pauli matrices into an $N \times N$ matrix. This configuration

[3] In the derivation of the equality, one has to use the fact that the term proportional to g_S^2 vanishes in $F^a_{\mu\nu} \widetilde{F}^{\mu\nu\, a}$, due to the Jacobi identity $f^{abc} f^{ade} - f^{abe} f^{adc} - f^{abd} f^{ace} = 0$ valid in the adjoint representation of any Lie group.

satisfies $\int \mathrm{d}^3x\, K^0 = 32\pi^2/g^2$, so that a field interpolating adiabatically between $A_\mu = 0$ at $t \to -\infty$ and the configuration of eq. (2.11) at $t \to +\infty$ satisfies

$$\int \mathrm{d}^4x\, F^a_{\mu\nu}\widetilde{F}^{\mu\nu\, a} = \int \mathrm{d}^3x\, K^0\Big|^{t\to+\infty}_{t\to-\infty} = \frac{32\pi^2}{g^2} \tag{2.12}$$

Such a field configuration exists and is called an *instanton* [22, 23]. The physical meaning of the instanton can be understood by looking at the topological number associated with a $SU(N)$ gauge field,

$$n = \frac{g^2}{32\pi^2}\int \mathrm{d}^4x\, F^a_{\mu\nu}\widetilde{F}^{\mu\nu\, a} \in \mathbb{Z}. \tag{2.13}$$

This quantity is topological in the sense that it is left invariant by any infinitesimal transformation, but can nevertheless take a discrete set of values, normalised here to be the set of integers. The existence of such a topological quantity implies that the space of possible field configurations is split into an infinite number of homotopy classes, such that field configurations belonging to different classes cannot be continuously deformed into each other. As can be seen from the equations above, an instanton is a field configuration with $n = 1$, i.e. interpolating between a given vacuum at $t \to -\infty$ and another topologically inequivalent vacuum at $t \to +\infty$. The probability for a tunnelling effect between two nearby vacua to occur is then related semi-classically to the energy associated with an instanton configuration, and is found to be

$$\exp\left(-\frac{8\pi^2}{g^2}\right). \tag{2.14}$$

The peculiar scaling of the coupling constant g is a typical signature of a non-perturbative effect. For weakly coupled theories, instanton effects are very much suppressed, while their importance in strongly-coupled theories is not well understood yet.

The presence of distinct homotopy classes in the theory implies that the true vacuum is not trivial, but is a linear combination of different states $|m\rangle$, each denoting the state of minimal energy within the class of configurations of topological charge m. When considering the vacuum expectation value of a given operator $\mathcal{O}$, the path integral can be split into different homotopy sectors, and one gets

$$\langle\Omega|\mathcal{O}|\Omega\rangle = \int \mathcal{D}A\, \mathcal{O}\, e^{i\int \mathrm{d}^4x\, \mathcal{L}_{YM}} = \sum_{m_{in},m_{out}} e^{i\theta(m_{out}-m_{in})}\langle m_{out}|\mathcal{O}|m_{in}\rangle, \tag{2.15}$$

where the phase on the right-hand side arises from the integration of the θ-term. The equality is then satisfied if the true vacuum is precisely the linear combination

$$|\Omega\rangle = \sum_m e^{-i\theta m}|m\rangle. \tag{2.16}$$

	$SU(3)_c$	$SU(2)_W$	$U(1)_Y$
$q_L = (u_L, d_L)$	**3**	**2**	$\frac{1}{6}$
u_R	**3**	**1**	$\frac{2}{3}$
d_R	**3**	**1**	$-\frac{1}{3}$
$l_L = (\nu_L, e_L)$	**1**	**2**	-$\frac{1}{2}$
e_R	**1**	**1**	-1

Table 2.1: The charge of fermions under the gauge groups in the Standard Model. The notations **1**, **2** and **3** correspond respectively to a singlet, doublet or triplet under the gauge group. The number describing the $U(1)_Y$ transformation is the hypercharge.

In general, under a topologically non-trivial gauge transformation U taking one vacuum to another as $\mathcal{U}|m\rangle = |m+1\rangle$, the vacuum $|\Omega\rangle$ is then invariant up to a phase as $\mathcal{U}|\Omega\rangle = e^{i\theta}|\Omega\rangle$. Adding a θ-term to the Yang-Mills Lagrangian is thus equivalent to specifying what is the true vacuum of the theory. The special case $\theta = 0$ corresponds to a particular choice of vacuum, but there is no reason to favour it over any non-zero value of θ as long as no symmetry principle is enforcing it. In the Standard Model, one can write down such a term for each gauge group, complementing the Lagrangian (2.2) with

$$\mathcal{L}_{\text{gauge}} \supset \frac{\theta_3\, g_S^2}{32\pi^2} G^a_{\mu\nu} \widetilde{G}^{\mu\nu\, a} + \frac{\theta_2\, g^2}{32\pi^2} W^i_{\mu\nu} \widetilde{W}^{\mu\nu\, i} + \frac{\theta_1\, g'^2}{32\pi^2} B_{\mu\nu} \widetilde{B}^{\mu\nu}. \tag{2.17}$$

2.1.2 Fermions and anomalies

In addition to being a gauge theory, the Standard Model is a chiral theory, in the sense that the left-handed and right-handed chiralities of fermions are treated independently. An equivalent formulation of this statement is that the fermions in the Standard Model are *Weyl fermions*. The fermion content of the Standard Model is summarised in Table 2.1. The fermions q_L, u_R and b_R charged under the colour gauge group are called *quarks*. They transform as triplets, and come therefore in three different colours. The remaining fermions l_L and e_R are called *leptons*. They do not couple to gluons.

A Lagrangian for the fermions can be written down in a gauge invariant way by defining a covariant derivative, given for example for q_L as

$$D_\mu q_L = \partial_\mu q_L - i\, g_S\, G^a_\mu \frac{\lambda^a}{2} q_L - i\, g\, W^i_\mu \frac{\sigma^i}{2} q_L - i\, g'\, B_\mu \left(\frac{1}{6}\right) q_L. \tag{2.18}$$

The form of the covariant derivative for the other fermions can be derived from Table 2.1: singlets do not couple to the gauge fields, and the hyper-

charge in brackets above has to be replaced by the appropriate value. The gauge-invariant kinetic terms for the fermions takes then the form

$$\begin{aligned}\mathcal{L}_{\text{fermions}} = & \, i\,\overline{q}_L\,\overline{\sigma}^\mu D_\mu\, q_L + i\,\overline{u}_R\,\sigma^\mu D_\mu\, u_R + i\,\overline{d}_R\,\sigma^\mu D_\mu\, d_R \\ & + i\,\overline{l}_L\,\overline{\sigma}^\mu D_\mu\, l_L + i\,\overline{e}_R\,\sigma^\mu D_\mu\, e_R,\end{aligned} \tag{2.19}$$

where $\sigma^\mu = \left(\mathbb{1}, \sigma^i\right)$, $\overline{\sigma}^\mu = \left(\mathbb{1}, -\sigma^i\right)$, and for Weyl fermions $\overline{f} = f^\dagger$. Note that fermions denoted with an index L differ from the ones denoted by an index R by the way they are contracted. The presence of a σ^μ of $\overline{\sigma}^\mu$ matrix defines the *helicity* of a fermion. A pair of Weyl fermions with opposite helicities can be combined into a Dirac fermion as

$$i\,\overline{f}_L\,\overline{\sigma}^\mu \partial_\mu\, f_L + i\,\overline{f}_R\,\overline{\sigma}^\mu \partial_\mu\, f_R = i\,\overline{f}\,\gamma^\mu \partial_\mu\, f \tag{2.20}$$

where the Dirac fermion f and γ^μ matrices are defined as

$$f = \begin{pmatrix} f_L \\ f_R \end{pmatrix}, \quad \overline{f} = f^\dagger \gamma^0 \quad \text{and} \quad \gamma^\mu = \begin{pmatrix} 0 & \sigma^\mu \\ \overline{\sigma}^\mu & 0 \end{pmatrix}. \tag{2.21}$$

Dirac fermions can acquire a mass in the form

$$\mathcal{L} \supset m_f\,\overline{f} f = m_f\left(\overline{f}_L f_R + \overline{f}_R f_L\right). \tag{2.22}$$

A crucial property of the Standard model is that there are no pairs of left-handed and right-handed fermions sharing the same quantum numbers, so that no Dirac fermions can be built, and subsequently no Dirac mass term is allowed. In addition, Majorana mass terms are forbidden as well by the $U(1)_Y$ gauge symmetry. At this stage, all Standard Model fermions have to be massless. We will see in the next section how they can finally get a mass after spontaneous breaking of the gauge symmetries. Another consequence of treating separately fermions with opposite helicity is that the theory breaks the parity symmetry $\vec{x} \to -\vec{x}$, and is therefore a *chiral theory*. Conversely, the time-reversing symmetry is preserved.

The Standard Model Lagrangian as described so far possesses in addition to the gauge symmetries a certain number of global symmetries. Noether's theorem relates each of these symmetries to a conserved current. Symmetries transforming the fermions as

$$f_{L,R} \to e^{i\alpha\, T} f_{L,R} \tag{2.23}$$

are of particular interest. Here T represents a generator acting on one of the spaces $SU(3)_C$, $SU(2)_W$ or $U(1)_Y$, and the $f_{L,R}$ are any fermions of the model. The Noether current associated with a transformation of this kind can be written as

$$J^\mu = \sum_{f_L} \overline{f}_L\,\overline{\sigma}^\mu\, T\, f_L + \sum_{f_R} \overline{f}_R\,\sigma^\mu\, T\, f_R. \tag{2.24}$$

While these current are automatically conserved at the classical level since their divergence is related to the field equation, their conservation is not guaranteed in the quantum theory. In the case where a symmetry of the Lagrangian is broken in the real world, one speaks of an *anomaly*. In the Standard Model, anomalies are induced by triangle diagrams of the form of fig. 2.1. The divergence of the current is then proportional to the external gauge fields as [24, 25]

$$\begin{aligned}\partial_\mu J^\mu = \pm N_f \Bigg(& \frac{g_S^2}{16\pi^2} \operatorname{Tr}\left[T \frac{\lambda^a}{2} \frac{\lambda^b}{2}\right] G^a_{\mu\nu} \widetilde{G}^{\mu\nu\, b} \\ & + \frac{g^2}{16\pi^2} \operatorname{Tr}\left[T \frac{\sigma^i}{2} \frac{\sigma^j}{2}\right] W^i_{\mu\nu} \widetilde{W}^{\mu\nu\, j} \\ & + \frac{g'^2}{16\pi^2} \operatorname{Tr}[T]\, Y^2\, B_{\mu\nu} \widetilde{B}^{\mu\nu} \Bigg),\end{aligned} \tag{2.25}$$

where N_f denotes the number of fermions running in the loop, and the sign should be taken positive for left-handed fermions and negative for right-handed ones. As an example, let us consider the $U(1)$ symmetry rotating the left-handed quark doublet by a phase, and the associated Noether current:

$$q_L \to e^{i\alpha} q_L, \qquad J^\mu_{q_L} = \overline{q}_L\, \overline{\sigma}^\mu\, q_L. \tag{2.26}$$

The anomaly in this case becomes

$$\partial_\mu J^\mu_{q_L} = 6 \left(\frac{g_S^2}{32\pi^2} G^a_{\mu\nu} \widetilde{G}^{\mu\nu\, a} + \frac{g^2}{32\pi^2} W^i_{\mu\nu} \widetilde{W}^{\mu\nu\, i} + \frac{g'^2}{16\pi^2} \left(\frac{1}{6}\right)^2 B_{\mu\nu} \widetilde{B}^{\mu\nu} \right) \tag{2.27}$$

As a consequence, the phase rotation of q_L generates in the Lagrangian a new term

$$\mathcal{L} \to \mathcal{L} + \alpha\, \partial_\mu J^\mu_{q_L}, \tag{2.28}$$

which brings a new contribution to the θ-terms (2.17), shifting in this case

$$\theta_3 \to \theta_3 + 6\alpha, \qquad \theta_2 \to \theta_2 + 2\alpha, \qquad \theta_1 \to \theta_1 + \frac{1}{3}\alpha. \tag{2.29}$$

A phase rotation can be associated with each of the Standard Model fields, and all of them are anomalous. Among the five $U(1)$ currents, only two independent linear combination can be built for which the anomalies cancel. The remaining three can be used to remove each of the three θ-terms, hence implying that all θ-vacua are equivalent. On the other hand, the anomaly-free linear combinations can be expressed as

$$J^\mu_{B-L} = \frac{1}{3}\left(J^\mu_{q_L} + J^\mu_{u_R} + J^\mu_{d_R}\right) - \left(J^\mu_{l_L} + J^\mu_{e_R}\right), \tag{2.30}$$

$$J^\mu_Y = \frac{1}{6} J^\mu_{q_L} + \frac{2}{3} J^\mu_{u_R} - \frac{1}{3} J^\mu_{d_R} - \frac{1}{2} J^\mu_{l_L} - J^\mu_{e_R}. \tag{2.31}$$

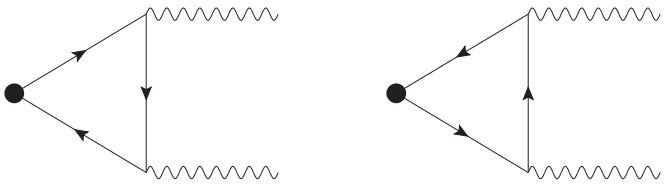

Figure 2.1: Chiral anomaly induced by loop diagrams. The blob symbolises the current (2.24) and fermions in the loops can be any quark or gluon coupling to this current.

The second of these currents is exactly the current associated with the hypercharge gauge symmetry $U(1)_Y$. Similarly, a study of the anomalies associated with the $SU(2)_W$ and $SU(3)_C$ gauge symmetries show that both vanish, as it is compulsory in a gauge theory in order to preserve the Ward identities.

Note finally that the fermion content given in Table 2.1 comes in three copies, called *generations*. This means for example that there are three quarks doublets $q_L^{(1)} = (u_L, d_L)$, $q_L^{(2)} = (c_L, s_L)$, $q_L^{(3)} = (t_L, b_L)$, which do not differ from each other as long as they remain massless, and similarly for the remaining fermions. Therefore, the global symmetry of the fermion sector is enhanced from $[U(1)]^5$ to the rotations among the three families of fermions independently for each of the five species, which can be written as

$$\big[U(3)\big]^5 = U(3)_q \times U(3)_u \times U(3)_d \times U(3)_l \times U(3)_e. \tag{2.32}$$

2.2 Spontaneous symmetry breaking

The theory described so far contains only massless states, in the gauge sector since gauge bosons are by definition massless, and in the fermion sector since no mass term preserving gauge-invariance can be written. There is a way of introducing masses for gauge fields without explicitly breaking the gauge invariance of the Lagrangian, known as *spontaneous symmetry breaking*. This mechanism is achieved by the introduction of one or more scalar fields, acquiring a vacuum expectation value different from zero due to a potential imposed by hand at the Lagrangian level, or generated via radiative corrections [26]. Although the Standard Model was constructed historically upon introducing a fundamental scalar field, preserving the renormalisability of the theory, we forget this requirement for now and address the question of mass generation in an effective approach.

2.2.1 The non-linear σ-model parametrisation

Of the four electroweak gauge bosons W^i_μ $(i = 1, 2, 3)$ and B_μ introduced above, only one massless state must be present in the model, the photon. The other three must therefore acquire a longitudinal component, arising from a scalar field after spontaneous symmetry breaking. The minimal content of the scalar sector consists therefore of three scalar fields $\chi^i(x)$ $(i = 1, 2, 3)$, whose kinetic term takes the form

$$\frac{1}{2}\partial_\mu\chi^i\partial^\mu\chi^i. \tag{2.33}$$

In order to become the longitudinal polarisation of the $W^\pm$ and Z^0 bosons, the fields χ^i must be charged under the electroweak gauge group. A straightforward choice would be to promote the space-time derivative to a covariant derivative

$$D_\mu\chi^i = \partial_\mu\chi^i - igW^k_\mu \left(T^k_{3\times3}\right)^{ij} \chi^j, \tag{2.34}$$

where $T^k_{3\times3}$ is a generator of $SO(3) \cong SU(2)$. In this case the fields χ^i transform linearly under gauge transformations as a triplet of $SU(2)_W$. Note that no $U(1)_Y$ term is allowed, so that the fields χ^i must have zero hypercharge. This choice is thus unsatisfying: Whatever vacuum expectation value $\langle\chi^i\rangle$ is imposed, the field B_μ remains massless, and there is no breaking of the gauge group from $SU(2)_W \times U(1)_Y$ down to $U(1)_{em} \neq U(1)_Y$.

A better choice is to use a non-linear parametrisation of the scalar fields, defining a 2×2 matrix

$$\Sigma(x) = \exp\left[i\chi^i\sigma^i/v\right] = \mathbb{1}_2 + i\frac{\chi^i}{v}\sigma^i + \dots, \tag{2.35}$$

where v is a dimensionful constant. The $SU(2)_W \times U(1)_Y$ covariant derivative is chosen to act on $\Sigma(x)$ as

$$D_\mu\Sigma = \partial_\mu\Sigma + igW^i_\mu\frac{\sigma^i}{2}\Sigma - ig'B_\mu\Sigma\frac{\sigma^3}{2}, \tag{2.36}$$

and a gauge-invariant Lagrangian can be written in the form

$$\mathcal{L}_\chi = \frac{v^2}{4}\,\mathrm{Tr}\left(D_\mu\Sigma^\dagger D^\mu\Sigma\right). \tag{2.37}$$

The term with two space-time derivatives is equivalent to the kinetic term (2.33) at lowest order in v, and yield additional interaction terms between the χ^i fields suppressed by powers of $1/v^2$. The minimum of the energy is attained for any static configuration $\partial_\mu\chi^i = 0$, and the vacuum state can always be chosen to correspond to $\langle\chi^i\rangle = 0$, since any other choice is

equivalent to it via a gauge transformation. Expanding around the vacuum, one gets therefore a mass term from the gauge fields in the form

$$\frac{v^2}{8}\left[g^2\left(W_\mu^1\right)^2+g^2\left(W_\mu^2\right)^2+\left(gW_\mu^3-g'B_\mu\right)^2\right]. \tag{2.38}$$

The mass and charge eigenstates can then be defined as

$$\begin{aligned} W_\mu^\pm &= \frac{1}{\sqrt{2}}\left(W_\mu^1 \pm iW_\mu^2\right), \\ Z_\mu &= \cos\theta_W W_\mu^3 - \sin\theta_W B_\mu, \\ A_\mu &= \sin\theta_W W_\mu^3 + \cos\theta_W B_\mu, \end{aligned} \tag{2.39}$$

where the Weinberg angle θ_W is defined by $\tan\theta_W = g'/g$. In this basis, the mass term (2.38) becomes

$$m_W^2\, W_\mu^+ W^{\mu-} + \frac{1}{2}m_Z^2\, Z_\mu Z^\mu, \tag{2.40}$$

where

$$m_W^2 = \frac{g^2v^2}{4}, \qquad m_Z^2 = \frac{g^2v^2}{4\cos^2\theta_W}. \tag{2.41}$$

These masses match the experimental measurement provided that $v \cong 246$ GeV. The constant v is called the *electroweak scale*.

Note that in addition to the electroweak gauge symmetry, the Lagrangian (2.37) has a global $SU(2)_L \times SU(2)_R$ symmetry, under which the scalar field transforms as

$$\Sigma \to L^\dagger \Sigma R, \qquad L, R \in SU(2). \tag{2.42}$$

The vacuum expectation value corresponding to $\langle\chi^i\rangle = 0$ or equivalently $\langle\Sigma\rangle = \mathbb{1}_2$ breaks this global symmetry spontaneously down to the diagonal subgroup $SU(2)_V$, realised in the transformation rule above, when $L = R$. The gauge field W_μ^i is a triplet of $SU(2)_L$, a singlet of $SU(2)_R$, and hence a triplet of $SU(2)_V$. For this reason, in the limit $g' \to 0$, the massive gauge bosons W^+, W^- and Z^0 form a triplet of an exact global symmetry, and their masses are equal: $m_W = m_Z$. With $g' \neq 0$, the ratio of masses can be expressed as

$$\rho = \frac{m_W^2}{m_Z^2\cos^2\theta_W} = 1. \tag{2.43}$$

At the loop level, the $W^\pm$ and Z^0 masses get radiative corrections induced by couplings to matter fields. The global $SU(2)_L \times SU(2)_R$ symmetry is called *custodial symmetry* and will play a central role in the construction of composite Higgs models, as discussed in section 3.2.2. If the custodial symmetry is preserved at all orders in perturbation theory, the parameter ρ remains exactly equal to one. In reality, we will see in the next section how fermion masses break the custodial symmetry, so that corrections to ρ will appear at loop level.

2.2.2 Fermion masses generation and flavour physics

The gauge transformation rules of the Σ field allows to write terms involving both Σ and fermions in the Lagrangian, fixed uniquely by the symmetry to

$$\mathcal{L}_{\text{Yukawa}} = \frac{v}{\sqrt{2}}\,\overline{q}_L^{(i)}\Sigma\begin{pmatrix} Y_u^{(i,j)}u_R^{(j)} \\ Y_d^{(i,j)}d_R^{(j)}\end{pmatrix} + \frac{v}{\sqrt{2}}\,\overline{l}_L^{(i)}\Sigma\begin{pmatrix} 0 \\ Y_e^{(i,j)}e_R^{(j)}\end{pmatrix} + \text{h.c.} \quad (2.44)$$

where the $Y_{u,d,e}^{(i,j)}$ are massless coefficients called *Yukawa couplings*, and the indices in parenthesis are flavour indices referring to the three generations of quarks and leptons. Expanding around the vacuum expectation value and writing the doublets explicitly in components, one finds

$$\mathcal{L}_{\text{Yukawa}} = \frac{v}{\sqrt{2}}\left(Y_u^{(i,j)}\overline{u}_L^{(i)}u_R^{(j)} + Y_d^{(i,j)}\overline{d}_L^{(i)}d_R^{(j)} + Y_e^{(i,j)}\overline{e}_L^{(i)}e_R^{(j)} + \text{h.c.}\right) + \mathcal{O}\left(v^0\right), \quad (2.45)$$

which acts now as a mass term for the fermions. The most general form of the $Y_{u,d,e}$ couplings can be simplified using the global flavour symmetry (2.32). For example, a $SU(3)_q \times SU(3)_d$ rotation allows to bring the down-type Yukawa matrix Y_d into a diagonal form. Similarly, Y_e can be diagonalised by an appropriate $SU(3)_l \times SU(3)_e$ rotation. However, the remaining $SU(3)_u$ symmetry is not sufficient to fully diagonalise the up-type Yukawa matrix Y_u. The most general Lagrangian for the fermion masses can hence be written as

$$\sum_{i,j} m_u^{(i)} V_{CKM}^{(i,j)}\overline{u}_L^{(i)}u_R^{(j)} + \sum_i m_d^{(i)}\overline{d}_L^{(i)}d_R^{(i)} + \sum_i m_e^{(i)}\overline{e}_L^{(i)}e_R^{(i)} \quad (2.46)$$

where $m_{u,d,e}^{(i)} = \lambda_{u,d,e}^{(i)} v/\sqrt{2}$ and $\lambda_{u,d,e}^{(i)}$ are the eigenvalues of the Yukawa matrices. V_{CKM} is here an unitary 3×3 matrix, called the *Cabibbo-Kobayashi-Maskawa matrix* [27, 28].

The Yukawa Lagrangian (2.44) is in general not invariant under the global $SU(2)_L \times SU(2)_R$ symmetry defined in eq. (2.42), unless the up- and down-type Yukawa couplings are equal. For this reason, the custodial $SU(2)_V$ symmetry is explicitly broken, but the breaking is at most proportional to the mass differences between quarks and leptons forming an isodoublet. The ρ parameter (2.43) gets subsequently corrections at the loop level, directly proportional to the fermion masses.

Note also that of the global $[U(1)]^5$ part of the full flavour symmetry (2.32), only two $U(1)$ subsist after fermion masses are generated. They are $U(1)$ factors associated with each term separately in the Lagrangian (2.44). The symmetry rotating quarks as $q_L \to e^{i\alpha/3}q_L$, $u_R \to e^{i\alpha/3}u_R$ and $d_R \to e^{i\alpha/3}d_R$ is called the *baryon number* $U(1)_B$, while the *lepton number* $U(1)_L$ is given by $l_L \to e^{i\alpha}l_L$ and $e_R \to e^{i\alpha}e_R$. Both baryon and lepton number symmetries are anomalous and are actually violated by non-perturbative processes. However, as seen in eq. (2.30), the linear combination $U(1)_{B-L}$

survives in the quantum theory and is thus a true symmetry of the Standard Model.

2.3 Renormalisability and unitarity

The Standard Model as described so far reproduces successfully the spectrum of all known particles and their properties. However, in the σ-model formalism adopted in the previous section, some issues of fundamental importance are present. Among them, the renormalisability of the theory and the unitarity of scattering amplitudes are going to be addressed now.

2.3.1 Renormalisability

The non-linear σ-model parametrisation is by definition non-renormalisable in four space-time dimensions. To see this, a divergence counting argument can be used. Expanding the field Σ into its scalar components χ^i and forgetting about the gauge fields, one gets from the Lagrangian (2.37) an infinite number of interaction terms, with any number of fields χ^i in them, but always exactly two space-time derivatives, of the form

$$\mathcal{L} \supset \frac{c_n}{v^{n-2}} \left(\partial_\mu \chi^{i_1}\right) \left(\partial^\mu \chi^{i_2}\right) \chi^{i_3} \cdots \chi^{i_n}. \tag{2.47}$$

Now let's consider a Feynman diagram involving only the scalar fields χ^i with N external legs and L loops. The diagram will also have P internal propagators and V vertices. The number of loops is related to the number of propagators and vertices as

$$L = P - V + 1. \tag{2.48}$$

The superficial degree of divergence of the diagram, defined as the expected power of momentum of the loop integral, is then, in d spatial dimensions

$$D = dL - 2P + 2V = (d-2)\, L + 2. \tag{2.49}$$

For $d \geq 2$, due to the fact that the superficial degree of divergence of any diagram increases with the number of loops (or equivalently with order in perturbation theory), an infinite number of counterterms is needed to cancel the divergences. The non-linear σ-model is therefore *non-renormalisable*. Since higher-dimension operators of the type (2.47) are suppressed by powers of v, the validity of the theory extends only in the range where the loop corrections are smaller than tree-level contributions, so naively up to the cutoff

$$\Lambda_{EW} \approx 4\pi\, v \cong 3.1 \text{ TeV}. \tag{2.50}$$

2.3.2 Unitarity violation in WW scattering

The second issue about our effective description of the Standard Model arises in the scattering amplitude of the longitudinal polarisation of W bosons, $W_L W_L \to W_L W_L$ [29, 30]. By the equivalence theorem [31], this scattering amplitude can be computed at energies larger than the $W^\pm$ and Z^0 masses in terms of the Goldstone bosons only. Consider the scattering $W^+W^- \to W^+W^-$, or equivalently $\chi^+\chi^- \to \chi^+\chi^-$: In the absence of gauge fields, the Lagrangian (2.37) can be rewritten as

$$\begin{aligned}\mathcal{L}_\chi &= \frac{1}{2\chi^2}\left[\left(\chi^i\partial_\mu\chi^i\right)^2 + \frac{v^2}{\chi^2}\sin^2\left(\frac{\chi^2}{v^2}\right)\left(\chi^2(\partial_\mu\chi^i)^2 - \left(\chi^i\partial_\mu\chi^i\right)^2\right)\right] \\ &= \frac{1}{2}\partial_\mu\chi^i\partial^\mu\chi^i + \frac{1}{6v^2}\left[\left(\chi^i\partial_\mu\chi^i\right)^2 - \chi^2(\partial_\mu\chi^i)^2\right] + \dots \end{aligned} \tag{2.51}$$

where $\chi^2 = (\chi^i)^2$, and in the second equality an expansion in inverse powers of v was performed. There is no vertex involving only three χ^i fields. Therefore, the scattering amplitude is given by fig. 2.2(a) only, and its cross-section is found to be

$$\mathcal{M}\left(W^+W^- \to W^+W^-\right) = \frac{s+t}{v^2}\left[1 + \mathcal{O}\left(\frac{m_W^2}{s}\right)\right] \tag{2.52}$$

where s and t are the usual Mandelstam variables. As the matrix element grows with the square of the energy of the scattered particles, one has to take care that the unitarity of the S-matrix is preserved. A simple way of achieving this goal is to use the optical theorem, relating the imaginary part of the forward scattering amplitude (i.e. at scattering angle $\theta = 0$) to the total cross section of $W^\pm$ bosons, as[4]

$$\begin{aligned}\operatorname{Im}\mathcal{M}\left(W^+W^- \to W^+W^-, \theta = 0\right) &= s\,\sigma\left(W^+W^- \to \text{anything}\right) \\ &\geq s\,\sigma\left(W^+W^- \to W^+W^-\right)\end{aligned} \tag{2.53}$$

To exploit this property it is convenient to expand the matrix elements into plane waves, as

$$\mathcal{M} = 16\pi\sum_{l=0}^{\infty}(2l+1)P_l(\cos\theta)\mathcal{M}_l \tag{2.54}$$

where $\mathcal{M}_l$ is independent on the angle θ, and the P_l are Legendre polynomials, the first two being $P_0(x) = 1$ and $P_1(x) = x$. Legendre polynomials satisfy an orthogonality condition

$$\int_{-1}^{1}\mathrm{d}x\,P_l(x)P_m(x) = \frac{2}{2l+1}\,\delta_{lm}. \tag{2.55}$$

[4] The matrix element is actually real at tree-level, see eq. (2.52), but will receive both real and imaginary corrections at higher loop order.

Using the property $P_l(1) = 1$, the left-hand side of eq. (2.53) becomes

$$\operatorname{Im}\mathcal{M}\left(\theta = 0\right) = 16\pi \sum_{l=0}^{\infty} (2l+1) \operatorname{Im}\mathcal{M}_l. \tag{2.56}$$

On the other hand, the total cross section for a $2 \to 2$ process involving the same particle in the initial and final states reads

$$\sigma = \int \mathrm{d}\Omega \frac{|\mathcal{M}|^2}{64\pi^2 s} = \int_{-1}^{1} \mathrm{d}(\cos\theta) \frac{|\mathcal{M}|^2}{32\pi s}, \tag{2.57}$$

which gives, upon expansion in plane waves,

$$\begin{aligned} \sigma &= \frac{(16\pi)^2}{32\pi s} \sum_{l=0}^{\infty} \sum_{m=0}^{\infty} (2l+1)(2m+1) \mathcal{M}_l \mathcal{M}_m^* \\ &\qquad \cdot \int_{-1}^{1} \mathrm{d}(\cos\theta) P_l(\cos\theta) P_m(\cos\theta) \\ &= \frac{16\pi}{s} \sum_{l=0}^{\infty} |\mathcal{M}_l|^2. \end{aligned} \tag{2.58}$$

Plugging this cross-section into the right-hand side of eq. (2.53), since the inequality has to hold for any angle θ, one obtains

$$\sum_{l=0}^{\infty} (2l+1) \operatorname{Im}\mathcal{M}_l \geq \sum_{l=0}^{\infty} (2l+1) |\mathcal{M}_l|^2 \tag{2.59}$$

For simplicity, this equality is assumed to hold for all l separately, hence

$$\operatorname{Im}\mathcal{M}_l \geq |\mathcal{M}_l|^2. \tag{2.60}$$

Now writing

$$\left(\operatorname{Re}\mathcal{M}_l\right)^2 + \left(\operatorname{Im}\mathcal{M}_l - \frac{1}{2}\right)^2 = |\mathcal{M}_l|^2 - \operatorname{Im}\mathcal{M}_l + \frac{1}{4} \leq \frac{1}{4}, \tag{2.61}$$

where the inequality follows directly from eq. (2.60), one finds then

$$|\operatorname{Re}\mathcal{M}_l| \leq \frac{1}{2}. \tag{2.62}$$

For the process $W^+W^- \to W^+W^-$, the matrix element is given, at tree-level, by

$$\mathcal{M} = \frac{s}{2v^2} \left(1 + \cos\theta\right) \tag{2.63}$$

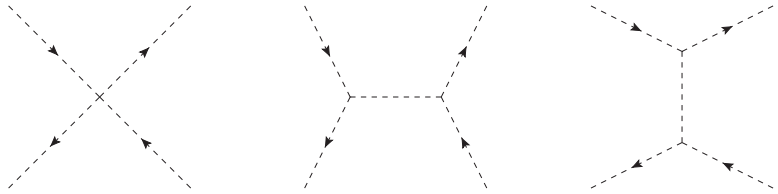

Figure 2.2: Diagrams contributing to the scattering of Goldstone bosons, or equivalently to the scattering of $W^{\pm}$ bosons in the high-energy limit.

which corresponds, in terms of planar waves, to

$$\mathcal{M}_0 = \frac{s}{32\pi v^2}, \qquad \mathcal{M}_1 = \frac{s}{96\pi v^2}, \qquad \mathcal{M}_{l\geq 2} = 0, \tag{2.64}$$

where s is the square of the W^+W^- centre-of-mass energy. The strongest unitarity bound comes from the $l = 0$ wave, and yields

$$E = \sqrt{s} \lesssim 4\sqrt{\pi}\, v \cong 1.7 \text{ TeV}. \tag{2.65}$$

This bound is of course only approximate, since it was derived from the tree-level matrix elements. More involved calculations can lead to a tighter bound. It shows however the need for new particle states to appear in addition to the spectrum described so far.

2.4 The Higgs boson

Both problems raised in the previous section can be solved by the simple addition of a massive scalar field to the theory, known as the *Higgs boson*. The presence of a fundamental scalar field nevertheless introduces a different issue, and one of the two known solutions to it out will turn out to have a composite Higgs boson.

2.4.1 Unitarity restoration by a scalar field

Let us add to the Standard Model as described so far a new scalar with the quantum numbers of the vacuum. This scalar is allowed to interact both with the χ^i fields and with the quark and leptons. Therefore, we replace the Lagrangian (2.37) by the most general form

$$\mathcal{L}_{h,\chi} = \frac{1}{2}\partial_\mu h \partial^\mu h - V(h) + \frac{v^2}{4}\,\mathrm{Tr}\left(D_\mu \Sigma^\dagger D^\mu \Sigma\right)\left(1 + 2a\,\frac{h}{v} + b\,\frac{h^2}{v^2} + \dots\right) \tag{2.66}$$

where the potential $V(h)$ is given by

$$V(h) = \frac{1}{2} m_h^2 h^2 + \frac{d_3}{2} \left(\frac{m_h^2}{v} \right) h^3 + \frac{d_4}{8} \left(\frac{m_h^2}{v^2} \right) h^4 + \dots \tag{2.67}$$

As indicated by the dots, higher powers of h might be present, but are irrelevant for the low-energy phenomenology. Note also that a can be always taken positive without loss of generality, since the theory is invariant under the transformation $a \to -a$, $h \to -h$. Similarly, the Lagrangian (2.44) can be enlarged to

$$\mathcal{L}_{\text{Yukawa}} = \frac{v}{\sqrt{2}} \overline{q}_L^{(i)} \Sigma \begin{pmatrix} Y_u^{(i,j)} u_R^{(j)} \\ Y_d^{(i,j)} d_R^{(j)} \end{pmatrix} \left(1 + c_{u,d}^{(i,j)} \frac{h}{v} + \dots \right) + \dots + \text{h.c.} \tag{2.68}$$

where the lepton part was omitted. The parametrisation used here is standard in the literature [32]. In general, flavour-changing neutral currents would arise at tree-level from exchange of the field h. One can constrain them by imposing

$$c_{u,d}^{(i,j)} = c_{u,d}\, \delta_{ij} \tag{2.69}$$

in the basis where the Yukawa matrices are diagonal. On the contrary, up-type quarks, down-type quarks and leptons can have different couplings to h.

In the presence of the scalar field h, new diagrams contribute to the scattering of $W^\pm$ gauge bosons at tree-level, as illustrated in fig. 2.2. They contribute to the matrix element (2.52) as

$$\begin{aligned} \mathcal{M}\left(W^+W^- \to W^+W^-\right) &= \frac{1}{v^2} \left(s + t - a^2 \frac{s^2}{s - m_h^2} - a^2 \frac{t^2}{t - m_h^2} \right) \\ &\xrightarrow{s,t \gg m_h^2} \left(1 - a^2\right) \frac{s+t}{v^2}. \end{aligned} \tag{2.70}$$

For the special choice of parameter $a = 1$, the terms growing with the square of the energy are exactly cancelled by the exchange of the h field, and the unitarity of the S matrix is ensured up to high energies. The matrix element then becomes, in the large energy limit,

$$\mathcal{M}\left(W^+W^- \to W^+W^-\right) = -\frac{m_h^2}{v^2} \left(\frac{s}{s - m_h^2} + \frac{t}{t - m_h^2} \right), \tag{2.71}$$

or equivalently for the s-wave $\mathcal{M}_0 = m_h^2/(8\pi v^2)$, which from the unitarity constraint (2.60) puts an upper bound on the Higgs mass:

$$m_h \lesssim 2\sqrt{\pi}\, v \cong 870 \text{ GeV}. \tag{2.72}$$

In general, any value of a in the vicinity of 1 does not unitarise the scattering of $W^\pm$ bosons completely but still allows to relax the unitarity bound

(2.65). As we will see in the next chapter, composite Higgs models generically predict values of a below one. The case $a > 1$ is nevertheless also a possibility, but in this case there is an "overunitarisation" which requires more involved new physics to cancel [33].

The presence of a new scalar particle requires however to investigate as well the status of unitarity in processes involving the h field as an external particle. For example the matrix element

$$\mathcal{M}\left(W^+W^- \to hh\right) = \frac{1}{2v^2}\left(b\,s + a^2 t + a^2 u\right), \tag{2.73}$$

computed here in the high-energy limit (for which s-channel h exchange diagram containing d_3 is subleading), gives a s-wave contribution

$$\mathcal{M}_0\left(W^+W^- \to hh\right) = \left(b - a^2\right)\frac{s}{32\pi v^2}, \tag{2.74}$$

which is vanishing in the limit $b = a^2$. A similar analysis of the process $W^+W^- \to \overline{f}f$, where f denotes any of the Standard Model fermions, shows that the amplitude grows linearly with the energy of the process, multiplied by a factor $(1 - a\,c)$. The condition for unitarity of scattering amplitudes up to arbitrarily high energy scales is thus

$$a = b = c = 1. \tag{2.75}$$

As of 2012, the LHC is starting to put direct experimental constraints on the parameters a and c, which indeed tend to favour a scenario where $0.5 \lesssim a \lesssim 1.5$ [34, 35].

2.4.2 The Standard Model Higgs doublet

We have seen in the previous section that unitarity can be restored provided that $a = b = c = 1$. This is not an accident, but corresponds instead to a special case in which the theory is renormalisable at all orders in perturbation theory [36]. For the choice of parameters $a = b = c = d_3 = d_4 = 1$ and $c_2 = 0$, one can rewrite the Lagrangian (2.66) as

$$\mathcal{L}_{h,\chi} = \frac{1}{4}\,\mathrm{Tr}\left(D_\mu \Phi^\dagger D^\mu \Phi\right) - V\left(\Phi^\dagger\Phi\right), \quad \text{where} \quad \Phi = (v+h)\,\Sigma, \tag{2.76}$$

with

$$V\left(\Phi^\dagger\Phi\right) = \frac{1}{8}\left(\frac{m_h^2}{v^2}\right)\left(\frac{1}{2}\,\mathrm{Tr}\,\Phi^\dagger\Phi - v^2\right)^2. \tag{2.77}$$

Moreover, defining

$$H = (v+h)\,\Sigma\begin{pmatrix}1\\0\end{pmatrix}, \qquad H^c = \left(i\sigma^2\right)H^* = (v+h)\,\Sigma\begin{pmatrix}0\\-1\end{pmatrix} \tag{2.78}$$

one has $\Phi = (H, -H^c)$, and the Lagrangian can be rewritten as

$$\mathcal{L}_{h,\chi} = \frac{1}{2} D_\mu H^\dagger D^\mu H - V\left(H^\dagger H\right). \tag{2.79}$$

Similarly, the Yukawa term becomes

$$\mathcal{L}_{\text{Yukawa}} = \frac{1}{\sqrt{2}} Y_u^{(i,j)} \overline{q}_L^{(i)} H u_R^{(j)} + \frac{1}{\sqrt{2}} Y_d^{(i,j)} \overline{q}_L^{(i)} H^c d_R^{(j)} + \ldots + \text{h.c.} \tag{2.80}$$

With this choice of parameters, H transforms linearly under the electroweak gauge group $SU(2)_W \times U(1)$. More precisely, it is a doublet with hypercharge $\frac{1}{2}$. The model is therefore a theory containing a fundamental scalar doublet H, and is completely renormalisable. The field h in this case is called the *Standard Model Higgs boson*.[5]

2.4.3 The hierarchy problem

While a fundamental Higgs doublet solves the problems of renormalisability and perturbative unitarity of the Standard Model, it introduces a new kind of issue, associated with the presence of fundamental scalars in general. It arises when one computes the radiative corrections to the Higgs boson mass. As for any other quantity in a renormalisable theory, the physical mass of the Higgs boson is given by

$$m^2_{\text{phys}} = m^2_{\text{bare}} + \delta m_h^2, \tag{2.81}$$

where m_{bare} is the *bare* mass of the Higgs, i.e. the parameter appearing in the potential (2.67), and δm_h^2 denotes the radiative corrections to the propagator of h, given schematically at leading order by the four diagrams in fig. 2.3. The loop diagrams contributing to the Higgs mass appear to be quadratically divergent: In a cutoff regularisation scheme, the leading term is

$$\delta m_h^2 = \frac{\Lambda^2}{32\pi^2}\left(\frac{9}{4}g^2 + \frac{1}{2}g'^2 - 6y_t^2 + \frac{3}{4}\frac{m_h^2}{v^2}\right) \tag{2.82}$$

where g and g' are the $SU(2)_W \times U(1)$ gauge couplings and y_t is the top Yukawa coupling (all remaining fermions give a negligible contribution). The contribution m_h^2/v^2 comes from the Higgs self-couplings. Quadratic divergences are actually not strictly a problem within the renormalisable Standard Model itself: an infinite δm_h^2 can be absorbed into an infinite

[5]Note that while the mechanism of gauge bosons acquiring a mass from spontaneous symmetry breaking was first discovered independently by Anderson [37], Englert and Brout [38], and later Higgs [39], Guralnik, Hagen and Kibble [40], Peter Higgs was the first to account for extra scalars remaining massive, as it is the case of the Standard Model Higgs boson [41]. The denomination "Higgs boson" is therefore accurate when one speaks of the particle, but the mechanism of mass generation through spontaneous symmetry breaking should strictly speaking also carry the name of its co-discoverers.

(a) (b) (c) (d)

Figure 2.3: One-loop radiative corrections to the Higgs boson propagator, from self-interactions (a), interactions with fermions (b) and with gauge bosons (c), (d).

bare mass for the Higgs, resulting in a finite result, as it is standard in a renormalisable theory. The only physical meaning of quadratically divergent corrections to the Higgs mass is that the latter cannot be calculated and remains a free parameter in the Standard Model.

Nevertheless, the Standard Model cannot account for all explained phenomena in nature, and new physics need to be added to the theory. The simplest example is gravity, which start becoming relevant for particle physics at the Planck scale

$$M_{\text{Planck}} = 1.22 \cdot 10^{19} \text{ GeV}. \tag{2.83}$$

Other observations indicate that new physics should probably appear at a much lower energy scale, as will be briefly explained in the next section. In the presence of new physics at a scale Λ, the radiative correction δm_h^2 will be cut-off at this very scale Λ, instead of being infinite. The requirement for the Higgs mass to be below the TeV scale as required by unitarity account therefore for a very strong fine-tuning of the bare Higgs mass. In case the cutoff is at the Planck scale, the bare mass of the Higgs should cancel the radiative contribution exactly up to the 35th digit. Such a cancellation is very unnatural. In other words, any small deviations from this precise value of m^2_{bare} in the Lagrangian would result in completely different physics. This tension is known as the *hierarchy problem*, or *naturalness* issue. Note that large scale hierarchies are not forbidden in nature, but require in principle a symmetry to protect them. One realisation of scale hierarchy occur naturally in asymptotically free theories, where masses are generated at the scale at which the theory becomes strongly interacting, instead of the cutoff scale of the theory. This principle is the fundamental idea behind composite Higgs models, and will be extensively discussed below.

Note finally that the presence of fundamental massive fermions in the Standard Model does not introduce a similar problem, since the radiative correction to their mass is controlled by the chiral symmetry: in the limit of vanishing Yukawa coupling, an exact symmetry acting as $f \to \exp\left(i\theta\gamma^5\right) f$ is present in the model. For this reason, loop corrections to the fermion masses arise only with coefficient proportional to the chiral symmetry break-

ing terms, namely to the fermion masses themselves. Corrections are thus naturally maintained at a reasonable level, and are only logarithmically sensitive to the new physics scale. Similarly, $W^{\pm}$ and Z^0 gauge bosons would be exact gauge bosons in the limit of vanishing masses, and are therefore protected from large loop corrections. The reason why fundamental scalars are problematic can be associated with the fact that massless and massive scalar fields have the same number of degrees of freedom, while extra degrees of freedoms have to be added to a theory in order to give a mass to fermions and vector fields.

2.5 The need to go beyond the Standard Model

Leaving apart the issues associated with the breaking of the electroweak symmetry, a number of other shortcomings arise in the Standard Model. We discuss here shortly the most obvious ones.

2.5.1 Neutrino masses

Since neutrinos appear only as left-handed fermions in the Standard Model, no Dirac mass term can be generated as for the other fermions. A Majorana mass term is forbidden as well by gauge invariance, since neutrinos are part a doublet of $SU(2)_W$. The theory described above predicts therefore that neutrinos of all three generations are exactly massless. Experimental evidence has however be accumulated that neutrino oscillate between the three physical eigenstates [42], a phenomenon which can only appear if they have a mass [43], at least for two of them. In this case, the neutrino fields coupling to the electroweak gauge bosons are superpositions of mass eigenstates. The past and present experiments allowed to determine with a reasonable precision the mass differences between the neutrino species, but not their sign nor their absolute mass scale. The latter is nevertheless constraint by an upper bound of a few eV [44].

A straightforward way of introducing masses for the neutrino in the Standard Model is to add a right-handed neutrino, with no charge under the electroweak gauge group but coupling to the left-handed neutrino via the Yukawa interaction [45]. Due to its absence of couplings to the gauge sector, such a neutrino is often called *sterile*. This setup can be achieved by completing the $SU(2)_R$ doublet in the Yukawa Lagrangian (2.44) as

$$\mathcal{L}_{\text{Yukawa}} \supset \frac{v}{\sqrt{2}}\, \bar{l}_L^{(i)} \Sigma \begin{pmatrix} Y_e^{(i,j)} N_R^{(j)} \\ Y_e^{(i,j)} e_R^{(j)} \end{pmatrix} + \text{h.c.} \tag{2.84}$$

where N_R denotes the new right-handed neutrino. Due to its absence of gauge couplings, a Majorana mass term for N_R is in principle allowed in the

model, despite its explicit violation of lepton number:

$$\mathcal{L}_N = \overline{N}_R^{(i)} i\partial\!\!\!/ N_R^{(i)} - M_N^{(i,j)}\, \overline{N}_R^{(i)c} N_R^{(j)}, \tag{2.85}$$

where c denotes charge conjugation, i.e.

$$\psi^c = \left(i\sigma^2\right)\psi^*, \qquad \overline{\psi}^c = \psi^T\left(-i\sigma^2\right). \tag{2.86}$$

As a result of the mixing between a massless ν_L and a massive Majorana neutrino N_R, the physical spectrum of the theory contains two massive fermions, whose masses are naturally hierarchical. This phenomenon is known as the *seesaw mechanism*, and is better illustrated with a single generation of leptons, for which the mass term after electroweak symmetry breaking can be written in a matrix notation as

$$\mathcal{L} \supset \left(\overline{\nu}_L\ \overline{N}_R^c\right) \begin{pmatrix} 0 & \frac{1}{\sqrt{2}}\, y_\nu v \\ \frac{1}{\sqrt{2}}\, y_\nu v & M_N \end{pmatrix} \begin{pmatrix} \nu_L \\ N_R \end{pmatrix} \tag{2.87}$$

Upon redefinition of the fields into mass eigenstates, the physical fermions have masses given by the eigenvalues of the 2×2 mass matrix, namely

$$m_1 = \frac{1}{2}\left(M_N - \sqrt{M_N^2 + 2(y_\nu v)^2}\right) \cong -\frac{(y_\nu v)^2}{2M_N} \tag{2.88}$$

$$m_2 = \frac{1}{2}\left(M_N + \sqrt{M_N^2 + 2(y_\nu v)^2}\right) \cong M_N \tag{2.89}$$

where the equalities on the right-hand side hold in the limit $y_\nu v \ll M_N$. The Majorana mass M_N can naturally be large since it is not protected by the chiral symmetry like quark and lepton masses are. The seesaw mechanism is thus not only a very economical way of introducing neutrino masses into the Standard Model, it provides simultaneously an explanation of why neutrino masses are tiny compared to the others fermion masses.

The problem of neutrino masses can equivalently be addressed in an effective theory approach. Considering only the Standard Model fields defined above and writing down all possible operators with increasing dimensions,[6] the first beyond-the-Standard-Model operator appears at dimension five and is [46]

$$\mathcal{L}_5 = c^{(i,j)}\frac{v^2}{M}\left(\bar{l}_L\Sigma\right)^c\left(\Sigma^\dagger l_L\right) \tag{2.90}$$

or equivalently in the renormalisable theory

$$\mathcal{L}_5 = c^{(i,j)}\frac{1}{M}\left(\bar{l}_L H\right)^c\left(H^\dagger l_L\right) \tag{2.91}$$

[6] Although the σ-model field Σ is actually dimensionless, for dimension counting arguments it always comes with a factor v and thus counts as dimension one like a scalar field. This property is better seen in the renormalisable realisation of the model, in which v is absorbed into the Higgs doublet H.

where M is the scale of the new physics leading to this operator and $c^{(i,j)}$ are coefficients naturally of order one (or smaller if the operator arises from integrating out a loop). The reason why no similar terms are allowed with a quark doublet replacing the lepton doublet is because of $U(1)_Y$ gauge invariance: the combination $\Sigma^\dagger l_L$ is not charged under the electroweak gauge group, while $\Sigma^\dagger q_L$ has a residual $U(1)_Y$ hypercharge.

From eq. (2.90) it is obvious that in the unitary gauge $\langle\Sigma\rangle = \mathbb{1}$, the dimension-five operator acts as a Majorana mass term for the left-handed neutrino ν_L. The resulting mass is then as in eq. (2.89) with the identification $M = M_N$ and $c = \frac{1}{2}y_\nu^2$. Integrating out the right-handed sterile neutrino from the model described above leads indeed to the operator (2.90). The effective theory approach allows us, however, to make a model-independent statement about the smallness of neutrino masses. It is for example possible to generate the dimension-five operator by introducing a scalar triplet instead of a right-handed neutrino (known as type II seesaw [47], while type I corresponds to the sterile neutrino setup described above), or even a fermion triplet (type III seesaw [48]).

As for the quarks, the global flavour symmetry (2.32) is not sufficient to diagonalise the form of the coefficients $c^{(i,j)}$ in (2.90). After diagonalising the lepton masses, there remains a 3×3 unitary matrix parametrising the mixing between the three generations of neutrino. Contrarily to the quark sector where the CKM matrix is quasi-diagonal (off-diagonal terms are subleading), in the lepton sector there is no such structure. Moreover, when a Majorana mass term is generated for the neutrinos, two additional CP-violating phases remain after rotation in the physical basis, in addition to the usual phase present in a 3×3 unitary matrix.

Note finally that there exist scenarios where, instead of being very massive, the sterile neutrino lives below the electroweak scale [49], in which case there is no new scale introduced in the theory. The presence of a light sterile neutrino could explain the dark matter problem [50], and there are even claims that the Standard Model extended in this way can solve all issues in cosmology including inflation, the baryon asymmetry and structure formation [51].

2.5.2 Dark matter, dark energy and baryon asymmetry

Many constraints on the Standard Model originate not directly from particle physics experiments, but rather from cosmology. The present and the past of the universe is known to some extent with high precision, and depend strongly on its particle content. The first evidence of physics beyond the Standard Model comes from discrepancies between the indirectly measured mass of some cosmological objects and their apparent luminosity. Indirect measurements are performed by observing the effects of the gravitational force, for example on the planets rotating inside a galaxy, from galaxies

rotating inside a cluster, and from gravitational lensing effects. When compared to the light they emit, these sources seem to be much heavier than expected. There must therefore exist a new form of matter, whose interactions with photons is strongly suppressed, the so-called *dark matter*. The current consensus from experimental observations is that ordinary, visible matter form only 27% of the total mass of the universe, while dark matter must account for the remaining 83%. Any new type of neutral and stable particle could possibly solve this problem. Among all the possibilities, it turns out that particles with a mass around the electroweak scale or higher and with no other couplings to the Standard Model fields than through the weak interaction have precisely the right pair-production and annihilation cross-sections so that if they are produced in thermal equilibrium in the early universe, their relic density at present day matches the dark matter density [52]. A hypothetical particle with these properties is called a WIMP (weakly-interacting massive particle). The condition that the WIMP mass lies above the GeV scale comes from the fact that dark matter particles should be slow-moving, or cold. In the opposite case, stable and neutral particles with relativistic velocities cannot aggregate enough to explain the formation of structures in the universe.

A problem similar to dark matter arise when one estimates the total energy of the universe. Evidence that the expansion of the universe is accelerating requires a new source of energy, which might arise from a cosmological constant term in the Einstein equation, or possibly from a new field. At present time, only 28% of the energy in the universe originates from dark and bright matter, while the remaining 72% is what is called *dark energy*.

The last of the cosmological problems mentioned here is the dominance of matter over antimatter in the universe, also known as the *baryon asymmetry*. The way out of this problem proceeds through the so-called baryogenesis, provided that the interactions producing baryons satisfy the three conditions set by Sakharov [53], namely that baryon number as well as CP-symmetry are violated, and that baryons are produced out of thermal equilibrium. The first two of these conditions are fulfilled in the Standard Model, although the only source of CP-violation comes from the complex phase in the CKM matrix, whose effects are too tiny to account for the observed asymmetry. Moreover, the third Sakharov condition can only be met if the electroweak phase transition is of first order, which is presently disfavoured by the best estimate of the Higgs boson mass. An elegant solution to the baryon asymmetry problem is available once neutrino masses are introduced in the model as explained above. In this case, the large CP-violating parameters in the Yukawa matrices can generate an asymmetry between leptons and anti-leptons, which in turn is transferred to baryons by non-perturbative processes breaking both lepton and baryon numbers but respecting the $U(1)_{B-L}$ symmetry. Such a scenario is called *leptogenesis* [54].

2.5.3 The strong CP problem

In the absence of matter fields, we have seen above that the θ-terms (2.17) are simply related to the non-trivial topological structure of the vacuum, and they have no physical effects. Moreover, when massless quarks and leptons are added to the theory, the θ-terms can even be removed by an appropriate redefinition of the fermion fields. However, once the quarks and leptons become massive, an important issue arises. The three anomalous linear combinations of the $[U(1)]^5$ global symmetry are being used for making the fermion masses real and positive. The resulting θ-terms in the Lagrangian are in principle non-vanishing, given as the sum of the bare term and the part arising from the rotation of the mass matrices. Symbolically, one can write

$$\overline{\theta}_i = \theta_i + \arg\left(\det M\right). \tag{2.92}$$

Non-zero θ-terms associated with the electroweak gauge group have no physical effects. However, the θ_3 term associated with QCD give a non-zero contribution to some physical observables, among which the most constraining is the electric dipole moment of the neutron [55], giving an experimental bound

$$\overline{\theta}_3 \lesssim 10^{-9}. \tag{2.93}$$

In the agnostic approach where the bare θ-terms and the entries of the Yukawa matrices take arbitrary values, a very precise cancellation must happen in eq. (2.92), which is highly unnatural if no symmetry reason can enforce it. This issue is called the *strong CP problem*. As for the hierarchy problem mentioned before, the naturalness principle is badly broken also here.

There exists a number of solutions to the strong CP problem [20]. For example, if any of the quarks is massless, the corresponding rephasing $q \to e^{i\alpha}q$ can be used to cancel the θ_3 term. Although experimental data disfavour this hypothesis, measuring the mass of light quarks is a very complicated task, and one might argue that a massless up quark is not completely excluded. An alternative solution consists in enforcing the CP symmetry as a fundamental symmetry of the Lagrangian, hence forbidding θ-terms at tree-level. In this case, the obvious CP-violation present in flavour physics should arise as an effect of spontaneous breaking of the CP symmetry, hence naturally preventing large corrections to the θ-terms.

An elegant solution to the strong CP problem is generated by introducing a *Peccei-Quinn axion* [56] in the theory: the idea is to promote θ to dynamical parameter, i.e. to add a scalar field $a(x)$ to the model, with a linear coupling to the CP-violating term,

$$\mathcal{L}_a = \frac{1}{2}\partial_\mu a \partial^\mu a + \frac{a}{f_a}\frac{g_S^2}{32\pi^2}G^a_{\mu\nu}\widetilde{G}^{\mu\nu\,a}, \tag{2.94}$$

where f_a is a massive parameter, known as the axion decay constant. The theory described here is then invariant under the Peccei-Quinn symmetry $a \to a + \alpha$. Whatever value of $\overline{\theta}$ is generated by anomalies, the vacuum expectation value $\langle a \rangle$ is going to adjust itself in order to minimise the energy, which is obtained when $\theta = 0$, hence solving naturally the issue of the neutron's electric dipole moment. The non-observation of this new field a is natural due to tiny couplings with matter. However, the axion can have important effects in cosmology, following large production rates in the early universe.

2.5.4 Grand unification

Finally, the Standard Model was defined above by giving the representation of the fermion under the gauge group in table 2.1. While the multiplets fit naturally into the lowest-dimensional representations of $SU(3)_C$ and $SU(2)_W$, there is a priori no reason to assign the hypercharge quantum numbers as they are. In particular, hypercharge must not in principle be quantised, and could take any non-fractional value. In this case the exact cancellation between the electric charge of a proton and of an electron would not happen, and no stable atoms could be form. The hypercharge assignment seems therefore to be accidental in the Standard Model, but is actually crucial for the cancellation of anomalies. In general, the requirement for a gauge theory to be free of anomalies can be expressed in terms of the generators of the gauge group. All triangle anomalies cancel if and only if

$$\mathrm{Tr}\left[T^a \left\{T^b, T^c\right\}\right] = 0, \tag{2.95}$$

is satisfied for all generators T^a. As a matter of fact, this property is automatically satisfied in all simple Lie groups, with the exception of $SU(N)$ with $N \geq 3$. It is hence natural to ask if the Standard Model gauge group could be embedded into a larger symmetry group. The simplest choice turns out to be $SU(5)$ [57]. There is a simple embedding of the $SU(3) \times SU(2) \times U(1)$ generators in a 5×5 unitary matrix as

$$T_C^a = \begin{pmatrix} \frac{\lambda^a}{2} & 0 \\ 0 & 0 \end{pmatrix}, \quad T_W^i = \begin{pmatrix} 0 & 0 \\ 0 & \frac{\sigma^i}{2} \end{pmatrix}, \quad Y = \begin{pmatrix} -\frac{1}{3}\mathbb{1}_3 & 0 \\ 0 & \frac{1}{2}\mathbb{1}_2 \end{pmatrix}. \tag{2.96}$$

Under the $SU(3) \times SU(2) \times U(1)$ subgroup of $SU(5)$ generated by T_C^a, T_W^i and Y, the lowest-dimensional representations of $SU(5)$ transform as

$$\mathbf{5} = (\mathbf{3}, \mathbf{1})_{-1/3} \oplus (\mathbf{1}, \mathbf{2})_{1/2}\,, \tag{2.97}$$

$$\mathbf{10} = (\mathbf{3}, \mathbf{2})_{1/6} \oplus \left(\overline{\mathbf{3}}, \mathbf{1}\right)_{-2/3} \oplus (\mathbf{1}, \mathbf{1})_{1}\,. \tag{2.98}$$

These are, respectively, the charge under the Standard Model gauge group of d_R, $\overline{l_L}$ (in the **5**), q_L, $\overline{u_R}$ and $\overline{e_R}$ (in the **10**). More precisely, all the Standard Model fermions are represented as right-handed helicity fermions in a $\mathbf{5}\oplus\overline{\mathbf{10}}$ representation of $SU(5)$. The cancellation of anomalies is however not trivial in $SU(5)$, following the argument presented above. Nevertheless, the anomaly associated with the **5** is the same as the anomaly of the **10**, so that the combination cancels. The breaking $SU(5) \to SU(3) \times SU(2) \times U(1)$ can be achieved spontaneously by introducing a scalar field in the 24-dimensional adjoint representation of $SU(5)$, which acquires a vacuum expectation value along the direction defined by Y at a high energy scale. Electroweak symmetry breaking and mass generation for fermions can occur due to the presence of a scalar field transforming like the Higgs doublet in the Standard Model as a $(\mathbf{1},\mathbf{2})_{1/2}$. Such a scalar exists for example in the **5** representation, as indicated in eq. (2.97).

The grand unification scenarios are moreover supported by the running of the gauge couplings. In the Standard model, the strong coupling g_S is much larger than the electroweak couplings g and g', but its strength decreases at large energies, while the electroweak coupling become always stronger. All three couplings become approximately equal at a scale[7]

$$M_{GUT} \approx 10^{16}\ \text{GeV}. \tag{2.99}$$

In minimal models, M_{GUT} corresponds to the scale at which the spontaneous symmetry breaking $SU(5) \to SU(3)\times SU(2)\times U(1)$ happens. The new gauge bosons associated with broken generators of $SU(5)$ obtain masses of order of M_{GUT}. Due to the fact that the second homotopy group of the coset space is non-trivial, (see chapter 4 for more details)

$$\pi_2\big(SU(5)/SU(3) \times SU(2) \times U(1)\big) = \mathbb{Z}, \tag{2.100}$$

magnetic monopoles are predicted as well in this theory [58, 59].

One of the drawbacks of grand unified theories is that once the quarks and leptons are embedded together in a representation of a larger symmetry group, the accidental baryon and lepton number symmetries do not survive. While in the Standard Model this breaking is due only to non-perturbative effects, largely suppressed as in (2.14) for weakly coupled theories, the explicit breaking of baryon number in grand unified theories lead to a relatively important decay rate for the proton. The experimental evidence of its stability puts therefore strong bounds on the unification scale, so that the simplest models based on the $SU(5)$ symmetry are ruled out. Other

[7] It is often argued that the unification of gauge couplings is better realised in the Minimal Supersymmetric Standard Model (MSSM). This assumptions relies however on the fact that no new particle states are present between the TeV scale and the Grand Unification scale M_{GUT}, and cannot be tested experimentally. In a sense, the approximate unification obtained in the Standard Model is nearly as good as in the MSSM.

models exist, involving semi-simple Lie groups [60], or even larger simple groups. An obvious example is $SO(10)$ [61], for which the 16-dimensional spinor representation splits under the $SU(5)$ subgroup of $SO(10)$ as

$$\mathbf{16} = \mathbf{5} \oplus \overline{\mathbf{10}} \oplus \mathbf{1}. \tag{2.101}$$

The advantage in this case is that all Standard Model fermions can be embedded into one single multiplet of $SO(10)$. The additional singlet has then exactly the quantum numbers of a right-handed sterile neutrino.

Note finally that the presence of new physics at the grand unification scale lowers the cutoff naively fixed at the Planck scale for the Standard Model. However, the hierarchy between M_{GUT} and the scale of electroweak symmetry breaking still remains huge, so that the hierarchy problem mentioned above remains as critical as in the Standard Model.

3
Composite Higgs Models

The Standard Model as presented in the previous chapter has been verified to a very high accuracy in numerous experiments. From the point of view of experimental physics, there are no conclusive results against the simple model that includes a Higgs doublet. From a theoretical point of view, however, many hints seem to indicate that the Standard Model is not complete and requires the introduction of new physics below the Planck scale. The challenge for theoretical physicists is therefore to write down a new theory solving the issues mentioned previously, while preserving the success of the Standard Model. The gauge and fermion sectors have been extensively tested and confirmed by experiments, and it is generally accepted that they should be kept as they are. The problematic part of the Standard model is the physics of electroweak symmetry breaking.

If one relaxes the requirement of having a fundamental Higgs scalar, the presence of the three massless scalar field required to provide a longitudinal polarisation for the $W^{\pm}$ and Z^0 gauge bosons should be explained otherwise. At the same time, the smallness of the electroweak scale v compared to the Planck scale must as well find an origin. It turns out that both can be explained in the presence of a new, strongly-interacting sector, of which the χ^a fields in eq. (2.33) are the Goldstone bosons, in a similar manner as the pions in low-energy QCD. This idea is called *technicolor*, and will be discussed in section 3.2.1. The relevant lessons which can be useful from low-energy QCD will first be presented in section 3.1.

As will be emphasised in section 3.2, the presence of a Higgs doublet in the theory not only unitarises the scattering of longitudinal gauge bosons, but is also favoured by indirect evidence from the LEP experiment. If the Higgs doublet is a fundamental scalar, a new kind of symmetry should pro-

tect its mass from large radiative corrections, in order to solve the hierarchy problem. Such a mechanism is provided by *supersymmetry*, in which fundamental scalars masses are protected from radiative corrections by a cancellation between bosonic and fermionic degrees of freedom running in the loops. Supersymmetry predicts a partner with opposite spin statistics for every fundamental particle in the theory, hence enlarging substantially the particle content of the Standard Model. The non-observation of such particles would require supersymmetry to be broken. It is nevertheless possible to break supersymmetry in a *soft* way, so that the cancellation of quadratic divergences in the Higgs sector is preserved, hence allowing the Higgs to remain light even in the presence of new physics at a higher energy scale. As already mentioned, many possible supersymmetric scenario have been extensively discussed in the literature and will not be treated further in this thesis.

Advantages of both technicolor and supersymmetry can be found in the so-called *composite Higgs* models, in which a Higgs doublet exists, as required by indirect evidence, and arises as a pseudo-Goldstone boson of some new strongly-interacting sector. In this case, the symmetry breaking scale can be naturally generated from a new, strongly-interacting gauge theory, if the latter displays asymptotic freedom and confinement as QCD does. These models are the main subject of this thesis and will be discussed in detail below.

Finally, a last class of models provide an elegant solution to the hierarchy problem and will be mentioned in section 3.2.4: In the presence of a *warped extra-dimension*, the Planck mass in the bulk of the five-dimensional space is equivalent, in terms of a four-dimensional effective theory, to a much lower scale, exponentially suppressed by the warping factor of the fifth dimension, hence reducing the huge hierarchy problem of the Standard Model to a much lower scale hierarchy. The latter can then be explained in a natural way by the spontaneous breaking of some global symmetry. The physics of five-dimensional models will only be addressed briefly in this thesis, since the recent development of AdS/CFT correspondences seem to indicate that the effective description of warped extra-dimensional models, in which the five-dimensional metric is of anti-de-Sitter type (AdS), is the same as the physics of composite Higgs models, which arise as the effective low-energy description of a strongly-coupled (nearly-)conformal field theory (CFT). We will therefore simply rely extra-dimensional models to the effective four-dimensional approach presented this thesis.

The material presented in this chapter is relatively recent, and there are to the best of our knowledge no textbooks treating it. The presentation of the different topics below is therefore based on a number lectures [62, 16] and reviews [63,64,65,66,67], while most of the material comes directly from original research papers. The sections 3.2.6, 3.3.3, 3.3.4, 3.3.6 and 3.3.7 are in particular directly extracted from the author's own papers [1, 2].

3.1 Lessons from low-energy QCD

Before moving to the description of composite Higgs models themselves, there is an important part of the Standard Model which remains to be discussed and whose importance will be crucial in the rest of the thesis. This regards the low-energy limit of QCD. The relevant aspects are presented here.

3.1.1 Asymptotic freedom and confinement

While in classical physics and in the tree-level approximation of a quantum theory the value of coupling constants is indeed constant, i.e. independent on the energy of the process under consideration, this is not the case at the loop-level in a quantum theory. The divergent nature of Feynman integrals and the renormalisation procedure required for the theory to make sense introduce a dependence on an arbitrary energy scale μ in the perturbative computation of physical observables. The statement of a theory being renormalisable is then equivalent to saying that the physical observables should not depend on this scale μ once all orders in perturbation theory are taken into account. Realistic computations rely however on the perturbative approach and the μ-dependence cannot be removed. This dependence can nevertheless also be used at our advantage, since it is possible to use it in order to infer the physics at different energy scales, using the so-called *renormalisation group* methods.

In the theory of electroweak interactions, the running of the couplings g and g' plays only a secondary role. This is not the case in QCD: The running of the strong coupling constant g_S depends at one-loop on the self-coupling of gluons, since $SU(3)_C$ is a non-abelian gauge group, and on the fermions content of the theory. This running is parametrised by the β-function, given at one-loop by

$$\beta(g_S) \equiv \mu \frac{\partial g_S}{\partial \mu} = -\frac{g_S^3}{16\pi^2}\left(11 - \frac{2}{3}N_f\right), \tag{3.1}$$

where N_f is the number of quark flavours running in a loop at a given energy scale, i.e. $N_f = 6$ above the top mass, $N_f = 5$ for $m_b \leq \mu \leq m_t$, and so on. The crucial feature of $\beta(g_S)$ is that it is negative as long as $N_f \leq 16$, hence g_S becomes arbitrarily small at very high energies. This property is called *asymptotic freedom* [68, 69]. This permits for example the computation of QCD observables in a perturbative framework at the LHC, due to the large enough energy at which the collisions occur. On the contrary, g_S increases at low-energy, first reaching the non-perturbative regime, and eventually diverging into a Landau pole. Integrating the β-function in eq. (3.1) yields

$$\alpha_S(\mu) \equiv \frac{g_S^2}{4\pi} = \frac{1}{b_0(N_f)\log\left(\mu^2/\Lambda(N_f)^2\right)} \tag{3.2}$$

where $b_0 = \frac{1}{4\pi}\left(11 - \frac{2}{3}N_f\right)$, and $\Lambda(N_f)$ is a new scale acting as the constant of integration. From the measured value of α_S at the Z^0 pole mass, the value α_S can be extrapolated down to arbitrarily low energies. Using results beyond the one-loop approximation made above, the scale at which the coupling g_S diverges is found to be

$$\Lambda_{QCD} \approx 220 \text{ MeV}. \tag{3.3}$$

It is however not clear if QCD really contains a Landau pole at Λ_{QCD}, at a different scale, or no pole at all, since the β-function can only be evaluated in the perturbative regime. The appearance of a physical pole at a given energy scale is nevertheless of highest physical interest: a theory like QCD is in principle scale-independent (at least in the limit of massless quarks), with a naturally small coupling strength at the Planck or GUT scale. It turns however at low-energy into a strongly-coupled theory, automatically implying new physical phenomena around the scale Λ_{QCD}. The huge hierarchy between the Planck or GUT scale and Λ_{QCD} is therefore naturally generated. Note that the running of the QCD coupling constant do not depend directly on the quark masses, so that the scale at which QCD becomes strongly coupled is a pure consequence of the size of the coupling at the Planck or GUT scale. The spontaneous generation of a physical mass scale in an *a priori* scale-invariant theory is sometime called *dimensional transmutation*.

At low energy, the strength of the QCD coupling has dramatic consequences. The energy required to separate two quarks from each another is increasing with the distance, up to a point where the creation of a new quark-antiquark pair from the vacuum is favoured by energy considerations. As a consequence no free quarks or gluons can be observed in nature, since they only appear confined into large colour-singlet objects, the hadrons. Although rather intuitive, the *confinement* of quarks in Yang-Mills theories is only a conjecture, and it remains an open problem in physics to prove it formally. At the TeV scale energies now under scrutiny of particle accelerators such at Tevatron and the LHC, the quarks and gluons appear to be weakly coupled, so that QCD computation can be performed in a perturbative expansion as in quantum electrodynamics. The asymptotic states observed in the detectors must on the contrary be colour neutral, and the transition between the two regimes happens in a process called *hadronisation*. This is the reason why collider experiments analyse the observed collision products in terms of leptons and jets, and not in terms of partons (quarks and gluons). The degrees of freedom of QCD at low energy are therefore colourless quark and gluon condensates. From symmetry reasons, as will be discussed below, the lightest states are the *mesons*, made of a pair of quark and antiquark. *Baryons* are the next category of hadrons, arising as antisymmetric bound states of quarks, and are naturally heavier than the mesons. Bound states

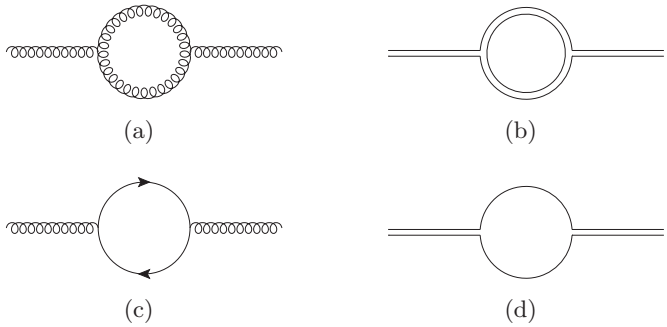

Figure 3.1: One-loop diagrams contributing to the gluon propagator, in the usual Feynman notation (left), and in the double-line notation of colour indices (right).

made purely out of gluons might also exist, as indicated by lattice QCD computations, but remain to be observed in nature.

Before addressing the methodology of low-energy QCD computations, note that the "hidden" way in which QCD arises suggests that new forces displaying a similar behaviour may be present in nature: above a certain energy scale, all QCD interactions are screened, and nearly all physical objects in our world are $SU(3)_c$ singlets. For this reason, our understanding of mesons and baryons as the bound state of quarks and gluons only followed many years after their observation by experiments [70, 71]. It is then straightforward to imagine that other such confined theory can exist. Technicolor and composite Higgs models are examples of models in which a new strongly-coupled force is responsible for the confinement of a new class of fermions, and the low-energy degrees of freedom in this case provide the Goldstone (and Higgs) bosons needed for the breaking of the electroweak symmetry.

3.1.2 The large N_c limit of QCD

In the absence of a small expansion parameter — g_S being larger than the loop factor 4π— it appears hopeless to describe the low-energy regime of QCD in the usual way, using a convergent series of Feynman diagrams. However, if one considers a generalisation of QCD with $N_c \gg 1$ colours, 't Hooft showed that $1/N_c$ can play the role of a valid expansion parameter [72]. Although QCD only has $N_c = 3$ and the expansion parameter is thus not much smaller than one, important qualitative results can be derived in this way.

The large-N_c expansion of QCD relies on the colour flow in physical processes involving quarks and gluons. Instead of using the usual Feynman diagrams, one can draw lines representing colour indices. Quarks transform

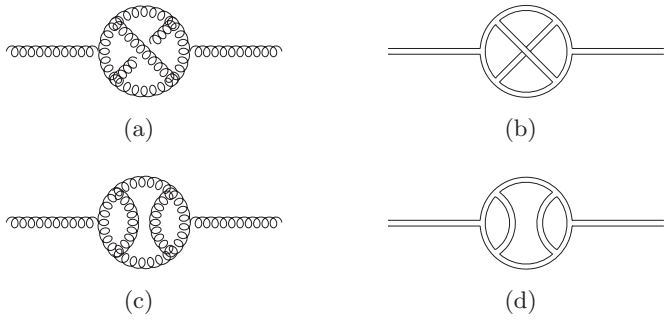

Figure 3.2: Multi-loop diagrams contributing to the gluon propagator, in the usual Feynman notation (left), and in the double-line notation of colour indices (right). Both diagrams contain 6 powers of the gauge coupling, g^6/N_c^3, but the top diagrams have only one internal colour line, hence suppressed by a factor $1/N_c^2$ while the bottom ones have three internal colour lines and are of order $N_c^0 = 1$.

in the fundamental representation of $SU(N_c)$, carry therefore one colour index, and are represented by a simple line. On the other hand, gluons carry two colour indices — the transform in the adjoint of $SU(N_c)$ — and are thus represented by two colour lines.[1] Since any propagating object must be a colour singlet, diagrams drawn in this way must contain only closed lines. There is an additional tricky point when one takes the limit of large N_c: The gluon self-energy has a contribution from gluon loops (see fig. 3.1 (a)–(b)) which includes summation over a colour index in the loop and is therefore proportional to N_c. Finiteness of the gluon self-energy in the limit $N_c \to \infty$ requires the strong coupling constant to scale as

$$g_S \propto \frac{1}{\sqrt{N_c}}. \tag{3.4}$$

Note that the one-loop diagram including a fermion loop (fig. 3.1 (c)–(d)) do not get enhanced by a factor of N_c, and hence vanishes in the limit $N_c \to \infty$ due to the vanishing of the QCD coupling in this limit. The double-line notations is particularly well-suited to compute the scaling with N_c of a given diagram: Each vertex contributes as $g\, N_c^{1/2}$ — $g^2\, N_c$ for the four-gluon vertex — and each internal line should be associated with a factor of N_c, since it corresponds to a trace over colour indices. The property illustrated on fig. 3.1 can then be turned into a general statement: In the limit of large N_c, diagrams with internal quark loops are suppressed compared with

[1] In the adjoint representation, there is in addition the requirement that the gluon field is represented by a traceless matrix. While the two-indices notation indicates that there should be N_c^2 different gluon species, there are actually only $N_c^2 - 1$. This different is however irrelevant in the limit $N_c \gg 1$.

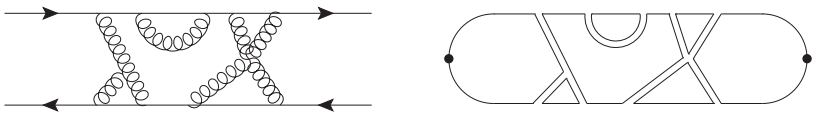

(a) (b)

Figure 3.3: Loop corrections to the meson propagator in the usual Feynman notation (left) and in the double-line notation (right). The diagram is proportional to g^{12}/N_c^6 and has 7 closed lines, i.e. a trace factor of N_c^7, so its overall scaling is N_c.

the same diagrams with gluons replacing the quarks. Moreover, among all diagrams with internal gluon loops, non-planar diagrams are suppressed as well with respect to planar ones. An example of this fact is given in fig. 3.2. As a consequence, only planar diagrams including internal gluons are relevant in large-N_c QCD.

Note that this property of large N_c QCD does not allow to compute an amplitude as a convergent series, since at each order in perturbation theory there are planar diagrams contributing to the zeroth order in N_c. The large N_c limit does not in this sense provide a small expansion parameter. Still, a lot of important information can be deduced from this limit. In order to do so, one should look at processes involving physical states, which are known from experiment to be mesons, i.e. bound states of a quark and an antiquark. The field theoretical description of mesons is made in terms of quark bilinears, which can be denoted by the quark current $J \propto \overline{q}q$. The propagation of a quark bilinear is illustrated on fig. 3.3. Following the rules which we derived above, the only relevant diagrams are planar, only contain gluons as internal fields, and in addition only have quarks on the exterior line. Since the mesons are colour singlets, the colour lines denoting the quark and the antiquark can be closed, see fig. 3.3 (b). The two-point function of a quark bilinear has therefore the scaling property

$$\langle 0|J(x_1)J(x_2)|0\rangle \propto N_c. \tag{3.5}$$

The spectrum of particles contributing to the meson propagator can be determined by cutting the diagram of fig. 3.3. By inspection, the intermediate state contains only two quark lines at the edges, and a number of gluons in between. Moreover, the colour indices are contracted in a way such that no colour-singlet combination of the gluons can be present. In terms of physical, colour-singlet states, the meson propagator contains therefore only one-meson states, i.e. there is no contribution from multi-quark states like $\overline{q}\overline{q}qq$, nor from glueballs states containing only gluons. A physical meson is thus a pure one-particle state in the large N_c limit. As such, the two-point

function (3.5) can be written in the spectral decomposition as

$$\langle 0|J(x_1)J(x_2)|0\rangle = \int \frac{d^4p}{(2\pi)^4} e^{i\,p\cdot(x_1-x_2)} \sum_i \frac{a_i(p)a_i^\dagger(p)}{p^2-m_i^2}, \tag{3.6}$$

where $a_i^\dagger(p)$ and $a_i(p)$ are respectively the creation and annihilation operators associated with a particle of mass m_i. The scaling with N_c deduced in eq. (3.5) can therefore only be obtained if the meson masses scale trivially with the number of colours, $m_i \propto N_c^0$, and if the field operators scale as $a_i(p), a_i^\dagger(p) \propto \sqrt{N_c}$. There are infinitely many meson states in this picture, but only the lightest ones are relevant in the low-energy limit. Mesons are known experimentally to be unstable. The scaling of the meson decay constant f_π with N_c can be determined from the scaling of the creation and annihilation operators. We have

$$f_\pi \propto \langle 0|J(x)|\pi\rangle \propto \big(\langle 0|J(x_1)J(x_2)|0\rangle\big)^{1/2} \propto N_c^{1/2}. \tag{3.7}$$

In the limit $N_c \to \infty$, f_π becomes therefore infinitely large. It is nevertheless immediate that the lightest mesons are stable in this very limit, since there is no allowed decay product. The decay width of the meson can therefore not be determined directly from the large N_c picture. We will see in the following that f_π is the only parameter which determines completely the low-energy QCD physics.

In addition to the property of a freely propagating meson, interactions between mesons can also be derived from the large N_c regime. The same arguments as above holds for the n-point function: the only relevant diagrams are the ones with a single quark line on the exterior and double gluon lines in the interior, as in fig. 3.4 (a). As for the two-point function, any cut in the diagram reveals that the intermediate states are made of mesons only, and that the interactions proceed either through contact terms or through the exchange of meson states at tree level, an example of which is given in fig. 3.4 (b). In particular, quark and gluons exchanges between mesons are subdominant in the N_c expansion. The scaling with N_c of the n-point function is the same as for the two-point function, and the strength of interaction between n mesons can be measured through the coupling $g_{n\pi}$ with the property

$$\langle 0|J(x_1)\cdots J(x_n)|0\rangle \propto g_{n\pi}\big(\langle 0|J(x)|\pi\rangle\big)^n \propto N_c, \tag{3.8}$$

from which we can deduce

$$g_{n\pi} \propto N_c^{1-n/2} \propto f_\pi^{2-n}. \tag{3.9}$$

g_{n_π} goes to zero as $N_c \to \infty$, so that in this limit QCD becomes a theory of stable, non-interacting mesons. For large but finite N_c, the leading meson-meson interactions are given by meson exchanges only, and the coupling given by eq. (3.9) is weak.

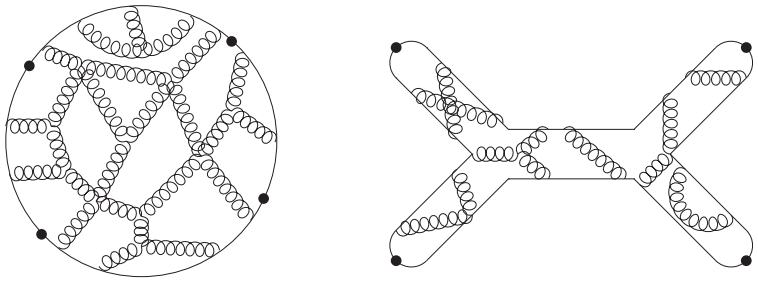

(a) (b)

Figure 3.4: Leading colour contribution to the interaction between a number of mesons (denoted by black points) in a general frame (left), and a possible interpretation as a meson exchange in the s-channel (right).

Extending the large N_c limit to the physics of baryons is less simple [73]: baryons in QCD are made of N_c quarks, and the diagrammatic picture is therefore failing since each internal line in any diagram is accompanied by a large combinatorics factor. However, due to the large number of quarks forming a baryon, the potential felt by each single quarks from the $N_c - 1$ other quarks is mostly independent of the wavefunctions of each other quarks. In other words, all quarks inside a baryon are subject to the same potential. Moreover, since the baryon wavefunction is totally antisymmetric in colour indices — from the requirement that a baryon is colourless — all quarks carry a different colour quantum number and their individual wavefunction are not constrained by the Pauli exclusion principle. The ground state for a baryon corresponds therefore to all quarks being in the same ground state, fixed only by the overall average potential. While the baryon mass is related to the sum of all separate quark energies, hence proportional to N_c, the baryon size is on the contrary fixed by the size of the ground state for one quark and is thus independent of N_c. A study of baryon scattering properties show that the amplitude for the process is as well proportional to N_c, hence to the overall kinetic energy of the baryon, and is therefore finite but non-vanishing in the limit $N_c \to \infty$. On the other hand, meson-baryon scattering amplitudes scale as N_c^0, and are therefore relevant for mesons but negligible compared to the kinetic energy of the baryon.

In summary, a consistent picture of low-energy QCD emerges when considering the number of colours N_c as large. The low-energy spectrum is described a theory of weakly-interacting mesons, where the coupling constant is proportional to $g \propto f_\pi^{-1} \propto N_c^{-1/2}$. Although $N_c = 3$ in nature is not really a large number, this approach is very successful in all its predictions. Baryons appear in this theory as heavy objects whose mass scales with the inverse of the weak coupling, $g^{-2} \propto N_c$. This behaviour is typical

of non-perturbative objects in a weakly-coupled theory, such as monopoles and other solitons. This interpretation is confirmed by the success of topological soliton models of baryons, which will be the subject of chapter 4. Note finally that all the large N_c considerations presented in this section are independent on the number of quark flavours, as well as on the quark masses.

3.1.3 Chiral symmetry breaking and the σ-model parametrisation

From large-N_c considerations, we have seen that the low-energy regime of QCD corresponds to a theory of weakly-interacting scalar fields only, i.e. written in terms of a number of meson fields $\pi^a(x)$. The way these scalar fields interact is however not obtained from the large-N_c approximation, and more information is required to write down an effective Lagrangian for the mesons. As we will now see, many constraints on the form of this Lagrangian can be determined from symmetry considerations. The lightest states observed experimentally are the pions, existing in three species, an electrically neutral π^0 and a pair π^+, π^- with unit electric charge. It turns out that their mass is much larger than the mass of the up and down quarks. The strange quark can to a to a certain extent also be considered very light with respect to the relevant QCD energy scale. It is therefore a good approximation to consider the three lightest quarks to be massless in QCD, not only in the high-energy limit used for computations at hadron colliders, but also in the low-energy limit. In the absence of quark masses, the Standard Model Lagrangian (2.19) is uniquely made of the kinetic terms for the fermions, and there is therefore an approximate global symmetry rotating the left-handed and right-handed chiralities of fermions by a unitary transformation among the different flavours. It is called the *chiral symmetry*, and in the presence of N_f massless flavours is of the form

$$U(N_f)_L \times U(N_f)_R = SU(N_f)_L \times SU(N_f)_R \times U(1)_L \times U(1)_R \qquad (3.10)$$

This symmetry is however only present at the Lagrangian level, and even in the absence of quark masses, the physical states do not possess this global symmetry. The reason for this apparent contradiction is the strength of the strong interaction, which create quark condensates in the vacuum. In other words, the vacuum is characterised by a non-zero expectation value for the quark bilinear operator $\overline{q}q$,

$$\langle 0|\overline{q}^{(i)}q^{(j)}|0\rangle \propto \delta^{ij}. \qquad (3.11)$$

Such condensates break the symmetry (3.10) to the diagonal subgroup $U(N_f)_V = SU(N_f)_V \times U(1)_V$, which is the group of unitary rotations acting simultaneously on the left- and right-handed quark flavours. As for the Higgs mechanism described in section 2.4, the symmetry at the Lagrangian

level is larger than the true symmetry of the vacuum. This is another realisation of the spontaneous symmetry breaking mechanism. As for the Higgs mechanism, there must be a certain number of Goldstone bosons associated with the broken directions of the symmetry group. In this case the broken group is the axial $U(N_f)_A = SU(N_f)_A \times U(1)_A$, and there should therefore be N_f^2 massless Goldstone bosons, which could be parametrised in terms of a field

$$\widetilde{U}(x) = \exp\left[2i\,\widetilde{\pi}^a(x)\,\widetilde{T}^a/f_\pi\right] = \exp\left[2i\,\sigma(x)/f_\pi\right]\exp\left[i\,\pi^a(x)\,T^a/f_\pi\right], \quad (3.12)$$

where the $\widetilde{T}^a$ are $U(N_f)$ generators, which are split in the second equality in terms of the $SU(N_f)$ generators T^a and the $U(1)_A$ term generated by the identity matrix. f_π is here a scale characterising the chiral symmetry breaking. We will see later that it can be identified with the pion decay constant, hence the overlap of notation with the previous section. The fields $\sigma(x)$ and $\pi^a(x)$ would be massless Goldstone bosons if the chiral symmetry (3.10) were to be exact. The lightness of the pions compared to the typical QCD scale arise indeed from the fact that they are the approximate Goldstone bosons associated with the breaking of $U(2)_A$ symmetry rotating up and down quarks [74]. The kaons K^+, K^-, K^0 and $\overline{K^0}$ are additional Goldstone bosons present in the limit of a massless strange quark, extending the symmetry to $U(3)_A$.

Following this rule, however, there should be four light pions instead of three. The solution to this puzzle, called the $U(1)_A$ problem of QCD, is provided by the discussion of anomalies in section 2.1. Due to the chiral nature of the Standard Model, the $U(1)_A$ symmetry is not a true symmetry of the quantum theory, since it is broken by loop-induced processes. The field $\sigma(x)$ associated with the breaking of $U(1)_A$ can therefore not be an exact Goldstone boson even in the limit of massless quarks, since a large mass term for it is automatically generated by anomalous processes involving electroweak instantons.[2] The correct parametrisation of the meson fields is therefore in terms of a $SU(N_f)$ matrix only, and eq. (3.12) should be replaced by

$$U(x) = \exp\left[2i\,\pi^a(x)\,T^a/f_\pi\right]. \quad (3.13)$$

In this parametrisation, under $SU(N_f)_L$ or $SU(N_f)_R$ transformations of the left- or right-handed quark flavours, the field $U(x)$ transforms as $U \to LUR^\dagger$. The vacuum state described by $\langle\pi^a(x)\rangle = 0$ or equivalently $\langle U(x)\rangle = \mathbb{1}$ is obviously only preserved by $SU(N_f)_V$ vector transformations for which $L = R$. Note that in this parametrisation the preserved $SU(N_f)_V$ symmetry is realised linearly, while the broken $SU(N_f)_A$ is not [76, 77].

[2] Note however that the notion of instanton is somehow ill-defined once the vacuum contains quark condensates, since the electroweak gauge symmetry is spontaneously broken. However, the $U(1)_A$ problem of QCD is still resolved in this case, as can be seen in the large N_c limit [75].

The quark condensate (3.11) does not only break the approximate chiral symmetry of QCD, but also the electroweak symmetry $SU(2)_W \times U(1)_Y$. In this sense, a tiny mass for the $W^\pm$ and Z^0 gauge bosons would be generated below the QCD scale even in the absence of the explicit electroweak symmetry breaking terms. A consequence is that the Goldstone bosons eaten by the electroweak gauge bosons are actually a linear combination of the quark bilinear $\overline{q}q$ and the Higgs field χ^a, while the other linear combination is the physical pion. The mixing is nevertheless very small due to the large hierarchy between the QCD scale and the scale of electroweak symmetry breaking, so that the physical consequences are negligible.

The Lagrangian describing meson interactions can then be written down in terms of the most general operators involving the field $U(x)$ of eq. (3.13) and derivative thereof. At low energy, the terms containing large number of derivatives will be subdominant. Note that all operators must nevertheless include derivatives, since the only invariants which can be built without them are trivial, i.e. proportional to $U^\dagger U = \mathbb{1}$. The leading order term is hence a kinetic term for the field U, which can be written in the form

$$\mathcal{L}_{\text{kin}} = \frac{f_\pi^2}{4} \operatorname{Tr}\left(\partial_\mu U^\dagger \partial^\mu U\right) \tag{3.14}$$

where the coefficient is uniquely fixed so that the fields $\pi^a(x)$ are canonically normalised, provided that the generators obey $\operatorname{Tr}\left(T^a T^b\right) = \frac{1}{2}\delta^{ab}$. Interactions between mesons are determined by expanding the exponential in the definition (3.13) of the field $U(x)$. In the two-flavour case, eq. (3.14) becomes for example

$$\mathcal{L}_{\text{kin}} = \frac{1}{2}\left(\partial_\mu \vec{\pi}\right)^2 + \frac{1}{6f_\pi^2}\left[\left(\vec{\pi}\cdot\partial_\mu\vec{\pi}\right)^2 - \vec{\pi}^2\left(\partial_\mu\vec{\pi}\right)^2\right] + \cdots, \tag{3.15}$$

where $\vec{\pi} = \left(\pi^1, \pi^2, \pi^3\right)$. It is obvious from here that the strength of interactions is regulated by the only parameter in the Lagrangian, f_π. As already mentioned above, the dimensionful constant f_π is related to the pion decay. The latter is an electroweak process, and its products are mostly leptons (for the charged pions) or photons (for the neutral pion). The relevant effective operator for the charged pion decay is

$$\mathcal{O}_{\pi^\pm \to l^\pm \nu} \propto \left(\overline{q}\,\gamma^\mu\gamma^5 q\right)\left(\overline{\ell}\,\gamma_\mu\gamma^5\ell\right), \tag{3.16}$$

and can be split into a hadronic axial current (first parenthesis) coupling to a leptonic axial current (second parenthesis). While the second term depends on the Standard Model described in the previous chapter, the first term can directly be extracted from the effective Lagrangian (3.14). The neutral pion decay is similar, in the sense that the hadronic axial current can also be factorised out of the process. The Noether current for an axial $SU(N_f)_A$

transformation is

$$\begin{aligned} J^a_{A\,\mu}(x) &= i\,\frac{f_\pi^2}{2}\left[\mathrm{Tr}\left(T^a U^\dagger \partial_\mu U\right) - \mathrm{Tr}\left(T^a U \partial_\mu U^\dagger\right)\right] \\ &= -f_\pi\,\partial_\mu \pi^a(x) + \mathcal{O}\left(\pi^2\right). \end{aligned} \tag{3.17}$$

The amplitude for an axial current to annihilate a meson state is then related to the constant f_π, as anticipated in eq. (3.7),

$$\langle 0|J^a_{A\,\mu}(x)|\pi^b(x)\rangle = i\,f_\pi\,\delta^{ab}\,p_\mu\,e^{-i\,x\cdot p} \tag{3.18}$$

f_π is therefore called the pion decay constant, and was determined from experiment to take the value

$$f_\pi \cong 93 \text{ MeV}. \tag{3.19}$$

Taking the derivative of the axial current (3.17) for on-shell pions shows an interesting relation between the conservation of the axial current and the pion mass:

$$\partial^\mu J^a_{A\,\mu}(x) = f_\pi\,m_\pi^2\,\pi^a(x) + \ldots \tag{3.20}$$

If the axial symmetry $SU(N_f)_A$ were to be exact, the pions would be exact Goldstone bosons, i.e. massless.

Acting as the inverse of the coupling constant between meson, f_π is also fixing the validity range of the theory. If one writes down an effective coupling g_π describing four-pions interactions — there are no three-pions terms — then the dependence of the coupling on the energy scale of the process is coming both from tree-level and loop contributions. Schematically, the two diagrams in fig. 3.5 contribute respectively as

$$g_\pi\left(p^2\right) \propto \frac{p^2}{f_\pi^2} + \frac{p^4}{16\pi^2 f_\pi^4}\log\left(\frac{p^2}{\mu^2}\right) + \ldots \tag{3.21}$$

where the dots denote corrections of higher order in $1/f_\pi$.[3] Naive dimensional analysis tells us that the theory stops being perturbative when all terms in the series contribute identically to the coupling. In addition to the suppression as $1/f_\pi^2$, the loop contribution carries a factor of $1/(4\pi)^2$, so that the naive cutoff of the theory is found to be

$$\Lambda_\pi = 4\pi f_\pi \cong 1.2 \text{ GeV}. \tag{3.22}$$

[3]The loop diagram in fig. 3.5 (b) contains actually quartically divergent terms, but these term do not depend on the energy of the external pions and can be renormalised away. The same apply to quadratic divergences. Only logarithmic divergent terms are relevant to the running of g as in eq. (3.21).

(a) (b)

Figure 3.5: Tree-level and one loop diagrams contributing to the four pions interaction.

Although subdominant in the low-energy regime, terms with more than two time derivatives are present as well in the theory. They become relevant for meson scattering processes below the cutoff Λ_π, and are mostly important in models where baryons emerges as topological solitons, as discussed in chapter 4. At the four-derivative order, there are exactly three such terms,

$$\begin{aligned}\mathcal{L}_4 = {} & c_1 \,\mathrm{Tr}\left(\partial_\mu U^\dagger \partial^\mu U \,\partial_\nu U^\dagger \partial^\nu U \right) + c_2 \,\mathrm{Tr}\left(\partial_\mu U^\dagger \partial_\nu U \,\partial^\mu U^\dagger \partial^\nu U \right) \\ & + c_3 \left[\mathrm{Tr}\left(\partial_\mu U^\dagger \partial^\mu U\right)\right]^2 \end{aligned} \tag{3.23}$$

Note however that in the two-flavour case, when $U \in SU(2)$, the operators with coefficients c_1 and c_3 are equivalent, so that only two operators are linearly independent. Dimension-four operators also contribute to the running of the pion coupling with energy, i.e. tree-level and loop terms should be added to eq. (3.21). The tree-level contribution starts however only at order $1/f_\pi^4$, since it is directly proportional to the coefficient c_i which do not contain any powers of the pion decay constant. They contribute nevertheless to constrain the validity range of the model.

3.1.4 Electromagnetic interactions

We have learnt from the large N_c limit that gluon exchanges are irrelevant to the phenomenology of mesons at low energy. Similarly, the large mass of the $W^\pm$ and Z^0 gauge bosons compared to the QCD scale turn the weak interaction into a negligible force in this regime. More precisely, the heavy gauge boson can be integrated out of the low-energy effective action and yield therefore current interactions such as the ones inducing pion decays. The only long-distance force between mesons apart from self-interactions is the electromagnetic force carried by the photon. It can be added into the non-linear σ-model by turning space-time derivatives into covariant ones, given by

$$D_\mu U = \partial_\mu U - i\, e\, \mathcal{A}_\mu \,[Q, U]\,, \tag{3.24}$$

where $e = g \sin\theta_W$ is the electromagnetic coupling and Q is a diagonal generator, whose entries are given by the charge of the quarks under consideration. In the three-flavour case, with the up, down and strange quarks taken as massless, the electric charge generator takes the form

$$Q = \mathrm{diag}\left(\frac{2}{3}, -\frac{1}{3}, -\frac{1}{3}\right). \tag{3.25}$$

The usual kinetic term for the photon, involving the field strength tensor $F_{\mu\nu}$, must be added to the Lagrangian as well. The resulting theory is invariant under the gauge transformation written in its infinitesimal form as

$$\delta U = i\,\alpha\,[Q, U], \qquad \delta \mathcal{A}_\mu = \frac{1}{e}\,\partial_\mu \alpha. \tag{3.26}$$

The electric charge of the various meson fields can then be determined by their transformation property under this very transformation. In the three-flavour case, one has

$$\pi^a\,T^a = \frac{1}{2}\begin{pmatrix} \pi^0 + \frac{1}{\sqrt{3}}\,\eta^0 & \sqrt{2}\,\pi^+ & \sqrt{2}\,K^+ \\ \sqrt{2}\,\pi^- & -\pi^0 + \frac{1}{\sqrt{3}}\,\eta^0 & \sqrt{2}\,K^0 \\ \sqrt{2}\,K^- & \sqrt{2}\,\overline{K}^0 & -\frac{2}{\sqrt{3}}\,\eta^0 \end{pmatrix}. \tag{3.27}$$

The Lagrangian describes in this case the interactions between pions, kaons, the η meson[4] and photons. Adding the electromagnetic force to the model explicitly breaks the global chiral symmetry (3.10), as in any case when only a subgroup of the global symmetry is gauged. A consequence is that the shift symmetry acting on the charged mesons is broken. The latter are not exact Goldstone bosons anymore and acquire therefore a radiatively generated potential, hence a mass, whose value is computed in the next section.

3.1.5 Heavy meson resonances

The form of the potential for the charged pions is however not completely fixed by the low-energy effective Lagrangian described above, but is also sensitive to the additional meson resonances expected from the large N_c considerations. These resonances are not Goldstone bosons in the chiral limit, and thus have much larger masses than the pions and kaons. Note that the presence of heavy vector and axial vector mesons is necessary in the theory for the same reason as the Higgs boson is necessary in the Standard Model: They contribute to unitarise the scattering processes of pions, like an elementary Higgs boson unitarises the scattering of longitudinally polarised

[4]The η described in this case is the pseudo-scalar state of mass 548 Mev, and is to be distinguished from the Goldstone boson associated with the $U(1)_A$ symmetry, the latter corresponding to the η' resonance of mass 958 MeV.

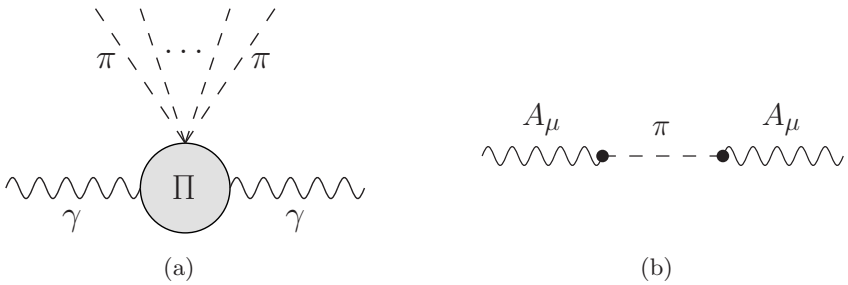

Figure 3.6: (a) Schematic description of the form factors of eq. (3.28). (b) Contribution to the axial form factor Π_{AA} from the exchange of a pion. This process contributes to the mass of the $W^\pm$ gauge bosons.

gauge boson, as discussed in section 2.3. QCD is ultimately a renormalisable theory, hence must preserve unitarity of the S-matrix at all loop levels. As indicated by the large-N_c limit, there is actually an infinite tower of scalar, pseudoscalar, vector and axial-vector mesons which contribute to the unitarisation. The finite mass of heavy mesons of non-Goldstone nature allows to write down an effective approach at low-energy, in which meson resonances are integrated out.

The interaction of pions with the electromagnetic field can be determined in this effective way, by writing down all possible operators involving the photon fields $\mathcal{A}_\mu$ and the Goldstone boson matrix $U(x)$, together with form factors encoding the dependence on the heavy fields. Note that both the photon propagator and the pion-photon interaction feel the effect of the heavy mesons. The effective Lagrangian can then be written as

$$\mathcal{L}_{\text{eff}} = \frac{e^2}{2}\mathcal{P}_\perp^{\mu\nu}\mathcal{A}_\mu\mathcal{A}_\nu\left[\Pi_1(p^2)\,\text{Tr}\left(Q^2\right) - \Pi_2(p^2)\,\text{Tr}\left(QUQU^\dagger\right)\right], \qquad (3.28)$$

where $\mathcal{P}_\perp^{\mu\nu} = \eta^{\mu\nu} - p^\mu p^\nu/p^2$ is the transverse projector, and the $\Pi_i(p^2)$ are form factors depending only on the energy of the electromagnetic field p^2. Additional terms including derivatives of the field $U(x)$ are absent here since they do not contribute to the potential for the mesons. The diagrammatic meaning of the form factors is depicted on fig. 3.6 (a).

The effective Lagrangian (3.28) is however not very useful in the absence of information about the form factors $\Pi_1(p^2)$ and $\Pi_2(p^2)$. Instead, the whole $SU(N_f)_L \times SU(N_f)_R$ chiral symmetry can be treated as a gauge symmetry and gauge fields L_μ and R_μ associated respectively with $SU(N_f)_L$ and $SU(N_f)_R$ transformations can be considered. The most general effective Lagrangian is then

$$\begin{aligned}\mathcal{L}_{\text{eff}} = \frac{1}{2}\mathcal{P}_\perp^{\mu\nu}\big[&\Pi_{LL}(p^2)\,\text{Tr}\left(L_\mu L_\nu\right) + \Pi_{RR}(p^2)\,\text{Tr}\left(R_\mu R_\nu\right) \\ &-\Pi_{LR}(p^2)\,\text{Tr}\left(L_\mu U R_\nu U^\dagger\right)\big]. \end{aligned} \qquad (3.29)$$

L_μ and R_μ are not real gauge fields, but rather Noether currents associated with the global symmetry. As such, they are not propagating, and the form factors Π_{LL} and Π_{RR} are not expected to be dominated by a term involving p^2. In the absence of pion fields, i.e. in the limit $U(x) \to \mathbb{1}$, the effective Lagrangian (3.29) must describe the interaction-free massive mesons, from which important properties were derived in the large-N_c limit. In order to make these properties apparent, one writes the (pseudo-)gauge fields in terms of vector and axial currents as $L_\mu = (V_\mu + A_\mu)/\sqrt{2}$ and $R_\mu = (V_\mu - A_\mu)/\sqrt{2}$, for which the effective Lagrangian becomes, in the vacuum $U(x) = \mathbb{1}$,

$$\begin{aligned}\mathcal{L}_{\text{eff}} = \frac{1}{2}\mathcal{P}_\perp^{\mu\nu} \big[&\Pi_{VV}(p^2)\,\mathrm{Tr}\,(V_\mu V_\nu) + \Pi_{AA}(p^2)\,\mathrm{Tr}\,(A_\mu A_\nu) \\ &+2\,\Pi_{VA}(p^2)\,\mathrm{Tr}\,(V_\mu A_\nu)\big]\,. \end{aligned} \tag{3.30}$$

The new form factors are defined as linear combinations of the previous ones,

$$\begin{aligned}\Pi_{VV}(p^2) &= \frac{1}{2}\left(\Pi_{LL}(p^2) + \Pi_{RR}(p^2) - \Pi_{LR}(p^2)\right), \\ \Pi_{AA}(p^2) &= \frac{1}{2}\left(\Pi_{LL}(p^2) + \Pi_{RR}(p^2) + \Pi_{LR}(p^2)\right), \\ \Pi_{VA}(p^2) &= \frac{1}{2}\left(\Pi_{LL}(p^2) - \Pi_{RR}(p^2)\right). \end{aligned} \tag{3.31}$$

The vector Π_{VV} and axial Π_{AA} form factors are then related to the propagators of the vector and axial currents respectively. These propagators are affected by the infinite tower of meson resonances, and using the spectral decomposition derived in eq. (3.6), one has then

$$\mathcal{P}_\perp^{\mu\nu}\Pi_{VV}(p^2) = \langle 0|V^\mu V^\nu|0\rangle = p^2\,\mathcal{P}_\perp^{\mu\nu}\sum_n \frac{f_{\rho_n}^2}{p^2 - m_{\rho_n}^2}, \tag{3.32}$$

$$\mathcal{P}_\perp^{\mu\nu}\Pi_{AA}(p^2) = \langle 0|A^\mu A^\nu|0\rangle = p^2\,\mathcal{P}_\perp^{\mu\nu}\left[\frac{f_\pi^2}{p^2} + \sum_n \frac{f_{a_n}^2}{p^2 - m_{a_n}^2}\right], \tag{3.33}$$

where m_{ρ_n} and m_{a_n} are the masses of vector and axial meson resonances, and f_{ρ_n} and f_{a_n} are coefficients parametrising their interactions with the currents L_μ and R_μ. It was made explicit in these equations that the tower of axial resonances have a zero-mode — the pions are massless in the chiral limit — while the vector resonances do not. If one consider the zero-momentum limit $p \to 0$, only the pion can contribute to the form factor, and one obtains $\Pi_{VV}(0) = 0$ and $\Pi_{AA}(0) = f_\pi^2$. The contribution to the axial form factor from the exchange of a massless pion is illustrated in fig. 3.6 (b).

From the information gathered in the large-N_c limit, one can now turn back to the effective pion-photon Lagrangian (3.28). The form factors Π_1

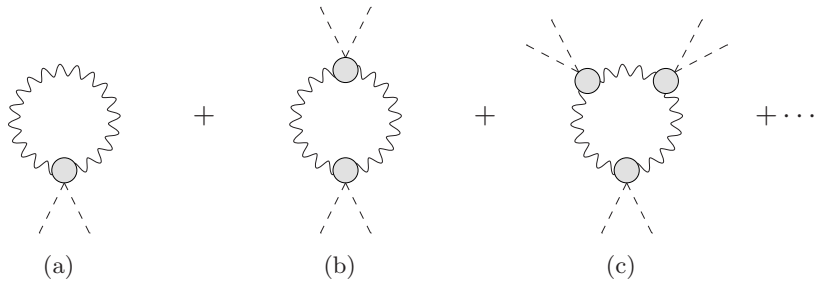

Figure 3.7: One-loop diagrams contributing to the Coleman-Weinberg potential for the pions.

and Π_2 can be expressed in terms of Π_{VV} and Π_{AA}. The electromagnetic current is a combination of left and right chiral currents, $L_\mu = R_\mu = e\,\mathcal{A}_\mu Q$, hence

$$\Pi_1 = \Pi_{LL} + \Pi_{RR} = \Pi_{VV} + \Pi_{AA}, \qquad \Pi_2 = \Pi_{LR} = \Pi_{AA} - \Pi_{VV}. \tag{3.34}$$

Writing down the expression $\mathrm{Tr}\left(QUQU^\dagger\right)$ of eq. (3.28) explicitly in terms of the pion fields, one obtains then

$$\begin{aligned}\mathcal{L}_{\text{eff}} &= \frac{e^2}{2}\mathcal{P}_\perp^{\mu\nu}\mathcal{A}_\mu\mathcal{A}_\nu\left[2\Pi_{VV}(p^2)\,\mathrm{Tr}\left(Q^2\right) + 2\,\Pi_{LR}(p^2)\,\pi^+\pi^-\frac{\sin^2(\pi/f_\pi)}{\pi^2}\right] \\ &= \mathcal{P}_\perp^{\mu\nu}\mathcal{A}_\mu\mathcal{A}_\nu\left[\frac{1}{2}\Pi_0(p^2) + e^2\Pi_{LR}(p^2)\,\pi^+\pi^-\frac{\sin^2(\pi/f_\pi)}{\pi^2}\right],\end{aligned} \tag{3.35}$$

where $\pi = \left((\pi^0)^2 + 2\,\pi^+\pi^-\right)^{1/2}$. In the second equality, we defined $\Pi_0(p^2) = 2e^2\,\mathrm{Tr}\left(Q^2\right)\Pi_{VV}(p^2)$. In this form, the Lagrangian contains obviously a kinetic term for the photon and an interaction term with pions. Note that there is no coupling to neutral pions only, thus no mass term for them will be generated by electromagnetic interactions, as anticipated in the previous section. On the contrary, a potential for the charged pions is generated. The Feynman diagrams relevant at one loop are shown on fig. 3.7. Each diagram is composed of a certain number of photon propagators and effective photon-pion vertices. The actual photon propagator is gauge-dependent and can be written in the form

$$\frac{i\,\mathcal{P}_\perp^{\mu\nu}}{\Pi_0(p^2)} + [\text{gauge-fixing terms}]\,\frac{p^\mu p^\nu}{p^2}. \tag{3.36}$$

The photon-pion vertex can be read directly from the effective Lagrangian to be

$$2\,i\,e^2\mathcal{P}_\perp^{\mu\nu}\Pi_{LR}(p^2)\,\pi^+\pi^-\frac{\sin^2(\pi/f_\pi)}{\pi^2}. \tag{3.37}$$

Due to the presence of a transverse projector $\mathcal{P}_\perp^{\mu\nu}$ at each vertex, the gauge-dependent part of the photon propagator is irrelevant. The one-loop potential is then given by the infinite sum of diagrams in fig. 3.7, yielding

$$\begin{aligned} V(\pi) &= 3\int \frac{\mathrm{d}^4p}{(2\pi)^4}\sum_{n=1}^{\infty}\frac{1}{2n}\left[-2e^2\frac{\Pi_{LR}(p^2)}{\Pi_0(p^2)}\,\pi^+\pi^-\frac{\sin^2(\pi/f_\pi)}{\pi^2}\right]^n \\ &= \frac{3}{2}\int \frac{\mathrm{d}^4p}{(2\pi)^4}\log\left(1+2e^2\frac{\Pi_{LR}(p^2)}{\Pi_0(p^2)}\,\pi^+\pi^-\frac{\sin^2(\pi/f_\pi)}{\pi^2}\right). \end{aligned} \tag{3.38}$$

The overall factor of three appearing in front of the potential comes from the contraction of the projectors $\mathcal{P}_\perp^{\mu\nu}$, and corresponds to the number of transverse polarisations of the photon field. While each individual diagram seems to be quadratically divergent, the series can be summed into a logarithm taking the form of the Coleman-Weinberg potential [26], and will eventually turn out to be finite. The momentum integral can be computed explicitly by rotating in Euclidean space. Defining $q^2 = -p^2$, the potential becomes[5]

$$V(\pi) = \frac{3}{32\pi^2}\int_0^\infty \mathrm{d}q^2\, q^2\,\log\left(1+2e^2\frac{\Pi_{LR}(q^2)}{\Pi_0(q^2)}\,\pi^+\pi^-\frac{\sin^2(\pi/f_\pi)}{\pi^2}\right) \tag{3.40}$$

This integral is finite provided that $\Pi_{LR}(q^2)$ goes to zero rapidly enough at large values of q^2. Indeed, $\Pi_{LR} = \Pi_{AA} - \Pi_{VV}$ is an order parameter sensitive to the breaking of the chiral symmetry, and is therefore expected to vanish above the chiral symmetry breaking scale. The exact momentum dependence of $\Pi_{LR}(q^2)$ can be determined performing an operator product expansion. From all possible operators contributing to the product of two vector and two axial currents, the leading one is a four-fermion operator of dimension six, whose contribution is suppressed by four powers of the momentum, yielding therefore

$$\Pi_{LR}(q^2) = \frac{\delta}{q^4} + \mathcal{O}\left(\frac{1}{q^6}\right). \tag{3.41}$$

δ is here a numerical coefficient which can be computed exactly in the large N_c limit [78]. From this asymptotic behaviour and using the spectral decompositions (3.32) and (3.33), the large q^2 limit of Π_{LR} provides a relation among the coefficients,

$$\lim_{q^2\to\infty}\Pi_{LR}(q^2) = f_\pi^2 + \sum_n f_{a_n}^2 - \sum_n f_{\rho_n}^2 = 0. \tag{3.42}$$

[5]The integral in Euclidean space can be split into a radial part and an angular part, giving

$$\int \mathrm{d}^4q = \int_0^\infty \mathrm{d}q\, q^3 \int \mathrm{d}\Omega = 2\pi^2\int_0^\infty \mathrm{d}q\, q^3 = \pi^2\int_0^\infty \mathrm{d}q^2\, q^2 \tag{3.39}$$

where $2\pi^2$ is the surface of the 3-sphere.

Moreover, the high-energy limit of the order parameter vanishes as well at the next order in q^2, implying

$$\lim_{q^2\to\infty} q^2\Pi_{LR}(q^2) = \sum_n m_{a_n}^2 f_{a_n}^2 - \sum_n m_{\rho_n}^2 f_{\rho_n}^2 = 0. \tag{3.43}$$

The relations (3.42) and (3.43) are called *Weinberg sum rules* [79]. In practice, the spectral functions are found to be dominated by the first resonance only. This property, known as *vector meson dominance* permits to write down relations between the masses of the lightest vector resonances. The sum rules reduce in this case to the approximate equalities

$$f_\rho^2 \cong f_\pi^2 + f_{a_1}^2, \qquad m_\rho^2 f_\rho^2 \cong m_{a_1}^2 f_{a_1}^2, \tag{3.44}$$

from which the mass of the axial vector resonance a_1 can be determined from the properties of the ρ vector meson. From the measured width of the latter, one finds $f_\rho^2 \cong 2f_\pi^2$, so that the ratio of axial to vector meson masses can be predicted to be

$$\frac{m_{a_1}}{m_\rho} \cong \sqrt{2}, \tag{3.45}$$

which is in reasonable agreement with experimental data, as indicated in table 3.1.

Contrarily to $\Pi_{LR}(q^2)$, the form factor $\Pi_0(q^2)$ is not vanishing at large q^2. Since it represents the inverse of the photon propagator, it must be given at leading order as $\Pi_0(q^2) = q^2 + \mathcal{O}(q^0)$. The ratio of form factors Π_{LR}/Π_0 appearing in the charged pion potential (3.40) is therefore a small number over most of the integration range, and the logarithm can then be expanded, giving

$$V(\pi) = \frac{3\,e^2}{16\pi^2}\,\pi^+\pi^-\frac{\sin^2(\pi/f_\pi)}{\pi^2}\int_0^\infty \mathrm{d}q^2\,\Pi_{LR}(q^2). \tag{3.46}$$

The exact value of Π_{LR} can then be computed from the spectral decomposition in eq. (3.32) and (3.33). Within the assumption of vector meson dominance, only the first resonance in each tower needs to be taken into account, i.e.

$$\Pi_{AA}(q^2) \cong f_\pi^2 + \frac{q^2}{q^2+m_{a_1}^2}\,f_{a_1}^2, \qquad \Pi_{VV}(q^2) \cong \frac{q^2}{q^2+m_\rho^2}\,f_\rho^2, \tag{3.47}$$

and using the values of f_ρ and f_{a_1} extracted from the truncated sum rule (3.44), one can deduce

$$\begin{aligned}\Pi_{LR}(q^2) &= f_\pi^2\left[1 + \frac{q^2}{q^2+m_{a_1}^2}\frac{m_\rho^2}{m_{a_1}^2-m_\rho^2} - \frac{q^2}{q^2+m_\rho^2}\frac{m_{a_1}^2}{m_{a_1}^2-m_\rho^2}\right]\\ &= f_\pi^2\,\frac{m_\rho^2 m_{a_1}^2}{(q^2+m_\rho^2)(q^2+m_{a_1}^2)}.\end{aligned} \tag{3.48}$$

	2-flavour scheme		3-flavour scheme	
	meson	mass in Mev	meson	mass in Mev
pseudoscalar	π^0	135.0	K^0	497.6
	$\pi^\pm$	139.6	$K^\pm$	493.7
	η'	957.8	η	547.9
vector	ρ	775.5	ω	782.6
axial vector	a_1	1230	f_1	1282

Table 3.1: Mass of the lightest unflavoured and strange mesons relevant to our discussion. All masses are taken from the Particle Data Group database [44].

The final form of the potential is obtained by performing the integral over q^2 in eq. (3.46), yielding

$$V(\pi) = \frac{3\,\alpha}{4\pi}\pi^+\pi^- \frac{\sin^2(\pi/f_\pi)}{(\pi/f_\pi)^2}\frac{m_\rho^2 m_{a_1}^2}{m_{a_1}^2 - m_\rho^2}\log\left(\frac{m_{a_1}^2}{m_\rho^2}\right), \tag{3.49}$$

where $\alpha = e^2/(4\pi)$ is the electroweak coupling constant. The potential is always positive, and most importantly is minimised around $\pi = 0$. If this were not the case, the true vacuum of the theory would correspond to $\langle\pi\rangle \neq 0$, which would indicate that the chiral symmetry is not broken to the diagonal subgroup, but to a different subgroup. In such a scenario, called *vacuum misalignment*, the photon would become massive. This is not the case in QCD, and can actually be extended to a more general statement: In any confining theory described by the effective Lagrangian (3.29), i.e. with a chiral symmetry broken down to the diagonal subgroup, the form factor $\Pi_{LR}(q^2)$ is positive for any q^2, hence the minimum of Coleman-Weinberg potential for the Goldstone fields preserves the alignment of the vacuum [80]. In other words, vector-like gauge bosons remain exactly massless at all orders in perturbation theory.

Note finally that the mass difference between the neutral and the charged pion can be read directly from the potential (3.49). The $\pi^+\pi^-$ term is directly proportional to the difference of masses squared $m_{\pi^\pm}^2 - m_{\pi^0}^2$, so that we have[6]

$$\Delta m_\pi \cong \frac{m_{\pi^\pm}^2 - m_{\pi^0}^2}{2m_{\pi^0}} = \frac{3\alpha}{8\pi m_{\pi^0}}\frac{m_\rho^2 m_{a_1}^2}{m_{a_1}^2 - m_\rho^2}\log\left(\frac{m_{a_1}^2}{m_\rho^2}\right) \cong 5.9\text{ MeV}, \tag{3.50}$$

[6]This results was first derived in ref. [81] before many of the large-N_c considerations discussed here were made.

where the masses given in table 3.1 were used. The agreement with the observed mass difference of 4.6 MeV is relatively good, considered that the derivation of this estimate relies on symmetry considerations and the large-N_c limit of QCD only.

3.1.6 Pion mass

In the effective theory for the mesons discussed so far, neutral pions are still exact Goldstone bosons and remain therefore massless. The pions are however massive in the real world, which is a consequence of the up and down quark being massive themselves. Since the latter do not exist as asymptotically free states, their mass is very difficult to determine experimentally. The best estimates at present time indicate $m_u \cong 2.5$ MeV and $m_d \cong 5.0$ MeV. These masses contribute directly to the pion mass as the mass of the up and/or down valence quark, but most importantly indirectly due to the explicit breaking of the chiral symmetry. In order to describe the low-energy theory of massive pions in an effective way, a term must be added to the Lagrangian which explicitly break the chiral symmetry. The simplest possibility in terms of the pion matrix $U(x)$ is the term $\mathrm{Tr}\,(U)$, which transforms under a $SU(N_f)_L \times SU(N_f)_R$ transformation into $\mathrm{Tr}\left(LUR^\dagger\right)$ and is therefore only invariant under the vector subgroup for which $L = R$, but not under axial transformations. In order to preserve the discrete symmetry $U \leftrightarrow U^\dagger$, whose crucial importance will be discussed in the next section, the mass term in the Lagrangian is introduced as

$$\mathcal{L}_{\mathrm{mass}} = \frac{1}{4} m_\pi^2 f_\pi^2 \left[\mathrm{Tr}(U) + \mathrm{Tr}(U^\dagger) - 4\right] \tag{3.51}$$

where the constant term proportional to $\mathrm{Tr}(\mathbb{1})$ is purely conventional, chosen so that $\mathcal{L}_{\mathrm{mass}}$ vanishes in the vacuum $\langle U \rangle = \mathbb{1}$. Note that since this Lagrangian preserves the diagonal $SU(N_f)_V$ symmetry, it describes actually a situation in which the mass term in the original QCD Lagrangian is diagonal, i.e. where the up and down quarks have equal masses. Although this is not the case in nature, the effects of the mass splitting between the lightest quark is negligible compared to the absolute effect of breaking the chiral symmetry, and the Lagrangian (3.51) is actually sufficient for all purposes discussed in this thesis. This is not the case anymore if one considers the three-flavour case, since the large mass $m_s \cong 100.0$ MeV of the strange quark contributes in a non-negligible way to the kaon masses, and the effective Lagrangian must necessarily contain terms explicitly breaking the $SU(3)_V$ symmetry. These issues are however beyond the scope of the present discussion.

Note finally that the quark masses provided above are only rough estimates. While the ratio of up to down and strange to down are extracted from the precisely measured pion and kaon masses, the uncertainty on the absolute mass scale is very large. The masses used here should be understood as

parameters in the QCD Lagrangian in a given renormalisation scheme, and can hardly be related with the mass of a propagating light quark, since the latter do not exist as such. The possibility for the up quark to be exactly massless is for example not totally excluded.

3.1.7 Wess-Zumino-Witten term

Before turning back to the physics of the electroweak symmetry breaking, a last piece of information must be added to the Lagrangian derived so far in order to get a complete low-energy effective theory of QCD. The Lagrangian is written at this stage in terms of the Goldstone field $U(x)$ and of (covariant) derivatives thereof, and contains a kinetic term (3.14) with two derivatives, higher order terms (3.23) with four derivatives or more, and the pion mass term (3.51). As already mentioned, the theory described in this way has a global $U(N_f)_V$ symmetry, not only at the Lagrangian level but also preserved by the vacuum expectation value $\langle U \rangle = \mathbb{1}$. In addition, two discrete symmetries exist in the theory. The first one, briefly mentioned in the previous section, is the exchange $U(x) \leftrightarrow U^\dagger(x)$, which corresponds to reversing the sign of the pion fields, $\pi^a(x) \leftrightarrow -\pi^a(x)$. The second discrete symmetry is the parity transformation under which spatial coordinates are reversed, $\vec{x} \leftrightarrow -\vec{x}$, while time is preserved $t \leftrightarrow t$. The presence of the latter symmetry seems to indicate that the light mesons are invariant under parity transformations. This is however not the case in nature, where pions and kaons are found to be pseudoscalar particles, i.e. they are only invariant under the transformation

$$\pi^a(\vec{x}, t) \quad \leftrightarrow \quad -\pi^a(-\vec{x}, t). \tag{3.52}$$

In order to match the observations, the low-energy effective Lagrangian of QCD should therefore be invariant under the combined transformation $U(x) \leftrightarrow U^\dagger(x)$ and $\vec{x} \leftrightarrow -\vec{x}$, but not under each of them separately. The invariance under parity in space is actually directly related to the fact that the Lorentz indices in the Lagrangian given so far are always contracted two-by-two using the metric tensor $g^{\mu\nu}$, which is symmetric in its indices. The extraneous parity symmetry could hence be removed by using the totally antisymmetric Levi-Civita tensor ε. The simplest term constructed out of it is however vanishing in four dimensions,

$$\varepsilon^{\mu\nu\rho\sigma} \operatorname{Tr}\left(\partial_\mu U \, \partial_\nu U^\dagger \partial_\rho U \, \partial_\sigma U^\dagger\right) = 0, \tag{3.53}$$

and any higher-order term including an ε tensor is also identically zero or equivalent to a total divergence term. Any local Lagrangian build out of the Goldstone field $U(x)$ is actually automatically invariant under the parity transformation.

Fortunately, this statement can be relaxed by considering a non-local term in the Lagrangian, which is carefully chosen so as not to affect the physics of meson otherwise. This uniquely defined term is called the *Wess-Zumino-Witten term* [82, 83] and can be introduced in the action as an integral over a five-dimensional space,

$$\Gamma_{\mathrm{WZW}} = i\lambda_{\mathrm{WZW}} \int_{\mathcal{M}_5} \mathrm{d}^5 x\, \varepsilon^{\mu\nu\rho\sigma\tau}\, \mathrm{Tr}\left(U^\dagger \partial_\mu U\, \partial_\nu U^\dagger \partial_\rho U\, \partial_\sigma U^\dagger \partial_\tau U\right). \quad (3.54)$$

The presence of an additional space coordinate is a notation artifact and has no physical consequences. When deriving the Euler-Lagrange equation for the field $U(x)$, the Wess-Zumino-Witten term appears as a total divergence over the five-dimensional space, and can therefore be written as a four-dimensional boundary term. The manifold $\mathcal{M}_5$ is chosen in particular such that its boundary $\partial\mathcal{M}_5$ matches the usual four-dimensional Minkowski space. The resulting four-dimensional term is then always in the form of eq. (3.53) and vanishes automatically. The Wess-Zumino-Witten term has therefore no effect on the field equations for the meson. It also preserves obviously the chiral symmetry of QCD, but breaks explicitly the parity symmetry and the exchange symmetry $U \leftrightarrow U^\dagger$, leaving only the combination of them invariant, as wanted in the first place. Note however that due to its five-dimensional nature, the Wess-Zumino-Witten term connects well separated points of the four-dimensional space-time through the fifth dimension, and is therefore a non-local object.

The coefficient λ_{WZW} in the definition (3.54) can not be chosen arbitrarily. Any choice of five-dimensional manifold must yield the same effective four-dimensional theory, which means that the actions given respectively by two manifolds $\mathcal{M}_5$ and $\mathcal{M}'_5$, satisfying $\partial\mathcal{M}_5 = \partial\mathcal{M}'_5$, must differ at most by an integer multiple of 2π,

$$\Gamma_{\mathrm{WZW}}\left(\mathcal{M}_5\right) - \Gamma_{\mathrm{WZW}}\left(\mathcal{M}'_5\right) = 2\pi n. \quad (3.55)$$

The integral in eq. (3.54) turns out to be the winding number of the field $U(x)$ in the five-dimensional space, so that choosing $\mathcal{M}_5$ and $\mathcal{M}'_5$ to form a five-sphere, the left-hand side of the equation above can be computed to be

$$\Gamma_{\mathrm{WZW}}\left(\mathcal{M}_5 \cup \mathcal{M}'_5\right) = 480\pi^3 \lambda_{\mathrm{WZW}} = 2\pi n. \quad (3.56)$$

The coefficient is then fixed to $\lambda_{\mathrm{WZW}} = n/(240\pi^2)$, where n can be *a priori* any integer number.

When one considers in addition the electromagnetic force in the low-energy description, the Wess-Zumino-Witten term is obviously not gauge-invariant. The space-time derivatives in (3.54) cannot be straightforwardly promoted to a covariant derivative, since the gauge field is not defined in five dimensions. However, as a confirmation that the fifth dimension is only an artifact of the theory, the variation of the action under a $U(1)_{em}$ gauge

transformation, defined by $\delta U = i\,\alpha(x)\,[Q,U]$, is a local, four-dimensional quantity, namely

$$\begin{aligned}\delta\Gamma_{\rm WZW} &= 5\lambda_{\rm WZW}\int_{\mathcal{M}_5}\mathrm{d}^5x\,\varepsilon^{\mu\nu\rho\sigma\tau}\partial_\mu\alpha(x)\Big[\mathrm{Tr}\left(Q\,\partial_\nu U^\dagger\partial_\rho U\,\partial_\sigma U^\dagger\partial_\tau U\right)\\ &\qquad\qquad -\mathrm{Tr}\left(Q\,\partial_\nu U\,\partial_\rho U^\dagger\,\partial_\sigma U\partial_\tau U^\dagger\right)\Big]\\ &= 5\lambda_{\rm WZW}\int\mathrm{d}^4x\,\varepsilon^{\mu\nu\rho\sigma}\partial_\mu\alpha(x)\Big[\mathrm{Tr}\left(Q\,U\,\partial_\nu U^\dagger\,\partial_\rho U\partial_\sigma U^\dagger\right)\\ &\qquad\qquad -\mathrm{Tr}\left(Q\,U^\dagger\partial_\nu U\,\partial_\rho U^\dagger\partial_\sigma U\right)\Big]\,, \qquad (3.57)\end{aligned}$$

where in the second equality we have used the fact that the integrand is a total divergence and integrated over the fifth dimension, using the fact that the gauge transformation is four-dimensional, i.e. $\partial_5\alpha(x) = 0$. In its last form, it is clear that the variation of the Wess-Zumino-Witten action can be compensated by the gauge variation of a local term in the Lagrangian including the antisymmetric contraction of gauge fields and derivatives of $U(x)$. The explicit form of this four-dimensional term is found to be

$$\begin{aligned}\mathcal{L}_{\rm WZW} = 5\lambda_{\rm WZW}\Big\{&e\mathcal{A}\,\mathrm{Tr}\left(QU^\dagger\mathrm{d}U\mathrm{d}U^\dagger\mathrm{d}U\right) \qquad (3.58)\\ &+i\,e^2\mathcal{A}\mathrm{d}\mathcal{A}\,\mathrm{Tr}\left(Q^2U\mathrm{d}U^\dagger + QUQ\mathrm{d}U^\dagger\right) - \left(U\leftrightarrow U^\dagger\right)\Big\}\end{aligned}$$

where we have used the notation of differential forms. The term linear in the photon field cancels the variation of the five-dimensional part but introduces additional gauge-variant operators, which in turn are cancelled by the terms quadratic in $\mathcal{A}_\mu$. Including these additional local terms, the variation of the effective Lagrangian under the $U(1)_{em}$ gauge transformation is a total divergence without physical significance. Note that the determination of the Lagrangian (3.58) requires to find the transformation properties of all possible gauge-invariant operators constructed from the fields $U(x)$ and $\mathcal{A}_\mu(x)$. In this process, it appears that an additional operator has a vanishing variation, namely

$$\mathcal{A}\mathrm{d}\mathcal{A}\left[\mathrm{Tr}\left(QUQ\mathrm{d}U^\dagger + QU^\dagger Q\mathrm{d}U\right)\right]. \qquad (3.59)$$

This operator is however parity-odd and simultaneously invariant under the exchange $U(x) \leftrightarrow U^\dagger(x)$, and would break the pseudoscalar nature of the pions. It must therefore be absent in the theory of low-energy QCD. The Lagrangian (3.58) contains a number of new meson-photon interaction terms, among which the most interesting involves one pion and two photon fields. The Wess-Zumino-Witten term describes, among other phenomena, the decay of pions into two photons, which was until know absent in the theory. An interesting relation can then be established between the weakly-interacting

scalar theory of mesons and the original QCD Lagrangian involving strongly-interacting quarks. On the one hand, the pion field is tightly related to the axial current of QCD through the relation (3.20), and on the other hand the latter suffers from an anomaly induced by the triangle diagram of figure 2.1, which permits an explicit computation of the pion decay into photon within the quark picture. The quark loop obtained in this way matches exactly the tree-level interaction appearing in the Wess-Zumino-Witten term provided that the integer coefficient n is equal to the number of quark colours, i.e. $n = N_c$, or explicitly

$$\lambda_{\mathrm{WZW}} = \frac{N_c}{240\pi^2}. \tag{3.60}$$

Note that the gauged form of the Wess-Zumino-Witten term can be extended to contain the massive electroweak gauge fields, and more generally the whole symmetry group $SU(N_f)_L \times SU(N_f)_R$. Many more local terms are needed in this case to cancel the variation of the five-dimensional action, as discussed again in section 4.2.2.

Looking back at the transformation rule of Γ_{WZW} under a vector transformation $\delta U \propto [T, U]$, one can see in eq. (3.57) that the four-dimensional variation of the Wess-Zumino-Witten term is proportional to $\delta\Gamma_{\mathrm{WZW}} \propto \{T, U\}$, which means that there can be symmetry transformations under which the Goldstone matrix U is invariant, but which still generate a non-zero current. This is the case of the baryon number symmetry $U(1)_V$, generated by $T = (1/N_c)\,\mathbb{1}$, for which $\delta U = 0$ and the associated Noether current is not vanishing,

$$B^\mu = \frac{1}{24\pi^2}\varepsilon^{\mu\nu\rho\sigma}\,\mathrm{Tr}\left(U^\dagger\partial_\nu U\,\partial_\rho U^\dagger\partial_\sigma U\right). \tag{3.61}$$

The current defined in this way is conserved, since its total divergence $\partial_\mu B^\mu$ is proportional to the vanishing topological term (3.53). The charge associated to it is the baryon number,

$$B = \int \mathrm{d}^3x B^0 = \frac{1}{24\pi^2}\varepsilon^{ijk}\int \mathrm{d}^3x\,\mathrm{Tr}\left(U^\dagger\partial_i U\,\partial_j U^\dagger\partial_k U\right), \tag{3.62}$$

which turns out actually to be a topological invariant quantity taking integer values, as will be discussed later in chapter 4. Note that the fact that only integer baryon number configurations can exist relies on the cancellation between the coefficient (3.60) of the Wess-Zumino-Witten term and the fractional baryon charge $1/N_c$ carried by each quark.

The necessity of the Wess-Zumino-Witten action can actually be derived in the completely different framework of the Nambu-Jona-Lasinio model [74, 84]. The latter is a model of mesons and baryons which do not refer to the strong interaction as the binding force of hadrons. Instead, quarks interact via four-fermion interactions whose form is dictated by symmetry arguments. As in the low-energy theory of QCD described above, the chiral

symmetry is present and broken only by a mass term for the quarks. The formation of a quark condensate is inspired in this case by solid state physics, where bosonic condensates can arise in a purely fermionic theory, adding an auxiliary scalar field to the Lagrangian and integrating out the fermions. This mechanism is called *bosonisation*. Performing finally a derivative expansion leads to an effective description in terms of a non-linear σ-model as in the discussion above. As a side-effect of the axial $U(1)_A$ anomaly, a non-zero phase appears in the fermion determinant of the path integral, which generates upon integration a Wess-Zumino-Witten term of the form of eq. (3.54), whose coefficient is indeed exactly fixed as in eq. (3.60).

3.2 Electroweak symmetry breaking from a strongly-interacting sector

From low-energy QCD, we have now seen that light scalars — although not elementary — exist in nature. They even trigger the breaking of the electroweak symmetry, although not at the correct energy scale. The same recipe can then be applied to build a model of electroweak symmetry breaking based on a strongly-interacting theory with a spontaneously broken global symmetry. As will be discussed, the lessons of QCD cannot be always applied straightforwardly at higher energies.

3.2.1 Technicolor

Looking back at the effective Standard Model Lagrangian without a Higgs introduced in chapter 2, one can see that the σ-model parametrisation used is readily adaptable to a strongly-coupled description of electroweak symmetry breaking. Let us assume in addition to the Standard Model gauge group the presence of a new force similar to the colour interaction, with gauge group $SU(N_{TC})$ (where TC stands for *technicolor*) and of a number of new fermions (called *technifermions*). If this new force is confining, as QCD is, the technifermions will not be observable as freely interacting particles. If in addition the new (techni-)fermionic sector possesses a global symmetry analogous to flavour and spontaneously broken down by the vacuum condensate, there will be a number of Goldstone bosons in the theory. Below a certain energy threshold, assumed to be beyond the scope of past and present experiments, the only new degrees of freedom in the theory will be scalars fields, the equivalent of mesons in QCD.

If one chooses for simplicity the global flavour symmetry breaking to be of the form $SU(2)_L \times SU(2)_R \to SU(2)_V$, as in the two-flavour case of QCD, then there are readily three massless Goldstone bosons which can play the role of the longitudinal degrees of freedom of the $W^\pm$ and Z^0 gauge bosons. Choosing to embed the electroweak gauge group in the $SU(2)_L$ and along

the third generator of $SU(2)_R$, the resulting low-energy effective description corresponds exactly to the electroweak symmetry breaking Standard Model σ-model of (2.37) [85, 86]. The scale playing the role of f_π in QCD is now the electroweak scale $v \cong 246$ GeV. The low-energy setup of the simplest technicolor models corresponds therefore naturally to the Standard Model without a Higgs boson. There is no hierarchy problem, since the electroweak scale v is generated as the scale at which the technicolor coupling g_{TC} becomes strong. Below the cutoff scale $\Lambda \approx 4\pi v$, the Standard Model as we know it arises as an effective theory. The notion of renormalisability is irrelevant in this framework. The unitarity in scattering processes of Goldstone bosons — or equivalently of the longitudinally polarised gauge bosons — is restored as in QCD by an infinite tower of (techni-)meson resonances. If the technicolor theory is similar to QCD, the first resonance needed beyond the Standard Model is the equivalent of the ρ meson, whose mass can be estimated from the large-N_c discussion made above. It was shown in section 3.1.2 that the meson masses are independent of the number of colours in the underlying theory, while the constant f_π scales with the square root of N_c. The two scales can then related as $f_\pi \propto \sqrt{N_c}\, m_\rho$, which can be transposed in the technicolor language into $v \propto \sqrt{N_{TC}}\, m_{\rho,TC}$. Assuming that the proportionality factor is of the same order, one gets an estimate of the mass of the first vector resonance,

$$m_{\rho,TC} \approx \left(\frac{N_c}{N_{TC}}\right)^{1/2} \frac{v}{f_\pi}\, m_\rho \approx \frac{3.5 \text{ TeV}}{\sqrt{N_{TC}}}. \tag{3.63}$$

We have for example $m_{\rho,TC} \approx 1.8$ TeV for $N_{TC} = 4$, which corresponds approximately to the energy (2.65) at which the scattering of $W^\pm$ bosons becomes strongly-interacting in the absence of a Higgs boson.

Apart from its kinetic term giving a mass to the gauge fields, the field $\Sigma(x)$ of chapter 2 also plays the crucial role of giving a mass to the fermions in the effective Standard Model. Obtaining from a strongly-interacting sector a Yukawa interaction like eq. (2.44) is not as straightforward giving a mass to the electroweak gauge bosons. In the low-energy description of QCD, there is no contact interaction between mesons and the fundamental, freely-propagating fermions of the theory (in this case the leptons). Similarly, since quarks and leptons are not charged under the technicolor gauge group, no Yukawa term is expected in technicolor models. The solution to this problem is to unify the Standard Model and technicolor interactions, in a similar manner as the grand unified theories were built. The *extended*

technicolor gauge group [87, 88] is thus of the form[7]

$$SU(N_{ETC}) \supset SU(3)_C \times SU(N_{TC}). \tag{3.64}$$

Assuming that this extended gauge symmetry breaks down spontaneously at an energy scale Λ_{ETC} above the electroweak scale, new massive gauge bosons will be present in the UV theory. When integrated out at low-energies, the new force carriers yield effective four-fermion interactions between Standard Model fermions and technifermions. The operators generated in this way are of three different types, schematically

$$\mathcal{O}_{QQ} \propto \frac{g_{ETC}^2}{\Lambda_{ETC}^2} \left(\overline{Q}Q\right)\left(\overline{Q}Q\right), \qquad \mathcal{O}_{Qq} \propto \frac{g_{ETC}^2}{\Lambda_{ETC}^2} \left(\overline{Q}Q\right)\left(\overline{q}q\right),$$

$$\mathcal{O}_{qq} \propto \frac{g_{ETC}^2}{\Lambda_{ETC}^2} \left(\overline{q}q\right)\left(\overline{q}q\right), \tag{3.65}$$

where q denotes generically Standard Model fermions and Q technifermions. γ-matrices and $SU(N_{ETC})$ group generators have been omitted on purpose. All three kinds of operators are naively generated with the same coefficients. The first of them generates masses for techni-mesons, but does not play any significant role in the low-energy regime. Note however that in the case where there exists additional Goldstone bosons not eaten by the electroweak gauge bosons, this provide an explanation why the latter can be naturally heavy and unobserved so far. The second operator above is exactly what was sought: When the technifermion condensate, i.e. $\langle\overline{Q}Q\rangle \neq 0$, $\mathcal{O}_{Qq}$ generates a mass term for the Standard Model quarks and leptons. The size of the technifermion condensate is *a priori* unknown, but can be estimated to be as in QCD

$$\langle\overline{Q}Q\rangle \approx \frac{\Lambda_{TC}^3}{(4\pi)^2} \approx 4\pi\, v^3, \tag{3.66}$$

for which we can read the fermion mass $m_q \approx 4\pi\, v^3/\Lambda_{ETC}^2$, assuming that the extended technicolor coupling is of order unity. Note that the large discrepancy between the masses of the Standard Model leptons and quarks requires actually that the spontaneous symmetry breaking of the extended group $SU(N_{ETC})$ proceeds in multiple steps. While leptons and light quarks have so tiny masses compared to the electroweak scale that they can be generated at very high energy scales, the charm and bottom quark masses require an extended technicolor mass scale of about 10 TeV. The top mass is so large that it cannot be generated by this mechanism, but other possibilities

[7] Note that in order to generate masses for the leptons, additional symmetries of the Standard Model must be included into the extended technicolor gauge group, such as the global flavour symmetries. This extended group has to feature technifermions transforming under $SU(N_{TC})$, quarks transforming under $SU(N_c)$ and leptons as singlets under both of these strongly-coupled gauge groups all belonging to the same extended multiplet.

exist and will be discussed below. With an extended technicolor scale only one order of magnitude above the electroweak cutoff, the third of the four-fermion operators above becomes however very dangerous. In the absence of additional symmetries, $\mathcal{O}_{qq}$ generates flavour-changing neutral currents, whose presence is very strongly constrained by experimental data. A naive dimensional analysis approach requires for example $\Lambda_{ETC} \geq 10^3$ TeV, much above the scale needed to give a mass to the quarks, hence clearly excluding such a scenario.

There is however a solution to this problem, which arise if the technicolor sector behaves differently from QCD at high energies. In QCD, the coupling g_S is decreasing very rapidly in the high-energy, weakly-coupled regime. As a consequence, the scaling of operators with energy is mostly given by their classical dimension. In other words, the anomalous dimension of operators is in general small for asymptotically free theory like QCD. Theories in which the strong-dynamics is nearly conformal present however a very different behaviour. The gauge coupling in such theories is not decreasing fast but stays constant over a large energy range [89]. Such a behaviour happens when the β-function has an infrared fixed point, which can occur depending on the number of flavours in the theory. There is in general a critical number of flavours in a theory which determines the direction of the running of the strong coupling constant [90]. If the number of flavours in a technicolor theory is close to its critical value, then the theory resembles a conformal field theory, the anomalous dimension of operators can become important, and the classical scaling rule loses its validity. *Walking technicolor* models are built upon this principle. They are theories with an extended symmetry at a very large scale $\Lambda_{ETC} \gg \Lambda_{TC}$, but where the coupling g_{TC} is nearly constant over the energy range between $\Lambda_{TC} \approx 2$ TeV and Λ_{ETC}. The suppression of flavour-changing neutral currents is therefore guaranteed from the size of Λ_{ETC}, which do not suffer anomalous scaling, while the quark masses are reduced as

$$m_q \propto \frac{1}{\Lambda_{ETC}^2}\langle \overline{Q}Q\rangle \propto \frac{\Lambda_{TC}}{(4\pi)^2}\left(\frac{\Lambda_{TC}}{\Lambda_{ETC}}\right)^{2+\gamma}, \tag{3.67}$$

where γ is the anomalous dimension of the operator $\mathcal{O}_{Qq}$. A moderate value of γ is sufficient to generate all quark masses with the exception of the top quark. Note that the anomalous dimension cannot be arbitrarily large. There is actually an important effort going on in order to understand the scaling of operators in conformal field theories and to put bounds of the size of the anomalous dimension γ [91, 92, 93]. As noted already twice, the top quark mass cannot be obtained purely from an extended technicolor sector. A possible way out of this problem is to consider a separate technicolor sector for the third generation of quarks, in which the physical top quark observed in experiments is not a fundamental fermion but rather a composite state of the strongly-interacting theory [94, 95]. An elementary top quark is present

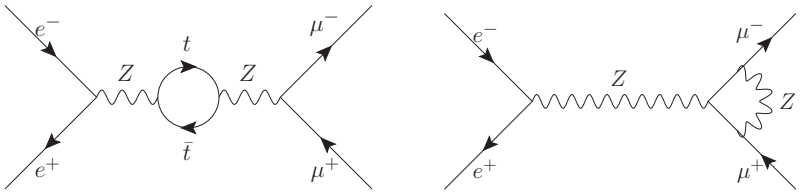

Figure 3.8: Oblique (left) and non-oblique (right) one-loop corrections to the process $e^+e^- \to \mu^+\mu^-$ at LEP.

like in the Standard Model, but cannot be observed due to its condensation, contributing to the breaking of the electroweak symmetry [96, 97, 98].

Note finally that while there is obviously no Higgs boson in the minimal version of technicolor described here, realistic models often have a light scalar in their spectrum, whose quantum numbers are those of the vacuum, like the Higgs boson itself. This happens for example when the strong dynamics is nearly conformal, in which case a Goldstone boson associated with the breaking of conformal symmetry can appear. The latter is usually called a *dilaton*. Although the dilaton can possibly be a narrow resonances with a mass of a few hundred GeV, exactly like a Higgs boson, its role in the theory is very different. A dilaton does not unitarise the scattering of longitudinal gauge boson, nor does he necessarily couple to fermions proportionally to their mass. In this sense, technicolor is truly a higgsless theory.

3.2.2 Electroweak precision tests

Apart from its difficulties to account for the fermion masses in a simple way, technicolor has to face an even more stringent issue regarding the precision data collected at LEP and at other collider facilities. LEP was an electron-positron collider, running in its first phase as a precision machine exactly at the energy of the Z^0 boson mass (LEP1), and in a second phase at higher energies with the goal to discover a light Higgs boson (LEP2). The data gathered from the resonant production of the Z^0 allowed for measuring a number of electroweak parameters with a very high accuracy, permitting to probe not only the tree-level processes involving a Z^0 boson in the s-channel, but also indirectly the physics at higher energies through the quantum radiative corrections. In this section, an analysis of this high-precision measurements is presented, which allows to constrain the physics beyond the Standard Model in a model-independent way.

Radiative corrections to the electron-positron annihilation processes can be separated into two classes, as illustrated in figure 3.8. An important class of corrections arise directly in the propagator of the Z^0 gauge boson through vacuum polarisation effects, and are called *oblique* corrections. All

other kinds of radiative corrections are subsequently denoted by *non-oblique* corrections. These include the vertex corrections shown in figure 3.8 (b), but also box diagrams and soft and collinear emission of massless gauge bosons. There is a deep reason behind the separation into these two classes. Whatever new physics enters beyond the Standard Model, its coupling to the light quarks and leptons is expected to be suppressed. From the success of the Weinberg-Salam model of quarks and leptons, the only interaction of the latter with new physics should proceed through their mass term, which is very tiny compared to the energy of the electron-positron annihilation process at LEP. On the contrary, the vacuum polarisation diagrams entering the oblique corrections are sensitive to all new fields with non-vanishing electroweak couplings, independently on their mass.

In order to parametrise the oblique corrections, one can write down an effective Lagrangian for the physical gauge bosons, proceeding as eq. (3.28) for the electromagnetic field in low-energy QCD:

$$\begin{aligned}\mathcal{L}_{\text{eff}} = \frac{1}{2}\mathcal{P}_{\perp}^{\mu\nu}\big[&\Pi_{\gamma\gamma}(p^2)\mathcal{A}_\mu\mathcal{A}_\nu + 2\Pi_{Z\gamma}(p^2)Z_\mu\mathcal{A}_\nu \\ &+\Pi_{ZZ}(p^2)Z_\mu Z_\nu + 2\Pi_{WW}(p^2)W_\mu^+W_\nu^-\big] + \mathcal{O}\left(\frac{p^\mu p^\nu}{p^2}\right).\end{aligned} \tag{3.68}$$

All radiative corrections to the propagators of the $W^\pm$, Z^0 and photon are contained in the form factors $\Pi(p^2)$. The terms proportional to the Lorentz tensor $p^\mu p^\nu$ are omitted on purpose, since when contracted with the fermion currents, their contribution to the electron-positron annihilation process is suppressed by the mass of the external particles and is therefore negligible. Note that the fields entering the effective Lagrangian are the physical gauge bosons, and need not necessarily be identical to the $SU(2)_W \times U(1)_Y$ electroweak gauge bosons. They contain for sure a large component of the latter, but might also be states mixed with new, heavy vector bosons with the same quantum numbers. The effective theory describing the precision physics at the Z-pole mass at LEP is therefore a theory of massless fermions (all leptons and quarks excepted the top), of a massless photon and of massive gauge bosons $W^\pm$ and Z^0. This corresponds to the Standard Model description of chapter 2, where the mass of the light fermions are put to zero and particles heavier than the boson Z^0 are integrated out — only the top quark in the effective description of the Standard Model without a Higgs boson. The only parameters entering the theory at this stage are therefore the gauge couplings g and g', as well as the electroweak scale v. Their values are fixed by the most precisely known observables, namely the mass of the Z^0 gauge boson $m_Z = g^2v^2/(2\cos\theta_W)$, the weak coupling constant $\alpha(m_Z) = g^2\sin\theta_W/(4\pi)$ at the Z-pole mass (different from the fine-structure constant), and the Fermi coupling constant $G_F = (\sqrt{2}v^2)^{-1}$ measured from the muon decay process. The Weinberg angle is defined here as the ratio of the $U(1)_Y$ and $SU(2)_W$ coupling constants, $\tan\theta_W = g'/g$. All other preci-

sion measurements performed at LEP can then be used to check the validity of the theory defined in terms of g, g' and v, and possibly to determine the effects of the heavy particles integrated out in the effective description. On the theoretical side, the form factors $\Pi(p^2)$ can be computed for any given theory. Instead of using the physical gauge bosons $W^\pm$, Z^0 and the photon, it will actually be more convenient to rotate the gauge field in a different basis defined by $Z_\mu = c_W W^3_\mu - s_W B_\mu$ and $\mathcal{A}_\mu = s_W W^3_\mu + c_W B_\mu$, where we have used the obvious notation $s_W \equiv \sin\theta_W$, $c_W \equiv \cos\theta_W$. Defining a new set of form factors, the effective Lagrangian becomes

$$\begin{aligned}\mathcal{L}_{\text{eff}} = \frac{1}{2}\mathcal{P}^{\mu\nu}_\perp \big[&\Pi_{BB}(p^2) B_\mu B_\nu + 2\Pi_{3B}(p^2) W^3_\mu B_\nu \\ &+\Pi_{33}(p^2) W^3_\mu W^3_\nu + 2\Pi_{+-}(p^2) W^+_\mu W^-_\nu \big] + \dots \end{aligned} \tag{3.69}$$

All form factors can then be expanded in powers of the energy squared as

$$\Pi(p^2) = \Pi(0) + p^2\Pi'(0) + \frac{p^4}{2}\Pi''(0) + \mathcal{O}\left(p^6\right), \tag{3.70}$$

and since the Z^0 boson is produced mostly on-shell in the electron-positron collisions at LEP1, only the first few terms in this expansion are relevant. Some of the form factors entering the Lagrangian (3.69) are constrained by the requirement that the photon remains exactly massless. Two constraints can be formulated as

$$\Pi_{\gamma\gamma}(0) = c^2_W \Pi_{BB}(0) + 2 s_W c_W\, \Pi_{3B}(0) + s^2_W \Pi_{33}(0) = 0, \tag{3.71}$$

$$\Pi_{Z\gamma}(0) = -s_W c_W\, \Pi_{BB}(0) + \left(c^2_W - s^2_W\right) \Pi_{3B}(0) + s_W c_W\, \Pi_{33}(0) = 0, \tag{3.72}$$

or equivalently, rearranging the two equalities,

$$\Pi_{BB}(0) = \tan^2\theta_W\, \Pi_{33}(0), \qquad \Pi_{3B}(0) = -\tan\theta_W\, \Pi_{33}(0). \tag{3.73}$$

In addition, there is still some freedom in defining the form factors, arising from the choice of counter-terms in the renormalisation procedure of the theory. There are three such counter-terms, corresponding to the three parameters g, g' and v, so that the definition of three of the form factors can be adjusted freely. A particular choice could be to canonically normalise the kinetic terms of the fields $W^\pm_\mu$ and B_μ by requiring

$$\Pi'_{BB}(0) = \Pi'_{+-}(0) = -1, \tag{3.74}$$

and to adjust the mass of the $W^\pm_\mu$ field to its experimentally measured value

$$\Pi_{+-}(0) = m^2_W. \tag{3.75}$$

From this point, the remaining form factors are totally determined by the theory under consideration. If one considers only the terms up to order

p^2 to be relevant in the form factor expansion (3.70), there are only three terms which are not fixed by $U(1)_{em}$ gauge invariance and by the freedom of renormalisation scheme. These three terms can be arranged in particular linear combinations, which can be then related to physical observables at LEP [99],[8]

$$\hat{S} = -\frac{g}{g'}\,\Pi'_{3B}(0), \tag{3.76}$$

$$\hat{T} = \frac{1}{m_W^2}\left[\Pi_{+-}(0) - \Pi_{33}(0)\right], \tag{3.77}$$

$$\hat{U} = \Pi'_{33}(0) - \Pi'_{+-}(0), \tag{3.78}$$

or in terms of the form factors of the physical gauge bosons,

$$\hat{S} = \Pi'_{ZZ}(0) - \frac{c_W^2 - s_W^2}{s_W c_W}\Pi'_{Z\gamma}(0) - \Pi'_{\gamma\gamma}(0), \tag{3.79}$$

$$\hat{T} = \frac{1}{m_W^2}\left[\Pi_{WW}(0) - c_W^2\Pi_{ZZ}(0)\right], \tag{3.80}$$

$$\hat{U} = c_W^2\Pi'_{ZZ}(0) + 2s_W c_W\Pi'_{Z\gamma}(0) + s_W^2\Pi'_{\gamma\gamma}(0) - \Pi'_{WW}(0). \tag{3.81}$$

The physical meaning of the parameters can be deduced from their definition. $\hat{T}$ measures the difference in mass between the $W^\pm$ and Z^0 gauge bosons. It is related to the parameter ρ defined in eq. (2.43) through the approximate equality

$$\rho \cong 1 + \hat{T}, \tag{3.82}$$

which is valid for small values of $\hat{T}$. ρ is found experimentally to be very close to one, which constraints very much the size of $\hat{T}$. The parameter $\hat{T}$ is actually related to isospin violation, or equivalently to the violation of the $SU(2)_R$ global symmetry acting on the right-handed fermions. Note that there is no contribution to $\hat{T}$ from the electroweak symmetry breaking sector in the Standard Model, since the latter possesses a global $SU(2)_L \times SU(2)_R$ symmetry and the spontaneous symmetry breaking mechanism preserves a global $SU(2)_V$ symmetry, which acts as a *custodial symmetry* for the $\hat{T}$ parameter. This statement is valid both in the absence or presence of a Higgs boson. The only source of $SU(2)_V$ violation in the Standard Model is the difference in mass — or equivalently in Yukawa coupling — between members of the same $SU(2)_W$ multiplet. In the effective approach discussed here, only the top quark is massive and can contribute to the $\hat{T}$ parameter when integrated out. Since it is part of a $SU(2)_W$ doublet together with the

[8]The definition given here does not match exactly the original definition of Peskin and Takeuchi, but refers instead to the notation of ref. [100]. The equivalence between the two parametrisations is follows from the equalities $\hat{S} = \alpha/(4s_W^2)S$, $\hat{T} = \alpha T$ and $\hat{U} = -\alpha/(4s_W^2)U$, where the parameters without a hat are the original ones as defined in ref. [99].

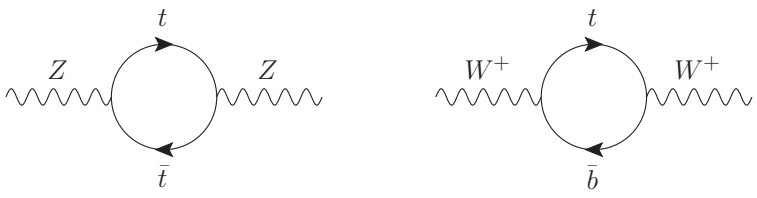

Figure 3.9: Vacuum polarisation diagrams contributing at one loop to the propagators of the gauge bosons Z^0 (left) and $W^\pm$ (right). The sum of these two diagrams is finite and give the Standard Model correction to the ρ parameter of eq. (3.83).

bottom quark, the top does not induce any contribution to the transverse polarisation of the gauge boson, since the custodial symmetry protects the gauge sector from such effects. The non-zero top Yukawa is however generating a contribution to the longitudinal polarisation of the $W^\pm$ and Z^0 gauge bosons, and the two relevant diagrams at the one-loop order are shown in figure 3.9. Quantitatively, the correction reads

$$\Delta\hat{T}_{\text{top}} = \frac{3m_t^2}{16\pi^2 v^2} \cong 9.2 \cdot 10^{-3}. \tag{3.83}$$

Note that the top loop correction is already very small, so that it is justified to neglect the contributions from lighter fermions. Despite its tiny size, the quantity $\Delta\hat{T}_{\text{top}}$ can be compared with the experimental measurement, and the agreement is found to be very good. Note that the agreement holds naturally at higher loop order as well [101]. More generally, the parameter $\hat{T}$ constrains the mass difference within isospin multiplets [102]. This constraint applies for example to an hypothetical fourth generation of fermions within the Standard Model, requiring the new quarks to be nearly degenerate in mass, and similarly for the leptons.

The meaning of the $\hat{S}$ parameter can be clarified by using the same trick as in the low-energy QCD effective Lagrangian (3.29). Considering the full $SU(2)_L \times SU(2)_R$ symmetry as a gauge symmetry, the form factor $\Pi_{3B}(p^2)$ plays precisely the same role as $\Pi_{LR}(p^2) = \Pi_{AA}(p^2) - \Pi_{VV}(p^2)$ above, it measures the violation of the left-right symmetry in the electroweak symmetry breaking sector. A straightforward example is again to consider a fourth generation of quarks and leptons in the Standard Model. Since only the left-handed fermions are charged under $SU(2)_W$, a non-zero contribution

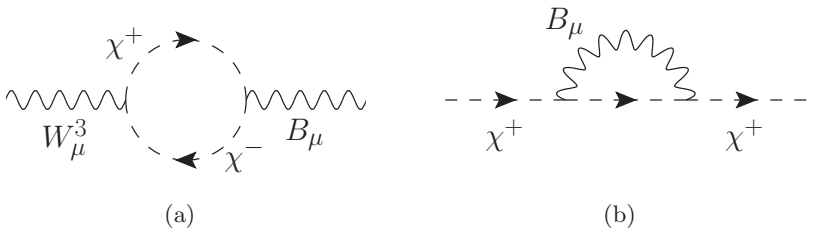

(a) (b)

Figure 3.10: Logarithmically divergent contributions to the $\hat{S}$ (left) and $\hat{T}$ (right) parameters from the longitudinal polarisation of the Gauge bosons, here written explicitly as the Goldstone fields χ^a.

to $\hat{S}$ is generated, namely [103]

$$\Delta\hat{S}_{\text{quarks}} = \frac{g^2}{32\pi^2}\left[1 - \frac{1}{3}\log\left(\frac{m^2_{u_4}}{m^2_{d_4}}\right)\right], \tag{3.84}$$

$$\Delta\hat{S}_{\text{leptons}} = \frac{g^2}{96\pi^2}\left[1 - \log\left(\frac{m^2_{l_4}}{m^2_{\nu_4}}\right)\right]. \tag{3.85}$$

Since $\hat{S}$ is also found experimentally to be small, a tension appears: the $\hat{S}$ parameter can only be small if for the fourth generation of fermions the hierarchies $m_{u_4} > m_{d_4}$ and $m_{l_4} > m_{\nu_4}$ are satisfied, while at the same time the smallness of $\hat{T}$ require the fermions within the same multiplet to be nearly degenerate in mass. Note however that a fourth generation cannot be completely excluded by the present experimental data, since a positive contribution to both $\hat{S}$ and $\hat{T}$ is allowed due to a large correlation among the experimental bounds on them, as will be discussed below. A complete analysis of the status of a fourth generation in the Standard Model can be found for example in ref. [104].

The parameter $\hat{U}$ is actually less important than $\hat{S}$ and $\hat{T}$ and is often taken to be zero in universal models of physics beyond the Standard Model. The reason for this is that no dimension-six effective operator can be built out of the Standard Model fields which would give a contribution to $\hat{U}$. Only operators of dimension eight or higher can give a non-zero $\hat{U}$, as opposed to $\hat{S}$ and $\hat{T}$, which are already generated by dimension-six operators [105]. The effective theory description of the electroweak precision test will be discussed in more detail in section 3.2.5.

There is nevertheless an important caveat in the effective description used so far: In a non-renormalisable theory, the parameters $\hat{S}$, $\hat{T}$ and $\hat{U}$ need not in general to be finite. This issue arises for example in the Standard Model without a Higgs boson, where the diagrams shown in figure 3.10 with Goldstone bosons χ^a running in the loop give logarithmically divergent contribution to the $\hat{S}$ and $\hat{T}$ parameters. The divergent diagrams are

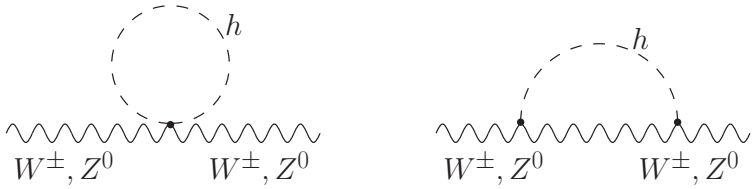

(a) (b)

Figure 3.11: Higgs boson contribution to the propagator of the $W^\pm$ and Z^0 gauge bosons at one loop. The sum of these two diagrams depends only logarithmically on the Higgs mass.

of course cut-off by the limited range of the effective theory, but cannot be evaluated quantitatively in the absence of information on the physics at the cutoff scale. We have already seen in chapter 2 that the theory can be made renormalisable by adding a single scalar field, which accounts here for making all three parameters $\hat{S}$, $\hat{T}$ and $\hat{U}$ finite by adding a single counterterm regulating the mass of the Higgs field m_h. The oblique parameters can thus only be defined relatively to a reference point in the Standard Model with a given Higgs mass. The reference point corresponds usually to a top quark mass $m_t = 175$ GeV and a Higgs boson mass $m_h = 115$ GeV. In this case, the renormalisation of m_t and m_h — or equivalently of the Higgs quartic λ_h — can be fixed so that $\hat{S} = \hat{T} = 0$ with these precise values. Experimental bounds on $\hat{S}$ and $\hat{T}$ can then be derived within this assumption, and possible deviations from zero indicate a different preferred value of m_t and m_h, or the presence of radiative effects from new physics. The dependence of the oblique parameters on the Higgs mass can be determined from the computation of the diagrams in figure 3.10, where the Higgs mass acts as a cutoff. Note that there is actually no contribution growing like m_h^2 as there is for the top, although the Higgs loop diagrams of figure 3.11 are superficially quadratically divergent [106]. The leading contribution to $\hat{S}$ and $\hat{T}$ is found to be

$$\Delta\hat{S}_h = \frac{g^2}{192\pi^2}\log\left(\frac{m_h^2}{\mu^2}\right), \qquad \Delta\hat{T}_h = -\frac{3g'^2}{64\pi^2}\log\left(\frac{m_h^2}{\mu^2}\right), \tag{3.86}$$

where μ indicates here the reference value of the Higgs mass. Note that there are additional terms dependent on m_h, which become however only important at large values of the Higgs mass.

Instead of using $\hat{S}$, $\hat{T}$ and $\hat{U}$, one can define an equivalent but more universal set of parameters ε_1, ε_2 and ε_3, which do not depend on the choice of a reference point in the Standard Model, but can be directly related to quantities measured experimentally independently of the top and Higgs

masses [107, 108]. They are defined as

$$\varepsilon_1 = \Delta\rho, \tag{3.87}$$

$$\varepsilon_2 = c_W^2 \Delta\rho + \frac{s_W^2}{c_W^2 - s_W^2}\Delta r_W - 2 s_W^2 \Delta k', \tag{3.88}$$

$$\varepsilon_3 = c_W^2 \Delta\rho + \left(c_W^2 - s_W^2\right)\Delta k', \tag{3.89}$$

where the three parameters $\Delta\rho$, Δr_W and $\Delta k'$ are in one-to-one correspondence with three physical observables, namely the mass m_W of the $W^\pm$ gauge boson, the partial decay width $\Gamma(Z \to \ell\ell)$ of the Z^0 boson into leptons and the forward-backward asymmetry A_{FB}^ℓ of leptonic final states, through the relations

$$\frac{m_W^2}{m_Z^2}\left(1 - \frac{m_W^2}{m_Z^2}\right) = \frac{\pi\alpha(m_Z)}{\sqrt{2}\, G_F m_Z^2 (1 - \Delta r_W)} \tag{3.90}$$

$$\Gamma(Z \to \ell\ell) = \frac{G_F m_Z^3}{6\sqrt{2}\,\pi}\left(g_V^2 + g_A^2\right), \tag{3.91}$$

$$A_{FB}^\ell = \frac{3 g_V^2 g_A^2}{(g_V^2 + g_A^2)^2}, \tag{3.92}$$

$$g_A = -\frac{1}{2}\left(1 + \frac{1}{2}\Delta\rho\right) \qquad \frac{g_V}{g_A} = 1 - 4 s_W^2\left(1 + \Delta k'\right). \tag{3.93}$$

With the exception of the W mass, all quantities defining the ε_i are measured with high precision at the Z-pole mass at LEP [109]. On the theory side, the ε_i are determined within the Standard Model to be[9]

$$\varepsilon_1^{(\mathrm{SM})} = [+5.60 - 0.86 \log(m_h/m_Z)] \cdot 10^{-3}, \tag{3.94}$$

$$\varepsilon_2^{(\mathrm{SM})} = [-7.09 + 0.16 \log(m_h/m_Z)] \cdot 10^{-3}, \tag{3.95}$$

$$\varepsilon_3^{(\mathrm{SM})} = [+5.25 + 0.54 \log(m_h/m_Z)] \cdot 10^{-3}. \tag{3.96}$$

New physics beyond the Standard Model enters then as corrections to the $\varepsilon_i^{(\mathrm{SM})}$. Their definition was carefully chosen so that each of them is proportional to one of the Peskin-Takeuchi parameter, i.e.

$$\varepsilon_1^{(th)} = \varepsilon_1^{(\mathrm{SM})} + \Delta\hat{T}_{\mathrm{BSM}}, \tag{3.97}$$

$$\varepsilon_2^{(th)} = \varepsilon_2^{(\mathrm{SM})} + \Delta\hat{U}_{\mathrm{BSM}}, \tag{3.98}$$

$$\varepsilon_3^{(th)} = \varepsilon_3^{(\mathrm{SM})} + \Delta\hat{S}_{\mathrm{BSM}}. \tag{3.99}$$

As discussed above, contributions to $\hat{U}$ from new physics proceed through a subleading operator only, and we will therefore generically take $\Delta\hat{U}_{\mathrm{BSM}} = 0$.

[9] The values quoted here are taken from ref. [110] and correspond to a fit for low Higgs mass of the full result obtained with the code TopaZ0 [111].

In order to have a complete picture of the effects of new physics, an additional constraint can be added, arising from the non-oblique corrections to the electron-positron annihilation process. As explained above, since the couplings of light quarks to gauge fields and to any new physics is assumed to be small, non-oblique corrections are less important than oblique ones. There is however one important exception. The longitudinal polarisation of the massive gauge bosons couple to the light fermions through the Yukawa interaction, so that the left-handed bottom quark, belonging to the same multiplet as the top, has a coupling to $W^\pm$ gauge boson of order one. Note that processes including only top quarks are irrelevant, since the energy of the LEP collider was not sufficient to produce pairs of top quarks. The only relevant non-oblique correction is therefore to the decay $Z \to \bar{b}_L b_L$. The effective correction to the vertex can be included in the Lagrangian through the parameter τ as[10]

$$\mathcal{L}_{\text{eff}} \supset i\frac{g}{2c_W}\left(1 - \frac{2}{3}s_W^2 + \tau\right) Z_\mu \, \bar{b}_L \gamma^\mu b_L \tag{3.100}$$

In the Standard Model, the one-loop correction involves a top quark running in the loop, and the diagrams contributing to this process are shown on figure 3.12. An explicit computation gives

$$\tau_{\text{top}} = -\frac{2m_t^2}{(4\pi)^2 v^2} \cong -6.2 \cdot 10^{-3}. \tag{3.101}$$

This result is obtained in the "gauge-less" limit, where only the Goldstone bosons run in the loop. Diagrams including internal transverse polarisation of the gauge bosons are proportional to g^2 and therefore subdominant. The parameter τ is constrained experimentally by the measurement of the partial decay width of Z^0 into bottom quarks. As before, it is convenient to define an alternative parameter to τ, called ε_b [112]. In analogy with the ε_i, the theoretical prediction for ε_b can be split into a Standard Model value and a correction from new physics effects, as

$$\varepsilon_b^{(th)} = -6.43 \cdot 10^{-3} + \Delta\tau_{\text{BSM}}. \tag{3.102}$$

The best experimental determination of ε_1, ε_2, ε_3 and ε_b still come from

[10] The notation τ for the correction to the $Z\bar{b}_L b_L$ vertex is taken from ref. [65]. Other conventions are also used frequently for the same quantity, such as δg_b.

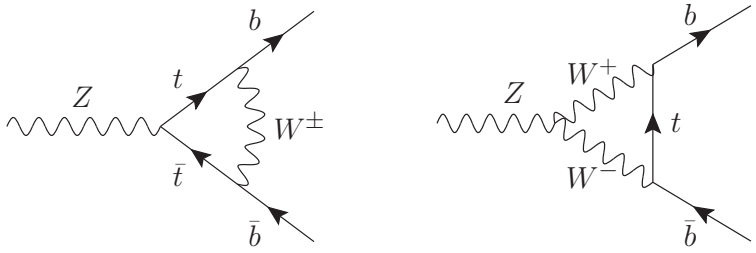

Figure 3.12: Vertex corrections to the decay $Z \to b\bar{b}$ at one loop.

the precision measurements at the Z-pole mass at LEP [109]:

$$\begin{aligned}
\varepsilon_1^{(exp)} &= (5.4 \pm 1.0) \cdot 10^{-3}, \\
\varepsilon_2^{(exp)} &= (-8.9 \pm 1.2) \cdot 10^{-3}, \\
\varepsilon_3^{(exp)} &= (5.34 \pm 0.94) \cdot 10^{-3}, \\
\varepsilon_b^{(exp)} &= (-5.0 \pm 1.6) \cdot 10^{-3},
\end{aligned} \qquad \rho = \begin{pmatrix} 1 & 0.57 & 0.90 & -0.32 \\ 0.57 & 1 & 0.40 & -0.22 \\ 0.90 & 0.40 & 1 & -0.22 \\ -0.32 & -0.22 & -0.22 & 1 \end{pmatrix}, \tag{3.103}$$

where ρ is the correlation matrix between the ε_i.[11] The status of electroweak precision observables did not change since LEP results, except for the mass of the W boson. The latter was recently updated based on Tevatron results [113, 114], and the new world average is now [115]

$$m_W = 80.385 \pm 0.015 \text{ GeV}. \tag{3.104}$$

The parameter ε_2 is the only one depending on the mass of the W, through the term Δr_W in eq. (3.88). The measurement of Δr_W is itself related to the W mass through eq. (3.90). The change of m_W from its value $m_W = 80.425 \pm 0.034$ GeV of 2006 to the most recent result (3.104) is then equivalent to a shift of ε_2 to

$$\varepsilon_2 = (-7.87 \pm 0.90) \cdot 10^{-3}. \tag{3.105}$$

Since the covariance between the different ε_i is unchanged by this update — except for the covariance of ε_2 with itself — the second row and column of the correlation matrix ρ are simply rescaled by the change in the uncertainty

[11] The correlation matrix ρ is directly obtained from the appendix E of ref. [109], marginalising over the three parameters m_Z, $\alpha_S(m_Z)$ and $\Delta\alpha^{(5)}_{had}(m_Z)$ defined there.

on ε_2. The best experimental values for the ε_i up-to-date are therefore

$$\begin{aligned}
\varepsilon_1^{(exp)} &= (5.4 \pm 1.0) \cdot 10^{-3}, \\
\varepsilon_2^{(exp)} &= (-7.87 \pm 0.90) \cdot 10^{-3}, \\
\varepsilon_3^{(exp)} &= (5.34 \pm 0.94) \cdot 10^{-3}, \\
\varepsilon_b^{(exp)} &= (-5.0 \pm 1.6) \cdot 10^{-3},
\end{aligned} \qquad \rho = \begin{pmatrix} 1 & 0.75 & 0.90 & -0.32 \\ 0.75 & 1 & 0.53 & -0.30 \\ 0.90 & 0.53 & 1 & -0.22 \\ -0.32 & -0.30 & -0.22 & 1 \end{pmatrix}. \tag{3.106}$$

The agreement between theoretical predictions and measured experimental values for the ε_i is then assessed by a χ^2 test, defined as

$$\chi^2 = \sum_{i,j} \left(\varepsilon_i^{(th)} - \varepsilon_i^{(exp)}\right) C_{ij}^{-1} \left(\varepsilon_j^{(th)} - \varepsilon_j^{(exp)}\right), \tag{3.107}$$

where C^{-1} is the inverse of the covariance matrix

$$C_{ij} = \Delta\varepsilon_i^{(exp)} \, \Delta\varepsilon_j^{(exp)} \, \rho_{ij}. \tag{3.108}$$

From the definition of the ε_i parameters, it is clear that the χ^2 is completely fixed by the mass of the Higgs and by the four quantities $\Delta\hat{S}_{\rm BSM}$, $\Delta\hat{T}_{\rm BSM}$, $\Delta\hat{U}_{\rm BSM}$ and $\Delta\hat{\tau}_{\rm BSM}$ only. Within the Standard Model, the only unknown is the Higgs mass. With our definition, the χ^2 test takes its minimum at

$$m_H^{\rm best} = 85.7 \text{ GeV}, \qquad \chi^2_{\rm min} = 1.73. \tag{3.109}$$

Moreover, a bound on the Higgs mass is obtained by requiring that $\chi^2 - \chi^2_{\rm min} \leq 13.28$, the latter corresponding to a 99% confidence level interval with four degrees of freedom. One finds

$$40.0 \text{ GeV} \leq m_H \leq 188.5 \text{ GeV}. \tag{3.110}$$

The lower bound is irrelevant, since it is overridden by the LEP2 limit on the direct Higgs search, $m_H \geq 114.4$ GeV. The upper bound is now also obsolete due to the recent Tevatron and LHC results, but was nevertheless a strong indication that the Higgs boson had to be relatively light, if Standard Model-like. The Higgs mass dependence of the electroweak precision parameters is mostly appearing in $\hat{S}$ and $\hat{T}$, and it is therefore insightful to look at the precision constraint in the two-dimensional plane $\left(\hat{S}, \hat{T}\right)$, or equivalently $(\varepsilon_3, \varepsilon_1)$. The experimental constraints imposed by the χ^2 test appear as an ellipse in this plane (see figure 3.13), whose inclination depends on the correlation between ε_1 and ε_3. Points corresponding to the Standard Model with various Higgs boson masses are shown for comparison. Note however that while projecting onto a two-dimensional plane, some information present in the χ^2 test is lost. The procedure used here to create fig. 3.13 is to minimise the χ^2 with respect to ε_2 and ε_b. The bound (3.110) can therefore

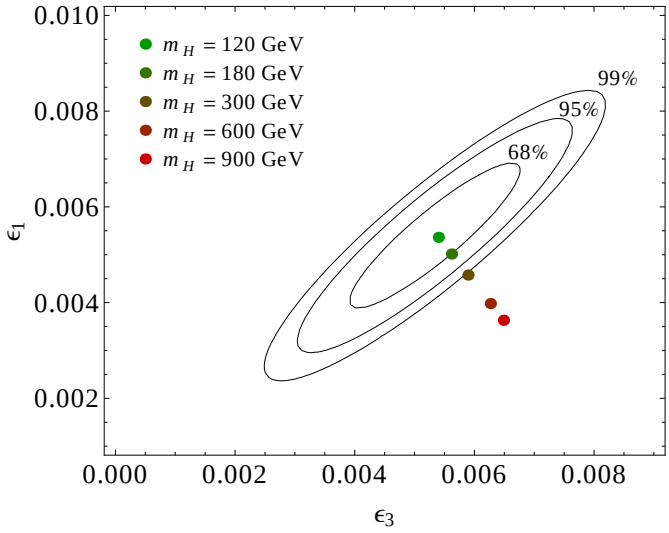

Figure 3.13: Allowed values of the ε_3 and ε_1 parameters (or equivalently $\hat{S}$ and $\hat{T}$) for the 68% (1σ), 95% (2σ) and 99% confidence intervals. The inclination of the ellipses shows an important correlation between the two parameters. The coloured points are Standard Model predictions for different values of the Higgs mass.

not be read directly from the intersection of the Standard Model prediction with the 99% confidence level ellipse. The important piece of information gathered from figure 3.13 is that the large-m_H direction is orthogonal to the major axis of the ellipse, hence providing a strong constraint on the Higgs mass. Conversely, one can see that the direction of positively correlated $\hat{S}$ and $\hat{T}$ is much less constrained. Important same-sign contributions to both $\hat{S}$ and $\hat{T}$ are thus not excluded by the data.

Despite its importance in the literature, the parametrisation of the effects of new physics in terms of the four ε_i parameters is not the most general. From the measurements obtained at LEP2, which are less precise than at the Z-pole mass but with a higher luminosity, the electroweak form factors can actually be constrained up to the term of order p^4 in the energy expansion (3.70). It is therefore possible to define an additional set of four electroweak

parameters, denoted by [100]

$$V = \frac{m_W^2}{2}\left[\Pi''_{33}(0) - \Pi''_{+-}(0)\right], \tag{3.111}$$

$$W = \frac{m_W^2}{2}\,\Pi''_{33}(0), \tag{3.112}$$

$$X = \frac{m_W^2}{2}\,\Pi''_{3B}(0), \tag{3.113}$$

$$Y = \frac{m_W^2}{2}\,\Pi''_{BB}(0). \tag{3.114}$$

As for the original three parameters, not all of them are equally relevant to the study of new physics: only Y and W are arising from dimension-six operators in an effective approach, while V and X are subdominant. The parameters Y and W are particularly sensitive to the presence of new gauge bosons, but will not be discussed further in this thesis.

After presenting the constraints imposed by LEP data on the Standard Model, the attention should now turn back to technicolor models, which were the original motivation for introducing the electroweak precision tests. The introduction of a new sector in the Standard Model without a Higgs can in principle generate important corrections both to the $\hat{S}$ and $\hat{T}$ parameters. It turns out however that the constraint on $\hat{T}$ can be easily accommodated by a simple mechanism. If the new, strongly interacting sector possesses the same custodial symmetry as the gauge and Higgs sectors of the Standard Model, then, by the same argument as above, no contribution to $\hat{T}$ is generated at tree-level. Models fulfilling this requirement must possess a global $SO(4) \cong SU(2) \times SU(2)$ symmetry, of which one of the $SU(2)$ and a subgroup of the second $SU(2)$ generated by a single generator are identified as the standard electroweak gauge group $SU(2)_W \times U(1)_Y$ [116]. The only non-zero contribution to $\hat{T}$ arises then from the custodially-breaking technifermion condensate, which is however identical in size to the mass term of the quarks in the Standard Model. The situation regarding the $\hat{S}$ parameter is much more severe. Since the effective theory below the technicolor scale is non-renormalisable and valid only up to the cutoff scale, the technicolor contribution to $\hat{S}$ cannot be computed exactly without knowing the physics present at this very scale. It can however be estimated in a similar fashion as the pion mass splitting was computed in QCD [103]. As explained above, the form factor $\Pi_{3B}(p^2)$ is indeed playing a similar role as $\Pi_{LR}(p^2)$ did in the low-energy effective Lagrangian (3.29), and assuming a similar behaviour — in particular vector meson dominance — one can use directly eq. (3.48), rescaled to the electroweak scale to estimate its size, namely

$$\Pi_{3B}(p^2) \approx \frac{gg'}{4}\Pi_{LR}(p^2) \approx \frac{gg'}{4}\,v^2\,\frac{m_\rho^2 m_a^2}{(p^2+m_\rho^2)(p^2+m_a^2)}. \tag{3.115}$$

The value of $\hat{S}$ is then straightforwardly computed to be

$$\Delta\hat{S}_{\mathrm{TC}} = -\frac{g}{g'}\,\Pi'_{3B}(0) \approx \frac{g^2}{4}\frac{v^2}{m_\rho^2}\left(1+\frac{m_\rho^2}{m_a^2}\right), \tag{3.116}$$

which turns out to be substantial. For a QCD-like strong sector, with $m_a^2 \cong 2m_\rho^2$, it becomes

$$\Delta\hat{S}_{\mathrm{TC}} \approx \frac{(100\ \mathrm{GeV})^2}{m_\rho^2}. \tag{3.117}$$

A typical value of $m_\rho = 1.8$ TeV, as estimated in eq. (3.63), yields then $\Delta\hat{S}_{\mathrm{TC}} \approx 3\cdot 10^{-3}$, which clearly exceeds the range allowed by precision measurements, as can be seen from figure 3.13. Instead, the experimental limits can be used to put a lower bound on the mass of the lightest vector resonance. Requiring $\Delta\hat{S}_{\mathrm{TC}} \lesssim 2\cdot 10^{-3}$, one finds

$$m_\rho \gtrsim 2.2\ \mathrm{TeV}. \tag{3.118}$$

This bound is incompatible with the original function of the ρ resonance in technicolor models, which was to unitarise the scattering of massive gauge bosons. The most naive version of technicolor — where the strong sector is just a rescaled version of QCD — is therefore excluded by electroweak precision tests. Note however that some non-QCD-like technicolor models are still viable. Models with a nearly conformal strong dynamics and a small number N_{TC} of technicolors permit for example to reduce the $\hat{S}$ parameter drastically [117]. The minimal walking technicolor models [118,119], making use of fermions in a different representation of the technicolor gauge group, are another example of realistic realisations of a strong dynamics without a Higgs boson. Technicolor will not be discussed further here, the focus being turned instead to an elegant alternative, in which both strong dynamics and a Higgs boson are present.

3.2.3 The Higgs as a pseudo-Goldstone boson

The situation described up to now in this thesis can now be summarised as follows: All the physics discovered so far in the high-energy regime is very well described by the Standard model without a Higgs boson, as introduced in chapter 2. The agreement between theoretical predictions and experimental measurements is valid not only at tree-level, but extends as well to the the loop level in many observables. The only remaining open problem concerns the physics of the electroweak symmetry breaking. There are three open questions, which can be formulated in this way:

(i) What gives a mass to the $W^\pm$ and Z^0 gauge bosons, or equivalently what is the nature of the scalar fields χ^a acting as the longitudinal polarisation for them? From unitarity and renormalisability arguments,

the χ^a were proved not to be elementary scalar fields and need therefore to have a different origin.

(ii) What gives a mass to the fermions? From the chiral structure of the gauge theory, no direct couplings are allowed between left- and right-handed chiralities of quarks and leptons, so that new fields are needed at this point. The answer to this question can — but must not — have the same origin as (i).

(iii) Why is the electroweak scale $v \cong 246.2$ GeV as it is, or more precisely why is it so much lighter than the scale at which new physics must enter, that is the GUT or Planck scale? Answering questions (i) and (ii) might provide a mechanism for the breaking of the electroweak symmetry, but do not necessarily fixes its scale.

Two attempts to answer this set of questions were formulated so far in this thesis. The first option, implying weakly coupled physics only, is to have an elementary Higgs boson. Through its kinetic term and its Yukawa interaction with fermions, the Higgs doublet answers both questions (i) and (ii), but fails at giving a natural explanation to (iii). The alternative discussed in the beginning of this chapter is to trigger the electroweak symmetry by a strong dynamics, adding a new technicolor sector to the model. In this case the electroweak scale can naturally be generated at a low scale, answering question (iii), but (i) and (ii) are not fully satisfied. On the one hand, the mechanism giving a mass to the gauge bosons has to face an important tension regarding the scale of the new, strongly-interacting physics, preferred to be light by size of the electroweak scale, but indicated to be heavy by indirect measurements. On the other hand, the generation of fermion masses is also delicate, and requires a nearly conformal behaviour of the theory in order to suppress flavour-changing currents. Needless to say, the discovery of a Higgs-like particle by ATLAS and CMS experiments also speaks against technicolor theories.

The class of models which are going to be described now belongs to a hybrid category, taking the advantages of a Standard Model Higgs boson in answering (i) and (ii), while possessing a strong sector above the TeV scale as in technicolor in order to solve the problem (iii). There is indeed the possibility that the strong dynamics, instead of generating only three Goldstone bosons transforming as a triplet of $SU(2)_V$ as in technicolor, has a larger global symmetry group and contains an electroweak doublet among its Goldstone bosons. In this case, the strong sector does not break the electroweak symmetry in itself, its role being limited to produce a light Higgs doublet. The low-energy effective description of the theory is therefore that of the Standard Model, with the difference that the Higgs doublet is not an elementary field anymore, but a *composite* bound state from the strong sector [120,121]. Being a Goldstone boson, the Higgs doublet is mass-

less at tree-level and only enters the Lagrangian with derivative couplings, hence being protected by a shift symmetry. A potential can then be generated radiatively by weak effects involving the exchange of gauge bosons and fermions in the loops [26]. Due to the composite nature of the Higgs boson, there is no hierarchy problem anymore. Above a certain energy scale, or equivalently at very short distances, the Higgs boson does not exist in itself, but only in terms of its constituent fermions.

As learnt from large-N_c considerations, the low-energy physics of the strong sector is described by a non-linear σ-model of the form

$$\mathcal{L} = \frac{f^2}{4} \operatorname{Tr}\left(D_\mu \Sigma^\dagger D^\mu \Sigma\right) + \dots \tag{3.119}$$

where $\Sigma(x)$ is the Goldstone field, whose exact form is not specified yet. Covariant derivatives include the electroweak gauge fields $SU(2)_W \times U(1)_Y$, and a fundamental requirement of the model is that Σ contains at least one electroweak doublet with the hypercharge assignment of a Higgs boson. Note that since the Higgs is not charged under the colour gauge group $SU(3)_C$, there is no need for the $\Sigma(x)$ field to have colour interactions. The non-linear σ-model (3.119) is not much different from the technicolor case, with the exception that the scale f fixing the strength of the interaction between Goldstone boson is now different from the electroweak scale v. A mass term for the Goldstone field $\Sigma(x)$ is forbidden by the shift symmetry, and provided that the electroweak gauge group remains unbroken at the scale f, the $W^\pm$ and Z^0 gauge bosons, as well as the four components of the complex Higgs doublet, all remain massless at this stage. In terms of the symmetry groups, composite Higgs models require a global symmetry $\mathcal{G}$ in the strong sector to be spontaneously broken to a subgroup $\mathcal{H} \subset \mathcal{G}$ by a condensate of (techni-)fermions. The number of Goldstone bosons appearing in this process is given by the difference between the dimensions of the two symmetry groups,

$$N_G = \dim(\mathcal{G}) - \dim(\mathcal{H}) \geq 4. \tag{3.120}$$

As indicated, this number must be larger than four in order to contain at least one Higgs boson among the Goldstone modes. In a model featuring such a global symmetry breaking $\mathcal{G} \to \mathcal{H}$, the Goldstone bosons are parametrising excitations of the vacuum in the *coset space* $\mathcal{G}/\mathcal{H}$. A gauge symmetry is assumed to be present in the strong sector, as a subgroup $\mathcal{G}' \subset \mathcal{G}$. The same spontaneous symmetry breaking which breaks $\mathcal{G} \to \mathcal{H}$ might also break the gauge symmetry to a subgroup $\mathcal{H}'$ of the unbroken global symmetry group $\mathcal{H}$. If $\mathcal{H}' \neq \mathcal{H}$, i.e. if a part of the gauge symmetry is broken by the vacuum of the strong sector, the gauge fields associated with broken generators of $\mathcal{G}'$ will become massive, with a mass fixed by the scale f of the strong sector and by the strength of the gauge coupling. For each gauge boson acquiring a mass, a Goldstone must be eaten and disappear

from the low-energy spectrum. The number of massive gauge bosons, or equivalently the number of eaten Goldstone bosons, is given by

$$N_G^{\text{eaten}} = \dim\left(\mathcal{G}'\right) - \dim\left(\mathcal{H}'\right) \geq 0. \tag{3.121}$$

The number of physical Goldstone bosons remaining after spontaneous symmetry breaking in the strong sector — but before electroweak symmetry breaking — is therefore

$$N_G^{\text{phys}} = N_G - N_G^{\text{eaten}} = \dim\left(\mathcal{G}\right) - \dim\left(\mathcal{H}\right) - \dim\left(\mathcal{G}'\right) + \dim\left(\mathcal{H}'\right) \geq 4, \tag{3.122}$$

and must be at least four in order to contain a Higgs doublet. Although infinitely many possible possibilities exist for the symmetry breaking pattern, a reasonable choice must be dictated by simplicity, since the only particles observed so far are those described by the Standard Model. This requirement applies at two different levels. For gauge groups, it implies that the symmetry $\mathcal{H}'$ surviving after spontaneous symmetry breaking is not larger than necessary. For Goldstone bosons, the absence of observation of new light scalars indicates that there might be only a Higgs doublet in the low-energy spectrum, hence taking $N_G^{\text{phys}} = 4$. The elementary Higgs doublet of chapter 2 is charged only under the electroweak gauge group, and it is therefore natural to consider the minimal gauge sector $\mathcal{H}' = SU(2)_W \times U(1)_Y$. Following the same argument, one could choose not to have any additional global symmetry apart from the gauge group, choosing $\mathcal{H} = \mathcal{H}'$. The latter having dimension four, our choice of the global symmetry group $\mathcal{G}$ is dictated by the requirements that $\mathcal{G}$ contains $SU(2)\times U(1)$ as a subgroup and has at least dimension eight, and possibly not more. There is a simple Lie group satisfying these wishes, namely $\mathcal{G} = SU(3)$. Choosing a gauge group $\mathcal{G}' = SU(2)\times U(1)$ preserved by the spontaneous breaking of $\mathcal{G}$, the theory described in this way has four Goldstone bosons, all of them remaining physical after spontaneous symmetry breaking. Their charge under the electroweak gauge group can moreover be adjusted to match those of a Higgs doublet, and it seems at first that this choice leads to a viable composite Higgs model. However, in spite of its correct electroweak charge assignment, the doublet obtained in this simplistic model has different symmetry properties than the Standard Model Higgs boson, and would therefore lead to a different phenomenology. The reason is that the global symmetry of the Standard Model Higgs sector is not simply given by its $SU(2) \times U(1)$ gauge symmetry, but corresponds actually to $SO(4)$, or equivalently $SU(2)_L \times SU(2)_R$ (up to a $\mathbb{Z}_2$ parity). While the importance of the global $SO(4)$ symmetry is not straightforward — it is broken both by gauge and Yukawa interactions — we have seen in section 3.2.2 that its presence is indirectly implied by electroweak precision measurements, since it acts as a custodial symmetry for the ρ parameter. In other words, any realisation of the spontaneous symmetry breaking pattern $SU(3) \to SU(2) \times U(1)$ would lead to unacceptable large corrections of

the $\hat{T}$ parameter and be excluded by LEP data. As in technicolor models, this issue can be cured by imposing the presence of a custodial symmetry already in the strong sector of the theory, and ensuring that the vacuum condensate do not break it [122]. This is realised in practice by requiring $\mathcal{H} \supset SO(4)$. The minimal composite Higgs model enforcing custodial symmetry must then have $\mathcal{H} = SO(4)$, which is a group of dimension six, hence requiring a global symmetry group $\mathcal{G}$ of dimension greater or equal to ten. $SO(5)$ is such a candidate. Indeed, the minimal composite Higgs model, which will be described in much detail in section 3.3, is based on the coset $SO(5)/SO(4)$. Many other realistic models can be constructed in the same way. Some of them reproduce similar features as the minimal supersymmetric extension of the Standard Model, in the sense that they have two Higgs doublets instead of one [123]. Other models can have additional singlets in their low-energy spectrum [124]. Although no experimental evidence of the latter has been found, such singlets cannot yet be excluded due to their very mild couplings with gauge bosons and fermions. Note that in the case where one or more singlets are much lighter than the Higgs boson, the decay of the latter can be much affected, possibly even "burying" the Higgs signal into QCD backgrounds at collider experiments [125, 126]. Such models are of course now ruled out by the Higgs discovery. Additional Higgs-like scalars which are not singlets but multiplets under the electroweak gauge group can acquire a vacuum expectation value from a radiatively generated potential, hence contributing to the electroweak form factors. In addition to direct detection constraints, multiplets a have thus to face indirect bounds from electroweak precision data. A non-exhaustive list of symmetry breaking patterns yielding a Higgs boson protected by a custodial symmetry is given in table 3.2. Note that apart from the simple cosets presented here, there is a large freedom to build models out of product groups, some of them being presented later in section 3.4.

The choice of a global symmetry breaking pattern is only the first step towards the construction of a realistic composite Higgs model. The question of whether the electroweak symmetry will then be broken by the radiative corrections remains open and does not have a trivial answer. When a subgroup $\mathcal{G}' \subset \mathcal{G}$ is gauged, not all vacua are equivalent. In general, the true vacuum tends to align with the gauge symmetry preserving direction [127, 128], which means that when the subgroup $\mathcal{H}$ is large enough to contain the gauge group $\mathcal{G}' = \mathcal{H}'$, then the latter is automatically preserved even after a potential is generated at the loop level. Such a situation is unsatisfactory, since the electroweak symmetry must eventually be broken in order to generate a mass for the $W^{\pm}$ and Z^0 gauge bosons. A solution to this problem can appear once additional gauge groups are added into the model. If the true vacuum state of the theory cannot preserve all of the gauge group $\mathcal{G}'$ at tree-level but only a subgroup $SU(2) \times U(1)$ of it, then radiative corrections can break this remaining gauge symmetry further down

$\mathcal{G}$	$\mathcal{H}$	N_G	$\mathcal{R}[\mathcal{H}]$	$\mathcal{R}\,[SU(2)_L \times SU(2)_R]$
$SO(5)$	$SO(4)$	4	$\mathbf{4}$	$(\mathbf{2},\mathbf{2})$
$SO(6)$	$SO(5)$	5	$\mathbf{5}$	$(\mathbf{2},\mathbf{2}) \oplus (\mathbf{1},\mathbf{1})$
$SO(6)$	$SO(4) \times SO(2)$	8	$\mathbf{4}_{+2} \oplus \mathbf{4}_{-2}$	$(\mathbf{2},\mathbf{2}) \oplus (\mathbf{2},\mathbf{2})$
$SO(7)$	$SO(6)$	6	$\mathbf{6}$	$(\mathbf{2},\mathbf{2}) \oplus (\mathbf{1},\mathbf{1}) \oplus (\mathbf{1},\mathbf{1})$
$SO(7)$	G_2	7	$\mathbf{7}$	$(\mathbf{2},\mathbf{2}) \oplus (\mathbf{1},\mathbf{3})$
$SO(7)$	$SO(5) \times SO(2)$	10	$\mathbf{10}_0$	$(\mathbf{2},\mathbf{2}) \oplus (\mathbf{1},\mathbf{3}) \oplus (\mathbf{3},\mathbf{1})$
$SO(7)$	$[SO(3)]^3$	12	$(\mathbf{3},\mathbf{2},\mathbf{2})$	$(\mathbf{2},\mathbf{2}) \oplus (\mathbf{2},\mathbf{2}) \oplus (\mathbf{2},\mathbf{2})$
$Sp(6)$	$Sp(4) \times SU(2)$	8	$(\mathbf{4},\mathbf{2})$	$(\mathbf{2},\mathbf{2}) \oplus (\mathbf{2},\mathbf{2})$
$SU(5)$	$SU(4) \times U(1)$	8	$\mathbf{4}_{-5} \oplus \mathbf{4}_{+5}$	$(\mathbf{2},\mathbf{2}) \oplus (\mathbf{2},\mathbf{2})$
$SU(5)$	$SO(5)$	14	$\mathbf{14}$	$(\mathbf{3},\mathbf{3}) \oplus (\mathbf{2},\mathbf{2}) \oplus (\mathbf{1},\mathbf{1})$

Table 3.2: Non-exhaustive list of cosets spaces $\mathcal{G}/\mathcal{H}$ satisfying the requirements to contain at least one Higgs boson transforming as a bidoublet $(\mathbf{2},\mathbf{2})$ under $SU(2)_L \times SU(2)_R$. The number of Goldstone bosons and their representation under the unbroken group is indicated in each case. This table is taken from ref. [123].

to the electromagnetic gauge group $U(1)$ [129, 130]. The vacuum misalignment is generated in this case by the new gauge bosons, which are however heavy enough to remain undetected by experiments. An alternative to this mechanism is provided by the top quark, whose large Yukawa coupling can generate important radiative corrections to the scalar potential, hence generating by itself a misalignment of the true vacuum of the theory [131]. This is the mechanism active in the minimal composite Higgs model of section 3.3.

Once the electroweak symmetry breaking is broken by radiative corrections, the next problem arises. Since the condensate of (techni-)fermions breaks the $SU(2) \times U(1)$ electroweak symmetry anyway, there is no valid symmetry reason that can prevent the breaking $\mathcal{G} \to \mathcal{H}$ and $SU(2)_W \times U(1)_Y \to U(1)_{em}$ to happen at different scales. Equivalently, v and f should naively be of the same order, which is obviously not acceptable, since the success of the Standard Model is only recovered within composite Higgs models in the limit $v \ll f$, when all new physics decouples from the low-energy effective description. The opposite limit $v \to f$ corresponds actually to technicolor, where electroweak symmetry breaking is again a direct consequence of the spontaneous symmetry breaking in the strong sector. These two limits illustrates the fact that composite Higgs models are somehow a continuous interpolation between the Standard Model with a Higgs boson and a technicolor theory. The problem of generating naturally a large hierarchy between v and f is better understood in terms of the Higgs potential,

$$V(\mathcal{H}) = \frac{\mu^2}{2}\,\mathcal{H}^2 + \frac{\lambda}{4}\,\mathcal{H}^4 + \mathcal{O}\left(\mathcal{H}^6\right) \tag{3.123}$$

where $\mathcal{H} = v + h$ is the Higgs field in the unitary gauge, later acquiring a vacuum expectation value $\langle \mathcal{H} \rangle = v$. Both terms μ^2 and λ are generated radiatively by loops of gauge bosons, top quarks, or whatever new physics enters the model. From a naive dimensional analysis perspective, it is expected that they are both proportional to the same loop factor κ, and to the appropriate power of f obtained by dimensional arguments, namely

$$\mu^2 \approx -\kappa f^2, \qquad \lambda \approx \kappa. \tag{3.124}$$

Neglecting terms of order $\mathcal{H}^6$ and higher in the Higgs potential, the electroweak scale v and the physical Higgs boson mass are then given by

$$v^2 = -\frac{\mu^2}{\lambda} \approx f^2, \qquad m_h^2 = -2\mu^2 \approx 2\kappa f^2. \tag{3.125}$$

While the loop factor κ can easily account for a light Higgs mass compared to the strong scale f, naive dimensional analysis indicate that v is naturally of order f. The required smallness of v with respect to f constitutes the *little hierarchy problem* of composite Higgs models, and there are two possible attitudes towards it. First, one can accept the idea that f lives at a scale

not much higher than v, which can be obtained with a moderate amount of tuning, and find a minimal realisation of the composite Higgs mechanism whose deviations from the Standard Model will be important but acceptable. The requirement of minimality is crucial in this case since the new physics appearing at the scale f is readily testable by collider experiments. A second approach consists in adding new symmetries to the model so as to protect the size of the electroweak scale v from strong radiative corrections, effectively reducing the size of the Higgs quadratic term μ^2 compared to the quartic λ. This is the goal of *little Higgs* models, discussed below in section 3.4.

The remaining issue to be discussed concerning the electroweak sector of composite Higgs models is their effects on electroweak precision parameters. Note first that due to the composite nature of the Higgs boson, its couplings to the gauge bosons are slightly modified compared to the Standard Model, as will be discussed below. As a consequence, the processes involving the longitudinal components of gauge bosons are not fully unitarised by the exchange of the physical Higgs boson. However, the scale at which unitarity is lost is pushed towards a higher energy compared to the Higgsless scenario, and unitarisation is eventually completed at this higher scale by the vector resonances of the strong sector. The implementation of a custodial symmetry guarantees the smallness of $\hat{T}$, while $\hat{S}$ gets a contribution which is formally the same as in technicolor, i.e. given by eq. 3.116, but effectively less important due to the higher scale at which the strong dynamics needs to appear. The mass m_ρ of the first resonance is in particular rescaled with a factor of f/v compared to the technicolor scale, so that one has roughly

$$\Delta\hat{S}_{\mathrm{CH}} \approx \frac{v^2}{f^2}\Delta\hat{S}_{\mathrm{TC}}. \tag{3.126}$$

It can be seen again that the limit $f \to \infty$ corresponds to the Standard Model with a Higgs, for which the electroweak precision tests are fully satisfied. This limit is nevertheless unnatural, since it reintroduces the hierarchy problem into the theory.

The success of the composite Higgs models in the gauge and electroweak sector is incomplete if the models do not provide a successful description of fermion mass generation. Since the low-energy spectrum of the theory contains a Higgs doublet, an effective interaction can be written down which reproduces exactly the Standard Model Yukawa interaction. This effective term must originate from the strong sector, and must contain the Goldstone field $\Sigma(x)$, since its vacuum expectation value is the only source of electroweak symmetry breaking in the theory. The transformation properties of $\Sigma(x)$ are however not those of a Higgs doublet, and the fermion mass generation requires to use mechanism more involved than a direct Yukawa interaction. There are in principle two ways of circumventing this issue. The first possibility is to proceed as in technicolor models, by coupling a fermion

bilinear to an operator of the strong sector,

$$\mathcal{L}_{\text{eff}} \supset y_0\, \overline{q}_L \mathcal{O}_{qq} q_R. \tag{3.127}$$

The quantum number of the operator $\mathcal{O}_{qq}$ are those of a Higgs boson, so that a quadratic term of the form $\mathcal{O}_{qq}^\dagger \mathcal{O}_{qq}$ cannot be forbidden in the effective Lagrangian description. From its classical scaling dimension, it is clear that the quadratic operator is relevant — it has a dimensionful coefficient — and is therefore sensitive to the cutoff of the theory. The bound on the four-fermion operators derived from the absence of flavour-changing neutral currents are therefore hard to combine with the generation of quark masses from a TeV-scale strong dynamics. Note that the situation can nevertheless be better in this case than in technicolor models, due to the larger scale of the strong dynamics in the limit $v \ll f$. Such a mechanism could be use in little Higgs models, but fails in the minimal composite Higgs models where the ratio v/f is close to one.

The second possibility to generate quark and lepton masses is to use linear couplings of the Standard Model fields to composite operators, in the form

$$\mathcal{L}_{\text{eff}} \supset y_L\, \overline{q}_L \mathcal{O}_R + y_R\, \overline{q}_R \mathcal{O}_L + \text{h.c.} \tag{3.128}$$

y_L and y_R are here *proto-Yukawa* couplings, and $\mathcal{O}_L$ and $\mathcal{O}_R$ are fermionic operators arising from the strong sector. Contrarily to the previous case, no relevant operator can be built out of $\mathcal{O}_L$ and $\mathcal{O}_R$, both of them having a classical mass dimension of $5/2$. Moreover, there are no simple quadratic operators of the form $\overline{\mathcal{O}}_L \mathcal{O}_L$, $\overline{\mathcal{O}}_R \mathcal{O}_R$ or $\overline{\mathcal{O}}_L \mathcal{O}_R$, since the former two are vanishing due to spinor identities, while the latter is forbidden by gauge invariance, resulting from the fact that the left and right chiralities of Standard Model fermions have different charges under the electroweak gauge group. The lowest-dimension operators built out of $\mathcal{O}_L$ and $\mathcal{O}_R$ are $\overline{\mathcal{O}}_L \partial\!\!\!/ \mathcal{O}_L$ and $\overline{\mathcal{O}}_R \partial\!\!\!/ \mathcal{O}_R$, whose classical dimension is six, so that their scaling is irrelevant, even for a large anomalous dimension. From the linear coupling (3.128), it appears that the elementary Standard Model fermions are not eigenstates of mass. The physical quark and leptons will therefore be a mixture of the massless, elementary fields and of some heavy composite states with the same quantum numbers, described as

$$|\psi_{\text{phys}}\rangle = \cos\varphi\, |\psi_{\text{elementary}}\rangle + \sin\varphi\, |\psi_{\text{composite}}\rangle. \tag{3.129}$$

This mechanism carries the name of *partial compositeness*. The mixing angles φ — one for each chirality of the Standard Model quarks and leptons — are fixed by the relative size of the proto-Yukawa couplings y_L and y_R with respect to the mass of the composite states entering the operators $\mathcal{O}_L$ and $\mathcal{O}_R$. In the absence of electroweak symmetry breaking, the light composite state remain massless. It is only when an operator including $\mathcal{O}_L$, $\mathcal{O}_R$ and

the field Σ is added into the Lagrangian that masses for the Standard Model fermions are generated. Note that as we already mentioned, the quantum numbers of the field Σ does not allow to couple it directly to the composite operators $\mathcal{O}_L$ and $\mathcal{O}_R$. Nevertheless, the latter can be embedded into larger operators as $\mathcal{O}_{L,R} = \mathcal{P}_{L,R}\mathcal{O}'_{L,R}$ where $\mathcal{P}_{L,R}$ are projectors onto a subgroup of the global symmetry, in such a way that the Yukawa-like term

$$\mathcal{L}_{\text{eff}} \supset y_* \overline{\mathcal{O}}'_L \Sigma \mathcal{O}'_R + \text{h.c.} \tag{3.130}$$

is allowed by the symmetries of the Lagrangian. Integrating out the heavy composite states yields then an effective Yukawa interaction of the form

$$\mathcal{L}_{\text{eff}} \supset y_* \sin\varphi_L \, \sin\varphi_R \, \overline{q}_L^{\text{phys}} H q_R^{\text{phys}}. \tag{3.131}$$

Note that contrarily to the mechanism of fermion mass generation in technicolor models, no hierarchy is needed in the composite sector within the partial compositeness scenario. The fermion mass hierarchy can be introduced purely at the level of the proto-Yukawa couplings. Note finally that flavour-changing neutral currents can in principle be generated at tree-level by the exchange of vector resonances, since the physical fermionic states have a component from the strong sector. The relevant effective operator is

$$\mathcal{O}_{FCNC} = \frac{g_\rho^2}{m_\rho^2} \sin\varphi_i \sin\varphi_j \sin\varphi_k \sin\varphi_l \, (\overline{q}_i q_j) \, (\overline{q}_k q_l) \tag{3.132}$$

where g_ρ is a coupling between the first vector resonance ρ and the composite fermions mixing with the elementary ones. Since the mixing angles are directly related to the relative mass of the physical quarks and leptons with respect to the strong scale, a large suppression factor for this operator is automatically provided by the lightness of the Standard Model fermions. The only processes which could have relevance for the current experimental bounds are those involving third-generation quarks. The status of flavour-changing neutral currents will be discussed in more detail within the minimal composite Higgs model in section 3.3.5.

3.2.4 Warped extra-dimensions and holography

It was chosen explicitly in this thesis to stick to an effective description of the physics of electroweak symmetry breaking, which involves describing the physics in terms of operators most relevant at low energy, but also to work exclusively in the $3+1$ dimensional framework. The present section is however a short diversion into the physics of extra-dimensional models. Some of the features of composite Higgs models which may seem somewhat unnatural — like the required spontaneous symmetry breaking patterns or the mechanism of partial compositeness — have a very natural description in the holographic picture. The current excitement about extra-dimensional

physics is a consequence of a number of theoretical advances in the last fifteen years. Additional space-like dimensions beyond the three experienced in everyday's life are well motivated by string theory, but the original idea goes back to the theory of Kaluza and Klein nearly one century ago [132,133]. One of the key ingredients in this theory is that fields living in the bulk of a five-dimensional manifold can be written in an effective way as a sum over a tower of resonances on the four-dimensional boundary of it. This process is called *Kaluza-Klein decomposition*. The presence of a massless mode depends on the boundary conditions of the field. The infinite tower of modes, with or without a massless component, is reminiscent of the infinite tower of meson resonances in QCD, deduced from large-N_c considerations in section 3.1.2. Indeed, it has been postulated that there is a correspondence between a quantum field theory on a slice of anti-de-Sitter space and a different, conformal field theory defined in one less space dimension [134, 135, 136]. The so-called *AdS/CFT correspondence* was first observed in a particular realisation of a string theory model and is conjectured to hold in a more general framework. In particle physics, the correspondence is mostly used to gain information on (nearly-)conformal four-dimensional field theories in the strong regime where perturbative methods are useless. The power of the correspondence is to allow for explicit computations in the five-dimensional dual theory. Extra-dimensional theories reproducing the low-energy spectrum of QCD have been looked for [137, 138, 139], and the special use of the correspondence in this case is often denoted by AdS/QCD. Pion form factors are reproduced with good accuracy within this class of models [140,141], and baryon also emerge in this picture, with the enormous advantage that they belong to the perturbative regime of the theory, as will be discussed in more detail in section 4.2.6.

The presence of extra-dimensions has also a very appealing consequence for the physics of electroweak symmetry breaking. Considering the low-energy physics described by the Standard Model to be confined onto a four-dimensional brane inside a five-dimensional manifold [142] can naturally explain the weakness of the gravitational force compared with the gauge interactions present in particle physics, since gravity automatically propagates in all physical dimensions — the space-time dimensions being actually defined by the metric tensor [143, 144]. The behaviour of gravity in four dimensions is however tested with great accuracy on large distances, and indicates therefore that the extra-dimensions must be compact and of very small size to be in agreement with observations. The latter assumptions can actually be relaxed if the metric of the additional space dimensions is not flat but rather *warped*. This happens in particular in anti-de-Sitter spaces entering the AdS/CFT correspondence. Gravity being defined in the bulk of the extra-dimension, the effective value of the Planck scale appears much reduced in the four-dimensional theory. Due to the exponential form of the five-dimensional anti-de-Sitter metric, the suppression is actually exponen-

tial as well, so that the cutoff of the four-dimensional theory induced by quantum gravitational effects may be as low as the TeV scale, and there is no hierarchy problem as defined in section 2.4.3 [145]. An equivalent formulation of this mechanism is that the electroweak scale is generated close to the Planck scale in the extra-dimensional theory, but appear as low as it is in nature due to the warped form of the fifth dimension. Note that this solution of the hierarchy problem does not actually rely on the size of the additional dimension, but rather on its curvature, such that extra-dimensions of infinite size are plausible as well [146].

Warped extra-dimensional models seem therefore to represent a third solution to the hierarchy problem after supersymmetry and strong dynamics, but are actually likely to be only a dual description of the latter. As mentioned already, fields living in the bulk of the five-dimensional space can be decomposed in Kaluza-Klein modes, i.e. the component of their wavefunction along the fifth-dimension can be integrated out, and they look eventually like composite objects in the effective four-dimensional description. Zero-modes appear as massless particles and correspond to the Goldstone bosons in a strongly-coupled theory language, while massive modes form a tower resonances like the vector mesons. The dependence on the fifth dimension has similar effects than the composite nature of mesons in a strongly-coupled theory. Their properties can both be described effectively in terms of energy-dependent form factors. In addition to the bulk fields, extra-dimensional models might contain fields confined to the boundaries of the 5D space. They correspond to elementary fields in the 4D description. In terms of symmetries, the gauge symmetry which might be present in the 5D bulk appears as well in the 4D theory as a global symmetry group $\mathcal{G}$, using the notation defined above. Depending on the boundary conditions on the UV brane, a part of it can be preserved at all energy scales and corresponds therefore to a true local symmetry of the 4D theory, namely the gauged subgroup $\mathcal{G}' \subset \mathcal{G}$. The part of the symmetry which is broken by the UV boundary conditions is only a global symmetry of the strongly-coupled theory. A different subgroup of $\mathcal{G}$ can be broken by the boundary conditions on the IR brane, so that only the subgroup $\mathcal{H} \subset \mathcal{G}$ is preserved at low energies. Although it is not straightforward that the explicit breaking $\mathcal{G} \to \mathcal{H}$ by IR boundary conditions corresponds effectively to a mechanism of spontaneous symmetry breaking in 4D, it is actually always possible to describe this process by considering a scalar field which acquires a vacuum expectation value [147].

From this perspective, five-dimensional models of electroweak symmetry breaking can easily be built and have an effective 4D description similar to technicolor theories, but they extend their predictivity in the sense that important information on the strong sector of the theory can be derived directly from computations within the 5D framework. The longitudinal polarisations of the $W^{\pm}$ and Z^0 are provided in this case by the zero-mode

of some gauge bosons living in the bulk, and the designation of *gauge-Higgs unification* is often used in this context, and the resulting 4D theory is effectively Higgsless [148]. The unitarity in scattering processes of gauge bosons is restored by the Kaluza-Klein tower of the same 5D gauge bosons [147]. Like in technicolor models, an important tension arises however when considering electroweak precision tests. Provided that a custodial symmetry is present, the parameter $\hat{T}$ is kept at a low level [149], but the lightness of the first Kaluza-Klein modes required to unitarise the effective theory give a large contribution to the $\hat{S}$ parameter.

The solution to this problem is to impose 5D boundary conditions wisely so as not to break the electroweak symmetry directly. An elementary scalar field confined to the IR brane or living close to it play eventually the role of the Higgs doublet and breaks the electroweak symmetry due to a potential generated purely in the weak regime. This scenario has an effective 4D description which matches exactly the definition of composite Higgs models given in the previous section [150]. Note that the large mass hierarchy of fermions finds an interesting explanation in terms of the overlap of their wavefunction with that of a Higgs field along the fifth dimension. More generally, the localisation of a field in the bulk fixes the anomalous dimension of the corresponding operator in the 4D conformal theory. Finally, note that unlike in the original conjecture, the strongly-coupled theory must not be exactly conformal at all energy levels and deviations from a pure anti-de-Sitter metric in 5D can actually lead to interesting effects. While AdS/QCD models are mostly independent on the warping factor of the metric [151], the latter affects the electroweak precision observables in extra-dimensional realisations of the Standard Model with a composite Higgs boson. A rather generic suppression of the $\hat{S}$ and $\hat{T}$ parameters is observed, up to the point in which the necessity of imposing a tree-level custodial symmetry into the theory disappears [152, 153, 154].

3.2.5 Effective theory approach

Going back to the four-dimensional description, the low-energy phenomenology of composite Higgs models is better examined with the tools of effective field theory. There is a variety of specific models which feature the Higgs as a composite, pseudo-Goldstone boson as described in section 3.2.3. Many predictions of these composite Higgs models are actually generic and can be studied in a model-independent approach. The effective field theory framework is particularly well-suited for this purpose, since composite Higgs models possess a mass gap between the electroweak scale v and the strong scale f, which motivates to integrate out the new physics beyond the Standard Model particles and the composite Higgs boson in order to study the phenomenological implications at and below the weak scale. The procedure is to write down all possible operators involving only Standard Model fields

and the Higgs doublet, and to use information from symmetry arguments and from our limited knowledge of the strong sector to estimate the size of their coefficients. Operators with the lowest classical scaling dimension play the most important role. As discussed already in section 2.5.1, the only operator of dimension five is the one of eq. (2.91), giving a mass to the neutrino. Going up to dimension six, many more operators are present [155]. Not all of them are relevant to the description of composite Higgs models. The discussion will be focused on deviations from the Standard Model, which arise in the low-energy sector mostly from the composite nature of the Higgs doublet [156]. The parametrisation used in the following is the so-called *strongly-interacting light Higgs* Lagrangian [157], which is a complete effective description of the Higgs physics relying on a small number of assumptions.

The first fundamental assumption is that the theory contains a scalar doublet with the quantum numbers of a Higgs field, which is moreover an exact Goldstone in the limit of vanishing Standard Model gauge and Yukawa couplings. As a consequence, the strength of operators involving only the Higgs doublet H is fixed by a unique parameter, which can be taken as the constant f entering σ-model parametrisation. Due to the shift symmetry associated with the Goldstone nature of the Higgs doublet, the latter can enter the Lagrangian only through the linear combination $\left(H^\dagger H\right)$ or through derivative terms of the form $(H^\dagger \overleftrightarrow{D}_\mu H) = (H^\dagger D_\mu H - D_\mu H^\dagger H)$ or $(D_\mu H^\dagger D^\mu H)$. Any other use of the Higgs field is prohibited. For example, there is no operator

$$\frac{1}{\Lambda^2}\left(H^\dagger \sigma^i H\right) W^i_{\mu\nu} B^{\mu\nu}, \tag{3.133}$$

which would in principle be allowed by the global and gauge symmetries of the Standard Model, but breaks the shift symmetry of the Higgs boson. Note that this operator would give a tree-level contribution to the parameter $\hat{S}$, and it size is therefore very much constrained by electroweak precision data. This argument shows the crucial importance of the Goldstone nature of the Higgs.

The second model-independent assumption on which the construction of the effective Lagrangian relies is that the effects of new physics in the strong sector beyond the composite Higgs can be described by a single mass scale m_ρ. The notation for this scale is a remnant of QCD-like theories, where the lightest state of the strong sector is the ρ vector meson resonance. In general, m_ρ needs not be associated with a vector resonance, but the latter is favoured since the new physics must somehow complete the partial unitarisation of $W^\pm$ bosons scattering initiated by the Higgs. m_ρ can be related to the scale f by the introduction of a coupling

$$m_\rho = g_\rho f, \tag{3.134}$$

where g_ρ denotes generically the coupling strength of the strong sector to the Goldstone bosons. Note that the description of the Goldstone sector in terms of a non-linear σ-model is valid up to the scale $\Lambda \approx 4\pi f$, at which new physics must appear. It is therefore legitimate to assume an upper bound for the strong coupling, $g_\rho \lesssim 4\pi$.

The effective Lagrangian can now be written down under these assumptions. Operators of dimension four form the renormalisable, Standard-Model-like part of the Lagrangian,

$$\mathcal{L} = D_\mu H^\dagger D^\mu H + \mu^2 \left(H^\dagger H\right) - \lambda \left(H^\dagger H\right)^2 - \left(y_f \, \overline{f}_L H f_R + \text{h.c.}\right). \quad (3.135)$$

The covariant derivatives of the Higgs doublet involve as usual the $SU(2)_W$ and $U(1)_Y$ gauge bosons. The constant y_f is the fermion Yukawa coupling defined as $y_f = \sqrt{2} m_f / v$. There is in principle one such coupling for each quark and lepton, but only the top mass will be relevant in the present discussion. μ^2 and λ are here the Higgs quadratic and quartic coupling respectively, corresponding in terms of physical quantities to $\mu^2 = m_h^2/(2v)$ and $\lambda = m_h^2/(2v^2)$. Note that the Goldstone shift symmetry forbids in principle a potential for the Higgs at tree-level, but that radiative corrections induced by gauge fields and by the top quark must eventually induce a quadratic and a quartic term for the Higgs doublet. Dimension-six operators can similarly be built following the rules established above, and one finds the following list of operators:

$$\begin{aligned}
\mathcal{O}_H &= \frac{c_H}{2f^2} \partial_\mu \left(H^\dagger H\right) \partial^\mu \left(H^\dagger H\right), \\
\mathcal{O}_T &= \frac{c_T}{2f^2} \left(H^\dagger \overleftrightarrow{D}_\mu H\right) \left(H^\dagger \overleftrightarrow{D}^\mu H\right), \\
\mathcal{O}_r &= \frac{c_r}{2f^2} \left(H^\dagger H\right) \left(D_\mu H^\dagger D^\mu H\right), \\
\mathcal{O}_\lambda &= -\frac{c_6 \lambda}{f^2} \left(H^\dagger H\right)^3, \\
\mathcal{O}_f &= \frac{c_y \, y_f}{f^2} \left(H^\dagger H\right) \left(\overline{f}_L H f_R\right) + \text{h.c.}, \\
\mathcal{O}_W &= i \frac{c_W \, g}{2m_\rho^2} \left(H^\dagger \sigma^i \overleftrightarrow{D}^\mu H\right) \left(D^\nu W^i_{\mu\nu}\right), \\
\mathcal{O}_B &= i \frac{c_B \, g'}{2m_\rho^2} \left(H^\dagger \overleftrightarrow{D}^\mu H\right) \left(D^\nu B_{\mu\nu}\right), \\
\mathcal{O}_{HW} &= i \frac{c_{HW} \, g}{16\pi^2 f^2} \left(D^\mu H^\dagger \sigma^i D^\nu H\right) W^i_{\mu\nu}, \\
\mathcal{O}_{HB} &= i \frac{c_{HB} \, g'}{16\pi^2 f^2} \left(D^\mu H^\dagger D^\nu H\right) B_{\mu\nu},
\end{aligned} \quad (3.136)$$

$$\mathcal{O}_\gamma = \frac{c_\gamma\, g'^2}{16\pi^2 f^2}\frac{g^2}{g_\rho^2}\left(H^\dagger H\right) B_{\mu\nu}B^{\mu\nu},$$
$$\mathcal{O}_g = \frac{c_g\, g_S^2}{16\pi^2 f^2}\frac{y_t^2}{g_\rho^2}\left(H^\dagger H\right) G^a_{\mu\nu}G^{\mu\nu\,a}.$$

All available information from the strongly-coupled nature of the theory is used in the definition of each operator and the coefficients c_i are thus expected to be of order unity, unless an additional symmetry protects them. The first five operators $\mathcal{O}_H$, $\mathcal{O}_T$, $\mathcal{O}_r$, $\mathcal{O}_\lambda$ and $\mathcal{O}_f$ arise as a consequence of the strongly-interacting nature of the Higgs boson, and come therefore directly from the expansion of the non-linear σ-model field $\Sigma(x)$. Since they are all issued from Standard model operators with two additional Higgs insertions, their suppression factor is naturally $1/f^2$. $\mathcal{O}_H$, $\mathcal{O}_T$ and $\mathcal{O}_r$ are generated by the kinetic term of the non-linear σ-model and contain therefore no additional coefficients, while $\mathcal{O}_\lambda$ and $\mathcal{O}_f$ are proportional to the coupling constants of the corresponding Standard Model operators with two Higgs fields less. Note that these five operators are not linearly independent in the general definition above. Under a field redefinition

$$H \to \left[1 + \alpha\left(H^\dagger H\right)/f^2\right] H, \tag{3.137}$$

the modification of the renormalisable Lagrangian (3.135) induces a change in the coefficients

$$c_H \to c_H + 2\alpha, \quad c_r \to c_r + 4\alpha, \quad c_6 \to c_6 + 4\alpha, \quad c_y \to c_y - \alpha. \tag{3.138}$$

This symmetry can be used for example to eliminate the operator $\mathcal{O}_r$. However, the most general basis including $\mathcal{O}_r$ as been proved useful for practical purposes [158]. The remaining six operators in eq. (3.136) are not generated by the σ-model Lagrangian, but involve the exchange of heavy particles at the tree- or loop-level and are thus proportional to the parameters m_ρ and g_ρ of the strong sector. The tree-level exchange of a vector resonance can in particular generate $\mathcal{O}_W$ and $\mathcal{O}_B$, so that their coefficients are simply suppressed by the inverse of the mass of the resonance, $1/m_\rho^2$. In general the same tree-level exchange could give rise to $\mathcal{O}_{HW}$ and $\mathcal{O}_{HB}$ as well, but the latter two operators contribute respectively to the gyromagnetic ratio $(g-2)$ of the $W^\pm$ gauge boson and to the coupling of an on-shell photon to neutral states, and such interactions are usually absent at tree-level in the most simple theories. This assumption is not universal, but is valid in the case of holographic composite Higgs models as well as in little Higgs models. Starting at the loop level, the suppression factor is then $1/(4\pi f)^2$. Note that for a maximal value $g_\rho = 4\pi$ of the strong coupling, there is no difference between the suppression factors from tree-level exchange of a ρ meson and from a loop process.The last two operators, $\mathcal{O}_\gamma$ and $\mathcal{O}_g$, cannot

be generated at tree-level since the Higgs bilinear term $\left(H^\dagger H\right)$ is uncharged under the electroweak gauge group. They are however generated by loops of fermions (for both of them) and gauge bosons (only for $\mathcal{O}_\gamma$). In addition, since the electroweak symmetry breaking is only generated by weak corrections from the low-energy sector, only elementary Standard Model fields contribute to the loop processes, and an additional suppression factor of g_{SM}/g_ρ enters the coefficient of these two operators. This suppression factor can be important if g_ρ is large.

The effective formalism derived here can easily be related to physical observables. This is valid for the phenomenology of the Higgs boson, which will be discussed in the next section, for flavour physics, and most straightforwardly for electroweak precision observables. The parameter $\hat{T}$ is actually directly related to the operator $\mathcal{O}_T$ through the relation

$$\Delta\hat{T}_{\text{SILH}} = c_T \frac{v^2}{f^2}, \tag{3.139}$$

and the experimental bounds derived in section 3.2.2 can be directly turned into a bound on the coefficient c_T, whose unnatural size indicate that an additional symmetry must be present in the model. The latter is exactly the custodial symmetry introduced above. If such a symmetry is present, the operator $\mathcal{O}_T$ is not generated at tree-level, but can still be non-zero due to loop processes. Naive dimensional analysis indicate a reduction

$$c_T \to \frac{c_T}{4\pi^2}\frac{y_t^2}{g_\rho^2}. \tag{3.140}$$

As mentioned already, there is no contribution to the parameter $\hat{S}$ coming directly from the strong nature of the Higgs boson. Heavy vector meson exchanges can nevertheless generate an important tree-level contribution, as in technicolor models. The relevant operators are $\mathcal{O}_W$ and $\mathcal{O}_B$, and we have

$$\Delta\hat{S}_{\text{SILH}} = (c_W + c_B)\frac{m_W^2}{m_\rho^2}. \tag{3.141}$$

Note that this contribution is exactly equal to the technicolor case given in eq. (3.116) when the coefficients are fixed to $c_W = c_B = 1$ as expected by naive dimensional analysis and when the strong sector has a chiral symmetry implying $m_a = m_\rho$. Effects induced by the mass differences $m_a \neq m_\rho$ can be enclosed in the effective theory approach into the coefficients c_W and c_B.

Another physical effect with direct experimental consequences is the decay of the Higgs boson into two real photons. The definitions (3.136) were chosen so that the operators $\mathcal{O}_W$, $\mathcal{O}_B$, $\mathcal{O}_{HW}$ and $\mathcal{O}_{HB}$ do not contribute to the process $h \to \gamma\gamma$, so that only $\mathcal{O}_\gamma$ is relevant for it. An estimate of this decay can be made in the framework of the low-energy theorem, which will

be presented in the next section in the different context of Higgs production through gluon fusion [2].

Note that the list of operators in eq. (3.136) is not complete. An operator including four derivatives of the Higgs field was for example omitted, since its effects are irrelevant to the energy ranges tested by present and near-future experiments. Additional operators including derivatives of the field strength tensors $W^a_{\mu\nu}$ and $B_{\mu\nu}$ were neglected as well. The later are also expected to give a subleading contribution to observables processes, but could nevertheless be relevant to electroweak precision tests through the parameters W and Y defined in eq. (3.111) and (3.114).

The coefficients in eq. (3.136) can be related to the parametrisation of chapter 2, given in eq. (2.66), (2.67) and (2.68) in terms of the parameters $a, b, c, \ldots$ The latter were introduced to parametrise the interactions of a scalar field h, which, like an elementary Higgs boson, has the quantum numbers of the vacuum. Since the low-energy spectrum of our effective description contains in addition to the Standard Model particles only a light composite Higgs, the two parametrisations are equivalent under the identification

$$\begin{aligned} a &= 1 - \tfrac{1}{4}\,\xi\,(2c_H - c_r)\,, \\ b &= 1 - \xi\,(2c_H - c_r)\,, \\ c &= 1 - \tfrac{1}{2}\,\xi\,(c_H + 2c_y)\,, \\ c_2 &= -\tfrac{1}{2}\,\xi\,\left(c_H + 3c_y + \tfrac{1}{4}c_r\right), \\ d_3 &= 1 + \xi\,\left(c_6 - \tfrac{3}{2}c_H - \tfrac{1}{4}c_r\right), \\ d_4 &= 1 + \xi\,\left(6c_6 - \tfrac{25}{3}c_H - \tfrac{11}{6}c_r\right), \end{aligned} \tag{3.142}$$

where the dimensionless parameter ξ is defined as

$$\xi = \frac{v^2}{f^2}. \tag{3.143}$$

ξ plays a fundamental role since it describes the strength of deviations from the Standard Model with an elementary Higgs boson. Eq. (3.142) makes it evident that the limit $\xi \to 0$ (or equivalently $f \to \infty$) is nothing but the Standard Model, as defined by the special choice of parameters $a = b = c = d_3 = d_4 = 1$ and $c_2 = 0$. Any deviation from these values in eq. (3.142) is proportional to the parameter ξ. In the opposite limit $\xi = 1$ or $v = f$, corresponding to technicolor, all parameters are getting corrections of order one, and the scalar field h does not have any of the characteristics of a Standard Model Higgs boson. Note that all linear combinations of the coefficients in eq. (3.142) are invariant under the shift symmetry (3.137). This notation also shows that in the case of a composite Higgs models, the coefficients a and b describing the Higgs interactions with gauge bosons have

the same origin in the strong sector, since their deviations from the Standard Model are scaling proportionally to each other.

Let us conclude this section with an important remark. The electroweak scale $v \cong 246$ GeV which was used throughout this thesis is defined from the experimental measurement of Fermi's constant G_F in leptonic processes at LEP, and corresponds to

$$v = \left(\sqrt{2}\, G_F\right)^{-1/2}. \tag{3.144}$$

It is therefore related to the mass of the $W^\pm$ gauge boson by the tree-level relation $m_W = gv/2$, which gets however corrected at the loop level. It should be stressed here that v is in this sense not directly related to the vacuum expectation value of the Higgs field H. Working in a general basis where $c_r \neq 0$ and in the unitary gauge

$$H = \frac{1}{\sqrt{2}} \begin{pmatrix} 0 \\ \mathcal{H} \end{pmatrix}, \tag{3.145}$$

the relation between $\langle \mathcal{H} \rangle$ and v is given by

$$v^2 = \langle \mathcal{H} \rangle^2 \left(1 + \frac{c_r}{4} \frac{\langle \mathcal{H} \rangle^2}{f^2}\right). \tag{3.146}$$

Similarly, the kinetic term for the field h is not necessarily properly normalised. The dimension-six operators (3.136) introduce a correction to the renormalisable part (3.135) of the Lagrangian given by

$$\Delta \mathcal{L}_{h\,\mathrm{kin}} = \frac{1}{2f^2} \left(c_H + \frac{c_r}{4}\right) \left(\langle \mathcal{H} \rangle + h\right)^2 \partial_\mu h \partial^\mu h. \tag{3.147}$$

At leading order in v/f, this term can be eliminated by the non-linear field redefinition

$$h \to h - \frac{v^2}{2f^2} \left(c_H + \frac{c_r}{4}\right) \left(h + \frac{h^2}{v} + \frac{h^3}{3v^2}\right). \tag{3.148}$$

Alternatively, one can use the freedom of the shift symmetry (3.137) to fix the coefficients such that $c_H + c_r/4 = 0$. Note that the latter equality is automatically realised in the non-linear σ-model description of a composite Higgs, for which the physical Higgs field h is canonically normalised at all orders in v/f.

3.2.6 Higgs low-energy theorem

Before constructing an explicit realisation of the composite Higgs idea, the maximum amount of information should be extracted from model-independent

considerations. The effective theory framework discussed here is the appropriate tool to do so. The phenomenology of composite Higgs models is in principle not very dramatic. Indeed, the theory is built such that the low-energy physics mimics the Standard Model in the decoupling limit. All the light particles are (mostly) elementary fields, and no severe deviations from Standard Model predictions are expected to be seen. The notable exception to this rule is the Higgs doublet, which is light but is nevertheless a composite object belonging to the strong sector of the theory. The effects of the Higgs compositeness can be noticed in electroweak precision tests, via the longitudinal polarisation of the gauge bosons, as discussed already. The other observables where significant deviations from the Standard Model could be observed are those involving the physical Higgs boson. In the Standard Model, for a light Higgs mass below the threshold for $W^\pm$ boson pair production, the decay width of the Higgs boson is small compared to its mass, so that the Higgs appears as a narrow resonance and its production and decay can be examined as separated processes. This behaviour is well reproduced in composite Higgs models. Electroweak precision observables indicated that the Higgs boson must be light, so that its decay can only proceed through particle lighter than the $W^\pm$ gauge boson, which are all very much like in the Standard Model. A possible exception to this rule is when additional Goldstone bosons lighter than the Higgs are present in the spectrum, as mentioned already. In all other cases, significant deviations from the Standard Model are only likely to occur in the Higgs production mechanism. At the LHC, Higgs single and pair production are dominated by gluon fusion processes, which involve a loop of fermions. Contrarily to its decay, heavy fermions contribute the most to Higgs production, so that large deviations from the Standard Model could in principle be expected.

The study of Higgs production via gluon fusion is made possible in a model-independent framework by the use of the low-energy theorem [159, 160]. The interactions of the physical Higgs boson with gluons, mediated by loops of heavy coloured particles, can be obtained by treating the Higgs H as a background field and taking the field-dependent mass of each heavy particle as a threshold for the running of the QCD gauge coupling. Assuming heavy particles p_i to transform in the fundamental representation of $SU(3)_C$, one obtains, after they are integrated out, the following effective Lagrangian

$$\mathcal{L}_{\text{eff}} = \frac{g_S^2}{64\pi^2}\, G^a_{\mu\nu} G^{\mu\nu\, a} \sum_{p_i} \delta b_{p_i} \log m^2_{p_i}(H), \tag{3.149}$$

where $\delta b = 2/3$ if the particle p_i is a Dirac fermion, and $\delta b = 1/6$ if it is a complex scalar. In composite Higgs models, the only relevant effects are those of the heavy fermion sector, which includes the top quark and new states required by the partial compositeness mechanism. By expanding the field-dependent masses of the heavy particles around the vacuum expecta-

tion value $\langle\mathcal{H}\rangle$, the couplings of the Higgs boson to gluons, mediated by loops of heavy fermions, is obtained as

$$\mathcal{L}_{h^n gg} = \frac{g_S^2}{96\pi^2}\, G^a_{\mu\nu} G^{\mu\nu\, a} \left(A_1 h + \frac{1}{2} A_2 h^2 + \dots \right), \tag{3.150}$$

where the coefficients A_n are defined as

$$A_n = \left[\frac{\partial^n}{\partial H^n} \log\det \mathcal{M}^2(H) \right]_{\langle\mathcal{H}\rangle}, \tag{3.151}$$

$\mathcal{M}$ is the heavy fermion mass matrix and $\mathcal{M}^2$ is a shorthand notation for $\mathcal{M}^\dagger\mathcal{M}$. Equivalently, the first two coefficients in the expansion can be written as

$$A_1 = \frac{1}{\langle\mathcal{H}\rangle} \left[\frac{\partial}{\partial(\log H)} \log\det \mathcal{M}^2(H) \right]_{\langle\mathcal{H}\rangle}, \tag{3.152}$$

$$A_2 = \frac{1}{\langle\mathcal{H}\rangle^2} \left[\left(\frac{\partial^2}{\partial(\log H)^2} - \frac{\partial}{\partial(\log H)} \right) \log\det \mathcal{M}^2(H) \right]_{\langle\mathcal{H}\rangle}. \tag{3.153}$$

In the Standard Model, only the top quark contributes with $\mathcal{M}(H) = m_t(H) = y_t H/\sqrt{2}$,[12] so that eq. (3.150) can be rewritten at all orders in h as [161]

$$\mathcal{L}_{h^n gg} = \frac{g_S^2}{48\pi^2}\, G^a_{\mu\nu} G^{\mu\nu\, a}\, \log\left(1 + \frac{h}{v}\right). \tag{3.154}$$

The corresponding gauge-invariant operator $G^a_{\mu\nu} G^{\mu\nu\, a}\, \log(H^\dagger H)$ is the generic contribution associated with a chiral fermion. The lowest-order operator arising from vector-like fermions is instead $G^a_{\mu\nu} G^{\mu\nu\, a}\, H^\dagger H$. The effects of these two different operators on double Higgs production are discussed in ref. [162].

In composite Higgs models, both the top quark and the heavy composite fermions give a contribution to the low-energy theorem. Working in the effective formalism of the previous section, one has to face the difficulty that the top is present as fundamental particle state in the effective theory, while the effects of composite fermions are already integrated out and enclosed in the operator $\mathcal{O}_g$ in eq. (3.136). Due to the presence of a logarithm in eq. (3.149), the determinant $\det \mathcal{M}^2(H)$ can however be split into a sum of two pieces,

$$\log\det \mathcal{M}^2(H) = \log m_t^2(H) + \log\det \mathcal{M}^2_{\text{comp}}(H). \tag{3.155}$$

The mass of the top quark is given in the effective formalism by

$$m_t(H) = \frac{y_t\, H}{\sqrt{2}} \left(1 - c_y \frac{H^2}{2f^2} \right). \tag{3.156}$$

[12] The contribution from the bottom quark is non-negligible but cannot be computed using the low-energy theorem due to the smallness of its mass.

In addition to the contribution from the top quark, computed explicitly from the expression above, the remaining fermionic states generate a term proportional to the coefficient c_g, and one has finally, at leading order in v^2/f^2,

$$\frac{1}{2}\left(\frac{\partial}{\partial(\log H)}\log\det\mathcal{M}^2(H)\right)_{H=v} = 1 - c_y\frac{v^2}{f^2} + 3c_g\,\frac{y_t^2 v^2}{m_\rho^2}, \tag{3.157}$$

$$\frac{1}{2}\left(\left(\frac{\partial^2}{\partial(\log H)^2} - \frac{\partial}{\partial(\log H)}\right)\log\det\mathcal{M}^2(H)\right)_{H=v} = -1 - c_y\frac{v^2}{f^2} + 3c_g\,\frac{y_t^2 v^2}{m_\rho^2}. \tag{3.158}$$

Note that the implicit expressions containing the determinant are in practice more useful than the explicit ones written in terms of c_y and c_g, because using the former avoids diagonalising the heavy fermion mass matrix, a rather complicated task in presence of multiple top partners. An additional subtle point has to be addressed. In eq. (3.150), it has been assumed that h is canonically normalised, which is actually not the case in the general parametrisation made above. The canonical normalisation of the Higgs boson is obtained at leading order in v^2/f^2 by performing the transformation (3.148), which yields the effective coupling of the Higgs to two gluons [163, 158]

$$\mathcal{L}_{hgg} = \frac{g_S^2}{48\pi^2}\,G^a_{\mu\nu}G^{\mu\nu\,a}\,\frac{h}{v}\left[\frac{1}{2}\left(\frac{\partial}{\partial(\log H)}\log\det\mathcal{M}^2(H)\right)_{H=v} - \frac{c_H}{2}\,\frac{v^2}{f^2}\right], \tag{3.159}$$

and the corresponding term with two Higgs bosons

$$\begin{aligned}\mathcal{L}_{hhgg} = {} & \frac{g_S^2}{96\pi^2}\,G^a_{\mu\nu}G^{\mu\nu\,a}\,\frac{h^2}{v^2} \\ & \cdot\left[\frac{1}{2}\left(\left(\frac{\partial^2}{\partial(\log H)^2} - \frac{\partial}{\partial(\log H)}\right)\log\det\mathcal{M}^2(H)\right)_{H=v} - \frac{c_r}{4}\,\frac{v^2}{f^2}\right].\end{aligned} \tag{3.160}$$

Putting everything together, the effective Higgs to gluons couplings read

$$\mathcal{L}_{hgg} = \frac{g_S^2}{48\pi^2}\,G^a_{\mu\nu}G^{\mu\nu\,a}\,\frac{h}{v}\left[1 - \left(c_y + \frac{c_H}{2}\right)\frac{v^2}{f^2} + 3c_g\,\frac{y_t^2 v^2}{m_\rho^2}\right], \tag{3.161}$$

$$\mathcal{L}_{hhgg} = \frac{g_S^2}{96\pi^2}\,G^a_{\mu\nu}G^{\mu\nu\,a}\,\frac{h^2}{v^2}\left[-1 - \left(c_y + \frac{c_r}{4}\right)\frac{v^2}{f^2} + 3c_g\,\frac{y_t^2 v^2}{m_\rho^2}\right]. \tag{3.162}$$

Equivalently, neglecting the effects of the strong sector suppressed by $1/m_\rho^2$, the top loop contribution can be written in terms of the parametrisation of chapter 2, using the relations (3.142)

$$\mathcal{L}_{hgg} = \frac{g_S^2}{48\pi^2}\,G^a_{\mu\nu}G^{\mu\nu\,a}\,\frac{h}{v}\,c, \qquad \mathcal{L}_{hhgg} = \frac{g_S^2}{96\pi^2}\,G^a_{\mu\nu}G^{\mu\nu\,a}\,\frac{h^2}{v^2}\left(2c_2 - c^2\right). \tag{3.163}$$

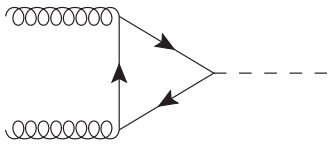

Figure 3.14: One-loop diagram contributing to the single Higgs production via gluon fusion at the LHC. All fermions carrying a colour charge can run into the loop.

In this last expression, the first term comes from the triangle top loop of fig. 3.15 (b), whereas the second corresponds to the box diagram of fig. 3.15 (c).

Single Higgs production via gluon fusion proceed through the diagram of fig. 3.14, where all fermions charged under $SU(3)_C$ contribute in the loop. Compared to the Standard Model, the process in composite Higgs model is modified by two effects: first the coupling of the Higgs to the top quark is modified, which give the contribution scaling with c in the computation above; second, the composite fermions running in the loop give an additional contribution to the process, whose strength is proportional to the coefficient c_g in eq. (3.161). It has been shown however that in explicit constructions the $gg \to h$ cross section is insensitive to the details of the heavy fermion spectrum, i.e. does not depend on the couplings and masses of composite states, but only on the ratio v/f [164, 158, 165, 166]. This was found to be true both in models with partial compositeness and in little Higgs theories. In fact, although the top Yukawa coupling receives a wave function renormalisation correction which depends on composite couplings, this contribution is exactly cancelled by the loops of extra fermions, leading to a dependence of the $gg \to h$ rate only on v/f. This also implies that the cross section can be obtained by simply multiplying the SM one by c^2, where c is the rescaling of the top Yukawa coming only from the nonlinearity of the σ-model, and neglecting corrections due to fermionic resonances. The cancellation arises due to the fact that the determinant of the heavy fermion mass matrix takes the form

$$\det \mathcal{M}^2(H) = F(H/f) \cdot P\left(\lambda_i, m_i, f\right), \tag{3.164}$$

where F is a function satisfying $F(0) = 0$, since the top becomes massless in the limit of unbroken electroweak symmetry, and P is a polynomial of the composite couplings λ_i and masses m_i, but independent of H. It is then immediate to see that the hgg coupling in eq. (3.159) does not depend on masses and couplings of the resonances. The origin of the factorisation (3.164) was explained in the context of partial compositeness by means of a spurion analysis [166]. Such a factorisation can break down if the top mixes with more than one composite operator, leading to a dependence of the hgg vertex on composite couplings. Nevertheless it holds in most explicit

constructions, including little Higgs models. Still, the independence of the hgg vertex on the composite couplings (collectively denoted by λ_i) is only valid in the approximation of the low-energy theorem, and corrections due to finite fermion mass effects are expected. We can estimate their size in a simple way. Assuming for simplicity the presence of only one top partner T whose mass dependence can be written at leading order in v^2/f^2 as

$$m_T(H) = \lambda_T f \left(1 + a_T \frac{H^2}{f^2}\right), \tag{3.165}$$

where a_T and λ_T are unknown numerical parameters. The hgg coupling reads then

$$\mathcal{L}_{hgg} = \frac{g_S^2}{48\pi^2} G^a_{\mu\nu} G^{\mu\nu\, a} \frac{h}{v} \left[1 - \left(c_y + \frac{c_H}{2} - 2a_T\right) \frac{v^2}{f^2} + \Delta\right], \tag{3.166}$$

where Δ indicates additional dependence on the spectrum of heavy fermions beyond the low-energy theorem approximation. The top loop diagram can be computed explicitly, using the expression of the top Yukawa coupling $(m_t/v)\left(1 - (c_y + c_H/2)v^2/f^2\right)$. Retaining the first subleading term in the $1/m_t^2$ expansion, which is the leading correction to the low-energy theorem in the limit $m_T \gg m_t$, one finds

$$\Delta = \frac{7}{120} \frac{m_h^2}{m_t^2} \left[1 - \left(c_y + \frac{c_H}{2}\right) \frac{v^2}{f^2}\right], \tag{3.167}$$

where we have fixed the energy of the process to $\hat{s} = m_h^2$. The independence of the hgg vertex of the composite couplings λ_i relies on the fact that $c_y - 2a_T$ is itself independent of them, as indicated by the determinant of the mass matrix

$$\det \mathcal{M}^2(H) = \frac{y_t^2 \lambda_T^2}{2} f^2 H^2 \left[1 - (c_y - 2a_T) \frac{H^2}{f^2}\right]. \tag{3.168}$$

If this is the case then the dependence of the hgg vertex with respect to the λ_i is due only to the term Δ, and we can estimate the sensitivity of the cross section on finite mass effects to be

$$\frac{\delta\sigma(gg \to h)}{\sigma(gg \to h)_{SM}} \approx \frac{7}{60} \frac{m_h^2}{m_t^2} \frac{v^2}{f^2} \cong 0.06 \frac{v^2}{f^2} \tag{3.169}$$

where in the last equality we assumed $m_h = 125\,\text{GeV}$. Corrections to the low-energy theorem are therefore expected to be very small even for a large value of the ratio v^2/f^2. This estimate will be confirmed in section 3.3.6, where the $gg \to h$ cross section will be computed in an explicit model retaining the full mass dependence.

Within the SM, double Higgs production via gluon fusion received interest mainly because it is sensitive to the trilinear Higgs self-coupling [167,

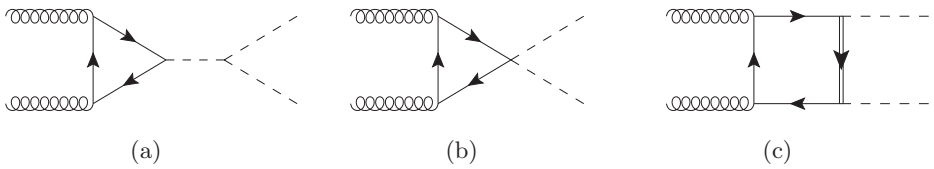

(a) (b) (c)

Figure 3.15: One-loop diagrams contributing to the Higgs pair production via gluon fusion at the LHC. Only one kind of fermion can run into the triangle loops in (a) and (b) since the strong interaction is diagonal in the mass basis, while two different kind of fermions can participate to the box diagram (c), as denoted by a single and a double line.

168, 169, 170] shown in fig. 3.15 (a). In composite Higgs models, the process $gg \to hh$ is affected essentially in two ways. First, the nonlinearity of the strong sector gives rise to a $f\bar{f}hh$ coupling and thus to a genuinely new contribution to the amplitude; the corresponding diagram of fig. 3.15 (b) is absent in the Standard Model. Second, one should take into account the effects of top partners, which include also new box diagrams involving off-diagonal Yukawa couplings, as illustrated in fig. 3.15 (c). A first study of $gg \to hh$ in composite Higgs models, neglecting top partners, was performed in ref. [171], where it was found that an enhancement of the cross section is possible due to the new $t\bar{t}hh$ coupling (see also ref. [172] for an earlier study in the context of little Higgs models). A model-independent study of the process in terms of the parameters $a, b, c, \ldots$ of chapter 2 and neglecting again the effects of top partners shows that the Higgs pair production cross-section is very sensitive to the the coefficient c_2 parametrising the $t\bar{t}hh$ coupling [173]. The effects of top partners in double Higgs production via gluon fusion are however important, especially since a light composite Higgs seems to be tightly correlated with the presence of light top partners [174], and were included for the first time in ref. [2].

Within the framework of the low-energy theorem where all heavy fermions are integrated out, the amplitude for Higgs pair production is given by the sum of two diagrams, one with the effective hgg coupling followed by a trilinear Higgs coupling, and the second involving the effective $hhgg$ coupling directly. The result can then be written as

$$\mathcal{A}_{\mathrm{LET}}\left(gg \to hh\right) = \frac{\alpha_S}{3\pi v^2}\delta^{ab}\left(p_1^\nu p_2^\mu - p_1 \cdot p_2\, g^{\mu\nu}\right) C_{\mathrm{LET}}(\hat{s}), \tag{3.170}$$

where p_1 and p_2 denote the momenta of the incoming gluons, the indices a

and b are colour indices and the coefficient $C_{\mathrm{LET}}(\hat{s})$ is defined as

$$\begin{aligned} C_{\mathrm{LET}}(\hat{s}) = \frac{3m_h^2}{\hat{s}-m_h^2}\Bigg[&\frac{1}{2}\left(\frac{\partial}{\partial(\log H)}\log\det\mathcal{M}^2(H)\right)_{H=v} \\ &+\left(c_6-2c_H-\frac{c_r}{4}\right)\frac{v^2}{f^2}\Bigg] \\ +\frac{1}{2}&\left(\left(\frac{\partial^2}{\partial(\log H)^2}-\frac{\partial}{\partial(\log H)}\right)\log\det\mathcal{M}^2(H)\right)_{H=v}-\frac{c_r}{4}\,\frac{v^2}{f^2} \\ =\frac{3m_h^2}{\hat{s}-m_h^2}&\left[1-\left(c_y-c_6+2c_H+\frac{c_r}{4}-3c_g\frac{y_t^2}{g_\rho^2}\right)\frac{v^2}{f^2}\right] \\ -&\left[1+\left(c_y+\frac{c_r}{4}-3c_g\frac{y_t^2}{g_\rho^2}\right)\frac{v^2}{f^2}\right] \end{aligned} \tag{3.171}$$

with $\hat{s}=(p_1+p_2)^2$ denoting the partonic centre-of-mass energy. Note that as expected, the combinations $c_y-c_6+2c_h+c_r/4$ and $c_y+c_r/4$ are invariant under the reparametrisation in eq. (3.137). For $v^2/f^2\to 0$, the Standard Model result in the limit of large top mass is correctly reproduces [175,176]:

$$C_{\mathrm{LET}}^{SM}(\hat{s})=\frac{3m_h^2}{\hat{s}-m_h^2}-1. \tag{3.172}$$

The low-energy theorem result (3.171) also indicates that in models where the factorisation (3.164) of $\det\mathcal{M}^2$ holds, the $gg\to hh$ cross section is insensitive to the details of the composite sector, due to a cancellation similar to the one present in single Higgs production. The equivalent of eq. (3.171) can also be computed using the effective formalism of chapter 2, where the effects of top partners are not taken into account, and one finds

$$C_{\mathrm{LET}}(\hat{s})=\frac{3m_h^2}{\hat{s}-m_h^2}\,c\,d_3+2c_2-c^2. \tag{3.173}$$

The partonic cross section can be computed from the amplitude (3.170), and reads

$$\hat{\sigma}_{gg\to hh}=\frac{G_F^2\alpha_s^2(\mu)\hat{s}}{128(2\pi)^3}\,\frac{1}{9}\sqrt{1-\frac{4m_h^2}{\hat{s}}}\,C_{\mathrm{LET}}^2(\hat{s}), \tag{3.174}$$

and the hadronic cross section is obtained by convolution with the parton distribution function $f_{g/P}$ of the gluon in the proton,

$$\sigma=\int\limits_{4m_h^2/s}^{1}\mathrm{d}\tau\int\limits_{\tau}^{1}\frac{\mathrm{d}x}{x}f_{g/P}(x,Q)f_{g/P}(\tau/x,Q)\hat{\sigma}_{gg\to hh}(\tau s) \tag{3.175}$$

where the collider centre-of-mass energy s is related to $\hat{s}$ by $\hat{s}=\tau s$. The renormalisation scale μ and the factorisation scale Q are chosen equal to

the invariant mass of the Higgs boson pair, $\mu = Q = \sqrt{\hat{s}}$. Note however that in the Standard Model, the limit $m_t \to \infty$ gives a cross section in agreement with the full result only within 20% for $m_h \lesssim 200$ GeV, and moreover produces incorrect kinematic distributions [177]. Thus we expect the low-energy theorem result for Higgs pair production to be in general less accurate than for single Higgs production processes. An explicit computation in section 3.3.7 will indeed confirm this statement.

3.3 The minimal composite Higgs model

We are now ready to apply all the model-independent results discussed so far to an explicit realisation of a composite Higgs model, and to compare its prediction to the current bounds provided by experiments. We have seen above that the minimal choice of symmetry group giving a set of Goldstone bosons which can be identified with the Higgs and featuring a custodial symmetry is the coset $SO(5)/SO(4)$, where the electroweak gauge group $SU(2)_W \times U(1)_Y$ is a subgroup of the unbroken global symmetry. The only possible source of electroweak symmetry breaking in such a model is coming from the fermion sector, mostly from the top quark. Generating a mass for the fermions while preserving enough of the global symmetry of the strong sector requires to use the partial compositeness mechanism, in which the fermion masses are generated through a mixing between elementary and composite states. The contribution of fermion loops to the Higgs potential is explicitly dependent on the physics at the strong scale $\Lambda \approx 4\pi f$, and cannot be approached in the perturbative way. We will therefore study a model arising in the holographic picture, where some of the physics at and above the strong scale can be computed within the five-dimensional dual description. A realisation of the minimal coset $SO(5)/SO(4)$ turns out to be compatible with the requirement that the electroweak symmetry is broken by top quark loops, provided that the strong sector is not exactly QCD-like [150]. We will consider for simplicity only the first stage in the tower of Kaluza-Klein of meson resonances: in the holographic picture, this is found to be as in QCD a vector ρ and an axial-vector a, characterised by the mass ratio [178]

$$m_a \cong \frac{5}{3} m_\rho, \tag{3.176}$$

as opposed to the QCD prediction $m_a \cong \sqrt{2}\, m_\rho$ obtained from the Weinberg sum rules (3.42-3.43). Note that the holographic description does not fix the ratio of the heavy vector resonance mass to the scale f fixing the strength of the Higgs interactions. The two scale are related as above by a coupling g_ρ which remains a free parameter in the theory, up to the requirement of perturbativity which can be expressed as

$$g_\rho \leq 4\pi, \quad \Leftrightarrow \quad m_\rho \leq 4\pi\, f. \tag{3.177}$$

Note also that the desirable hierarchy $v \ll f$ can only be accounted for via some fine-tuning of the parameters in the model. A realistic potential requires for example the introduction of a Higgs quartic coupling at tree-level [150]. We will not describe explicit solutions to this problem, but remember that the ratio of scale

$$\xi = \frac{v^2}{f^2} \tag{3.178}$$

is a measure of the fine-tuning of the model, and that $\xi \ll 1$ is disfavoured by naturalness arguments.

3.3.1 The SO(5)/SO(4) σ-model

The four Goldstone fields arising from the breaking of the global $SO(5)$ symmetry to a subgroup $SO(4)$ can be parametrised in terms of a five-vector subject to a constraint $\Sigma^T\Sigma = 1$, as the part of the $SO(5)$ transformations which do not leave the vacuum invariant,

$$\Sigma(x) = \exp\left[\sqrt{2}i\, h^{\hat{a}} T^{\hat{a}}\right] \Sigma_0, \qquad \langle\Sigma(x)\rangle = \Sigma_0. \tag{3.179}$$

Note that the factor $\sqrt{2}$ is purely conventional, chosen in order to have a useful definition for the generators $T^{\hat{a}}$ in the following. The $T^{\hat{a}}$ form a set of linearly-independent broken generators which do not preserve the vacuum expectation value Σ_0, i.e. $T^{\hat{a}}\Sigma_0 \neq \Sigma_0$. The Goldstone fields h^a transforms non-linearly under a general $SO(5)$ transformation

$$\Sigma(x) \to V\Sigma(x), \qquad V = \exp\left[i\,\theta^a T^a / f\right] \in SO(5), \tag{3.180}$$

where the θ^a are real parameters defining the transformation, and the T^a are generators of the $SO(5)$ group. The ten T^agenerators can be split into the subsets $\{T^a\} = \{T^a_L, T^a_R, T^{\hat{a}}\}$, where T^a_L and T^a_R with $a = 1, 2, 3$ generate the subgroup $SU(2)_L \times SU(2)_R \cong SO(4)$ preserved by the vacuum Σ_0, and the remaining four broken operators are denoted by $T^{\hat{a}}$, $\hat{a} = 1, 2, 3, 4$. It is convenient to choose the $SO(4)$ subgroup to live in the upper-left 4×4 block of the 5×5 matrix representation of the generators, defining

$$\begin{aligned}
(T^a_L)_{ij} &= -\frac{i}{2}\left[\varepsilon^{abc}\delta^b_i\delta^c_j + \delta^a_i\delta^4_j - \delta^4_i\delta^a_j\right], \\
(T^a_R)_{ij} &= -\frac{i}{2}\left[\varepsilon^{abc}\delta^b_i\delta^c_j - \delta^a_i\delta^4_j + \delta^4_i\delta^a_j\right], \\
(T^{\hat{a}})_{ij} &= -\frac{i}{\sqrt{2}}\left[\delta^{\hat{a}}_i\delta^5_j - \delta^5_i\delta^{\hat{a}}_j\right],
\end{aligned} \tag{3.181}$$

The definition are chosen so as to satisfy the normalisation condition

$$\mathrm{Tr}\left(T^a T^b\right) = \delta^{ab}, \tag{3.182}$$

and such that the T^a_L and T^a_R form $\mathfrak{su}(2)$ algebras

$$\left[T^a_{L,R}, T^b_{L,R}\right] = i\,\varepsilon^{abc}\,T^c_{L,R}. \tag{3.183}$$

The gauge group can therefore be chosen straightforwardly along the $SU(2)_L$ subgroup and the third generator of $SU(2)_R$. In order to give the correct hypercharge to the fermions, an additional $U(1)_X$ symmetry will be required in the model, under which the Goldstone field is uncharged. The definition of the hypercharge generator is then

$$Y = T^3_R + X. \tag{3.184}$$

As discussed above, before including radiative corrections to the potential for the fields $h^{\hat{a}}$, the vacuum state chooses to align with the gauge-preserving direction, in our case

$$\Sigma_0 = (0, 0, 0, 0, 1)^T, \tag{3.185}$$

for which the broken generators used in the parametrisation (3.179) correspond indeed to the definition of eq. (3.181). Note that although the $SO(5)$ transformation (3.180) acts non-linearly on the Goldstone bosons $h^{\hat{a}}$, the unbroken subgroup $SO(4)$ acts linearly on them [76,77], so that the Goldstone fields $\{h^{\hat{a}}\}$ transform as a **4** of $SO(4)$, i.e. in the fundamental representation. Using the definition (3.181) for the generators, the field Σ can be computed to be

$$\Sigma(x) = \left(\frac{h^1}{h}\sin(h/f),\ \frac{h^2}{h}\sin(h/f),\ \frac{h^3}{h}\sin(h/f),\ \frac{h^4}{h}\sin(h/f),\ \cos(h/f)\right), \tag{3.186}$$

with $h = \sqrt{(h^{\hat{a}})^2}$. A covariant derivative of the field can be constructed as

$$D_\mu\Sigma(x) = \partial_\mu\Sigma(x) - i\left(g\,W^a_\mu\,Q^a + g'\,B_\mu\,Y\right)\Sigma(x). \tag{3.187}$$

Note that since the generators (3.181) are purely imaginary, the covariant derivative is real, as is the field $\Sigma(x)$. The σ-model Lagrangian can then be constructed as the sum of all gauge-invariant operators built out of the fields $\Sigma(x)$ and of covariant derivative thereof. Due to the shift symmetry of the Goldstone bosons, which in this case in manifested by the relation $\Sigma^T\Sigma = 1$, only derivative interactions are present in the Lagrangian. The lowest order term is simply the kinetic term

$$\mathcal{L}_\Sigma = \frac{f^2}{4} D_\mu\Sigma^T D^\mu\Sigma, \tag{3.188}$$

whose coefficient is completely fixed by the canonical normalisation of the kinetic terms for the Goldstone fields $h^{\hat{a}}$. Terms with a higher number of derivatives, starting at order four, are also present in the model but will be

ignored here due to their negligible role on the low-energy phenomenology.[13] The electroweak gauge freedom can be used to rotate the field $\Sigma(x)$ in a unitary gauge, where $h_1 = h_2 = h_3 = 0$ and $h_4 = \mathcal{H}$, for which

$$\Sigma = (0, 0, 0, \sin(\mathcal{H}/f), \cos(\mathcal{H}/f)) \,. \tag{3.189}$$

The Lagrangian (3.188) becomes then

$$\mathcal{L}_\Sigma = \frac{1}{2}\partial_\mu \mathcal{H}\, \partial^\mu \mathcal{H} + \frac{f^2}{4}\sin^2\left(\frac{\mathcal{H}}{f}\right)\left[g^2 W_\mu^+ W^{\mu-} + \frac{g^2}{2\cos\theta_W} Z_\mu Z^\mu\right], \tag{3.190}$$

and a mass term for the gauge bosons is generated when $\mathcal{H}$ gets a vacuum expectation value. The usual mass relations $m_W^2 = g^2 v^2/4$ and $m_Z^2 = (g^2 + g'^2)v^2/4$ satisfying the custodial symmetry are recovered provided that the electroweak scale v is identified as

$$v = f \sin\left(\frac{\langle \mathcal{H}\rangle}{f}\right) = \langle \mathcal{H}\rangle \left[1 - \frac{1}{6}\frac{\langle \mathcal{H}\rangle^2}{f^2} + \ldots\right]. \tag{3.191}$$

The equality $\langle \mathcal{H}\rangle = v$ happening in the Standard Model is in this case only valid in the limit $f \to \infty$. Expanding the Higgs field around its vacuum expectation value, $\mathcal{H} = v + h$, one obtains a Lagrangian including only a scalar field h, a photon and massive gauge bosons $W^\pm$ and Z^0, which turns out to be identical to the Standard Model description of eq. (2.66) and (2.67), with the identification of parameters [32]

$$\begin{aligned} a &= \sqrt{1-\xi}, \\ b &= 1 - 2\xi, \\ d_3 &= (1-2\xi)/\sqrt{1-\xi}, \\ d_4 &= \left[1 - \tfrac{28}{3}\,\xi(1-\xi)\right]/(1-\xi)\,. \end{aligned} \tag{3.192}$$

3.3.2 Fermion masses from a composite sector

In addition to the scalar and gauge sector, the minimal composite Higgs models contains the same elementary fermion content as the Standard Model, described by the Lagrangian

$$\mathcal{L}_{\text{elementary}} = i\,\bar{q}_L \not{D} q_L + i\,\bar{t}_R \not{D} t_R + i\,\bar{b}_R \not{D} b_R. \tag{3.193}$$

We indicated here for simplicity only the quarks of the third generation. The remaining fermions are irrelevant to our discussion, since their tiny mass compared to the energy scale of electroweak interactions make them irrelevant to Higgs physics. The partial compositeness scenario is then enforced

[13] A model-independent parametrisation of the chiral Lagrangian in composite Higgs models including terms up to four derivatives is provided in ref. [179].

by adding a set of massive, composite fermions with the same quantum numbers and opposite chirality as the left-handed doublet q_L and the right-handed singlet t_R, respectively a new doublet $Q_R = (T_R, B_R)^T$ and a new singlet $\widetilde{T}_L$. Note that the fermions in the strong sector must therefore also be charged under the colour gauge group. The mixing between elementary and composite fermion states arises from the operators

$$\mathcal{L}_{\text{mixing}} = \Delta_L \, \overline{q_L} Q_R + \Delta_R \, \overline{t}_R \widetilde{T}_L + \text{h.c.} \tag{3.194}$$

where Δ_L and Δ_R are proto-Yukawa couplings with dimension of mass. There is no mixing term for the right-handed bottom quark, since the latter can be considered massless for all our purposes. Note that in general the mass for the light fermions need not be generated by the same partial compositeness mechanism, since they are small enough to arise for example from contact interactions as in technicolor theories. The composite fermions Q_R and $\widetilde{T}_L$ can however not exist alone, but must belong to multiplets of the full $SO(5)$ global symmetry of the strong sector. Moreover, in order to acquire a tree-level mass, the composite fermions must be vector-like, i.e. exist in both chiralities. The $SO(5)$-invariant Lagrangian describing them is therefore

$$\mathcal{L}_{\text{composite}} = i \, \overline{\psi}_L \not{D} \psi_L + i \, \overline{\psi}_R \not{D} \psi_R - M_0 \left(\overline{\psi}_L \psi_R + \overline{\psi}_R \psi_L \right). \tag{3.195}$$

Up to this point, there are still various possibilities to realise the partial compositeness scenario: the vector-like fermions ψ can be in any representation of the $SO(5)$ global symmetry group, with the imperative condition that a subset of them must transform as a doublet and a singlet under the electroweak gauge group, and can thus be identified with Q_R and $\widetilde{T}_L$.

The simplest choice fulfilling this condition is to embed the fermions into a spinorial representation of $SO(5)$ [131]. The spinorial representation decomposes under the $SO(4) \cong SU(2)_L \times SU(2)_R$ unbroken subgroup as

$$\mathbf{4} = (\mathbf{2}, \mathbf{1}) \oplus (\mathbf{1}, \mathbf{2}), \tag{3.196}$$

which indicates that there is one $SU(2)_W$ doublet and two singlets. As mentioned already, the correct hypercharge for them can be obtained by adding an extra $U(1)_X$, under which the fermion field ψ has a charge $X = 1/6$. Examining the phenomenology of this model, in turns out however that a large tree-level correction to the $Z\bar{b}_L b_L$ vertex is induced by the composite fermions, which makes the model incompatible with the precision measurement related to ε_b [110].

The next-to-minimal choice of representation for the composite fermions is the fundamental of $SO(5)$ [180], which decomposes under the unbroken subgroup as

$$\mathbf{5} = (\mathbf{2}, \mathbf{2}) \oplus (\mathbf{1}, \mathbf{1}), \tag{3.197}$$

and also contain the required doublet and singlet. Apart from the latter two, a new electroweak doublet of fermions is present here. Note that the

presence of additional fermions is a generic consequence of imposing the tree-level custodial symmetry in the strong sector of the theory; such fermions are usually denoted as *custodians* and play a very important role in the phenomenology of composite Higgs and little Higgs models [180, 166]. As for the fermions in the spinorial representation, the correct electric charge for the fermions in the fundamental can be obtained by simply adding a $U(1)_X$ gauge group to the model, and fixing this time the charge of the composite fermion five-plet ψ to $X = 2/3$. The covariant derivative appearing in the Lagrangian (3.195) is then given by

$$D_\mu \psi_{L,R} = \partial_\mu \psi_{L,R} - i \left(g\, W_\mu^a\, T_L^a + g'\, B_\mu \left(T_R^3 + \frac{2}{3} \right) \right) \psi_{L,R}. \qquad (3.198)$$

In addition to the fermions in the singlet $\widetilde{T}$ and doublet $Q = (T, B)$ which have the usual electric charge of top and bottom quarks, the additional doublet can be written as $X = \left(X^{5/3}, X^{2/3}\right)$, where the indices indicate the electric charge. The model contains therefore apart from required partners for the top and the bottom quarks an exotic fermion of charge $5/3$. Contrarily to the previous attempt, there is with this choice no tree-level contribution to the $Z\bar{b}_L b_L$ vertex from loops of composite fermions. The reason for this is the presence of a custodial symmetry protecting in general the vertex $Z\overline{f}f$, where f denotes any elementary fermion, from tree-level corrections arising from the mixing with composite states [181]. This symmetry is realised if and only if the elementary fermion f mixes with a composite fermion which transform in the same representation under $SU(2)_L$ and $SU(2)_R$, and whose quantum numbers under T_L^3 and T_R^3 are the identical. This situation was not satisfied in the case of composite fermions in the spinorial representation of $SO(5)$, but can be realised with fermions in the fundamental: both the singlet $\widetilde{T}$ and the bidoublet (Q, X) satisfy the first condition, while the second condition is only fulfilled by the singlet $\widetilde{T}$ and the members B and $X^{5/3}$ of the bidoublet. In the minimal composite Higgs model with fermions in the fundamental representation, there are therefore no tree-level corrections to the vertices $Z\bar{b}_L b_L$ nor to $Z\bar{t}_R t_R$, while corrections to $Z\bar{t}_L t_L$ can be important, but are nevertheless not yet relevant to constrain the model from experimental data.

A proof of the custodial protection described above can be sketched as follows. Let us consider an elementary fermion f_L mixing with a composite fermion F_R, where the latter is massive through its interactions with the composite fermion of opposite parity, F_L. The correction to the coupling $Z\overline{f}_L f_L$ comes not only from F_R, although f_L naively only mixes with the latter, but also from F_L, whose mixing with F_R is induced at tree-level by the mass term $M_0(\overline{F}_L F_R + \text{h.c.})$. Corrections to the vertex $Z\overline{f}_L f_L$ are therefore proportional to Q_L^3 and Q_R^3, which denote the charge of the composite fermion F under $SU(2)_L$ and $SU(2)_R$ respectively. By definition, the cancellation only works for fermions satisfying $Q_L^3 = Q_R^3$. At the same time,

however, the custodial symmetry $SU(2)_V$ is an exact global symmetry of the Lagrangian, even after electroweak symmetry breaking, and its action on the composite state F must be trivial, hence implying $Q_L^3 + Q_R^3 = 0$. From the two equalities, one derives $Q_L^3 = Q_R^3 = 0$, which indicates that corrections to the $Z\overline{f}_L f_L$ vertex vanishes. Note that since the custodial symmetry is broken by the top quark mass, non-zero radiative corrections will appear in diagrams like fig. 3.12 involving fermions in the loop.

The breaking of electroweak symmetry is introduced in the fermion sector by a Yukawa-like term of the form

$$\mathcal{L}_{\text{Yukawa}} = -y_* f \left(\overline{\psi}_L \cdot \Sigma\right) \left(\Sigma^T \cdot \psi_R\right) + \text{h.c.} \tag{3.199}$$

With our definitions of the generators, the five-vector ψ can be decomposed as

$$\psi_{L,R} = \begin{pmatrix} \frac{1}{\sqrt{2}}\left(B - X^{5/3}\right) \\ -\frac{i}{\sqrt{2}}\left(B + X^{5/3}\right) \\ \frac{1}{\sqrt{2}}\left(T + X^{2/3}\right) \\ -\frac{i}{\sqrt{2}}\left(T - X^{2/3}\right) \\ \widetilde{T} \end{pmatrix}_{L,R} \tag{3.200}$$

where we recognise the singlet $\widetilde{T}$ mixing with t_R, the doublet $Q = (T, B)^T$ mixing with q_L and the custodian doublet $X = \left(X^{5/3}, X^{2/3}\right)$. In order to preserve the perturbativity of our theory, the size of the coupling y_* is bounded as

$$|y_*| \leq 4\pi. \tag{3.201}$$

Note the use of the absolute value, since both signs for y_* are possible and will describe very different situations.[14] The full Lagrangian of the minimal composite Higgs model is then simply the sum of its parts given in eq. (3.188), (3.193), (3.194), (3.195) and (3.199), as

$$\mathcal{L}_{\text{MCHM}} = \mathcal{L}_\Sigma + \mathcal{L}_{\text{elementary}} + \mathcal{L}_{\text{composite}} + \mathcal{L}_{\text{mixing}} + \mathcal{L}_{\text{Yukawa}}. \tag{3.202}$$

After electroweak symmetry breaking, the last three terms contribute to give a mass to the top quark. It is convenient to write the mass term in the matrix notation

$$\mathcal{L}_{\text{mass}} = -\overline{\psi}_L^{-1/3} M_{-1/3}\, \psi_R^{-1/3} - \overline{\psi}_L^{2/3} M_{2/3}\, \psi_R^{2/3} - \overline{\psi}_L^{5/3} M_{5/3}\, \psi_R^{5/3} \tag{3.203}$$

where the fermions are grouped by their electric charge,

$$\psi_{L,R}^{-1/3} = \left(b, B\right)_{L,R}^T, \quad \psi_{L,R}^{2/3} = \left(t, T, X^{2/3}, \widetilde{T}\right)_{L,R}^T, \quad \psi_{L,R}^{5/3} = \left(X^{5/3}\right)_{L,R}^T, \tag{3.204}$$

[14] Only the relative sign of y_* and M_0 is actually physical, since they can be both flipped by a redefinition of the composite fermion field ψ. By convention, M_0 is chosen to be positive here.

and the mass matrices are defined as

$$M_{-1/3} = \begin{pmatrix} 0 & \Delta_L \\ 0 & M_0 \end{pmatrix}, \qquad M_{5/3} = \big(M_0\big), \tag{3.205}$$

$$M_{2/3} = \begin{pmatrix} 0 & -\Delta_L & 0 & 0 \\ 0 & M_0 + \frac{1}{2}s_H^2 y_* f & \frac{1}{2}s_H^2 y_* f & \frac{1}{\sqrt{2}}s_H c_H y_* f \\ 0 & \frac{1}{2}s_H^2 y_* f & M_0 + \frac{1}{2}s_H^2 y_* f & \frac{1}{\sqrt{2}}s_H c_H y_* f \\ -\Delta_R & \frac{1}{\sqrt{2}}s_H c_H y_* f & \frac{1}{\sqrt{2}}s_H c_H y_* f & M_0 + c_H^2 y_* f \end{pmatrix}, \tag{3.206}$$

where we used the shordhand notations $s_H = \sin\left(\langle\mathcal{H}\rangle/f\right)$ and $c_H = \cos\left(\langle\mathcal{H}\rangle/f\right)$. The mass matrix $M_{2/3}$ cannot be straightforwardly diagonalised. However, performing the redefinition

$$\begin{pmatrix} q_L \\ Q_L \end{pmatrix} \to \begin{pmatrix} \cos\phi_L & -\sin\phi_L \\ \sin\phi_L & \cos\phi_L \end{pmatrix} \begin{pmatrix} q_L \\ Q_L \end{pmatrix}, \qquad \tan\phi_L = \frac{\Delta_L}{M_0}, \tag{3.207}$$

$$\begin{pmatrix} t_R \\ \widetilde{T}_R \end{pmatrix} \to \begin{pmatrix} \cos\phi_R & -\sin\phi_R \\ \sin\phi_R & \cos\phi_R \end{pmatrix} \begin{pmatrix} t_R \\ \widetilde{T}_R \end{pmatrix}, \qquad \tan\phi_R = \frac{\Delta_R}{M_0 + y_* f}, \tag{3.208}$$

$M_{-1/3}$ is rotated into a diagonal matrix

$$M_{-1/3} \to \begin{pmatrix} 0 & 0 \\ 0 & m_Q \end{pmatrix} \tag{3.209}$$

and $M_{2/3}$ into

$$\begin{pmatrix} \frac{1}{\sqrt{2}}s_H c_H s_L s_R y_* f & \frac{1}{2}s_H^2 s_L y_* f & \frac{1}{2}s_H^2 s_L y_* f & \frac{1}{\sqrt{2}}s_H c_H s_L c_R y_* f \\ \frac{1}{\sqrt{2}}s_H c_H c_L s_R y_* f & m_Q + \frac{1}{2}s_H^2 c_L y_* f & \frac{1}{2}s_H^2 c_L y_* f & \frac{1}{\sqrt{2}}s_H c_H c_L c_R y_* f \\ \frac{1}{\sqrt{2}}s_H c_H s_R y_* f & \frac{1}{2}s_H^2 y_* f & m_X + \frac{1}{2}s_H^2 s_L y_* f & \frac{1}{\sqrt{2}}s_H c_H c_R y_* f \\ -s_H^2 s_R y_* f & \frac{1}{\sqrt{2}}s_H c_H y_* f & \frac{1}{\sqrt{2}}s_H c_H y_* f & m_T - s_H^2 c_R y_* f \end{pmatrix} \tag{3.210}$$

where we defined

$$\begin{aligned} m_Q &= \sqrt{M_0^2 + \Delta_L^2} = \frac{M_0}{c_L}, \\ m_X &= M_0, \\ m_{\widetilde{T}} &= \sqrt{(M_0 + y_* f)^2 + \Delta_R^2} = \frac{M_0 + y_* f}{c_R}. \end{aligned} \tag{3.211}$$

The rotated form of $M_{2/3}$ is diagonal in the limit $(v/f) \approx s_H \to 0$, so that the masses m_Q, m_X and $m_{\widetilde{T}}$ can be identified with the physical mass of the two heavy doublets and of the singlet in the same limit. The top quark mass can be read from the first entry of the matrix to be

$$m_t = \sqrt{\frac{\xi(1-\xi)}{2}}\, \sin\phi_L\, \sin\phi_R\, y_*\, f + \mathcal{O}\left(\xi^3\right). \tag{3.212}$$

The top mass — and equivalently the mass of other fermions generated by the same mechanism — can be made arbitrarily small by choosing small mixing angles ϕ_L and ϕ_R. This feature is welcome for light quarks and leptons, whose compositeness is very much constrained by the size of four-fermion operators. For the top quark, however, the mixing angles ϕ_L and ϕ_R have to be sizable: in the limit $v \ll f$, the equivalent of the Standard Model top Yukawa coupling, defined so that $m_t = y_t v/\sqrt{2}$, is extracted from eq. (3.212) to be

$$y_t \cong \sin\phi_L\, \sin\phi_R\, y_*. \tag{3.213}$$

Requiring $y_t \approx 1$ as measured for the top quark and noting that the perturbativity bound (3.201) does not allow for an arbitrarily large coupling y_*, one finds the constraint

$$\sin\phi_L\, \sin\phi_R \gtrsim \frac{1}{4\pi} \tag{3.214}$$

on the compositeness of the top quark. Large mixing angles are on the other hand constrained by experimental data, both from flavour physics and from electroweak precision tests: a large $\sin\phi_L$ imply for example a hierarchical structure among the composite fermions of the bidoublet, as indicated by eq. (3.211), which creates an important breaking of the custodial symmetry. A complete study of the radiative corrections induced by composite fermions on electroweak precision observables is thus needed, and will be performed in the next section. Note finally that while the mass of the fermion doublet Q and X is bounded from below by composite mass term M_0, this is not the case for the singlet $\widetilde{T}$, which can become very light in case of an approximate cancellation $y_* f \approx -M_0$. Such a cancellation is actually rather natural, since a naive estimate of the composite mass $f \lesssim M_0 \lesssim \Lambda \approx 4\pi f$ corresponds to the same naive estimate (in absolute value) of the term $y_* f$, i.e. $1 \lesssim |y_*| \lesssim 4\pi$.

The interaction of the physical Higgs field h with the top quark can be extracted as well from the Lagrangian (3.202), and matching the result with our model-independent parametrisation of eq. (2.68), one finds

$$\begin{aligned} c &= (1-2\xi)/\sqrt{1-\xi}, \\ c_2 &= -2\xi. \end{aligned} \tag{3.215}$$

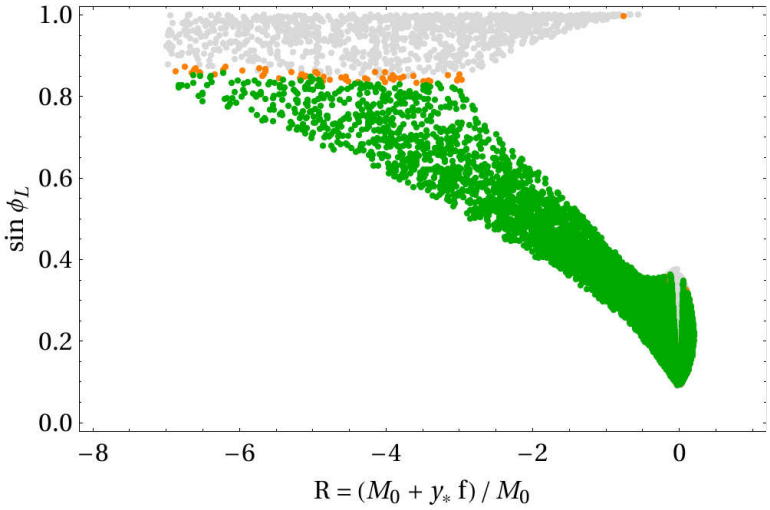

Figure 3.16: A sample of 20 000 points passing the electroweak precision tests as defined in the text, shown in the plane $(R, \sin\phi_L)$ for fixed values $\xi = 0.25$ and $m_h = 125$ GeV. The light grey points are excluded by direct collider constraints, see section 3.3.4. Green and orange points are still allowed, although the latter will be tested in 2012 by the LHC running at 8 TeV with a total integrated luminosity of 15 fb^{-1}.

Unlike in the Standard Model, a non-vanishing contact interaction $\bar{t}tthh$ is present in the theory. Note also that around the special value $\xi = \frac{1}{2}$, the coupling of one Higgs field to fermions can be drastically reduced compared to the Standard Model, which corresponds to the so-called *fermiophobic* Higgs boson scenario.

3.3.3 Electroweak precision tests

The strongest experimental constraints on the minimal composite Higgs model still come from the electroweak precision measurements at the Z-pole mass at LEP. We use the ε_i parameters defined in section 3.2.2 to constrain the model. In addition to the Standard Model contribution present in the decoupling limit $f \to \infty$, there are three different effects contributing to the ε parameters. First, the modified coupling of the Higgs to W and Z gauge bosons induces a logarithmically divergent contribution to the oblique parameters $\hat{S}$ and $\hat{T}$, or equivalently to ε_1 and ε_3. Using the $\hat{S}$ dependence on the Higgs mass derived in eq. (3.86) and recalling that the Higgs coupling to gauge bosons is rescaled by the parameter a in composite Higgs models, we find

$$\Delta\hat{S}_{\text{MCHM}} = \Delta\hat{S}_h^{\text{MCHM}} - \Delta\hat{S}_h^{\text{SM}} = \frac{\alpha}{48\pi\sin\theta_W}\left(a^2 - 1\right)\log\left(\frac{m_h^2}{\mu^2}\right). \quad (3.216)$$

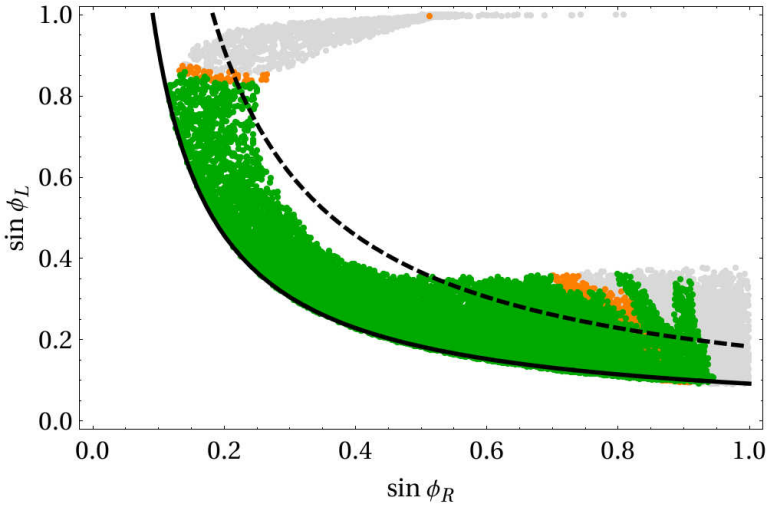

Figure 3.17: Same as fig. 3.16, in the plane $(\sin\phi_R, \sin\phi_L)$. The black dashed line corresponds to a correct top mass prediction as given in eq. (3.212) with the maximal coupling $y_* = 4\pi$ (solid line) and half its value $y_* = 2\pi$ (dashed line). The value of the compositeness parameter is fixed at $\xi = 0.25$.

Using the relation derived in eq. (3.192), we find $(a^2 - 1) = -\xi$. The loop contribution to $\hat{S}$ involving a Higgs boson is logarithmically divergent, as indicated by the dependence on μ^2, but is the cutoff by the physical mass m_ρ of the first composite vector resonance [182], so that we have finally for $\hat{S}$ and for $\hat{T}$, for which the same argument can be used,

$$\Delta\varepsilon_1^{\rm IR} = -\frac{3\,\alpha(m_Z)}{16\pi\cos^2\theta_W}\xi\log\left(\frac{m_\rho^2}{m_h^2}\right), \qquad \Delta\varepsilon_3^{\rm IR} = \frac{\alpha(m_Z)}{48\pi\sin^2\theta_W}\xi\log\left(\frac{m_\rho^2}{m_h^2}\right). \tag{3.217}$$

This correction is usually referred to as the *infrared* one, since it arises from a modification of the physics at low energy. The second effect on electroweak precision tests beyond the Standard Model is the direct contribution of the vector ρ and axial-vector a resonances to the $\hat{S}$ parameter, which is exactly the contribution derived in eq. (3.116),

$$\Delta\varepsilon_3^{\rm UV} = \frac{m_W^2}{m_\rho^2}\left(1 + \frac{m_\rho^2}{m_a^2}\right) \cong 1.36\,\frac{m_W^2}{m_\rho^2}. \tag{3.218}$$

The index refers to the *ultraviolet* origin of this contribution. In the second equality, we have used the relation $m_a/m_\rho \cong 5/3$ of eq. (3.176). The third and last contribution to electroweak precision parameters comes from the top partners at one loop, giving contributions both to the $\hat{T}$ parameter and the $Z\bar{b}b$ vertex, i.e. respectively to ε_1 and ε_b [110,183,1,184]. Computing the precise value of these contributions requires to the numerical diagonalisation

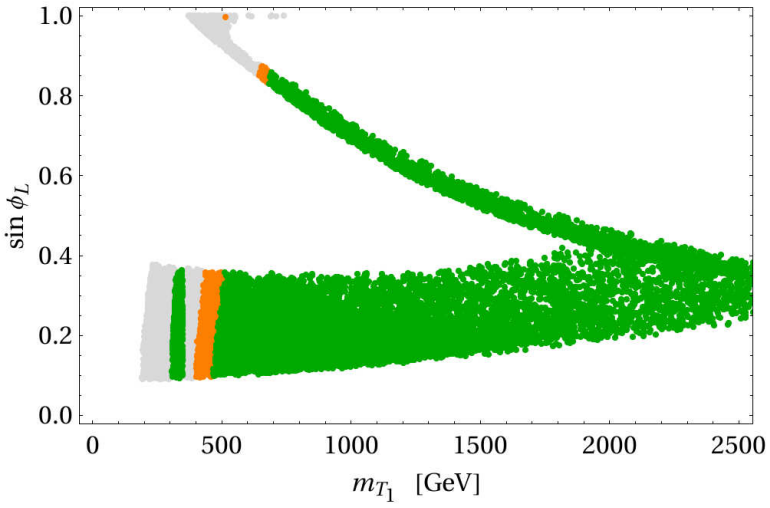

Figure 3.18: Same as fig. 3.16, where the mass of the lightest top partner is shown on the abscissa. The value of the compositeness parameter is fixed at $\xi = 0.25$.

of the mass matrix of the top quark and its partners, which depends on the parameters Δ_L, Δ_R, M_0, y and f. The requirement that the top mass matches the measured value $m_t = 173.3$ GeV allows, however, to express the corrections to ε_1 and ε_b in terms of four dimensionless parameters,

$$\Delta\varepsilon_1^{fermions} = f_1\left(\xi, \phi_L, \phi_R, R\right), \qquad \Delta\varepsilon_b^{fermions} = f_b\left(\xi, \phi_L, \phi_R, R\right), \tag{3.219}$$

where ξ, ϕ_L, ϕ_R are defined above and $R = (M_0 + yf)/M_0$. The function f_1 is computed exactly at one loop, while for f_b only the longitudinal polarisations of the gauge bosons are taken into account in the loop. The values obtained in this way are consistent with the full one-loop result [184]. The agreement of the model with experimental data is then assessed through a χ^2 test described in section 3.2.2. Fixing the Higgs mass to $m_h = 125$ GeV, as indicated by experimental results, the model is completely determined by the five parameters ξ, ϕ_L, ϕ_R, R and m_ρ. The results of a scan over the last four of these parameters for a fixed value of $\xi = \frac{1}{4}$ is shown in figures 3.16 and 3.17. Note that the value of R is bounded by the requirement $y \leq 4\pi$, and the we take $m_\rho \leq 4\pi f$ as required by perturbativity arguments.[15] We impose furthermore the constraint $|V_{tb}| > 0.77$ [185], discussed in more details in section 3.3.5. The mass of the lightest top partner in the allowed regions of parameter space is shown in fig. 3.18. For comparison, the same plot is made in fig. 3.19 for a lower value $\xi = 0.1$, corresponding to a higher energy scale of the strong sector. As expected, there are more points pass-

[15] Imposing a lower bound on m_ρ is not necessary here, since small values are automatically disfavoured by the large contribution to ε_3 from eq. (3.218).

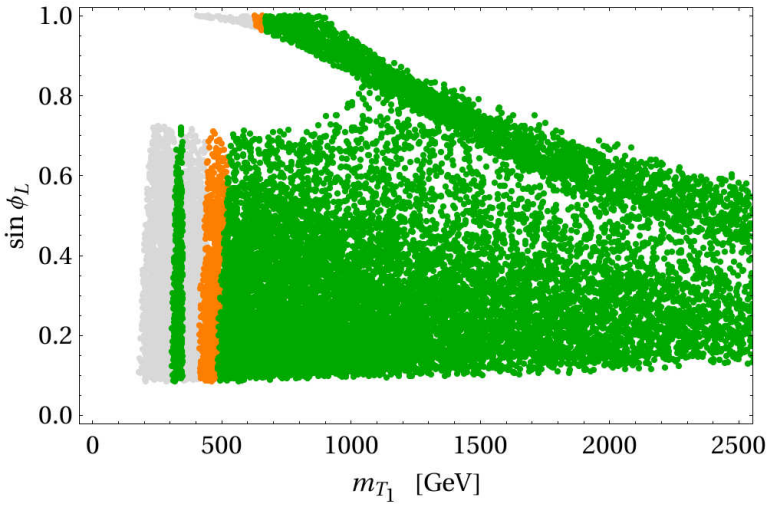

Figure 3.19: Same as fig. 3.18, with a smaller compositeness parameter $\xi = 0.1$.

ing the electroweak precision tests, but the fine-tuning required with this choice is higher. The mass spectrum of the whole fermion sector is shown in fig. 3.20 for $\xi = 0.25$. After rotating in the physical basis, it makes not much sense to distinguish fermions with the same electric charge, since their mixing can be important. It is however visible in fig. 3.20 that the fermion B of charge $-1/3$, shown in green, always come with a fermion of charge $2/3$, in blue (partially hidden behind the green region), which can obviously be interpreted as the T. Similarly, the $X^{5/3}$ (red points) is accompanied by a partner of charge $2/3$, corresponding to the $X^{2/3}$. The remaining fermion, appearing as a blue point well separated from the green and red regions, can therefore be interpreted as the $SO(4)$ singlet $\widetilde{T}$. There are two 'natural' regions of the allowed parameter space with light top partners. The first one corresponds to low values of the top compositeness angle ϕ_L, where the lightest top partner is generically the singlet $\widetilde{T}$. In this case the fermion bidoublet is always heavier than 1.5 TeV and decouples. The important mass hierarchy between the singlet and the bidoublet can only be explained by a cancellation $M_0 \approx -y_* f$, as shown in fig. 3.16. Note that the right-handed top must then be very composite in order to yield the correct top Yukawa coupling y_t (see fig. 3.17). The second region with light top partners corresponds to large values of $\sin\phi_L$, for which the top-bottom doublet becomes fully composite. In this second region, the custodian doublet X is very light, having a mass well below a TeV. Since the X doublet contains an exotic charge $5/3$ fermion (which turns out to be the lightest new fermion for large $\sin\phi_L$), this region is very sensitive to direct collider constraints, as will be discussed in the next section. An intermediate region with moderate

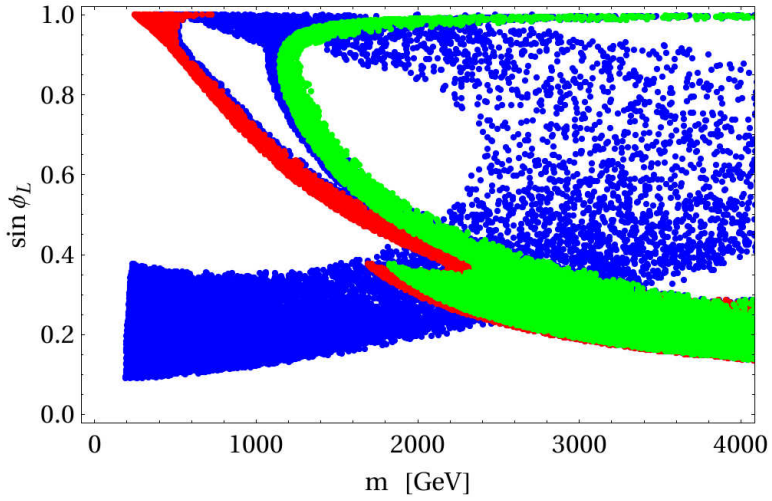

Figure 3.20: Mass spectrum of the composite fermions for a sample of points passing the electroweak precision tests. Each set of parameters corresponds to five fermions: the bottom partner B is shown in green, the exotic-charge $X^{5/3}$ is shown in red, and the three top partners T, $X^{2/3}$ and $\widetilde{T}$ are shown in blue. The value of the compositeness parameter is fixed at $\xi = 0.25$.

values of $\sin\phi_L$ is also allowed by precision data, although all new fermions are rather heavy, above 1 TeV. In most regions of the allowed parameter space, the coupling y_* must be close to its maximal value of 4π in order to compensate for the values of $\sin\phi_L$ and $\sin\phi_R$ which are preferably small, as shown in fig. 3.17. A notable exception to this rule happens at values of $\sin\phi_L$ very close to one, which are nevertheless fully excluded by direct collider constraints. Note finally that the constraints on the parameter space from electroweak precision data can be significantly relaxed by extending the fermion sector of the model [184].

3.3.4 Direct experimental constraints

Expanding the composite Higgs coupling to fermions, we obtain the leading interactions between one heavy fermion and two SM particles, which mediate the decay of the heavy states. After the rotations (3.207) and (3.208) are performed, one finds

$$\begin{aligned}\mathcal{L} \supset\ & y_* s_L c_R \left(\bar{b}_L \pi^- + \bar{t}_L \frac{h - i\,\pi^0}{\sqrt{2}}\right) \widetilde{T}_R \\ & + y_* s_R \left(-\overline{X}_L^{5/3} \pi^+ + \overline{X}_L^{2/3} \frac{h + i\,\pi^0}{\sqrt{2}}\right) t_R \\ & + y_* s_R c_L \left(\overline{B}_L \pi^- + \overline{T}_L \frac{h - i\,\pi^0}{\sqrt{2}}\right) t_R + \text{h.c.}\end{aligned} \tag{3.220}$$

The branching ratios of composite fermions into Standard Model particles can then be deduced from the Goldstone equivalence theorem, in the limit $m_\psi \gg m_Z, m_h$, for which we find for the top partners,

$$\begin{aligned}
&\mathrm{BR}(\widetilde{T} \to Wb) &&= \tfrac{1}{2}, && \mathrm{BR}(\widetilde{T} \to Zt) &&= \mathrm{BR}(\widetilde{T} \to ht) &&= \tfrac{1}{4},\\
&\mathrm{BR}(X^{2/3} \to Wb) &&= 0, && \mathrm{BR}(X^{2/3} \to Zt) &&= \mathrm{BR}(X^{2/3} \to ht) &&= \tfrac{1}{2},\\
&\mathrm{BR}(T \to Wb) &&= 0, && \mathrm{BR}(T \to Zt) &&= \mathrm{BR}(T \to ht) &&= \tfrac{1}{2},
\end{aligned} \tag{3.221}$$

while the partner of the bottom quark and the exotic new fermion can only decay to a $W^\pm t$ final state, hence

$$\mathrm{BR}(X_{5/3} \to Wt) = 1, \quad \mathrm{BR}(B \to Wt) = 1. \tag{3.222}$$

For a decent analysis of the electroweak and collider constraints, one needs however to use the exact branching ratios, obtained by performing a full numerical diagonalisation of the mass matrix in the top sector and computing the couplings of the mass eigenstates to gauge bosons and to the Higgs boson in the unitary gauge. The interaction of the Higgs boson with top partners can be read from the Lagrangian (3.199), expanding $\Sigma(x)$ in powers of the gauge fields. One obtains

$$\mathcal{L} \supset -y_* h \overline{\psi}_L^{2/3} G_{h\overline{f}f} \psi_R^{2/3} - \frac{y_*}{2f} h^2 \overline{\psi}_L^{2/3} G_{hh\overline{f}f} \psi_R^{2/3} + \text{h.c.}, \tag{3.223}$$

where the coupling matrices $G_{h\overline{f}f}$ and $G_{hh\overline{f}f}$ are defined as

$$G_{h\overline{f}f} = \begin{pmatrix} 0 & 0 & 0 & 0 \\ 0 & s_H c_H & s_H c_H & \frac{1}{\sqrt{2}}\left(c_H^2 - s_H^2\right) \\ 0 & s_H c_H & s_H c_H & \frac{1}{\sqrt{2}}\left(c_H^2 - s_H^2\right) \\ 0 & \frac{1}{\sqrt{2}}\left(c_H^2 - s_H^2\right) & \frac{1}{\sqrt{2}}\left(c_H^2 - s_H^2\right) & -2 s_H c_H \end{pmatrix}, \tag{3.224}$$

$$G_{hh\overline{f}f} = \begin{pmatrix} 0 & 0 & 0 & 0 \\ 0 & c_H^2 - s_H^2 & c_H^2 - s_H^2 & -2\sqrt{2} s_H c_H \\ 0 & c_H^2 - s_H^2 & c_H^2 - s_H^2 & -2\sqrt{2} s_H c_H \\ 0 & -2\sqrt{2} s_H c_H & -2\sqrt{2} s_H c_H & -2\left(c_H^2 - s_H^2\right) \end{pmatrix}. \tag{3.225}$$

After performing the rotations (3.207) and (3.208), the matrix $G_{h\bar{f}f}$ becomes

$$\begin{pmatrix} \frac{1}{\sqrt{2}} s_L s_R \left(c_H^2 - s_H^2\right) & s_L s_H c_H & s_L s_H c_H & \frac{1}{\sqrt{2}} s_L c_R \left(c_H^2 - s_H^2\right) \\ \frac{1}{\sqrt{2}} c_L s_R \left(c_H^2 - s_H^2\right) & c_L s_H c_H & c_L s_H c_H & \frac{1}{\sqrt{2}} c_L c_R \left(c_H^2 - s_H^2\right) \\ \frac{1}{\sqrt{2}} s_R \left(c_H^2 - s_H^2\right) & s_H c_H & s_H c_H & \frac{1}{\sqrt{2}} c_R \left(c_H^2 - s_H^2\right) \\ -2 s_R s_H c_H & \frac{1}{\sqrt{2}} \left(c_H^2 - s_H^2\right) & \frac{1}{\sqrt{2}} \left(c_H^2 - s_H^2\right) & -2 c_R s_H c_H \end{pmatrix}, \tag{3.226}$$

The first row and column indicate respectively the couplings of left- and right-handed top partners T, $X^{2/3}$ and $\widetilde{T}$ to a top quark and a Higgs boson, which are relevant to their decay into Standard Model particles. At leading order in v/f, one has therefore

$$\begin{aligned} \lambda_{ht\,L}^{T} &\cong 0, & \lambda_{ht\,R}^{T} &\cong \tfrac{1}{\sqrt{2}} y_* c_L s_R, \\ \lambda_{ht\,L}^{X^{2/3}} &\cong 0, & \lambda_{ht\,R}^{X^{2/3}} &\cong \tfrac{1}{\sqrt{2}} y_* s_R, \\ \lambda_{ht\,L}^{\widetilde{T}} &\cong \tfrac{1}{\sqrt{2}} y_* s_L c_R, & \lambda_{ht\,R}^{\widetilde{T}} &\cong 0. \end{aligned} \tag{3.227}$$

Working in the physical mass basis requires to diagonalise the mass matrix $M_{2/3}$ to all orders in v/f, a task which can in general only by realised numerically. We define the rotation matrix $U_L, U_R \in O(4)$ such that

$$M_{2/3} \to U_L^T M_{2/3} U_R = \mathrm{diag}\left(m_t, m_{T_1}, m_{T_2}, m_{T_3}\right), \tag{3.228}$$

where the masses of the top partners are ordered as $m_{T_1} < m_{T_2} < m_{T_3}$ and are all positive by convention. Note that since the sign of the determinant of the mass matrix $M_{2/3}$ depends on the sign of y_* and of the mass scale $M_0 + y_* f$, this might require $\det U_L = -1$ or $\det U_R = -1$. In this exact basis, the coupling of the lightest top partner T_1 to a Higgs boson and a top quark becomes

$$\lambda_{ht\,L}^{T_1} = y_* \left(U_L^T G_{h\bar{f}f} U_R\right)_{12}, \qquad \lambda_{ht\,R}^{T_1} = y_* \left(U_L^T G_{h\bar{f}f} U_R\right)_{21}. \tag{3.229}$$

The width of the decay $T_1 \to ht$ is therefore readily computable to be

$$\Gamma\left(T_1 \to ht\right) = \frac{m_{T_1}}{32\pi} \sqrt{\zeta_{ht}} \left[\left(\lambda_{ht\,L}^2 + \lambda_{ht\,R}^2\right) \left(1 + \frac{m_t^2}{m_{T_1}^2} - \frac{m_h^2}{m_{T_1}^2}\right) + 4 \frac{m_t}{m_{T_1}} \lambda_{ht\,L} \lambda_{ht\,R} \right], \tag{3.230}$$

where

$$\zeta_{ht} = 1 - 2\frac{m_t^2 + m_h^2}{m_{T_1}^2} + \frac{\left(m_t^2 - m_h^2\right)^2}{m_{T_1}^4}. \tag{3.231}$$

In order to compute the decay width of the lightest top partner into final states involving gauge bosons, one has to determine the relevant couplings. From the kinetic term of the fermions, one obtains the terms

$$\mathcal{L} \supset \frac{g}{c_W} Z_\mu \left(\overline{\psi}_L^{2/3} \gamma^\mu G_{Z\,L} \psi_L^{2/3} + \overline{\psi}_R^{2/3} \gamma^\mu G_{Z\,R} \psi_R^{2/3} \right), \tag{3.232}$$

where the coupling matrix G_Z are defined as

$$\begin{aligned} G_{Z\,L} &= \mathrm{diag}\left(\tfrac{1}{2}, \tfrac{1}{2}, -\tfrac{1}{2}, 0\right) - \tfrac{2}{3} s_W^2 \mathbb{1}_{4\times 4}, \\ G_{Z\,R} &= \mathrm{diag}\left(0, \tfrac{1}{2}, -\tfrac{1}{2}, 0\right) - \tfrac{2}{3} s_W^2 \mathbb{1}_{4\times 4}. \end{aligned} \tag{3.233}$$

Note that since the rotations (3.207) and (3.208) only involve particles with the same quantum numbers under the electroweak gauge group $SU(2)_W \times U(1)_Y$, the matrices $G_{Z\,L}$ and $G_{Z\,R}$ are left invariant under this very rotation. As a consequence, there are no off-diagonal couplings of the Z^0 boson to fermions at leading order in v/f. The leading couplings can be obtained from the equivalent description in terms of the Lagrangian (3.221), and are indeed suppressed by ratio of the Z^0 mass over the mass of the heavy fermion,

$$\begin{aligned} \lambda_{Zt\,L}^{T} &\cong 0, & \lambda_{Zt\,R}^{T} &\cong \tfrac{1}{\sqrt{2}} y_* c_L s_R \tfrac{m_Z}{m_Q}, \\ \lambda_{Zt\,L}^{X^{2/3}} &\cong 0, & \lambda_{Zt\,R}^{X^{2/3}} &\cong \tfrac{1}{\sqrt{2}} y_* s_R \tfrac{m_Z}{m_X}, \\ \lambda_{Zt\,L}^{\widetilde{T}} &\cong \tfrac{1}{\sqrt{2}} y_* s_L c_R \tfrac{m_Z}{m_{\widetilde{T}}}, & \lambda_{Zt\,R}^{\widetilde{T}} &\cong 0. \end{aligned} \tag{3.234}$$

The general result is again proportional to the rotation matrices U_L and U_R, and reads

$$\lambda_{Zt\,L}^{T_1} = \frac{g}{c_W} \left(U_L^T G_{Z\,L} U_L \right)_{12}, \quad \lambda_{Zt\,R}^{T_1} = \frac{g}{c_W} \left(U_R^T G_{Z\,R} U_R \right)_{12}. \tag{3.235}$$

The decay $T_1 \to Zt$ has then the width

$$\begin{aligned} \Gamma\left(T_1 \to Zt\right) = \frac{m_{T_1}}{32\pi} \sqrt{\zeta_{Zt}} \Bigg[& \left(\lambda_{Zt\,L}^2 + \lambda_{Zt\,R}^2 \right) \frac{m_{T_1}^2}{m_Z^2} \\ & \cdot \frac{m_Z^2 \left(m_{T_1}^2 + m_t^2 \right) + \left(m_{T_1}^2 - m_t^2 \right)^2 - 2 m_Z^4}{m_{T_1}^4} \\ & - 12 \frac{m_t}{m_{T_1}} \lambda_{Zt\,L} \lambda_{Zt\,R} \Bigg], \end{aligned} \tag{3.236}$$

where

$$\zeta_{Zt} = 1 - 2 \frac{m_t^2 + m_Z^2}{m_{T_1}^2} + \frac{\left(m_t^2 - m_Z^2 \right)^2}{m_{T_1}^4}. \tag{3.237}$$

The decay $T_i \to W^+ b$ is characterised by the width — neglecting the bottom quark mass —

$$\Gamma\left(T_1 \to W^+ b\right) = \frac{m_{T_1}}{32\pi}\lambda^2_{Wb\,L}\frac{m^2_{T_1}}{m^2_W}\left(1 - 3\frac{m^4_W}{m^4_{T_1}} + 2\frac{m^6_W}{m^6_{T_1}}\right). \tag{3.238}$$

Working at leading order in v/f, the coupling $\lambda_{W\,L}$ is vanishing since only the top quark couples to the bottom. The leading order coupling are thus given by the Lagrangian (3.221), and read

$$\lambda^T_{Wb\,L} \cong \lambda^{X^{2/3}}_{Wb\,L} \cong 0, \qquad \lambda^{\widetilde{T}}_{Wb\,L} \cong y_* s_L c_R \frac{m_W}{m_{\widetilde{T}}}. \tag{3.239}$$

The all-order result is in this case simply

$$\lambda^{T_1}_{Wb\,L} = \frac{g}{\sqrt{2}}\left(U_L\right)_{12}. \tag{3.240}$$

The decay widths of fermions with other electric charges can be derived in the same way:

$$\begin{aligned}\Gamma\left(B \to W^- t\right) = \frac{m_Q}{32\pi}\sqrt{\zeta_{Wt}}\Bigg[&\left(\lambda^{B\;2}_{Wt\,L} + \lambda^{B\;2}_{Wt\,R}\right)\frac{m^2_Q}{m^2_W} \\ &\cdot\frac{m^2_W\left(m^2_Q + m^2_t\right) + \left(m^2_Q - m^2_t\right)^2 - 2m^4_W}{m^4_Q} \\ &-12\frac{m_t}{m_Q}\lambda^B_{Wt\,L}\lambda^B_{Wt\,R}\Bigg],\end{aligned} \tag{3.241}$$

with

$$\zeta_{Wt} = 1 - 2\frac{m^2_t + m^2_Z}{m^2_{T_1}} + \frac{\left(m^2_t - m^2_Z\right)^2}{m^4_{T_1}}, \tag{3.242}$$

and similarly for $\Gamma\left(X^{5/3} \to W^+ t\right)$, replacing m_Q by m_X and λ^B by $\lambda^{X^{5/3}}$. The couplings are given by

$$\lambda^B_{Wt\,L} = \frac{g}{\sqrt{2}}\left(U_L\right)_{21}, \qquad \lambda^B_{Wt\,R} = \frac{g}{\sqrt{2}}\left(U_R\right)_{21}, \tag{3.243}$$

$$\lambda^{X^{5/3}}_{Wt\,L} = \frac{g}{\sqrt{2}}\left(U_L\right)_{31}, \qquad \lambda^{X^{5/3}}_{Wt\,R} = \frac{g}{\sqrt{2}}\left(U_R\right)_{31}, \tag{3.244}$$

and can be estimated at leading order in v/f by the coefficients in the Lagrangian (3.221) to be

$$\lambda^B_{Wt\,L} \cong 0, \qquad \lambda^B_{Wt\,R} \cong y_* s_R c_L \frac{m_W}{m_Q}, \tag{3.245}$$

$$\lambda^{X^{5/3}}_{Wt\,L} \cong 0, \qquad \lambda^{X^{5/3}}_{Wt\,R} \cong y_* s_R \frac{m_W}{m_X}. \tag{3.246}$$

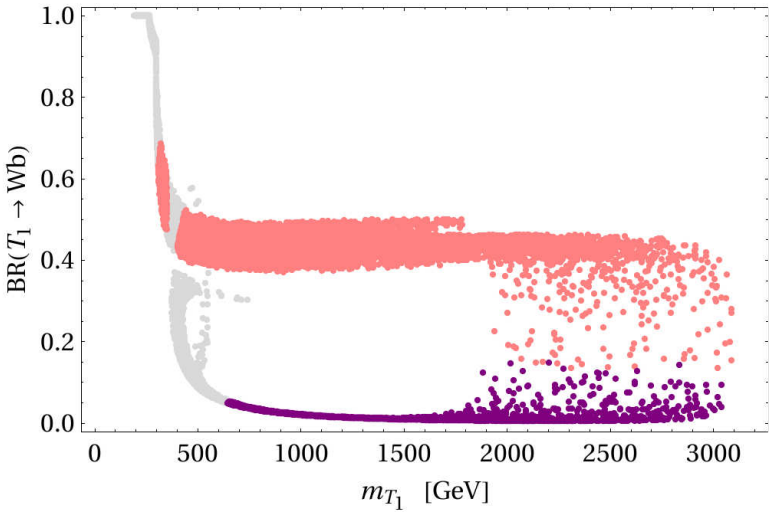

Figure 3.21: Branching ratio of the lightest top partner into a $W^{\pm}$ and a bottom quark for a sample of points passing the electroweak precision tests. Points satisfying the condition $|M_0 + y_* f| < |M_0|$, corresponding approximately to the region in which the singlet $\widetilde{T}$ is the lightest top partner are shown in pink; the purple satisfy $|M_0 + y_* f| \geq |M_0|$.

The formulae for the partial decay widths given here are consistent at leading order in v/f with those obtained in ref. [186]. The branching ratios can then be computed numerically for a given set of parameters, and the results for a sample of points passing the electroweak precision tests discussed in the previous section are shown on fig. 3.21, 3.22 and 3.23, as a function of the mass of the lightest top partner and for $\xi = 0.25$. A different colour scheme is used for the points in which a cancellation of the mass of the singlet $\widetilde{T}$ happens. Compared to the approximate formulae obtained by at leading order in ξ, the branching ratios into ht are a bit enhanced while the ones into Zt are somewhat reduced.

In certain regions of the parameter space, some fermionic resonances can be very light, thus rendering constraints from direct searches for heavy fermions at the LHC and Tevatron relevant. The experimental collaborations have performed several searches for pair-produced heavy fermions, with subsequent decay into the final states $WbWb$, $ZtZt$, $WtWt$ [187, 188, 189, 190, 191, 192, 193, 194, 195, 196, 197]. Since pair-production of the heavy fermions is a purely QCD process, the cross section $\sigma(pp,\, p\overline{p} \to \psi\overline{\psi})$, where ψ is a generic heavy fermion, only depends on its mass m_ψ. The constraint from a search for $\psi\overline{\psi} \to XX$, where X denotes one of the final states Wb, Zt, ht or Wt, will be given by

$$\sigma_{QCD}(pp \to \overline{\psi}\psi) \cdot \mathrm{BR}(\psi \to X)^2 \leq \sigma_{exp}\left(\overline{\psi}\psi \to XX\right) \tag{3.247}$$

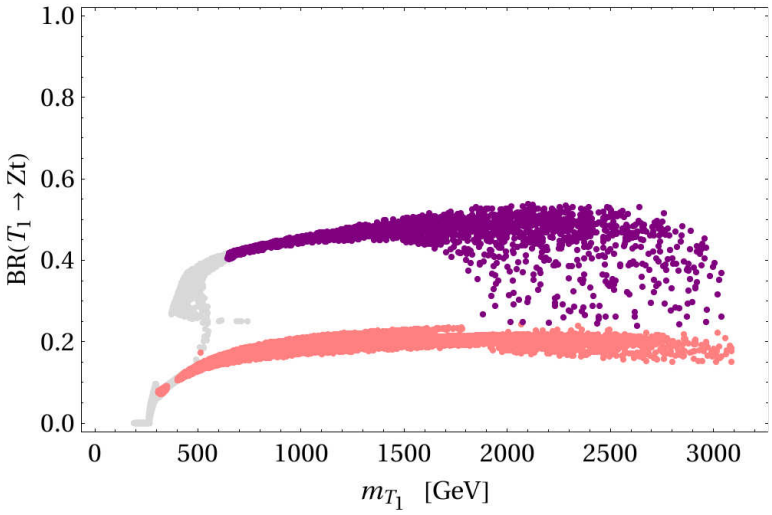

Figure 3.22: Same as fig. 3.21 for the branching ratio of the lightest top partner into a top quark and a Z^0 boson.

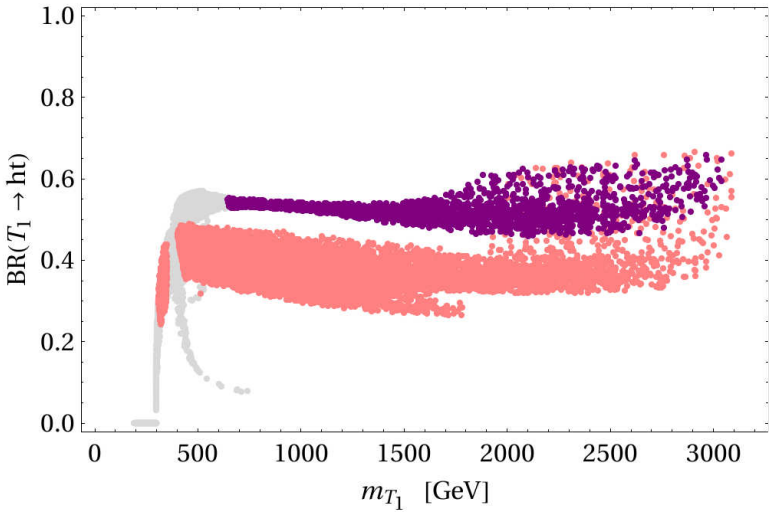

Figure 3.23: Same as fig. 3.21 for the branching ratio of the lightest top partner into a top quark and a Higgs boson.

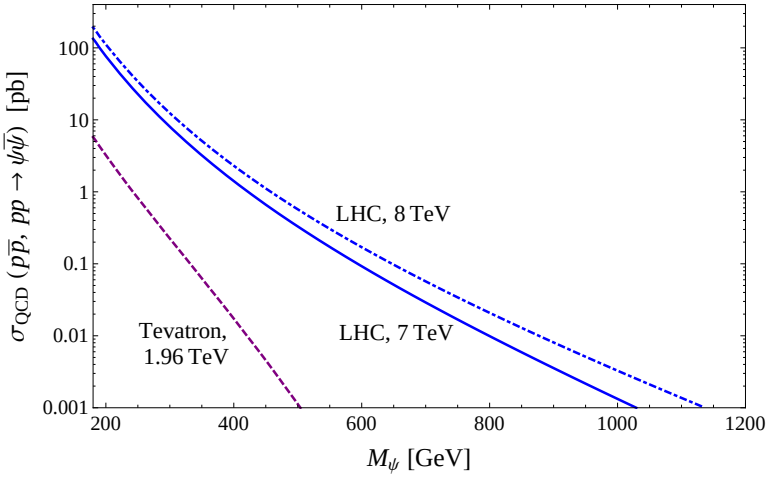

Figure 3.24: Cross-section for QCD production of heavy fermions at approximate NNLO, at the Tevatron, and the LHC with a centre-of-mass energy of 7 and 8 TeV, computed using the program HATHOR [198] and the MSTW2008 parton distribution functions [199].

where σ_{exp} is the upper bound on the cross section, as provided by the experiment for several values of the heavy fermion mass. The QCD pair-production cross sections can be obtained at approximate next-to-next-to-leading order (NNLO) [198] and are shown in fig. 3.24. Note that the branching rations are non-trivial only for the top partners $T, X^{2/3}$ and $\widetilde{T}$, whereas B and $X^{5/3}$ decay with unity branching ratio into $W^{\pm}t$. We summarise in table 3.3 all the searches for pair-produced heavy fermions which we included in our analysis. The analyses of $tWtW$ final states, although intended by the experiments to be searches for heavy charge $-1/3$ quarks such as the B, apply straightforwardly also to the $X_{5/3}$, which decays into the same final state. The decay products of $\overline{B}B$ and $\overline{X^{5/3}}X^{5/3}$ have a different kinematics — for example same-sign leptons both originate from the same $X^{5/3}$ particle in the second case, while they have to be produced one by each of the B in the first case — but since current searches only apply basic cuts, there is no sensitivity to kinematical effects.

The region of the parameter space corresponding to $\sin\phi_L \sim 1$ is the most constrained by direct searches. The lightness of the $X_{5/3}$ fermion in this case (see fig. 3.20) is prohibited by both Tevatron and LHC searches in $WtWt$ final states. For a lower degree of compositeness of the left-handed top quark, the lightest top partner is generically the singlet $\widetilde{T}$, which decays in all three final states Wb, Zt and ht. The Tevatron only has enough sensitivity to exclude top partners below 300 GeV, while the relevant LHC constraints — the ones including the full luminosity of 5 fb-1 — start

exp.	final state	$\mathcal{L}$ [fb^{-1}]	mass range [GeV]	ref.
CMS	$WbWb$ (1 lepton)	4.7	$400 - 625$	[187]
	$WbWb$ (2 leptons)	5.0	$350 - 600$	[188]
	$WtWt$	1.14	$350 - 550$	[189]
	$WtWt$	4.9	$450 - 650$	[190]
	$ZtZt$	1.14	$250 - 550$	[191]
ATLAS	$WbWb$	1.04	$250 - 500$	[192]
	$WqWq$	1.04	$300 - 500$	[193]
	$WtWt$ (1 lepton)	1.04	$300 - 600$	[194]
	$WtWt$ (2 leptons)	1.04	$300 - 600$	[195]
CDF	$WbWb$	5.6	$180 - 500$	[196]
	$WtWt$	4.8	$260 - 425$	[197]

Table 3.3: List of experimental searches for pair-produced heavy fermions included in our analysis.

only at 350 GeV. This leaves a region of the parameter space in the range $m_{\tilde{T}} \in [300, 350]$ GeV which is not directly excluded by present constraints, as can be seen in fig. 3.18 and 3.19.

In addition to the present exclusion limits, we show in fig. 3.16–3.19 an estimate of the reach of the LHC in 2012. The increase in energy enhances significantly the production cross section of heavy fermion pairs, as shown in fig.3.24. On the other hand, the present exclusion limits quoted by ATLAS and CMS will be modified due to the changes in the background and to the additional integrated luminosity. Backgrounds in searches for top partners are dominated by top quark pair production, which is increased by 42% when going from 7 to 8 TeV c.m. energy at the LHC. The search strategy relies on a cut on the $t\bar{t}$ invariant mass, whose distribution is not significantly affected by the increase in energy, as explicitly checked using MadGraph 5 [200]. The upper limit on the top partner production cross section is therefore softened in the Gaussian approximation by a factor $\sqrt{1.42} \cong 1.19$. The total luminosity of 15 fb^{-1} expected to be attained in 2012 is nevertheless tightening the limit on the cross section, lowering it by a square root factor of the luminosity in every channel. More refined searches after the LHC upgrade to 14 TeV will be needed in order to explore the full parameter space [201, 202]. Among the most interesting strategies belong the same-sign dilepton final states arising from the decay of a $X^{5/3}$ fermion [203], and

final states with multiple bottom quarks [204] or leptons [205].

3.3.5 Flavour physics

Additional constraints from past experiments come from flavour physics. As any strongly-interacting model of electroweak symmetry breaking, composite Higgs models give rise to four-fermion operators which contribute to flavour-changing processes and to electric dipole moments. Low values of the compositeness scale f as required by naturalness are only allowed if the strong sector is flavor-symmetric, hence effectively implementing *minimal flavour violation* [206]. The hierarchy among the quark and lepton masses and the mixing angles in the CKM matrix have as a unique origin the hierarchical structure of the proto-Yukawa couplings $\Delta_{L,R}$ of the type of eq. (3.194), or equivalently of the mixing angle $\phi_{L,R}$ defined in eq. (3.207) and (3.208). In this case both flavor-changing processes and electric dipole moments are automatically inhibited. The large compositeness of the top quark might nevertheless affect the V_{tb} entry of the CKM matrix. The part of the Lagrangian involving top and bottom quarks can be written as

$$\mathcal{L} \supset f \psi_L^{-1/3} G_{tb} \psi_R^{2/3}, \tag{3.248}$$

where the coupling matrix is defined as

$$G_{tb} = \begin{pmatrix} 0 & 0 & 0 & 0 \\ 0 & \frac{1}{\sqrt{2}} y_* s_H & \frac{1}{\sqrt{2}} y_* s_H & y_* c_H \end{pmatrix}. \tag{3.249}$$

After rotation in the mass basis and upon identification with the Standard Model definition of V_{tb}, one obtains

$$V_{tb} = \frac{v}{\sqrt{2} m_t} \left(U_L^{-1/3\,T} G_{tb} U_R \right)_{11} \tag{3.250}$$

where $U_L^{-1/3\,T}$ is the rotation matrix associated with the rotation (3.207) in the bottom quark sector,

$$U_L^{-1/3} = \begin{pmatrix} c_L & -s_L \\ s_L & c_L \end{pmatrix}. \tag{3.251}$$

At leading order in v/f, one finds therefore

$$V_{tb} \cong \frac{v}{\sqrt{2} m_t} \left(s_L s_R y_* s_H \right) \cong 1 \tag{3.252}$$

where in the second equality we used the top mass (3.212). Computing V_{tb} with the full dependence in v/f is however necessary in order to compare

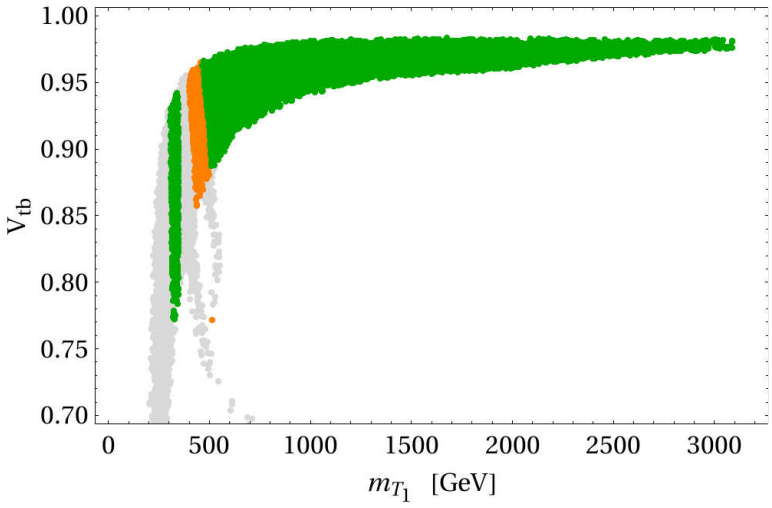

Figure 3.25: $|V_{tb}|$ as a function of the mass of the lightest top partner, as computed from eq. (3.250). The meaning of the colours is the same as in fig. 3.16 to 3.19.

it with the experimental constraints. The result are shown in fig. 3.25 for the same sample of points used above in the study of electroweak precision tests. The result turns out to be very dependent on the mass of the lightest top partner: significant deviations from unity are only seen for low values of m_{T_1}, where the direct collider constraints are most severely constraining the parameters space. The experimental bound of $|V_{tb}| > 0.77$ [185] does not actually constraint the parameter space more than our previous analysis.

The assumption of minimal flavour violation in the strong sector require nevertheless a non-zero degree of compositeness also for light quarks, which is very much constrained by experimental data. The latter can be described in an effective formalism, in which four-fermion operators arise after integrating out the vector resonances. The most relevant operator is

$$\frac{g_\rho^2}{4m_\rho^2}\,(\sin\phi_L)^4\,(\bar{q}_L\gamma^\mu t^a q_L)\,(\bar{q}_L\gamma_\mu t^a q_L)\,, \tag{3.253}$$

which imposes a constraint on the size of the mixing angle ϕ_L. From the most recent experimental dijet angular distribution [207], the bound is

$$\frac{g_\rho^2}{4m_\rho^2}\,(\sin\phi_L)^4 \lesssim \frac{2\pi}{(7.5\text{ TeV})^2} \quad \Rightarrow \quad (\sin\phi_L)^2 \lesssim \frac{f}{1.5\text{ TeV}}, \tag{3.254}$$

or equivalently $\sin\phi_L \lesssim 0.6$ for $\xi = 0.25$ and $\sin\phi_L \lesssim 0.7$ for $\xi = 0.1$. Similar bounds apply to the compositeness of right-handed quarks. Note that the recent proposal of using dijet observables may enhance even more the limit on four-fermion operators [208]. An even more stringent constraint arises

from the compositeness of the left-handed bottom quark, which affects the mass splitting between neutral B mesons, yielding the bound [157]

$$\xi \, (\sin \phi_L)^4 \lesssim 2 \cdot 10^{-3}. \tag{3.255}$$

Flavor constraints are therefore strongly disfavouring the region of the parameter space where $\sin \phi_L \approx 1$. They rely nevertheless on a number of estimates, and we will therefore not consider this region as fully excluded in our analysis of Higgs physics.

3.3.6 Single Higgs production

The cross section for single Higgs production can be readily estimated using the low-energy theorem of section 3.2.6. Note that the Higgs kinetic term is canonically normalised, so that only the term $\log \det \left[\mathcal{M}^\dagger(H)\mathcal{M}(H)\right]$ must be evaluated. Only the top partners of charge 2/3 have a non-vanishing interaction with the Higgs field H in the limit where the remaining quarks and leptons are massless, and we have

$$\det \left[M^{2/3\dagger}(H)M^{2/3}(H)\right] = \frac{1}{8}\Delta_L^2\Delta_R^2 \, (y_* f)^2 M_0^2 \sin^2\left(2\frac{H}{f}\right). \tag{3.256}$$

The determinant satisfies the factorisation condition (3.164). We obtain therefore $A_1 = (2/v)(1-2\xi)/\sqrt{1-\xi}$, where we have used $\xi = \sin^2(\langle H \rangle / f)$, and the modification of the cross-section with respect to the Standard Model value is directly found to be

$$\frac{\sigma(pp \to h)}{\sigma(pp \to h)_{SM}} = \frac{(1-2\xi)^2}{1-\xi}, \tag{3.257}$$

which is valid to all orders in ξ and is independent of the details of the fermion spectrum. While this result holds exactly only in the low-energy theorem limit, as discussed in section 3.2.6 we expect that retaining the full mass dependence will give corrections to the cross section at most of a few percent. This is confirmed by a full computation of the cross section in which the dependence on the fermion masses is retained, as shown in fig. 3.26. The figure shows the cross section of single Higgs production through gluon fusion including new fermionic resonances, normalised to the SM cross section computed with finite m_t, as a function of the mass of the lightest resonance. Note that the important K-factors arising from QCD corrections cancel out under the assumption that the higher order corrections are the same in both cases [165][16] A parameter scan has been performed, selecting

[16]This assumption is actually only valid at next-to-leading order (NLO). Effects due to the presence of different mass scales can play a role at NNLO. It was shown however that for parameters similar to the one used here the differences in the K-factors are of the order of a few percent only [165], so that the SM NNLO K-factor can safely be applied also to this composite Higgs model.

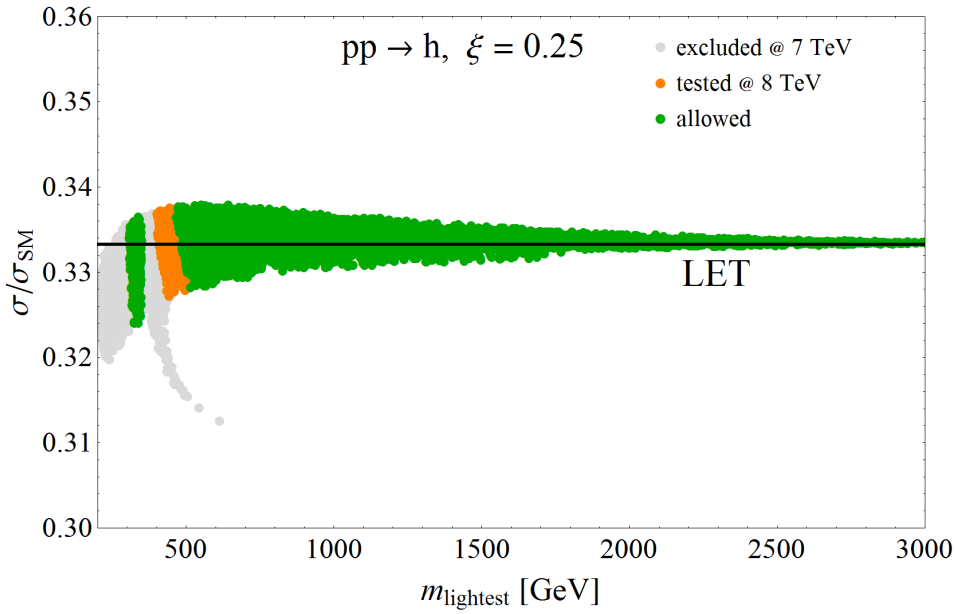

Figure 3.26: The cross-section for single Higgs production via gluon fusion including the exact dependence on the top and its heavy partners, normalised to the SM cross section (computed retaining the m_t dependence), as a function of the mass of the lightest fermion resonance m_{T_1}. The compositeness parameter has been fixed to $\xi = 0.25$. Green points are allowed by all present experimental data, grey points are excluded by current collider constraints, and orange points will be tested by the LHC run of 2012. For comparison, the cross section ratio computed with the low-energy theorem, eq. (3.257), is shown as a black line.

only points passing the electroweak precision tests. The agreement with the prediction of the low-energy theorem confirms that the cross section is to an excellent approximation independent of the details of the spectrum, and is fixed only by the composite scale f, or equivalently by the parameter ξ. The sensitivity to the composite couplings is at most $2\% \times \sigma_{SM}$ for light top partners, in agreement with our previous estimate, and vanishes for heavy partners.

Note however that additional operators have been omitted in the definition of our minimal composite Higgs models: the Lagrangian can be augmented with the operators

$$\mathcal{L} \supset i\, y'_L \left(\overline{\psi}_L \cdot \Sigma\right) \not{D} \left(\Sigma^T \cdot \psi_L\right) + i\, y'_R \left(\overline{\psi}_R \cdot \Sigma\right) \not{D} \left(\Sigma^T \cdot \psi_R\right), \qquad (3.258)$$

where the $SO(5)$-invariant combinations $(\Sigma \cdot \psi)$ is only charged under the $U(1)_X$ gauge group, so that the covariant derivative reads $D_\mu = \partial_\mu - i\, g' \frac{2}{3} B_\mu$. The new operators introduce in principle a rescaling of the ki-

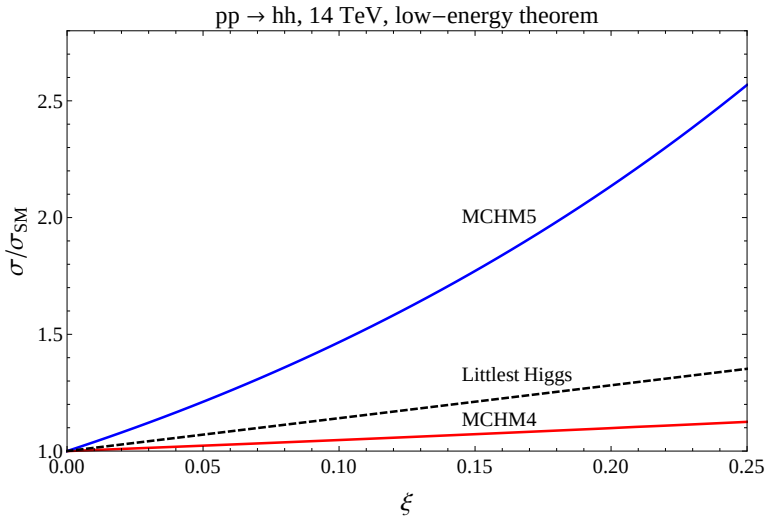

Figure 3.27: Cross-section for the process $pp \to hh$ at the LHC with a centre-of-mass energy of 14 TeV, as computed in eq. (3.259) from the low-energy theorem, normalised to the Standard Model cross-section also computed in the low-energy limit $m_t \to \infty$. The minimal composite Higgs model discussed in this section is denoted MCHM5. For the details of the computation in a model with fermions in the spinorial representation (MCHM4) and within the littlest Higgs model, see ref. [2].

netic term for the Higgs, and may affect its physics. It is however possible to perform a redefinition of the fermion fields for which the Higgs remains canonically normalised even in the presence of the operators (3.258) [166], and for which the factorisation condition (3.164) of the mass matrix determinant is preserved, so that the amplitude for the process $gg \to h$ remains insensitive to the coefficient y'_L and y'_R.

On the other hand, the Higgs derivative interactions in eq. (3.258) contribute in general to the pair production process, since they enter box diagrams. Therefore the cross section for $gg \to hh$ will be sensitive to $y'_{L,R}$. We will however only consider the minimal Lagrangian, setting $y'_{L,R} = 0$.

3.3.7 Double Higgs production

From the determinant of the fermion mass matrix (3.256), one derives $A_2 = (-2/v^2)/(1-\xi)$, which determines the $hhgg$ coupling via fermion loops. Together with the form of A_1 previously derived and with the coefficient c_2 in eq. (3.215), this allows us to write down the amplitude for $gg \to hh$ at all orders in ξ as

$$C_{\mathrm{LET}}(\hat{s}) = \frac{3m_h^2}{\hat{s}-m_h^2}\left(\frac{1-2\xi}{\sqrt{1-\xi}}\right)^2 - \frac{1}{1-\xi}. \tag{3.259}$$

As for single Higgs production, the cross-section derived from the low-energy theorem is insensitive to the details of the heavy fermion spectrum, and is fixed only by the compositeness scale ξ. The corresponding $pp \to hh$ cross section at the LHC with nominal energy is shown in fig. 3.27: the limit $\xi \to 0$ reproduces the Standard Model cross-section as expected, while a large enhancement is visible for non-zero values of ξ.

As anticipated in section 3.2.6, the low-energy theorem is expected to deviate from the numerical result retaining the full dependence on fermion masses: in single Higgs production, the expansion parameter is truly m_h^2/m_t^2 and hence works extremely well; in double Higgs production on the other hand, the expansion parameter is given by $\hat{s}/(4m_t^2)$ with $4m_t^2 \leq \hat{s} \leq (14\,\text{TeV})^2$, which is not anymore a small parameter. The discrepancy in the Standard Model is about 20%, but become worse in composite Higgs models due to the presence of the non-linear coupling of two Higgs bosons to the fermion loop, shown in fig. 3.15 (b), which does not vanish at large $\hat{s}$ contrarily to the triangle diagram involving the virtual Higgs boson exchange. An estimate of the importance of this diagram can be made by considering the full dependence on the top quark, but without including the top partners in the spectrum. A computation in this limit shows that the low-energy theorem underestimates the ratio σ/σ^{SM} by about 50% [171]: for $\xi = 0.25$, applying eq. (3.259) gives a cross section of 2.6 times the SM, whereas the enhancement factor is 3.6 when including the effects of the top quark.

Including heavy top partners in the fermion loop shows in addition that although the factorisation condition (3.164) of the mass matrix determinant is satisfied at all orders in ξ, there is a non-negligible dependence on the parameters of the strong sector, as shown in fig. 3.28 and 3.29 for two different values of the compositeness parameter ξ. The details of the full computation are given in ref. [2]. Heavy fermions decouple as expected when they become really heavy, and the limit obtained taking only the top to run in the loop is recovered with a reasonable accuracy. This is not the case however for light top partners. To estimate the reach of the 14 TeV run of the LHC on Higgs pair production, we focus on the final state $hh \to b\bar{b}\gamma\gamma$, which was shown to be the most promising for a light Higgs boson [177, 209, 210, 211]. Assuming a luminosity of 600 fb^{-1}, a benchmark computation showed that 6 signal events could be obtained after all cuts, with a background of 11 events [211]. The number signal events in the minimal composite Higgs model can be estimated by computing $\sigma(pp \to hh) \cdot \text{BR}(hh \to b\bar{b}\gamma\gamma)$ for each point in the parameter space, taking into account the QCD production K-factor of 1.9 and the non-standard Higgs branching ratios, and multiplying it times the acceptance for all cuts as computed in ref. [211] for the Standard Model. It is given on the right-hand side of fig. 3.28 and 3.29, also quoting the number of events needed for a 3σ (5σ) evidence with a luminosity of 300 (3000) fb^{-1}, based on the background estimate of ref. [211], which is likely to be conservative.

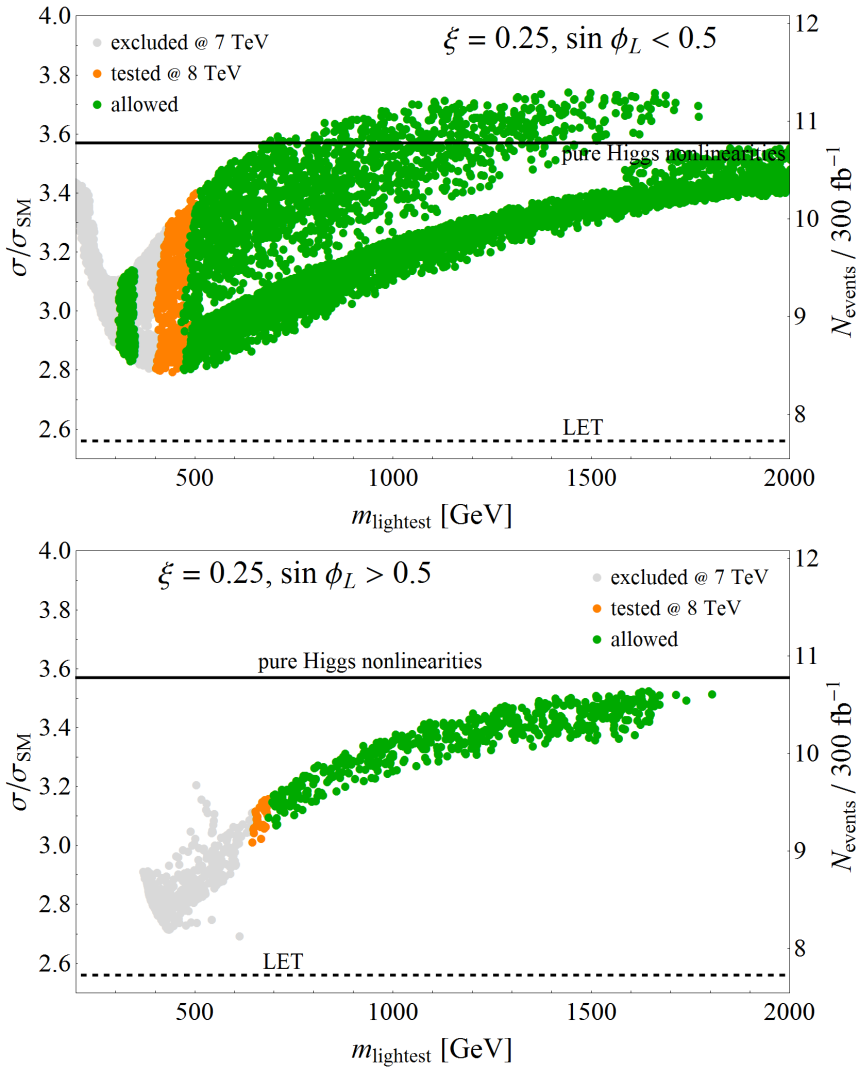

Figure 3.28: The cross-section for Higgs pair production via gluon fusion including the exact dependence on the top and its heavy partners, normalised to the SM cross section (computed retaining the m_t dependence), as a function of the mass of the lightest fermion resonance m_{T_1}. The compositeness parameter has been fixed to $\xi = 0.25$. Green points are allowed by all present experimental data, grey points are excluded by current collider constraints, and orange points will be tested by the LHC run of 2012. The result of the low-energy theorem, eq. (3.259), is shown as the dashed line. The solid line is the result of integrating out the heavy fermions but keeping the exact top mass dependence. The sample of points is separated in two sets corresponding to different values of the left-handed top compositeness, as indicated on the upper and lower panels. The estimated number of events shown on the right axis corresponds to the LHC running at 14 TeV with a luminosity of 300 fb^{-}1 (see ref. [2] for details).

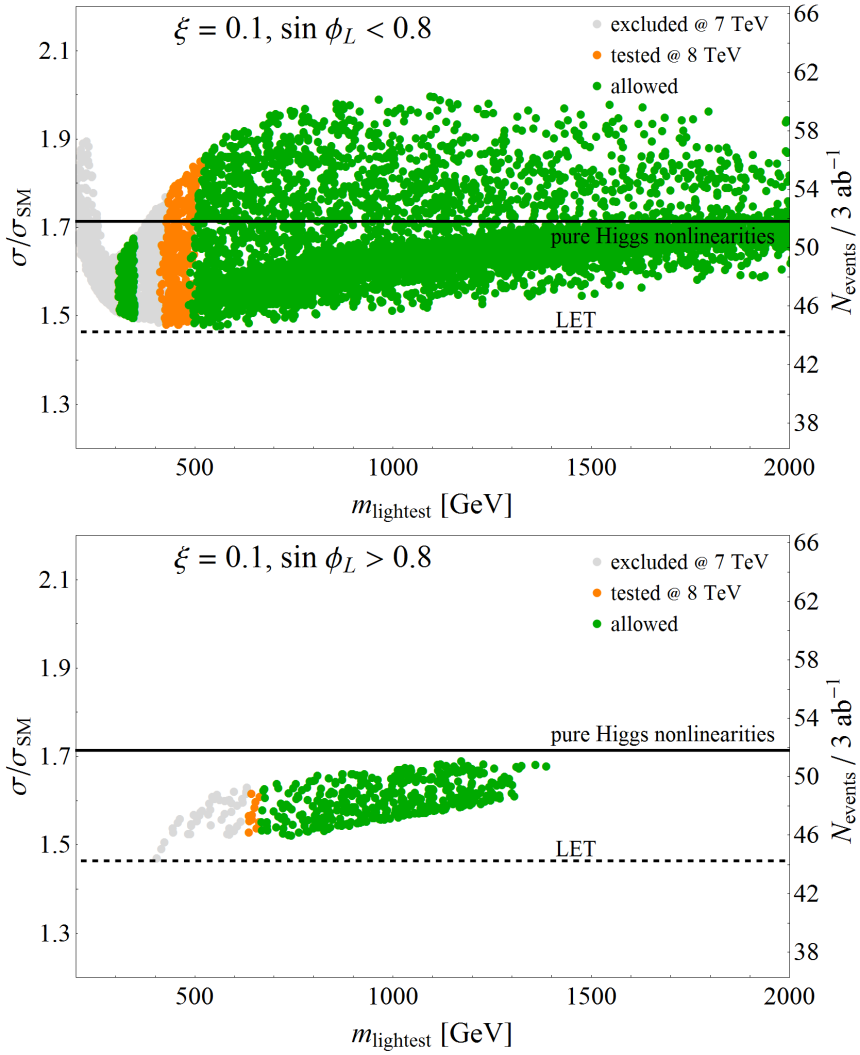

Figure 3.29: Same as fig. 3.28, for a different value of the compositeness parameter $\xi = 0.1$. The estimated number of events is based in this case on a luminosity of 3000 fb^{-}1.

3.4 Little Higgs models

Our discussion on composite Higgs models demonstrated that while the latter are still well compatible with the most recent experimental data, they are in many phenomenological areas dangerously close to the current limits. This is particularly true for electroweak precision data, constraints on direct detection of fermion and vector resonances, and flavour physics in general. If the LHC does not observe any new physics beyond the Standard Model, the current models will be excluded within a few years. All potential issues mentioned during the discussion above arise from a single problem, namely that the manifestation of the strong scale is naturally happening at too low energy. Formulated the other way around, if a small ratio $\xi = v^2/f^2$ could be naturally generated, composite Higgs models would probably become the most appealing solution to the hierarchy problem.

In this spirit, one can try and implement additional symmetries in the strong sector in order to justify a suppression of the scale v compared to f. The only known solution to this problem so far proceeds through the mechanism of *collective symmetry breaking*, and models defined in this way are supposed to feature a *little Higgs* much lighter than the strong scale. Reviews on little Higgs models can be found in ref. [212, 213].

3.4.1 Collective symmetry breaking

As discussed in section 3.2.3, the difficulty in generating a small value of v compared to the compositeness scale f is related to the problem of generating a small quadratic (mass) term in the Higgs potential while keeping the Higgs quartic coupling large. The second part of this problem will be discussed in the next section. First of all, the central ingredient in little Higgs model is to reduce the value of the Higgs quadratic term. As soon as the Goldstone shift symmetry is broken by any kind of phenomena — for example top quark or gauge boson loops — no remaining symmetry can protect a quadratic term of the form $(H^\dagger H)$, since the latter has the quantum properties of the vacuum and can be generated at all loop orders. Note however that we do not want to eliminate completely the quadratic term, only to reduce its size: cancelling the one-loop corrections from the top and gauge boson loop which are shown in fig. 2.3 would therefore be sufficient, pushing the leading contribution to the quadratic term to the two-loop order, and effectively gaining a loop factor of $1/(4\pi)^2$ in the relative ration of v/f.

A complete cancellation of the Higgs potential at one-loop is actually not possible: the efforts of theorists concentrate therefore on cancelling the quadratically divergent contributing to it, which permits already to improve the ratio v/f by a significant factor. The latter is possible through the collective symmetry breaking mechanism, in which the electroweak symmetry breaking is only introduced through the interplay of two different operators,

but is absent if any of the two operators vanishes [214, 215]. The diagrams of fig. 2.3 all involve a single vertex — or twice the same vertex — and their contribution to the Higgs potential will therefore be zero with this new symmetry. We focus first on the gauge sector of the theory, in which the freedom of adding new fields is limited: all unobserved gauge bosons must either not couple at all to the Standard Model fields or be eaten and get a mass proportional to the compositeness scale f. Implementing the collective symmetry breaking mechanism in the top Yukawa sector is made easier by the possibility to give tree-level masses to new fermions.

There are two slightly different possibilities of implementing a collective symmetry breaking in the gauge sector. The first option is to consider a single Goldstone field $\Sigma(x)$ but two different gauge groups. A simple example is given by the littlest Higgs model [216], in which the scalar field $\Sigma(x)$ is a 5×5 symmetric matrix, transforming in the two-index symmetric representation of $SU(5)$ as

$$\Sigma(x) \to U \cdot \Sigma(x) \cdot U^T, \quad U \in SU(5). \tag{3.260}$$

When the field $\Sigma(x)$ acquires a vacuum expectation value $\langle \Sigma \rangle = \mathbb{1}_{5\times5}$, the global symmetry is broken to the real subgroup $SO(5)$, and 14 Goldstone bosons appear in the low-energy spectrum. The gauge group is chosen to be a $[SU(2) \times U(1)]^2$ subgroup of the global $SU(5)$ symmetry, such that the vacuum state cannot be aligned in a direction preserving all of it. Only a diagonal subgroup $SU(2) \times U(1)$ is preserved, which is to be identified with the electroweak gauge group, and the four gauge bosons associated with broken gauge generators eat four Goldstone bosons and become massive, with a mass fixed by f much above the electroweak scale. The remaining ten Goldstone bosons transform under the electroweak group as a complex doublet, the Higgs boson, and an additional complex triplet. More details on the model are given below in section 4.5. The presence of a collective breaking mechanism appears when looking at the symmetries of the model. The true global symmetry after gauge interactions are taken into account is only given by the gauge subgroup $[SU(2) \times U(1)]^2$, which is spontaneously broken down to its diagonal subgroup. There are therefore only four exact Goldstone bosons, all of which are eaten by the gauge bosons of the broken $SU(2) \times U(1)$ gauge group. This indicates that the remaining 10 pseudo-Goldstone bosons are charged under the electroweak gauge group and might acquire a mass from radiative corrections. However, when taking to zero the gauge couplings of one of the $SU(2) \times U(1)$ gauge subgroups, the true global symmetry is enhanced to a $SU(3) \times SU(2) \times U(1)$ subgroup of $SU(5)$, which is spontaneously broken to $SU(2) \times U(1)$ by the vacuum expectation value $\langle \Sigma \rangle$. There are thus 8 exact Goldstone bosons in this case, only four of which are eaten: the remaining four are exact in this limit, and actually corresponds to the Higgs doublet. As a consequence, all diagrams including only one set of $SU(2) \times U(1)$ gauge boson do not contribute to

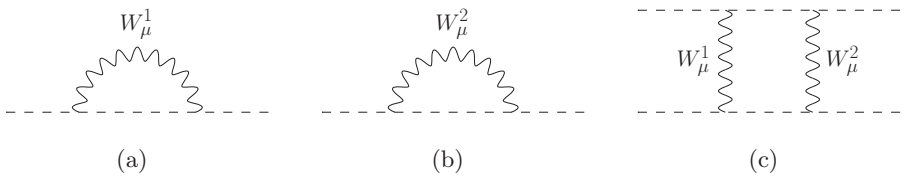

Figure 3.30: Quadratic (a) and (b) and logarithmic (c) divergent contributions to the Higgs potential in the littlest Higgs model. Diagram (a) and (b) only contribute a constant term since the include only one gauge field.

the Higgs potential; this applies to the quadratically divergent loops shown in fig. 3.30 (a) and 3.30 (b). The first non-zero contribution appearing at the one-loop level is that of fig. 3.30 (c), which includes two different gauge bosons. The mandatory presence of two different gauge boson propagators in any diagram contributing to the Higgs potential imply that the leading contribution arises only from logarithmically divergent diagrams. Note that although fig. 3.30 (c) seems to have four external Higgs legs, the field depicted there is a non-linear representation of the Higgs, which contribute both to the quadratic and to the quartic interactions of the physical Higgs doublet. In this sense, the suppression of the quadratically divergent contribution to the Higgs potential does not yet explain the smallness of the ratio v/f.

A second version of the collective symmetry breaking mechanism can be realised with only a single entity of the electroweak gauge group, but with two Goldstone fields $\Sigma_1(x)$ and $\Sigma_2(x)$. This setup is realised in the simplest little Higgs model [217,218]. Both fields $\Sigma_1(x)$ and $\Sigma_2(x)$ are 3-vectors transforming in the fundamental representation of $SU(3)$; the whole $SU(3)$ symmetry is then gauged. Both scalar fields acquires a vacuum expectation value, each of them breaking the global and gauge $SU(3)$ symmetry down to $SU(2) \times U(1)$.[17] The vacuum expectation values of the two fields tend to be aligned in order to preserve the largest possible gauge symmetry. Each scalar field describes four Goldstone bosons, and only four linear combinations of them remain massless before electroweak symmetry breaking, the orthogonal combinations being eaten by the massive gauge fields. The collective symmetry breaking mechanism is again manifest when the gauge coupling to either Σ_1 or Σ_2 are turned to zero: in this case, the scalar fields with non-vanishing gauge couplings to the gauge bosons are all eaten during the spontaneous breaking of the gauge symmetry, while the scalars with vanishing gauge couplings remains obviously massless even after electroweak sym-

[17] For the spontaneous symmetry breaking to preserve not only a $SU(2)$ subgroup of $SU(3)$ but also a $U(1)$ associated with the electroweak hypercharge, an additional $U(1)_X$ gauge symmetry must be added to the model. It plays no role in the mechanism of collective symmetry breaking and is therefore just ignored in our discussion.

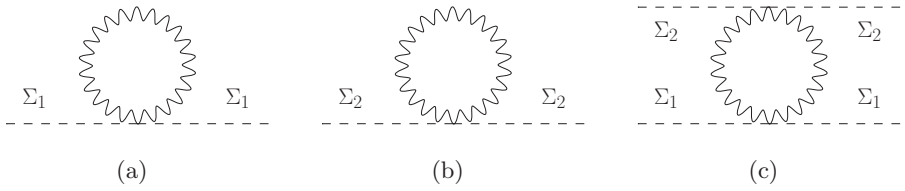

Figure 3.31: Quadratic (a) and (b) and logarithmic (c) divergent contributions to the Higgs potential in the simplest little Higgs model. Diagram (a) and (b) only contribute a constant term since the include only one of the two scalar fields.

metry breaking. As for the model previously described, quadratically divergent diagrams contributing to the Higgs potential involve only one species of Goldstone fields and are therefore vanishing, as illustrated in fig. 3.31 (a) and 3.31 (b), while logarithmically divergent diagrams involving both $\Sigma_1(x)$ and $\Sigma_2(x)$ contribute to the Higgs quadratic and quartic terms, see fig. 3.31 (c). Note that all little Higgs models must not fall into one or the other category of collective symmetry breaking mechanism described above, but might also feature a hybrid situation with multiple Goldstone fields and in which the gauge symmetry is enlarged compared to the Standard Model. This is the case of "moose" models inspired by dimensional deconstruction [219, 220].

Implementing the mechanism of collective symmetry breaking in the fermion sector follows the same lines: the key ingredient is to use two couplings for each fermion, and chose the symmetries appropriately so that the loop of fermions contributing to the Higgs potential vanishes in the limit where either of the two couplings is taken to zero. Note that since only the top quark gives a non-negligible contribution to the Higgs potential, we will only refer to it and forget about the other quarks and leptons. In the simplest little Higgs model, which corresponds to the second case discussed above, the cancellation of quadratic divergences is simply obtained by promoting the $SU(2)$ doublet of left-handed fermions $q_L = (t_L, b_L)$ to a $SU(3)$ triplet $\psi_L = (t_L, b_L, T_L)$, where T_L is a new fermion identical to the top quark so far. Two different Yukawa term can be written down, each involving one of the two scalar fields $\Sigma_1(x)$ and $\Sigma_2(x)$, which require as well to introduce two right-handed fermion singlets t_R^1 and t_R^2,

$$\mathcal{L} \supset \lambda_1 f \left(\overline{\psi}_L \cdot \Sigma_1\right) t_R^1 + \lambda_2 f \left(\overline{\psi}_L \cdot \Sigma_2\right) t_R^2, \tag{3.261}$$

where λ_1 and λ_2 are the two couplings mentioned above. After spontaneous symmetry breaking in the strong sector, and expanding the Goldstone fields in terms of the Higgs doublet H, the Yukawa terms become

$$\mathcal{L} \supset \lambda_T f \, \overline{T}_L T_R + \lambda_t \, \overline{q}_L H t_R + \mathcal{O}\left(H^\dagger H\right), \tag{3.262}$$

where the right-handed fields t_R and T_R are linear combinations of t_R^1 and t_R^2, and the couplings λ_t and λ_T are fixed by λ_1 and λ_2. The fermion spectrum of the model contains therefore one massless fermion, the bottom quark, and two massive ones, one of which is the top quark t, whose mass is generated at the electroweak scale v after electroweak symmetry breaking, and the other is its partner T, whose mass is fixed by the strong scale. In the limit where any of the two couplings λ_1 or λ_2 goes to zero, the corresponding Goldstone field Σ_1 or Σ_2 does not couple to the fermions and remains exactly massless — ignoring the effects of gauge fields — while the other scalar field gets a potential from its interactions with the fermions: the presence of a massless Higgs doublet is guaranteed in both cases. Subsequently, only diagrams involving both coupling λ_1 and λ_2, i.e. both Goldstone fields Σ_1 and Σ_2, contribute to a potential for the true Higgs doublet. Such diagrams are at most logarithmically divergent as wanted. A similar mechanism can be used to generate fermion masses in the littlest Higgs model, which was discussed in our first example above. The minimal choice is again to enlarge the Standard Model doublets into a triplet $\psi_L = (t_L, b_L, T_L)$. Although not trivial to see, such a triplet can be contracted with two entities of the Goldstone field $\Sigma(x)$ into a gauge-invariant product, adding the following operators to the Lagrangian:

$$\mathcal{L} \supset \lambda_1 f \left(\overline{\psi}_L \times \Sigma \times \Sigma\right) t_R^1 + \lambda_2 \overline{T}_L t_R^2. \tag{3.263}$$

The leading order terms in the Higgs field are then

$$\mathcal{L} \supset \lambda_t \overline{q}_L H \, t_R + \lambda_T \overline{q}_L H \, T_R + \lambda' f \overline{T}_L T_R + \mathcal{O}\left(H^\dagger H\right), \tag{3.264}$$

which contains in addition to the top Yukawa interaction and the mass term for the field T an interaction between q_L and T_R. Going to the mass basis requires an additional field redefinition after the Higgs doublet gets a vacuum expectation value, but it is obvious from the form of the Lagrangian that one of the mass eigenstates is generated with a mass close to the compositeness scale f, while the other is proportional to the electroweak scale v. The limit $\lambda_1 \to 0$ is trivial in this case since it removes all interactions of the Higgs field to the fermions. In the opposite limit $\lambda_2 \to 0$, the Higgs interacts with fermions but is protected by a $SU(3)$ shift symmetry which imply the cancellation of quadratic divergences between the loop diagram involving the quarks t and T, so that the leading contribution to the Higgs potential is again arising as a logarithm divergent diagram.

3.4.2 Higgs quartic and dangerous singlets

The realisation of a collective symmetry breaking mechanism requires to extend the global and local symmetries of the theory compared to the minimal composite Higgs models described before, which is not an easy task but

finds a satisfactory solution in different realisations. The most constraining task in the process of building a little Higgs model is actually the implementation of a large quartic coupling. In the general procedure described in the previous section, quadratic divergences in the Higgs potential are all removed at a time by the collective symmetry breaking mechanism, so that not only the Higgs quadratic term is naturally reduced, but also the quartic term. The large mass hierarchy between the scales v and f was seen to be natural only in the limit where the quartic term is more important than the quadratic one. Equivalently, the experimentally measured value of the Higgs mass requires imperatively an important quartic coupling in the Higgs potential.

Different solutions to this problem are provided in various realistic models, but often requires to extend the particle content of the model. In the simplest little Higgs model described above, it turns out that a Higgs quartic cannot be generated collectively: the model may still be viable in fine-tuned regions of the parameter space [218], but is not properly a true realisation little Higgs scenario in the original sense. A way out consists in extending the global symmetry from $SU(3)$ to $SU(4)$ [217], which also involve additional particles in the low-energy spectrum. An alternative solution to the quartic problem in this model was realised by adding a third copy of the global symmetry $SU(3)$ [221], but turns out not to work properly due to quadratically divergent contributions to the Higgs mass from a pseudo-Goldstone singlet [222]. The idea to extend the number of Goldstone fields is also the one used in product group models. Note that in the presence of two fields Σ_1 and Σ_2, the only non-trivial combination of them is of the form $\Sigma_1^\dagger \cdot \Sigma_2$, which does not generate a quartic term alone but also a mass term in the Higgs potential. Adding more Goldstone fields, whose contraction two-by-two is forbidden by the symmetry, permits to solve the problem: "plaquette" operators involving four fields can be written down, including terms of the form $\Sigma_1 \cdot \Sigma_2 \cdot \Sigma_3 \cdot \Sigma_4$ and similar terms with permutations of the Σ_i [219]. The situation is better in the littlest Higgs model, where a quartic term is automatically generated when the physical complex triplet among the Goldstone fields is integrated out [216].

The collective generation of a quartic Higgs coupling realised in the littlest Higgs model is actually an indication of the crucial role played by additional Goldstone bosons which are not the Higgs doublet [222]. This result can be explained in the following way: in the presence of a Higgs doublet H alone, the symmetry respected by the scalar, the gauge and the fermion sectors can act on the Higgs doublet as a shift symmetry parametrised by a small parameter ε with the quantum numbers of a Higgs doublet,

$$\delta H = \varepsilon + \dots \tag{3.265}$$

where the dots indicate a possible non-linear dependence on the Higgs field itself. Either the symmetry is preserved at the one-loop level, in which

case any term is forbidden in the Higgs potential, or it is somehow broken, allowing for a Higgs quartic term but at the same time for a quadratic term as well. This problem can only be solved if there is an additional Goldstone field ϕ, and two different symmetries acting on it under which the Higgs transforms as above and ϕ is shifted as

$$\delta\phi_{\pm} = \pm\frac{H\cdot\varepsilon + \varepsilon\cdot H}{f} + \dots \tag{3.266}$$

The two shift symmetries with opposite sign cannot be realised simultaneously, but can exist in two different limits in the model. Consider for example the Lagrangian

$$\mathcal{L}_{\text{quartic}} = -\lambda_1 f^2 \left|\phi + \frac{H\cdot H}{f} + \dots\right|^2 - \lambda_2 f^2 \left|\phi - \frac{H\cdot H}{f} + \dots\right|^2 . \tag{3.267}$$

If either λ_1 or λ_2 is put to zero, one of the shift symmetries acting simultaneously on H and ϕ is realised, and no potential for the Higgs can be generated, even radiatively. When both terms proportional to λ_1 and λ_2 are present at the same time, however, none of the two shift symmetries is preserved. The Lagrangian can be rewritten as

$$\mathcal{L}_{\text{quartic}} = -\left(\lambda_1+\lambda_2\right) f^2 \left[\phi + \frac{\lambda_1-\lambda_2}{\lambda_1+\lambda_2}\frac{H\cdot H}{f^2}\right]^2 + \frac{4\lambda_1\lambda_2}{\lambda_1+\lambda_2}\left(H\cdot H\right)^2 + \dots \tag{3.268}$$

and one can see that upon integrating out the field ϕ, only a quartic term for H remains. Quadratically divergent diagrams generated radiatively only include one type of vertex, either including λ_1 or λ_2 but not both, and are therefore vanishing since protected by the shift symmetries. Only logarithmically divergent diagrams which involve both couplings are then generating a mass term for the Higgs doublet, whose size is then naturally suppressed compared to the tree-level quartic coupling.

Note that for such a scenario to be realised, ϕ must have the quantum numbers of a Higgs bilinear $H\cdot H$. The meaning of the dot product was left undefined on purpose: the Higgs bilinear can be a either a real singlet or a real or complex triplet under the electroweak gauge group. If it happens to be a singlet, which is only realised by the combination $H^\dagger H$ of Higgs doublets, then ϕ has the quantum numbers of the vacuum, and tadpole diagrams can be generated, which induce radiatively the presence of the operators

$$\mathcal{L} \supset \lambda_1 f \frac{\Lambda^2}{4\pi^2}\left(\phi + \frac{H^\dagger H}{f}\right) - \lambda_2 f \frac{\Lambda^2}{4\pi^2}\left(\phi - \frac{H^\dagger H}{f}\right) \tag{3.269}$$

in the Lagrangian. Such operators yield eventually a divergent mass term for the Higgs doublet, and spoil the success of the collective symmetry breaking

mechanism. Note that if only one of those operators were present, the Higgs quadratic divergence could be absorbed in a field redefinition of ϕ, but this is not the case when both operators are generated. The presence of singlets carrying no electroweak quantum numbers is therefore dangerous in little Higgs models. This pathology is present in the extension of the simplest little Higgs model to the global symmetry breaking pattern $SU(9)/SO(8)$ [221], as well as in the attempt to implement a custodial symmetry in the littlest Higgs model based on the group structure $SO(9)/(SO(5) \times SO(4))$ [223]: both model fail to properly implement the collective symmetry breaking mechanism and require therefore the introduction of fine-tuning.

In the presence of one Higgs doublet, the only possibility to generate collectively a Higgs quartic is therefore to have a physical Higgs triplet, either real or complex. The latter case is realised in the littlest Higgs model, while there exist no model based on a real triplet yet. The situation is slightly better in models featuring two Higgs doublets. In this case a singlet can carry an additional $\mathbb{Z}_2$ symmetry associated with the sign flip of the two Higgs doublets with respect to each other, which prevent the singlet from generating quadratic divergent contribution to the Higgs potential through tadpole diagrams. The "antisymmetric condensate" model based on the breaking pattern $SU(6)/Sp(6)$ [224] and the "bestest little Higgs" [220] are examples of models realising this possibility.

3.4.3 Phenomenology

Little Higgs models feature a natural hierarchy between the electroweak scale v and the compositeness scale f. However, the construction of realistic models seems to indicate that a scale $f \gg 1$ TeV still requires some fine-tuning, the natural scale for f being around the TeV scale. The deviations from the Standard Model at low energy due to the new physics are then of order of a few percents, and can therefore still be very much constrained by the electroweak precision data gathered at LEP. In the littlest Higgs model, for example, new physics effects require $f > 4$ TeV [225, 226, 227].[18] The main issue in this model is arising from the tree-level contribution to the $\hat{T}$ parameters due to the mixing of the two $U(1)$ gauge bosons. The extension of the symmetry breaking pattern to $SO(9)/(SO(5) \times SO(4))$ in order to preserve a custodial symmetry yields a model which suffers from the dangerous singlet pathology [223], and is therefore unsatisfying. A similar tension in the electroweak precision observables is present in different

[18] The lightness of the gauge boson associated with the broken $U(1)$ symmetry may in this case even be sensitive to the direct detection bounds; it might therefore be convenient to consider a variation of the littlest Higgs model in which the problematic gauge boson is removed, i.e. the gauge symmetry before spontaneous symmetry breaking is $[SU(2)]^2 \times U(1)$ [228]. Radiative corrections arising from the $U(1)$ gauge boson are thus not suppressed by the collective symmetry breaking mechanism, but are sufficiently small so as not to destabilise the hierarchy $v \ll f$.

realisations of the little Higgs idea [229]. The necessity of having a electroweak triplet in the spectrum, and more importantly the fact that this triplet must acquire a non-zero vacuum expectation value, lead to important breaking of the custodial symmetry even in models where it is imposed at the Lagrangian level.[19] A similar problem appears in the extension of the "moose" model [219] in which the global symmetry group, appearing in multiple copies, is enlarged from $SU(3)$ to $SO(5)$ [231]: a custodial symmetry is present in the model, but the required misalignment of the vacuum expectation value of both Higgs doublets is inducing large corrections to it. A solution can be found when extending the global symmetry even further to $SO(6)$ [220]. Other models with two little Higgs doublets, such as the $SU(6)/Sp(6)$ "antisymmetric condensate" model [224] are doing better when confronting electroweak precision tests.

Models with a single little Higgs doublet can nevertheless be delivered from tree-level contributions to the gauge boson form factors by a different mechanism: many model permit the implementation of a discrete $\mathbb{Z}_2$ symmetry called *T-parity*, under which all Standard Model fields are even — including the Higgs boson – while all new particles introduced in the model are odd [232, 233]. In this case, no physical process can involve only one heavy field from the new physics sector, but at least two of them are required. Tree-level contributions to the electroweak parameters $\hat{S}$ and $\hat{T}$ are therefore prohibited. The implementation of such a parity cannot be realised in models with a simple gauge group: at least two copies of $SU(2)\times U(1)$ are needed, which break down into the T-even $W^{\pm}$ and Z^0 gauge bosons, and a new set of four T-odd massive gauge bosons, W'^a and Z'. The difficulty in building models with a T-parity comes from the fermion sector, since it is not trivial to add fermions as eigenstates of the T-parity. The most obvious choice to introduce them as transforming under the unbroken global symmetry group [234] lead to an important tension between the required large mass for the top partners and the vertex corrections involving the set of new fermions [235].[20] Realistic models need to introduce two different type of fermions, some of them transforming under the global symmetry group present before the spontaneous symmetry breakdown, and others belonging to the unbroken subgroup but transforming therefore non-linearly under the overall global symmetry [234, 236]. The presence of numerous new fermions beyond the Standard Model ones lead to a rich phenomenology [237], but is an important drawback in the quest of finding an elegant model with minimal content.

The presence of T-parity in little Higgs models has also very dramatic consequences for cosmology: the lightest T-odd particle turns out to be

[19] A small breaking of the custodial symmetry might actually be favoured by precision data, and could be generated by the vacuum expectation value of a triplet [230].

[20] The realisation of ref. [234] also require to enlarge the symmetry group of the model.

stable due to the absence of possible decay products, and can therefore become a promising dark matter candidate provided it is electrically neutral [238, 239, 240, 241, 242]. In all little Higgs models discussed so far, T-parity is however only an accidental symmetry of the low-energy effective description and is broken by anomalies which arise in the effective description from a Wess-Zumino-Witten term [243, 244]. As a consequence, the lightest T-odd particle can generically decay into gauge bosons [245,246], and its ability in playing the role of dark matter is spoiled. Note that the anomalous breaking of T-parity can be counteracted in some realisations of the little Higgs idea by the presence of additional discrete symmetries [247]: specific models featuring a stable dark matter candidate have been built [248, 249]. Alternatively, the presence of a weakly-coupled, anomaly-free UV completion of the model could prevent the presence of a Wess-Zumino-Witten term. Such a UV completion exists for example for the littlest Higgs model [250], but requires the introduction of a very large number of new fields, hence missing the requirement of minimality. Note that such a UV completion reintroduces the hierarchy problem between the "little Higgs scale" of a few TeV and the Planck scale. Other weakly coupled UV completions aiming at solving this problem use many copies of the little Higgs mechanism in order to explain the smallness of the electroweak scale. Most little Higgs models are however meant as being the low-energy description of a strongly-interacting theory, either purely in four-dimensional space-time [251] or in a holographic description [252, 253].

Note finally that the current status of little Higgs theories is somewhat disappointing: only the littlest Higgs model provide a single Higgs doublet and fully realises the cancellation of quadratic divergences in the Higgs potential, which was the original goal of little Higgs theories. The model is at the same time only viable in the presence of a T-parity, introducing therefore mild issues in the fermion sector. It will be moreover shown in the next chapter that strongly-coupled UV completion of the littlest Higgs model have to deal with a much worse problem, the presence of an electrically charged stable particle in their spectrum. A minimal and fully viable little Higgs model is thus still missing. If such a model exists, it must probably possess apart from the Higgs doublet only a real triplet in its spectrum, and possibly implement a custodial symmetry in its construction. The coset $SO(7)/G_2$ mentioned in table 3.2 might provide a good candidate, and is currently under scrutiny of the author.

4

The Skyrme Model and its Applications

The previous chapter was dedicated to showing that electroweak symmetry breaking can arise from a strongly-coupled sector added to the Standard Model. Among the models realising this possibility, only the ones containing a pseudo-Goldstone Higgs doublet were in agreement with experimental data in the perturbative regime. An important number of assumptions came from extrapolating the knowledge of low-energy QCD to the electroweak scale, since the former is up to now the only known strongly-coupled theory in particle physics. There is however a point that we overlooked so far: the immense majority of particles present in the visible universe appear in QCD as baryons, which are not describe in terms of Goldstone bosons like the mesons are. The most striking consequence of adding a new, strongly-interacting sector to the Standard Model could therefore in principle be the presence of new, stable, heavy objects, the equivalent of protons and neutrons in QCD. While these hypothetical new particles could maybe explain the missing mass in our universe, usually denoted by dark matter, they are above all subject to very stringent constraints. If such particle exists, they must interact with the Standard Model quarks and leptons at most through the weak or colour interaction, but should definitely be electrically neutral, hence not coupling directly to the photon. Moreover, their relic density must obviously not exceed that of the dark matter. Alternatively, if the strongly-coupled theory of the electroweak symmetry breaking is not QCD-like, the possibility exists that no stable, heavy bound state are created.

These issues are precisely going to be investigated in this chapter. Note however that we want again to take an effective approach to the theory of electroweak symmetry breaking, which departs from our discussion of QCD made in chapters 2 and 3. For QCD, we started with a theory of

fundamental fermions — the quarks — and demonstrated that the theory is confined, hence leading to the presence of mesons and baryons as the low-energy degrees of freedom. Such an approach permits to learn a lot about the physics of baryons and their interactions, but cannot be used for composite Higgs and little Higgs models when one takes above perspective of being agnostic about the UV completion of these models. In analogy with QCD, our task is therefore to study the physics of baryons while using only information taken from the meson sector.

Interestingly, there exists such a description of baryons in QCD, in which they arise as the topological solitons of the σ-model describing pions and kaons. This is the so-called Skyrme model described below in section 4.1. After reviewing the model, its methods and its predictions, we will show that it can be extended to fit the requirements of composite Higgs and little Higgs theories, and study its phenomenological consequences. The content of sections 4.1 and 4.2 is based on reviews of the Skyrme model given in textbooks [254, 255, 14], as well as on research papers cited directly in the text. Sections 4.3, 4.4 and 4.5 are directly taken from the original work of the author, published in ref. [5, 3, 4].

4.1 Skyrmions as the baryons of QCD

Before studying the topological solitons directly in composite Higgs models, we review the results obtained in QCD. Our starting point is therefore the low-energy theory describing the Goldstone modes only, given by the non-linear σ-model Lagrangian of eq. (3.14). We will see that solitons arise in this model — requiring however to include other terms irrelevant in the perturbative approach — and compute their properties.

4.1.1 Topological charge and baryon number

Let us consider a general theory describing a field $\Phi(x) \in SU(N)$, and where the vacuum state corresponds to the identity matrix $\langle \Phi(x) \rangle = \mathbb{1}_{N\times N}$. The field $\Phi(x)$ contains $N^2 - 1$ degrees of freedom, and describes therefore a set of scalar fields π^a, related to the $SU(N)$-valued field through the generators T^a of the group as

$$\Sigma(x) = \exp\left[i\,\pi^a(x) T^a / f_\pi\right]. \tag{4.1}$$

Assuming that the generators satisfy $\mathrm{Tr}\left(T^a T^b\right) = \frac{1}{2}\delta^{ab}$, the canonically-normalised kinetic term for the fields π^a is then

$$\mathcal{L}_2 = \frac{f^2}{4}\,\mathrm{Tr}\left(\partial_\mu \Phi^\dagger \partial^\mu \Phi\right). \tag{4.2}$$

Note that since $\Phi^\dagger\Phi = \mathbb{1}$, no potential can be written for the fields π^a; they can be seen as Goldstone bosons, although this characteristic is not

necessary in our approach. Any other operators written in terms of the field $\Sigma(x)$ contain at least four space-time derivatives, and are thus subdominant at very low energy.

We are now interested in studying static field configurations, i.e. time-independent solutions to the equations of motion for the field $\Sigma(x)$. In order to have a finite energy, any such field configuration must be in the vacuum at the boundaries of the three-dimensional space, i.e. the energy must be localised somewhere in space. The field considered at the moment can therefore be described by the mapping

$$\Phi : \begin{cases} \mathbb{R}^3 \to SU(N) \\ \vec{x} \mapsto \Phi(\vec{x}) \end{cases} \qquad \text{with } \Phi(|\vec{x}| \to \infty) = \mathbb{1}_{N\times N}. \tag{4.3}$$

Upon these requirement, any field configuration can be characterised by an integer number

$$B(\Phi) = -\frac{1}{24\pi^2}\varepsilon_{ijk}\int d^3x \ \mathrm{Tr}(\Phi^\dagger\partial_i\Phi)(\Phi^\dagger\partial_j\Phi)(\Phi^\dagger\partial_k\Phi) \ \in \mathbb{Z}. \tag{4.4}$$

This integral has very special properties. First, it is a topological quantity in the sense that it is invariant under any infinitesimal transformation of Φ. Second, the integral (4.4) is additive with respect to multiplication of two fields $\Phi_1(x)$ and $\Phi_2(x)$: an explicit computation gives

$$B(\Phi_1\Phi_2) = B(\Phi_1) + B(\Phi_2) - \int d^3x \ \partial_i\Omega_i, \tag{4.5}$$

where

$$\Omega_i = \frac{1}{8\pi^2}\varepsilon_{ijk}\,\mathrm{Tr}(\Phi_1^\dagger\partial_j\Phi_1)(\Phi_2\partial_k\Phi_2^\dagger). \tag{4.6}$$

The last term above is a surface term and therefore vanishes provided that the fields are in the vacuum at the spatial boundaries. Note also that the integral is zero when evaluated on the vacuum state, $B(\mathbb{1}) = 0$, and that the relation $B(\Phi^\dagger) = -B(\Phi)$ follows from the unitarity of the matrix $\Phi \in SU(N)$. From these properties, the integral (4.4) must takes its values in a finite set of numbers, symmetric around zero. There must therefore be a field configuration Φ_0 for which $B(\Phi_0)$ is the closest possible to zero, and such that other non-zero values for B can be generated as integer multiples of it. The normalisation in eq. (4.4) was actually chosen such that the lowest possible value of the integral is one, so that B takes indeed its values in the set of integer numbers $\mathbb{Z}$. $B(\Phi)$ is therefore called the *winding number* of the field $\Phi \in SU(N)$. This denomination comes from the fact that the three-dimensional space $\mathbb{R}^3$ can be identified with the three-sphere S^3 when the requirement (4.3) is satisfied: in this case, all points at spatial infinity take the same vacuum value in $SU(N)$ and can therefore be identified to

a unique point, for example through the use of a stereographic projection. The field Σ can thus be seen mathematically as a mapping $S^3 \to SU(N)$, which is characterised by the third homotopy group of $SU(N)$,

$$\pi_3\big(SU(N)\big) = \mathbb{Z}. \tag{4.7}$$

In the low-energy limit of QCD, where the meson fields were described by a $SU(N)$ valued matrix $U(x)$ in eq. (3.13) — N corresponding then to the number of light quark flavours — the winding number integral (4.4) matches exactly the baryon number, written in terms of the field $U(x)$ in eq. (3.62). This finally explains our statement made in section 3.1 that the baryon number is a topological quantity.

Field configuration of different winding number — i.e. belonging to different homotopy classes — cannot be continuously deformed one into another. The lightest configuration in each homotopy class is therefore absolutely stable over time. If all minima are degenerate in energy, then they all represent a vacuum state of the theory, and we recover a typical θ-vacuum situation similar to the one discussed in section 2.1.1. If on the contrary not all the minima have the same energy, then only the lightest one will be the true vacuum of the theory; in this case, the lightest field configuration belonging to a homotopy class which do not include the true vacuum will appear as a stable, massive object in the complete theory, with finite size and finite energy. It corresponds then to a *topological soliton*. Determining which of the two situations is realised in our theory requires to look at the Hamiltonian of the system. For the Lagrangian (4.2), the latter is

$$H_2 = \frac{f^2}{4} \int \mathrm{d}^3x \left[\mathrm{Tr}\left(\partial_0 \Phi^\dagger \partial_0 \Phi\right) + \mathrm{Tr}\left(\partial_i \Phi^\dagger \partial_i \Phi\right)\right] \geq 0 \tag{4.8}$$

and indicates that the energy of the system is bounded below by zero. The bound is saturated by our choice $\langle \Phi \rangle = \mathbb{1}_{N\times N}$, which indicates that it is indeed the true vacuum of the theory. The homotopy class corresponding to $B(\Phi) = 0$ is therefore called topologically trivial. In this simple case, however, field configurations with non-zero winding number can also saturate the bound on the energy, as proved by Derrick's theorem [256]: in our $3+1$ dimensional world, under a rescaling of the spacetime coordinates $x \to \lambda\, x$, the energy associated with the kinetic term scales as $H_2 \to \lambda\, H_2$ and can thus be made arbitrarily small. The mass and size of any soliton satisfying $B(\Phi) \neq 0$ can shrink to zero, and all homotopy classes contain excitations of arbitrarily small energy. Derrick's theorem can nevertheless be evaded by adding terms with more derivatives to the Lagrangian. As a first step, one can add the terms with four derivatives, which were given in eq. (3.23) and are reminded here:

$$\begin{aligned} \mathcal{L}_4 = {} & c_1 \,\mathrm{Tr}\left(\partial_\mu \Phi^\dagger \partial^\mu \Phi\, \partial_\nu \Phi^\dagger \partial^\nu \Phi\ \right) + c_2 \,\mathrm{Tr}\left(\partial_\mu \Phi^\dagger \partial_\nu \Phi\, \partial^\mu \Phi^\dagger \partial^\nu \Phi\ \right) \\ & + c_3 \left[\mathrm{Tr}\left(\partial_\mu \Phi^\dagger \partial^\mu \Phi\right)\right]^2 . \end{aligned} \tag{4.9}$$

Since the field $\Phi(x)$ is itself invariant under rescaling, adding more derivatives changes the overall scaling of the energy: the Hamiltonian associated with $\mathcal{L}_4$ scales as $H_4 \to (\lambda)^{-1} H_4$, and prevents the size of an hypothetical soliton to shrink to zero in the limit $\lambda \to 0$. In the presence of both terms $\mathcal{L}_2$ and $\mathcal{L}_4$, the energy of the system is bounded by a minimum reached when the respective Hamiltonians H_2 and H_4 contribute equally.

4.1.2 The Skyrme model

The Skyrme model corresponds to a particular choice among the operators of dimension four in the Lagrangian (4.9), under which the solitons has peculiar properties. Note first that the third homotopy group $\pi_3(SU(N))$ is identically equal to the set of integers for any $N \geq 2$. The reason for this is that the winding number integral (4.4) actually counts the number of windings around an $SU(2)$ subgroup of $SU(N)$, as will be discussed below, such that all information about the solitons appearing as topologically non-trivial field configurations can be learnt — at least at the classical level — from the case $N = 2$. The latter case corresponds also to the natural choice in the low-energy theory of QCD, since the up and down quark masses are much lighter than the strange quark's one. As discussed in the previous chapter, there are only two linearly-independent operators with four derivatives of the field $\Phi(x)$, so that the term proportional to the coefficient c_3 in eq. (4.9) can be dropped. The second crucial choice made in the definition of the Skyrme model is to limit the number of time derivatives to two, so that a Hamiltonian can be easily constructed and a canonical quantisation performed. This requirement is achieved by building the dimension four operator as an antisymmetric product of identical Lorentz structure: the so-called *Skyrme model* can then be written with the help of commutators as [257]

$$\begin{aligned}\mathcal{L}_{\text{Skyrme}} = & \frac{f_\pi^2}{4} \operatorname{Tr}\left(\partial_\mu \Phi^\dagger \partial^\mu \Phi\right) \\ & + \frac{1}{32e^2} \operatorname{Tr}\left[\Phi^\dagger \partial_\mu \Phi, \Phi^\dagger \partial_\nu \Phi\right]\left[\Phi^\dagger \partial^\mu \Phi, \Phi^\dagger \partial^\nu \Phi\right], \end{aligned} \tag{4.10}$$

and corresponds to the special choice $c_1 = -c_2 = -1/(16e^2)$. The model will turn out to provided a good, yet very simple, description of the baryons as topological solitons. The only parameter entering the model apart from the dimensionful constant f_π fixed by pion interactions is the Skyrme parameter e, which is naively of order unity. For a static field configuration such as the ones discussed in the previous section, the total energy of the system can be

written as

$$E(\Phi) = \int \mathrm{d}^3x \left\{ \frac{f^2}{4} \operatorname{Tr}\left(\partial_i \Phi^\dagger \partial_i \Phi\right) + \frac{1}{16e^2} \left[\operatorname{Tr}\left(\partial_i \Phi^\dagger \partial_i \Phi \partial_j \Phi^\dagger \partial_j \Phi\right) - \left(\partial_i \Phi^\dagger \partial_j \Phi \partial_i \Phi^\dagger \partial_j \Phi\right) \right] \right\}. \tag{4.11}$$

It will be convenient in the following to introduce dimensionless units $\widetilde{x} = (fe)\, x$, for which the dependence of the energy on the parameters f_π and e can be factorised out of the integral, and becomes

$$E(\Phi) = \frac{f}{e} \int \mathrm{d}^3\widetilde{x} \left\{ \frac{1}{4} \operatorname{Tr}\left(\partial_i \Phi^\dagger \partial_i \Phi\right) + \frac{1}{16} \left[\operatorname{Tr}\left(\partial_i \Phi^\dagger \partial_i \Phi \partial_j \Phi^\dagger \partial_j \Phi\right) - \left(\partial_i \Phi^\dagger \partial_j \Phi \partial_i \Phi^\dagger \partial_j \Phi\right) \right] \right\} \tag{4.12}$$

The integrand is then a dimensionless quantity and can be directly computed from the shape of the field $\Phi(\widetilde{x})$. The notation $\widetilde{x}$ will often be implicit in the rest of this chapter. A very crucial feature of the Skyrme model is that this energy is bounded below by a positive, non-zero quantity for field configuration with non-trivial topology, $B(\Phi) \neq 0$. This is better seen by defining a quantity

$$K_i^\pm = i \left[\frac{f}{2}\, \Phi^\dagger \partial_i \Phi \pm \frac{1}{4e} \varepsilon_{ijk}\, \partial_j \Phi^\dagger \partial_k \Phi \right], \tag{4.13}$$

which is Hermitian by definition, $\left(K_i^\pm\right)^\dagger = K_i^\pm$, so that its square is positive definite. Computing explicitly the trace of the operator $(K_i^\pm)^2$, one finds

$$\operatorname{Tr}\left(K_i^\pm K_i^\pm\right) = E(\Phi) \pm 6\pi^2 \frac{f}{e}\, B(\Phi) \geq 0, \tag{4.14}$$

where the right-hand side of the equality is written in terms of the energy density (4.11) and of the winding number (4.4). Since this quantity is positive for both signs K_i^+ and K_i^-, one can write down a lower bound on the energy as

$$E(\Phi) \geq 6\pi^2 \frac{f}{e}\, |B(\Phi)|\,. \tag{4.15}$$

This inequality reminds of the BPS bound [258,259] on the mass of 't Hooft-Polyakov monopoles [58,59] mentioned in chapter 2, and is accordingly often called the *Bogomolny bound*.[1] The presence of this bound unambiguously lifts the degeneracy among the ground states of each homotopy class, so that only the state $\langle\Phi\rangle$ is the true vacuum of the theory, while other configurations

[1] Note however that the bound was already derived many years earlier by Skyrme in its own work [257].

minimising the energy (4.11) corresponds to solitons, called in this case *skyrmions*.

An interesting comment on the scaling of meson and baryon masses with the number of colours N_c of the underlying theory can be made here. As explained in eq. (3.7), the pion decay constant f_π scales proportionally with the square root of the number of colours, $f_\pi \propto (N_c)^{1/2}$. At leading order, the Skyrme terms yields a four-pions interaction with a coupling proportional to $1/(f_\pi^4 e^2)$. From the required scaling of pion interactions as given in eq. (3.9), one finds the relation $e \propto (N_c)^{-1/2}$, or more importantly, $f/e \propto N_c$. The latter indicates that the mass of the skyrmion scales with one power of N_c. On the contrary, the size of the skyrmion is fixed only by the interplay of the two terms in the integrand of eq. (4.12), and is therefore independent of the number of colours. The skyrmion's scaling properties match therefore exactly the ones of the baryons obtained in the quark picture in section 3.1.2. Together with the observation that the winding number integral (4.4) corresponds exactly to the baryon number in QCD, there is a strong evidence that the skyrmions represent indeed baryon states in the low-energy picture of QCD [260].

Note finally that in order to account for a realistic theory of both mesons and baryons, a mass term breaking the chiral symmetry must be added to the Lagrangian, as in eq. (3.51):

$$\mathcal{L}_{\text{mass}} = \frac{1}{4} m_\pi^2 f_\pi^2 \left[\text{Tr}(\Phi) + \text{Tr}(\Phi^\dagger) - 4 \right]. \tag{4.16}$$

Such a term is only present in the theory of pions with $N = 2$, although other terms might be constructed for a field $\Phi \in SU(N)$ with $N > 2$. It also formally breaks the Bogomolny bound (4.15), although it will be seen in the next section that the skyrmion masses only increase with $m_\pi \neq 0$.

4.1.3 The hedgehog ansatz

It is well accepted that for solitons, the field configurations of highest symmetry tend to yield the lowest energy solutions to the field equations. This is the case of the 't Hooft-Polyakov monopole [58, 59], of the Julia-Zee dyon [261], and of the original skyrmion solution which will be presented here. All these solitonic field configurations are spherically symmetric, reflecting the rotational invariance of the Lagrangian density. Notice however that this is not the case for solitons of winding number larger than one. For monopoles, it has been proved in ref. [262] that only the unit winding number solutions preserve the spherical symmetry, since the mass of a spherically symmetric configuration of magnetic charge $n > 1$ is larger than n times the mass of the solution of magnetic charge one. A similar behaviour is found for skyrmions, where the solutions of multiple winding number will be shortly discussed in section 4.1.6.

In the Skyrme model, the solution of unit winding number with the lowest energy is found using the *hedgehog ansatz* [263]

$$\Phi_h = \exp\left[2i\,F(r)\,\hat{x}_i\,T^i\right], \tag{4.17}$$

where $F(r)$ is a function of the radial variable $r = \sqrt{x_i^2}$, the $\hat{x}_i = x_i/r$ are angular coordinates, and the T^i are generators of $SU(N)$ satisfying a proper normalisation condition and simultaneously forming a $\mathfrak{su}(2)$ algebra,

$$\mathrm{Tr}\left(T^a T^b\right) = \frac{1}{2}\delta^{ab}, \qquad \left[T^i, T^j\right] = i\,\varepsilon^{ijk}\,T^k. \tag{4.18}$$

The boundary condition for F at spatial infinity is fixed without loss of generality to $F(\infty) = 0$ in order to recover the vacuum $\Phi(x \to \infty) = \mathbb{1}$. Definiteness at the origin requires on the other hand $F(0)$ be an integer multiple of π, $F(0) = k\pi$. The hedgehog ansatz is built so that a spatial $SO(3)$ rotation of the coordinates $x_i \to R_{ij}x_j$ is equivalent to a $SU(2) \subset SU(N)$ transformation $\Phi \to U\Phi U^\dagger$, where the equivalence between the two formulations is given by

$$R_{ij} = 2\,\mathrm{Tr}\left(T_i U T_j U^\dagger\right). \tag{4.19}$$

Since the Skyrme Lagrangian above is symmetric under diagonal $SU(N)$ transformations — even in the presence of a mass term for the pions — and hence under any $SU(2)$ subgroup, it is also invariant under spatial rotations. For this reason, the skyrmion built using this hedgehog ansatz is said to be spherically symmetric. An important point about the $SU(N)$ skyrmion construction is that it only makes use of a $SU(2)$ subgroup of the target space. This is the minimal choice, as proved in a theorem due to Bott [264, 265]: the winding number integral (4.4) is actually only counting the number of times the field is winding around any $SU(2)$ subgroup of $SU(N)$, which makes it sufficient to embed all the non-trivial components of the field $\Phi(x)$ into a $SU(2)$ subgroup, while the other can be taken in the vacuum. In the absence of interactions with gauge or matter fields, the embedding of the $SU(2)$ subgroup can be chosen without loss of generality to be in the upper-left 2×2 block of the $SU(N)$ matrix as

$$\Phi(x) = \begin{pmatrix} \Phi_0(x) & \\ & \mathbb{1}_{N-2} \end{pmatrix}, \tag{4.20}$$

where $\Phi_0(x)$ is the $SU(2)$ hedgehog ansatz, given in terms of Pauli matrices σ^i as

$$\begin{aligned} \Phi_0(x) &= \exp\left[i\,F(r)\,\hat{x}_i\,\sigma_i\right] \\ &= \cos F(r)\,\mathbb{1}_{2\times 2} + i\sin F(r)\,\hat{x}_i\sigma^i. \end{aligned} \tag{4.21}$$

The energy (4.12) of a field configuration, as well as the winding number (4.4) can then be evaluated with this ansatz. Note that all terms can be expressed in terms of the current

$$\Phi^\dagger \partial_i \Phi = 2i \left[\frac{\sin F \cos F}{r} \left(\delta_{ij} - \hat{x}_i \hat{x_j}\right) + F'(r) \hat{x}_i \hat{x_j} - \frac{\sin^2 F}{r} \varepsilon_{ijk} \hat{x}_k \right] T^j. \tag{4.22}$$

One obtains then straightforwardly

$$B(\Phi) = -\frac{2}{\pi} \int_0^\infty \mathrm{d}r \, F' \sin^2 F = \left. \frac{\sin F \cos F - F}{\pi} \right|_{F=k\pi}^{F=0} = k, \tag{4.23}$$

which takes integer values as expected. Choosing $k = 1$ or equivalently the boundary conditions $F(0) = \pi$ ensures a unit winding number. Note that the solution with winding number -1, obtained from the boundary condition $F(0) = -\pi$, corresponds simply to exchanging $\Phi \leftrightarrow \Phi^\dagger$ in the Lagrangian, and is therefore equivalent in all characteristics to the solution of positive winding number. The equivalence of the solution with opposite winding numbers holds as well for $B > 1$.

The energy density (4.12) becomes as well a functional of the profile function $F(r)$, and reads

$$E[F] = 4\pi \frac{f_\pi}{e} \int_0^\infty \mathrm{d}r \left[\left(r^2 + 2\sin^2 F\right) F'^2 + \left(2r^2 + \sin^2 F\right) \frac{\sin^2 F}{r^2} \right], \tag{4.24}$$

where we used the dimensionless units defined above. As expected, there is no explicit dependence on the angular coordinates due to the spherical symmetry of the ansatz. The energy is minimised when $F(r)$ is a solution of the Euler-Lagrange equation

$$\frac{\partial}{\partial r} \left(\frac{\partial E[F]}{\partial F'} \right) - \frac{\partial E[F]}{\partial F} = 0, \tag{4.25}$$

which becomes in our case

$$\left(r^2 + 2\sin^2 F\right) F'' + 2rF' + \sin 2F \left(F'^2 - 1 - \frac{\sin^2 F}{r^2} \right) = 0. \tag{4.26}$$

Solving this highly non-linear equation subject to the boundary conditions $F(0) = \pi$ and $F(r \to \infty) = 0$ is a non-trivial task, and can only be realised numerically, as explained in the appendix. The function $F(r)$ solving the equation (4.26) is shown on fig. 4.1. Plugging this solution in the energy density (4.24), one finds the distribution shown in fig. 4.2, which upon integration gives the classical skyrmion mass

$$M_0 = 72.9 \, \frac{f}{e}. \tag{4.27}$$

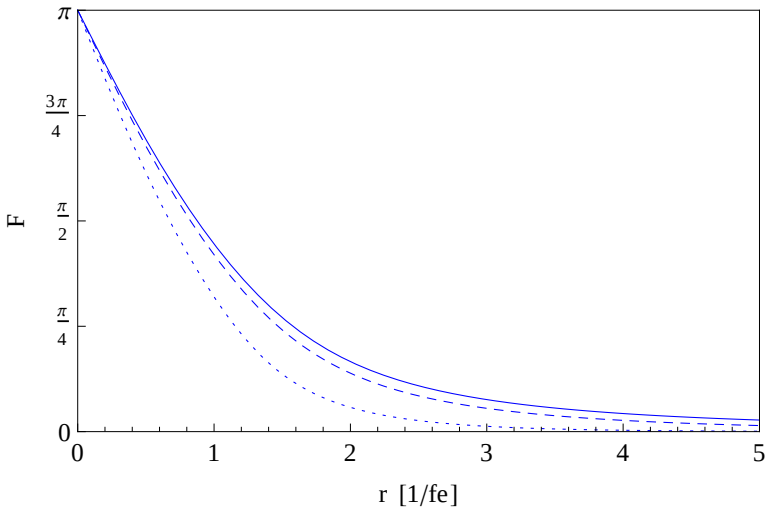

Figure 4.1: The profile function $F(r)$ solving eq. (4.26). The discontinuous lines corresponds to the solution in the presence of the pion mass term (4.32), with $m_\pi = 0.3 f_\pi e$ (dashed) and $m_\pi = f_\pi e$ (dotted).

Note that the terms with two and four powers of the spatial derivative both contribute half the mass of the skyrmion, as illustrated in fig. 4.2. They follow however different distribution along the radial direction, which stabilises the size of the skyrmion against rescaling $x \to \lambda x$.

The physical radius of the skyrmion can be defined in different ways. An obvious choice is to take the mean square value of the energy density as

$$\langle r^2 \rangle_E = \frac{1}{M_0} \int_0^\infty \mathrm{d}r \, r^2 \frac{\partial E[F]}{\partial r} \tag{4.28}$$

where $E[F]$ is the energy found in eq. (4.24). The numerical value obtained in this way is

$$\langle r^2 \rangle_E = \left(1.46 \frac{1}{fe} \right)^2 . \tag{4.29}$$

The skyrmion's size relevant to its interactions with fields other than gravity is however not provided by its energy, but rather by the distribution of its baryon number in space. The latter is shown in fig. 4.3, plugging the numerical solution for $F(r)$ in the baryon charge defined in eq. (4.23). This definition of the radius, which can be made clearer using the topological current of eq. (4.78), is then

$$\langle r^2 \rangle_B = \int d^3x \; r^2 B^0 = \left(1.06 \frac{1}{fe} \right)^2 , \tag{4.30}$$

and is found to be slightly smaller than the previous one.

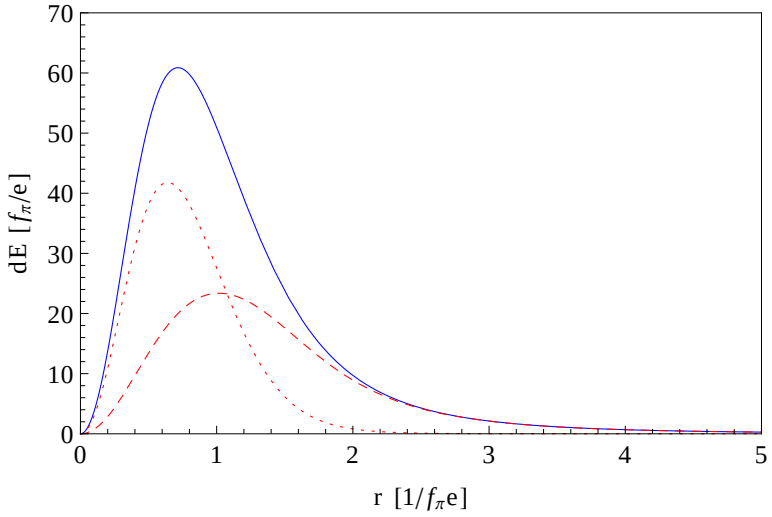

Figure 4.2: The radial energy density of the skyrmion of unit winding number, corresponding to the integrand of eq. (4.24). The dashed and dotted line represent the relative contributions of the kinetic and Skyrme term respectively; both contribute exactly to half the total energy.

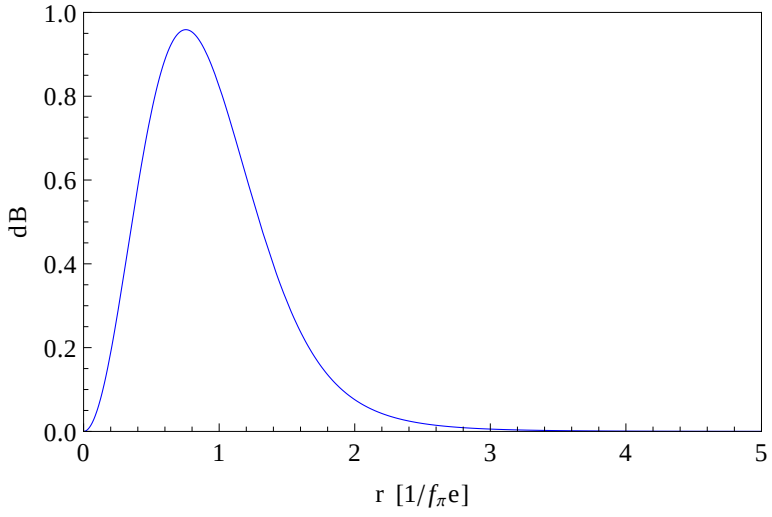

Figure 4.3: The radial distribution of the baryon density, given as the integrand of eq. (4.23).

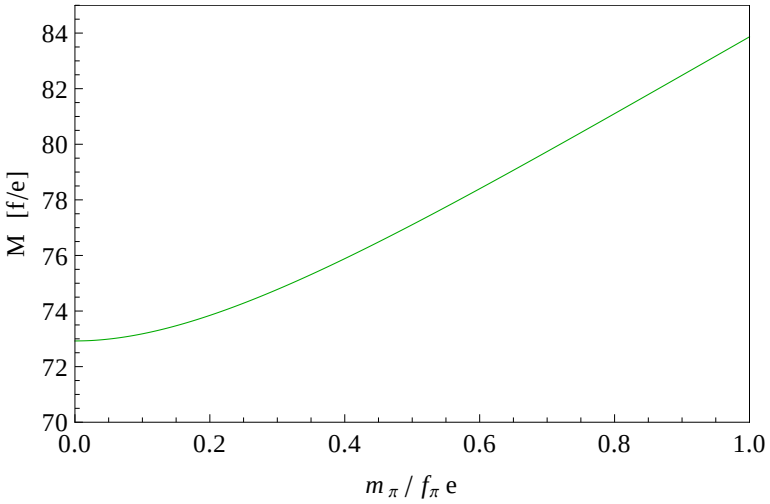

Figure 4.4: Classical mass of the skyrmion in terms of the ratio $(m_\pi/f_\pi e)$. The mass (4.27) is recovered in the limit $m_\pi \to 0$.

The classical energy of the skyrmion is obviously affected by the presence of the pion mass term (4.16). The presence of the additional parameter m_π in the model does not allow to factorise the parameter dependence out of the integral over space as before. The solution in this case is still provided by the hedgehog ansatz [266], under which the pion mass term reads

$$\mathcal{L}_{\text{mass}} = m_\pi^2 f_\pi^2 \left(\cos F - 1\right), \tag{4.31}$$

and gives a contribution to the energy functional (4.24) as

$$\Delta E[F] = 4\pi \frac{f_\pi}{e} \left(\frac{m_\pi}{f_\pi e}\right)^2 \int_0^\infty \mathrm{d}r\, r^2 \left(1 - \cos F\right) \geq 0. \tag{4.32}$$

Note that as indicated, this quantity is always positive. The Euler-Lagrange equation for $F(r)$ will also be enhanced by a term proportional to the dimensionless coefficient $(m_\pi/f_\pi e)$, and differs from the case $m_\pi = 0$ as shown in fig. 4.1. With the physical value of m_π, f_π and choosing $e \approx 5$ — shown later to be a reasonable choice — one finds as a typical value $(m_\pi/f_\pi e) \approx 0.3$. The dependence of the skyrmion's classical mass on this coefficient is only mild, as illustrated in fig. 4.4. Nevertheless, the presence of the pion mass term has a dramatic consequence on the asymptotic behaviour of the profile function $F(r)$: while in the case $m_\pi = 0$ the function decreases as $1/r^2$ at large r (see appendix), the decrease is exponential when a non-zero pion mass is taken into account, $F \propto e^{-m_\pi r}/r$.

Before proceeding to the quantisation of the classical skyrmion solution, not that there is no formal proof that the hedgehog ansatz provides the

lightest energy configuration. The mass (4.27) is nevertheless relatively close to the Bogomolny bound (4.15), and it is a fact that the latter cannot be saturated in the Skyrme model. It will also be shown in section 4.1.6 that naively adding angular dependence to the function F in the hedgehog ansatz can only lead to an increase in energy.

4.1.4 Zero-mode quantisation and static properties

The static solution found with the hedgehog ansatz is invariant under spatial translations and rotations, as well as under global symmetry transformations. Such transformations are called *zero-modes*. There is therefore an energy degeneracy, which will be removed once the theory is quantised. The quantisation procedure consists in promoting the zero-mode transformations to time-dependent ones parametrised by collective coordinates, then compute the Hamiltonian of the system, and finally perform a canonical quantisation of the collective coordinates [263]. The Lorentz translations and boosts lead to the quantisation of the skyrmion momentum and are not interesting in this context, as we want to derive the static properties of the skyrmion Moreover, for the simplicity of the argument, we will restrict our analysis to the case $N = 2$.[2] Among the relevant symmetry transformations are the global $SU(2)$ transformations which can be parametrised by a matrix $A = \exp[i\,\alpha_i\sigma^i/2]$ depending on the three collective coordinates α_i, with Φ transforming as $\Phi \to A\phi A^\dagger$. The quantisation procedure then promotes the global transformation parameters α_i to dynamical variables $\alpha_i(t)$. The other class of transformations playing a role in the quantisation procedure is the rotation in physical space. However, as explained above, the latter are equivalent to global $SU(2)$ transformations and it is therefore not necessary to introduce additional collective coordinates at this point. The time-dependent ansatz for Φ is then

$$\Phi(x,t) = A(t)\Phi(x)A(t)^\dagger, \tag{4.33}$$

where $A \in SU(2)$ was defined above. It will be convenient for our computation to define a different set of collective coordinates than the $\alpha_i(t)$, describing the matrix $A(t)$ in terms of Euler angles θ_i as

$$A(t) = \exp\left[i\,\theta_1(t)\frac{\sigma^3}{2}\right]\exp\left[i\,\theta_2(t)\frac{\sigma^2}{2}\right]\exp\left[i\,\theta_3(t)\frac{\sigma^3}{2}\right]. \tag{4.34}$$

Plugging this ansatz into the Lagrangian of the theory, one can see that the time dependence only appears in factors of $A^\dagger\partial_0 A$. An explicit computation yields

$$\begin{aligned}\mathcal{L}_{\text{Skyrme}} &= -M_0 + \Lambda\,\mathrm{Tr}\left(\partial_0 R\,\partial_0 R^\dagger\right)\\ &= -M_0 + \frac{1}{2}\Lambda\left(\dot\theta_i^2 + 2\dot\theta_1\dot\theta_3\cos\theta_2\right),\end{aligned} \tag{4.35}$$

[2] A complete treatment of the case $N = 3$ can be found for example in ref. [14].

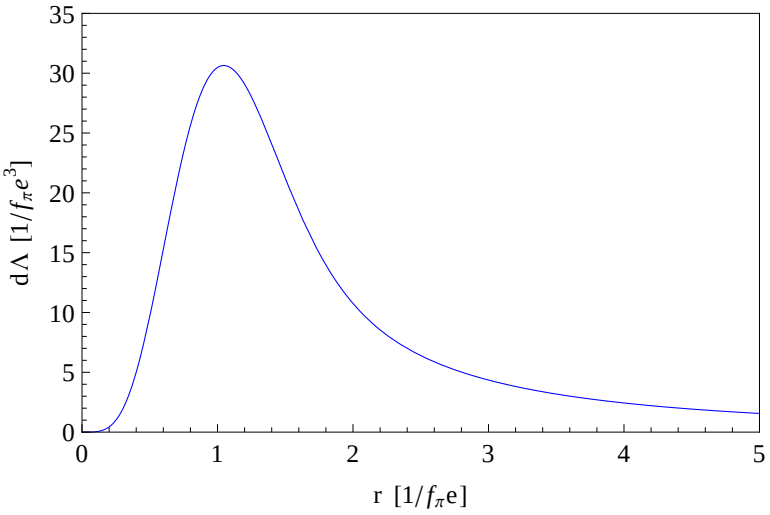

Figure 4.5: Radial distribution of the moment of inertia Λ given by the integrand in eq. (4.36).

where M_0 corresponds to the energy of the static skyrmion solution given in eq. 4.27, and Λ is quantity which can be identified with the moment of inertia of the classical solution, given by

$$\Lambda = \frac{8\pi}{3}\frac{1}{f_\pi\, e^3}\int_0^\infty \mathrm{d}r\, r^2 \sin^2 F \left(\left(F'\right)^2 + 1 + \frac{\sin^2 F}{r^2} \right). \tag{4.36}$$

The distribution of the integrand with the numerical solution for $F(r)$ is shown in fig. 4.5, and upon integration gives the value

$$\Lambda = 53.4 \frac{1}{f_\pi\, e^3} \tag{4.37}$$

The Hamiltonian of the system is obtained by performing a Legendre transformation of the Lagrangian: the canonical momenta reads

$$\Theta_i = \frac{\partial \mathcal{L}}{\partial \dot{\theta}_i} = \Lambda \begin{pmatrix} \dot{\theta}_1 + \dot{\theta}_3 \cos\theta_2 \\ \dot{\theta}_2 \\ \dot{\theta}_3 + \dot{\theta}_1 \cos\theta_2 \end{pmatrix}_i \tag{4.38}$$

and we find, inverting the previous equality,

$$\mathcal{H} = \Theta_i \dot{\theta}_i - \mathcal{L} = M_0 + \frac{1}{2\Lambda}\left[\frac{1}{\sin^2\theta_2}\left(\Theta_1^2 - 2\Theta_1\Theta_3\cos\theta_2 + \Theta_3^2\right) + \Theta_2^2 \right] \tag{4.39}$$

Upon canonical quantisation, the collective coordinates θ_i and momenta Θ_i are promoted to operators, and do not commute anymore. Using the usual

identification $\Theta_i \to -i\partial/\partial\theta_i$, the Hamiltonian can be written as a differential operator as

$$H = E_0 - \frac{1}{2\Lambda}\left[\frac{1}{\sin^2\theta_2}\left(\frac{\partial^2}{\partial\theta_1^2} + \frac{\partial^2}{\partial\theta_3^2} - 2\cos\theta_2\frac{\partial^2}{\partial\theta_1\partial\theta_3}\right) + \frac{1}{\sin\theta_2}\frac{\partial}{\partial\theta_2}\sin\theta_2\frac{\partial}{\partial\theta_2}\right]. \tag{4.40}$$

which turns out to be the Laplacian on a three-sphere, whose eigenfunctions are the Wigner D-functions $D^j_{mm'}(\theta_i)$ with eigenvalues

$$E^j_{mm'} = E_0 + \frac{j(j+1)}{2\Lambda}. \tag{4.41}$$

The operators Θ_i are actually related to the physical spin and isospin of the skyrmion. The $SU(2)$ isospin transformation $\delta^a\Phi = i[T^a, \Phi]$ is associated with the Noether current

$$\begin{aligned} I^\mu_k = &-i\frac{f_\pi^2}{2}\left[\mathrm{Tr}\left(T^k\Phi^\dagger\partial^\mu\Phi\right) + \mathrm{Tr}\left(T^k\Phi\partial^\mu\Phi^\dagger\right)\right] \\ &+\frac{i}{8e^2}\Big(\mathrm{Tr}[T^k, \Phi^\dagger\partial_\nu\Phi][\Phi^\dagger\partial^\mu\Phi, \Phi^\dagger\partial^\nu\Phi] \\ &\qquad + \mathrm{Tr}[T^k, \Phi\partial_\nu\Phi^\dagger][\Phi\partial^\mu\Phi^\dagger, \Phi\partial^\nu\Phi^\dagger]\Big). \end{aligned} \tag{4.42}$$

The conserved charge defined as the spacetime integral of the zeroth component of this current is nothing but the isospin of the skyrmion. Plugging in the time dependent ansatz (4.33) and neglecting the terms cubic in time derivatives (in the semiclassical limit the skyrmion rotates slowly, so the higher order terms in time derivatives are subdominant), we obtain:

$$I_k = \int \mathrm{d}^3x\, I^0_k = i\Lambda\,\mathrm{Tr}\left(A\,\partial_0 A^\dagger T^k\right), \tag{4.43}$$

where Λ is defined as above. Similarly, computing the spin charge J_k, one obtains

$$J_k = -i\Lambda\,\mathrm{Tr}\left(A^\dagger\partial_0 A\,T^k\right). \tag{4.44}$$

The two operators obey the $SU(2)$ commutation relations

$$[I_i, I_j] = i\,\varepsilon_{ijk}I_k, \qquad [J_i, J_j] = i\,\varepsilon_{ijk}J_k, \tag{4.45}$$

and are related to each other via a rotation as

$$I_k = -\Omega_{kl}J_l, \tag{4.46}$$

where Ω is a time-dependent rotation matrix defined as

$$\Omega_{kl} = \frac{1}{2}\,\mathrm{Tr}\left(T^k A\,T^l A^\dagger\right) \in SO(3). \tag{4.47}$$

This relation is particularly important, since it implies that physical skyrmion states have the same total spin and isospin quantum numbers,

$$I^2 = J^2. \tag{4.48}$$

The operator $I^2 = J^2$ turns out to be exactly the differential operator in (4.40), so that the Hamiltonian of the system can be rewritten as

$$H = M_0 + \frac{1}{2\Lambda} J^2 \tag{4.49}$$

with eigenvalues $j(j+1)$. The Hilbert space of the quantum theory is therefore described in terms of states

$$|i = j; m, m'\rangle, \tag{4.50}$$

where j corresponds to the total spin (or isospin) of the physical state, taking either integer or half-integer values, depending if the skyrmion is a boson or a fermion. The quantum numbers m and m' have to be identified subsequently with the eigenvalues of the operators I_3 and J_3 respectively and run from $-j$ to $+j$ in integer steps. Note that they do not contribute to the energy of the skyrmion, but imply a certain degeneracy in energy among the skyrmion's spectrum, which can eventually be lifted by interactions with gauge fields. Note that due to the different scaling of the terms M_0 and $1/\Lambda$ in eq. (4.41) with respect to the Skyrme parameter e, the mass of the lightest skyrmion state is bounded from below if the skyrmion is a fermion ($j = \frac{1}{2}$): in this case, the minimal energy is $12.7f$, for $e \cong 7.7$. All energy states are displayed in fig. 4.6 as a function of e, for both cases where the skyrmion is a boson or a fermion.

The skyrmion cannot however take any spin value in general. In theories where the path integral is double-valued, the wavefunction of a skyrmion moving along a closed path in configuration space can pick up a phase of -1 when the path is non-contractible, but is left unchanged when the path is contractible [267]. In this case, the spin statistics of the skyrmion is a free parameter of the theory. Such a property of the path integral can only happen if the fourth homotopy group π_4 of the target space contains a $\mathbb{Z}_2$ subgroup. This is actually the case in QCD with two flavours, but does not extend to the general case with $N_f \geq 3$,

$$\begin{cases} \pi_4\big(SU(2)\big) &= \mathbb{Z}_2, \\ \pi_4\big(SU(N)\big) &= 0 \quad \text{for } N \geq 3. \end{cases} \tag{4.51}$$

Quantising the skyrmion using the Finkelstein-Rubinstein rule [267] is therefore usually not considered as a valid attitude in QCD, and the bosonic or fermionic nature of the skyrmion is completely fixed by the theory. Although

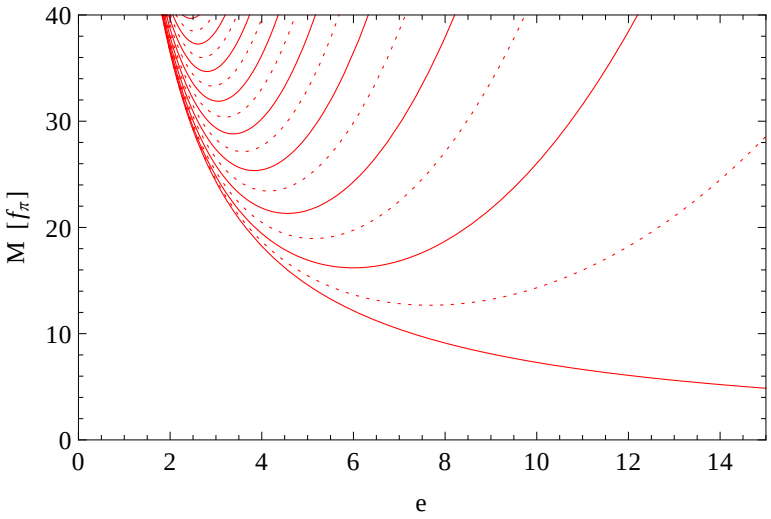

Figure 4.6: The mass of the bosonic (solid line) and fermionic (dotted line) skyrmion states as a function of the parameter e, in units of f_π, as given by eq. (4.41).

the σ-model described here contains only bosonic degrees of freedom, there is still the possibility for the skyrmion to be quantised as a fermion: in the presence of a Wess-Zumino-Witten term (3.54), an adiabatic 2π rotation of the skyrmion in space adds to the action a constant term $\Delta S = iN_c\pi$, where N_c is the coefficient of the Wess-Zumino-Witten term, equal to the number of colours in the underlying strongly-interacting theory. If N_c is odd, the wavefunction of the skyrmion picks a minus sign when rotated in space, which indicates a fermionic nature. On the contrary, if N_c is even, the skyrmion is a boson. In QCD, with $N_c = 3$, the skyrmion is therefore a fermion, and the lightest skyrmion states form an isospin doublet, corresponding to the proton and the neutron.

Note that the Wess-Zumino-Witten term neither contributes to the energy of the skyrmion field configuration, nor to the isospin current (4.42), so that all the results obtained above still hold. It can play however a crucial role for symmetries that are hidden in our σ-model formalism, but which are present in the underlying theory. This is the case for example of hypercharge in QCD: at the quark level, both the left- and right-handed quarks are charged under the $U(1)_Y$ gauge group, but the field Φ has a trivial transformation rule under this very symmetry. This can be seen when looking at the generator of the electric charge as given in eq. (3.25): in the two-flavour case, one has

$$Q = \begin{pmatrix} \frac{2}{3} & \\ & -\frac{1}{3} \end{pmatrix} = T^3 + Y, \tag{4.52}$$

and as suggested by the notation, Q can be split in a part T^3 coming from the $SU(2)$ isospin symmetry and a hypercharge generator Y, which are respectively defined as

$$T^3 = \begin{pmatrix} \frac{1}{2} & \\ & -\frac{1}{2} \end{pmatrix}, \qquad Y = \frac{1}{6}\,\mathbb{1}_{2\times 2}. \tag{4.53}$$

Under an electromagnetic gauge transformation, $\delta\Phi \propto [Q, \Phi]$, only the isospin part of Q plays a role, since the hypercharge generator commutes with the field Φ independently of its space-time configuration. Similarly, the electromagnetic Noether current is given by the equivalent of the isospin current (4.42), with the generator Q replacing T^a, but essentially only the part T^3 of it contributes. With the hedgehog ansatz, we find according to eq. (4.43)

$$I_3 = \int \mathrm{d}^3x\, I_3^0 = i\Lambda\,\mathrm{Tr}\left(A\,\partial_0 A^\dagger T^3\right) = \frac{1}{2}\Theta_1, \tag{4.54}$$

which as expected takes the value $\pm\frac{1}{2}$ when applied on the physical proton and neutron states. The radial distribution of the isospin charge around the spherically symmetric skyrmion can be written as

$$\rho_I(r) = \frac{1}{\Lambda}\,\frac{4\pi}{3f_\pi\, e^3}\, r^2 \sin^2 F \left(\left(F'\right)^2 + 1 + \frac{\sin^2 F}{r^2}\right) \tag{4.55}$$

which is normalised such that $\int_0^\infty \mathrm{d}r\,\rho_I(r) = \frac{1}{2}$. In our naive approach, since the hypercharge of the field Φ is vanishing, one would expect the two lightest skyrmion states to have electric charges $\pm\frac{1}{2}$, as given by the isospin component. This is however not what is observed in nature, and the reason is the presence of the Wess-Zumino-Witten term (3.54). Under a vector transformation $\delta\Phi \propto [T, \Phi]$, the non-local, five-dimensional Wess-Zumino-Witten term induces a Noether current of the form

$$\begin{aligned} J^\mu_{WZW} = \frac{N_c}{48\pi^2}\varepsilon^{\mu\nu\rho\sigma}\Big[&\,\mathrm{Tr}\,T(\Phi^\dagger\partial_\nu\Phi)(\Phi^\dagger\partial_\rho\Phi)(\Phi^\dagger\partial_\sigma\Phi) \\ &- \mathrm{Tr}\,T(\Phi\partial_\nu\Phi^\dagger)(\Phi\partial_\rho\Phi^\dagger)(\Phi\partial_\sigma\Phi^\dagger)\Big]. \end{aligned} \tag{4.56}$$

This quantity vanishes when T is taken to be a generator of $SU(2)$, hence confirming that the Wess-Zumino-Witten term do not contribute to the isospin current (4.42). Surprisingly, there is however a non-zero contribution from the $U(1)_Y$ hypercharge generator: taking $T = \mathbb{1}$, although the field Φ is left unchanged, the current J^μ_{WZW} is non-vanishing

$$J^\mu_{\mathbb{1}} = \frac{N_c}{24\pi^2}\varepsilon^{\mu\nu\rho\sigma}\ \mathrm{Tr}(\Phi^\dagger\partial_\nu\Phi)(\Phi^\dagger\partial_\rho\Phi)(\Phi^\dagger\partial_\sigma\Phi), \tag{4.57}$$

and induces a conserved charge

$$J_{\mathbb{1}} = \frac{N_c}{24\pi^2}\varepsilon_{ijk}\int \mathrm{d}^3x\ \mathrm{Tr}(\Phi^\dagger\partial_i\Phi)(\Phi^\dagger\partial_j\Phi)(\Phi^\dagger\partial_k\Phi) = N_c\,B(\Phi), \tag{4.58}$$

which turns out to be exactly N_c times the winding number integral of eq. (4.4). With the definition $Y = \frac{1}{6}\mathbb{1}$, the Wess-Zumino-Witten term contributes to the electric charge of all skyrmion states of unit winding number, independently of their quantum numbers, with a charge

$$J_Y = \frac{N_c}{6}, \tag{4.59}$$

which is exactly 1/2 in QCD. The isospin doublet found to be the lightest skyrmion state is therefore composed of two skyrmions of charge +1 and 0, corresponding respectively to the proton and the neutron. The non-trivial character of the charge cancellation inside a neutron appears here clearly from the requirement that the electric charge generator Q is written in integer multiples of $1/N_c$, so that the hypercharge of the skyrmion arising from the Wess-Zumino-Witten term takes half-integer values as the isospin does. The radial distribution of the hypercharge is then given by the baryon number distribution of eq. (4.23), namely

$$\rho_Y(r) = -\frac{1}{\pi} F' \sin^2 F. \tag{4.60}$$

The radial distribution of the electric charge in protons and neutrons can then be written as

$$\rho_P(r) = \rho_I(r) + \rho_Y(r), \qquad \rho_N(r) = -\rho_I(r) + \rho_Y(r), \tag{4.61}$$

and are shown in fig. 4.7. A number of physical observables can be extracted from the quantised skyrmions, which turns out to be in reasonable agreement with the proton and neutron's properties determined experimentally. The success of the model is undeniable if one considers one the one hand the number of predictions which are given an correct order-of-magnitude estimate, and on the other hand that the model contains only one free parameter, the Skyrme coupling e. The best fit between experiment and theory is provided by $e \approx 4.5$. Note that there exist many possibilities to improve the model by adding more input parameters (see ref. [14] for a review). Important corrections to the skyrmions' mass and static properties are also generated by radiative corrections [268].

4.1.5 Long-range interactions

The interactions between skyrmions depend of course of their charge under the electroweak gauge group, which can be derived from the quantisation presented in the next section. There is however also a contribution arising from strong-interactions, which as we saw in section 3.1.2 is dominated by the exchange of light mesons. With the hedgehog ansatz derived above, the skyrmion are very much localised in space, but still contain a non-zero component of the meson field $\Phi(x)$ up to arbitrarily large distances from the

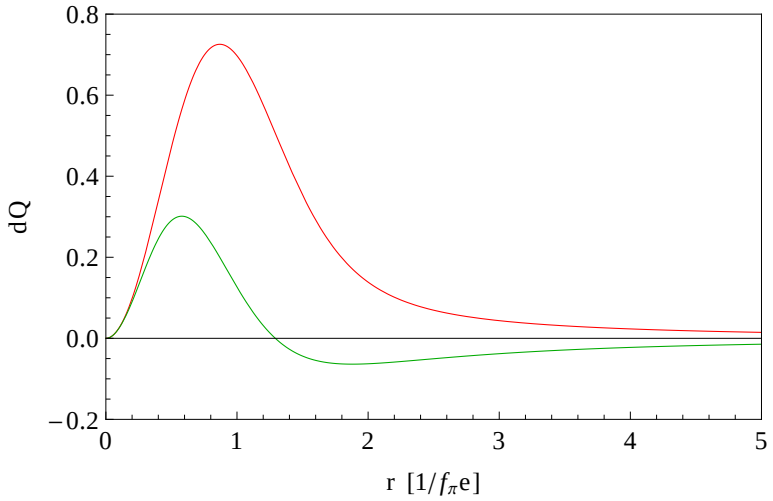

Figure 4.7: Radial distribution of the electric charge in a proton (red) and a neutron (green) as given by eq. (4.61). Upon integration over r, the curves yield respectively the value $+1$ and 0.

skyrmion centre. As long as the distance between two skyrmions is much larger than their radius, we can assume that they behave locally like single skyrmions, and that the overall field configuration can simply described by a multiplicative ansatz [269]

$$\Phi_\times(x; x_1, x_2) = \Phi(x - x_1)\Phi(x - x_2), \tag{4.62}$$

where $\Phi(x - x_0)$ describes a hedgehog configuration centred at the space point x_0. This approximation only holds if the distance between the two points x_1 and x_2 is large, otherwise the presence of one skyrmion will significantly distort the field $\Phi(x)$ around to the other skyrmion from its hedgehog shape. At short distances, two skyrmions of opposite winding number can annihilate into a topologically trivial final state, but this process cannot be described in the static approach used here. If the two skyrmions both have winding number $+1$, they might or might not form a bound state of winding number $+2$. This subject will be discussed in the next section. At large distances, however, the potential energy between the two skyrmions can simply be estimated as the difference in energy between the product ansatz (4.62) and the energy of two isolated skyrmions, as

$$V\left(|x_1 - x_2|\right) = E[\Phi_\times] - 2\,E[\Phi]. \tag{4.63}$$

At large distances, for the hedgehog solution of section 4.1.3 and in the absence of a pion mass term, the profile function $F(r)$ follows asymptotically a power law,

$$F(r) \xrightarrow{r\to\infty} \frac{\alpha}{r^2} \tag{4.64}$$

where α is a constant whose numerical value is computed in the appendix. The current $\Phi^\dagger \partial_i \Phi$ of eq. (4.22) goes therefore to zero as

$$\Phi^\dagger(x)\partial_i\Phi(x) = 2i\frac{\alpha}{r^3}\left(\delta_{ij} - 3\hat{x}_i\hat{x}_j\right)T^j, \tag{4.65}$$

at large r. The leading term in the energy $E[\Phi_\times]$ of the multiplicative ansatz is given by the kinetic term for the field $\Phi(x)$, which is quadratic in the current $(\Phi^\dagger\partial_i\Phi)$ and decreases therefore as $1/r^6$. The potential becomes then

$$V\left(|x_1 - x_2|\right) \cong \frac{f_\pi}{2}\int d^3x\, \mathrm{Tr}\left(\Phi(x-x_1)^\dagger\partial_i\Phi(x-x_1)\right)\left(\Phi(x-x_2)^\dagger\partial_i\Phi(x-x_2)\right). \tag{4.66}$$

In the multiplicative ansatz (4.62), we have implicitly chosen the isospin orientation of both skyrmions to be aligned. This is not true in general, and the potential should actually not only be a function of the distance between the two skyrmions, but also of their relative orientation. Since isospin transformations acts as spatial rotations on the hedgehog solution, one can consider without loss of generality to rotate one of the two skyrmions, replacing $\Phi(x - x_2)$ by $\Phi\big(R \cdot (x - x_2)\big)$, where R is an $SO(3)$ matrix which can be parametrised in terms of three angles β_1, β_2 and β_3 as

$$R = \begin{pmatrix} c_1c_2c_3 - s_1s_3 & s_1c_2c_3 + c_1s_3 & -s_2c_3 \\ -c_1c_2s_3 - s_1c_3 & -s_1c_2s_3 + c_1c_3 & s_2s_3 \\ c_1s_2 & s_1s_2 & c_2 \end{pmatrix}. \tag{4.67}$$

Note that we used the shorthand notation $c_i = \cos\beta_i$, $s_i = \sin\beta_i$. With this choice, after integration over space, the potential between the two skyrmions is found to be

$$V(d,\beta_i) = \frac{8\pi}{3}\,\frac{\alpha^2}{f^2e^4}\,\frac{1}{d^3}\left[2\cos\beta_2 - (1+\cos\beta_2)\cos(\beta_1+\beta_3)\right]. \tag{4.68}$$

This potential can be both attractive or repulsive, and is vanishing when both skyrmions are aligned, corresponding to $\beta_i = 0$. Interpreting this potential in terms of exchange of light particle states goes beyond the scope of this work. However, the dependence with the cube of the inverse of the distance shows that the attraction force between skyrmions vanishes very rapidly at large distances, so that no macroscopic force can be observed between well-separated nucleons. Note finally that the hedgehog solution obtained in the presence of pion masses yield a very different large-distance behaviour due to the exponential asymptotic behaviour. Since pions are indeed massive in nature, the suppression of strong forces between nucleons is even more drastic than in eq. (4.68).

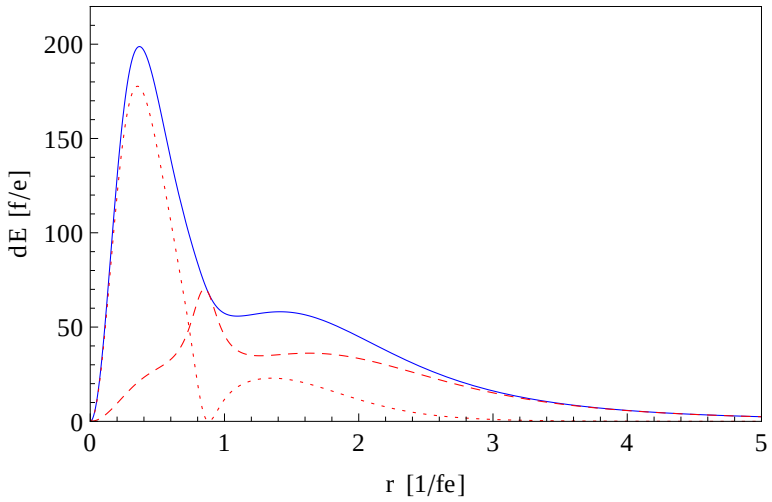

Figure 4.8: The radial energy density as a function of r, for an hedgehog ansatz with boundary condition $F(0) = 2\pi$. The dashed and dotted line represent the relative contributions of the kinetic and Skyrme term respectively.

4.1.6 Skyrmions of higher winding number

Skyrmion solutions with winding number larger than one are more difficult to construct. We show here as an example the construction of the skyrmion of winding number $B = 2$, which gives a satisfying picture of the deuteron, bound state of one proton and one neutron, and will also be relevant to our discussion in section 4.3.

A naive choice to construct the skyrmion of winding number two is to use the hedgehog ansatz (4.17) and adapt the boundary condition to $F(0) = 2\pi$ in order to get the correct winding number from eq. (4.23). The energy density is identical to the one given in eq. (4.24), but the function $F(r)$ is now required to solve the Euler-Lagrange equation (4.26) with the new boundary condition mentioned above. The energy is found numerically to follow the distribution in fig. 4.8, and corresponds to a total mass of 217 f/e. The two peaks visible in the energy distribution seems to indicate that this configuration corresponds to two skyrmions superimposed at the same place, one having a slightly larger radius than the other. Note that this configuration is nevertheless unstable, since its energy is much above the energy of two single skyrmions. It does not therefore represent a physical state.

The description of a system of winding number two requires to abandon the spherical symmetry of the hedgehog ansatz. However, one can expect to preserve an axial symmetry, since the true solution interpolates between a situation where two skyrmions are well separated, hence defining an axis of symmetry, and a (unphysical) situation where the two units of baryonic

charge are located at the same point in space. An general axially symmetric ansatz can be made in terms of the spherical coordinates (r, θ, φ) defined as

$$(x_1, x_2, x_3) \equiv (r\ \sin\theta\cos\varphi, r\ \sin\theta\sin\varphi, r\ \cos\theta) \tag{4.69}$$

in the form [270]

$$\begin{aligned}\Phi_{\|} = \exp\left[-i\,m\,\varphi\frac{\sigma^3}{2}\right]\cdot\exp\left[i\,F(r,\theta)\left(\sin G(r,\theta)\frac{\sigma^1}{2}+\cos G(r,\theta)\frac{\sigma^3}{2}\right)\right]\\ \cdot\exp\left[i\,m\,\varphi\frac{\sigma_3}{2}\right]\end{aligned} \tag{4.70}$$

where m is an integer, which will turn out to give the winding number of the ansatz, and $F(r,\theta)$ and $G(r,\theta)$ are two unknown functions of two variables. The ansatz built in this way is obviously invariant under a rotation along the angle φ, since the latter is explicitly written as a diagonal $SU(2)$ transformation, preserved by the Skyrme Lagrangian. The boundary conditions are chosen as

$$\begin{cases} F(0,\theta) &= \pi, \\ F(\infty,\theta) &= 0, \end{cases} \qquad \begin{cases} G(r,0) &= 0, \\ G(r,\pi) &= \pi, \end{cases} \tag{4.71}$$

such that the vacuum state is recovered at spatial boundaries, $\Phi_{\|}(r\to\infty) = \mathbb{1}$. The boundary condition for $F \neq 0$ at $r = 0$ forces the field to have a non-trivial topology, and π is the lowest possible value for F compatible with the requirement that the field is singled-valued at the origin. Similarly, the boundary conditions for G fulfil the requirement that Φ is well-defined along the axis of symmetry $\theta = 0, \pi$, and such that G is forced to take non-vanishing values. With this ansatz, the winding number integral (4.4) becomes

$$B\left(\Phi_{\|}\right) = \frac{m}{\pi}\int_0^\infty \mathrm{d}r \int_0^\pi \mathrm{d}\theta\ \sin^2 F \sin G\left(\partial_r F\partial_\theta G - \partial_r G\partial_\theta F\right). \tag{4.72}$$

The integrand can be rewritten as a difference of two surface terms

$$\frac{1}{2}\partial_r\left[(F-\sin F\cos F)\sin G\,\partial_\theta G\right] - \frac{1}{2}\partial_\theta\left[(F-\sin F\cos F)\sin G\,\partial_r G\right]. \tag{4.73}$$

The second term above is vanishing upon integration due to the value $\sin G = 0$ at the θ-boundaries. Performing the integration over r on the first term, one gets, using the boundary values for F at $r = 0$ and $r\to\infty$,

$$B\left(\Phi_{\|}\right) = \frac{m}{\pi}\int_0^\pi \mathrm{d}\theta\ \left(-\frac{\pi}{2}\sin G\,\partial_\theta G\right) = m. \tag{4.74}$$

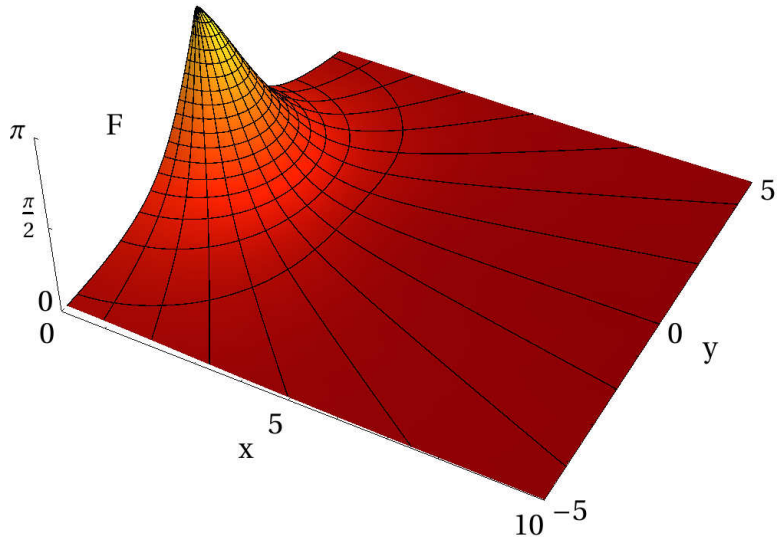

Figure 4.9: The numerical solution for F in the deuteron case, in the plane $(x, y) = (\widetilde{r}\sin\theta, \widetilde{r}\cos\theta)$.

m is thus as announced fixing the winding number of the field $\Phi_{\|}$. Plugging the ansatz (4.70) into the energy density (4.12), one obtains

$$E[F,G] = 2\pi\frac{f_\pi}{e}\int_0^\infty \mathrm{d}r \int_0^\pi \mathrm{d}\theta\, r^2 \sin\theta \left\{ \left(1 + m^2 \frac{\sin^2 F \sin^2 G}{r^2 \sin^2\theta}\right) \right. \tag{4.75}$$
$$\cdot \left[(\partial_r F)^2 + \frac{1}{r^2}(\partial_\theta F)^2 + \sin^2 F \left((\partial_r G)^2 + \frac{1}{r^2}(\partial_\theta G)^2\right)\right]$$
$$\left. + \frac{1}{r^2}\left(\partial_r F \partial_\theta G - \partial_r G \partial_\theta F\right)^2 + m^2 \frac{\sin^2 F \sin^2 G}{r^2 \sin^2\theta} \right\}.$$

Although much more complicated than for the hedgehog ansatz, the minimisation of the energy proceeds similarly: Euler-Lagrange equations can be derived for F and G and solved numerically with the proper boundary conditions (4.71). For $m = 1$, the numerical solution takes a familiar form: F has no dependence on the angle θ, i.e. $F(r,\theta) = F(r)$, and G is found to take the value $G(r,\theta) = \theta$. Looking at the energy density, one can see that it is then exactly equivalent to eq. (4.24) giving the energy of the hedgehog ansatz of unit winding number. This shows once again that the solution of minimal energy chooses automatically the largest possible symmetry, in this case a spherical one.

The skyrmion of winding number two can similarly be obtained by min-

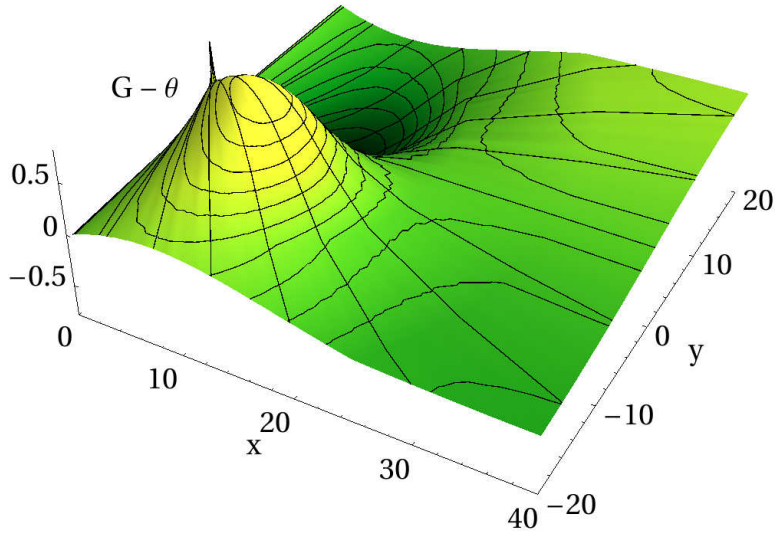

Figure 4.10: The numerical solution for the difference $G - \theta$ (right) in the deuteron case, in the plane $(x, y) = (\widetilde{r}\sin\theta, \widetilde{r}\cos\theta)$.

imising the energy functional (4.75) with $m = 2$. The solution for F and G are shown respectively on fig. 4.9 and 4.10. The total energy of the solution obtained in this way gives the mass of the $B = 2$ skyrmion as

$$M_{B=2} = 139.6\,\frac{f}{e}, \tag{4.76}$$

and its distribution, shown in fig. 4.11 is not anymore spherical symmetric. Note that the energy of the field $\Phi_{\|}$ is interestingly vanishing on the axis of symmetry of the solution, most of it being located along a torus. The solution obtained in this way is stable, since its energy (4.76) is slightly more than twice the energy (4.27) of a single skyrmion. The deuteron arises therefore in the Skyrme model as a weakly-bounded composite state of two nucleons, corresponding to the situation observed in nature.

Skyrmions with winding number larger than two lose the remaining axial symmetry of the deuteron solution. They can be built in general using the rational map ansatz of ref. [271], and solutions up to very high winding numbers have been found numerically [272]. For a review on the subject, see for example ref. [273]. Note that the presence of a pion mass can alter the very structure of the skyrmion for solutions of high winding numbers [274].

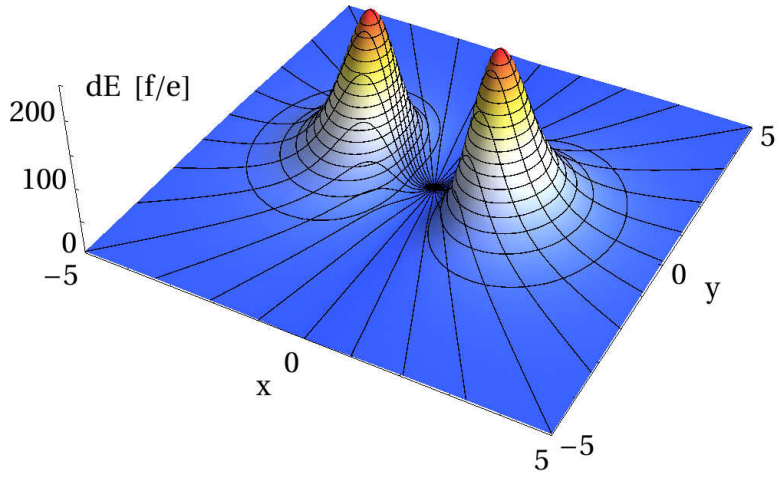

Figure 4.11: The energy density of the deuteron solution in a plane containing the axis of symmetry of the skyrmion (located along $x = 0$).

4.2 Extensions of the Skyrme model

The simple model used so far was sufficient to gain a qualitative understanding of baryons as topological solitons in the low-energy limit of QCD. Turning to our main concern, which is the presence of baryon-like state in composite Higgs models, requires however to extend or modify the Skyrme model in a number of ways, which may or may not influence the classical and quantum properties of the skyrmion. We will first discuss the presence of additional terms in the Lagrangian, including operators of dimension higher than four and gauge interactions, and then turn to completely different realisations of the Skyrme model, where the symmetry structure is not any more that of QCD.

4.2.1 Stabilisation through higher-order terms

The Skyrme model described above contains only two operators in its Lagrangian. In a general $SU(N)$ non-linear σ-model, an infinity of terms can be present. While in the perturbative regime only the terms with a low number of derivatives are present, all terms could potentially play an important role in the non-perturbative description of baryons. The requirement from Derrick's theorem is that at least two operators with different classical scaling dimensions are present in the Lagrangian, so that the balance between their

scaling can define a preferred scale for the skyrmion size. It is important to note here that there exists models in which none of these higher-order terms is present, and for which no stable skyrmions can be formed. This scenario is realised when the scalar field $\Phi(x)$ is a elementary field, as for example in some little Higgs models where the scalar field playing the role of the Higgs is described before spontaneous symmetry breaking by a linear sigma-model [275,250]. In this case, however, the lightness of the electroweak scale is not explained anymore by the presence of a natural scale fixed by strong dynamics, and the hierarchy problem is reintroduced in the theory. Introducing for example supersymmetry at a higher scale could solve the problem. Models realised following this path are non-minimal and won't be discussed further in this thesis.

If one wants to keep the property of the Skyrme model that higher-dimensional operators involve at most two time derivatives, then the structure of the Lagrangian is importantly constrained. No additional term can be added to the Skyrme Lagrangian up to operators with six space-time derivatives. At this level, a simple term can be added which uses two instances of the completely antisymmetric tensor $\varepsilon^{\mu\nu\rho\sigma}$: this term, often present as an alternative to the Skyrme term or in addition to it [276, 277], is then proportional to the square of the topological current B_μ, as

$$\mathcal{L}_6 = -c_6\, \mathcal{B}_\mu \mathcal{B}^\mu, \tag{4.77}$$

where $\mathcal{B}^\mu$ is defined as the integrand of eq. (3.61),

$$\mathcal{B}^\mu = \frac{1}{24\pi^2}\varepsilon^{\mu\nu\rho\sigma}(\Phi^\dagger\partial_\nu\Phi)(\Phi^\dagger\partial_\rho\Phi)(\Phi^\dagger\partial_\sigma\Phi). \tag{4.78}$$

For a static configuration, only the component $\mathcal{B}^0$ of the current is non-vanishing. With the hedgehog ansatz (4.17), $\mathcal{B}^0$ can be read directly from eq. (4.23) to be

$$B^0 = -\frac{2}{\pi}\, F' \,\frac{\sin^2 F}{r^2}, \tag{4.79}$$

so that the Lagrangian $\mathcal{L}_6$ contributes to the energy as

$$H_6 = \frac{16}{\pi}\int_0^\infty \mathrm{d}r\, \left(F'\right)^2 \frac{\sin^4 F}{r^2}. \tag{4.80}$$

Note that since the operator (4.77) preserves all the symmetries of the Skyrme Lagrangian, the spherical symmetry of the hedgehog ansatz is preserved. Both the energy (4.24) and the moment of inertia (4.36) are affected by the presence of the higher-order term and take therefore different numerical values in this case, the quantum numbers of the skyrmion states derived from the canonical quantisation procedure remains unchanged. This example illustrates an very important point about skyrmions: while the exact

form of the Lagrangian — which remains in principle unknown, even in theories with a well-defined UV completion — decides of the mass, radius and other static properties of the skyrmion, it has no effects on its symmetries nor on its quantum properties. This statement will play a crucial role below, when discussing the skyrmion appearing in composite Higgs models: while their mass can only be estimated roughly, important constraints on the models will arise from the skyrmion quantum numbers, which can be computed exactly.

4.2.2 Gauge interactions

The second important modification of the Skyrme model consists in adding gauge interactions. As seen already in section 3.1, the non-linear σ-model describing meson interactions can be augmented to include electromagnetic interactions. Before discussing them in the next-section, we want to address the more general case where all the global symmetries of field $\Phi(x)$ are promoted to local ones. This trick was used already in our discussion on vector mesons in QCD, and will be proved useful also in the following. Let us therefore consider general $SU(N)_L \times SU(N)_R$ transformations associated with gauge field $L_\mu, R_\mu \in SU(N)$, with the transformation properties

$$\begin{aligned} \Phi(x) &\to U_L(x)^\dagger \Phi(x) U_R(x), \\ L_\mu(x) &\to U_L(x)^\dagger L_\mu(x) U_L(x) - \frac{i}{g_L} U_L(x)^\dagger \partial_\mu U_L(x), \\ R_\mu(x) &\to U_R(x)^\dagger R_\mu(x) U_R(x) - \frac{i}{g_R} U_R(x)^\dagger \partial_\mu U_R(x). \end{aligned} \tag{4.81}$$

These transformations define a local symmetry of the Skyrme Lagrangian, provided that the space-time derivatives are replaced by covariant ones,[3]

$$D_\mu \Phi = \partial_\mu \Phi - i\, g_L\, L_\mu \Phi + i\, g_R\, \Phi\, R_\mu, \tag{4.82}$$

and adding to the Lagrangian a kinetic term for the gauge fields

$$\mathcal{L}_{YM} = -\frac{1}{2} \mathrm{Tr}\left(L_{\mu\nu} L^{\mu\nu}\right) - \frac{1}{2} \mathrm{Tr}\left(R_{\mu\nu} R^{\mu\nu}\right), \tag{4.83}$$

where the field strength tensors associated with the $SU(N)_L$ and $SU(N)_R$ gauge symmetries are defined as

$$L_{\mu\nu} = \partial_\mu L_\nu - \partial_\nu L_\mu - i\, g_L\, [L_\mu, L_\nu], \tag{4.84}$$

$$R_{\mu\nu} = \partial_\mu R_\nu - \partial_\nu R_\mu - i\, g_R\, [R_\mu, R_\nu]. \tag{4.85}$$

[3]Note that the sign of the terms $L_\mu \Phi$ and ΦR_μ is chosen so as to get a canonical form for the field strength tensors in eq. (4.84) and (4.85).

The normalisation of $\mathcal{L}_{YM}$ is chosen such that for gauge fields defined as $L_\mu(x) = L^a_\mu(x)T^a$ and $R_\mu(x) = R^a_\mu(x)T^a$, where the T^a are $SU(N)$ generators satisfying the normalisation $\mathrm{Tr}\left(T^aT^b\right) = \frac{1}{2}\delta^{ab}$, then the kinetic terms for $L^a_\mu(x)$ and $R^a_\mu(x)$ are canonically normalised.

While promoting the Skyrme Lagrangian to a gauge-invariant theory is rather straightforward, the situation is different for the winding number. The integrand in the definition (4.4) is obviously not invariant under gauge transformations, and simply promoting the derivative to covariant ones adds new terms in the integral which are not topologically invariant. However, one can consider a gauge-invariant variation of the topological current (4.78),

$$\begin{aligned}\overline{B}^\mu = \frac{1}{24\pi^2}\varepsilon^{\mu\nu\rho\sigma}\Big[&\mathrm{Tr}\left(\Phi^\dagger D_\nu\Phi D_\rho\Phi^\dagger D_\sigma\Phi\right) \\ &+\frac{3i}{2}g_L\ \mathrm{Tr}\left(L_{\nu\rho}\Phi D_\sigma\Phi^\dagger\right) - \frac{3i}{2}g_R\ \mathrm{Tr}\left(R_{\nu\rho}\Phi^\dagger D_\sigma\Phi\right)\Big].\end{aligned} \tag{4.86}$$

The charge associated with this current can be written as

$$\overline{B} = \int \mathrm{d}^3x\ \overline{B}^0 = B(\Phi) + \frac{1}{2}\left[n(R_\mu) - n(L_\mu)\right] + \int \mathrm{d}^3x\ \partial_i\Omega_i, \tag{4.87}$$

where $B(\Phi)$ is the winding number (4.4) for the scalar field Φ,

$$\begin{aligned}\Omega_i = \frac{1}{8\pi^2}\varepsilon_{ijk}\Big[&i\,g_L\ \mathrm{Tr}\left(L_j\Phi\partial_k\Phi^\dagger\right) - i\,g_R\ \mathrm{Tr}\left(R_j\Phi^\dagger\partial_k\Phi\right) \\ &+ 3\,g_L\,g_R\ \mathrm{Tr}\left(L_j\Phi R_k\Phi^\dagger\right)\Big]\end{aligned} \tag{4.88}$$

and $n(A_\mu)$ is a quantity including only gauge fields and defined as

$$\begin{aligned}n(A_\mu) &= \frac{g^2}{8\pi^2}\varepsilon_{ijk}\int \mathrm{d}^3x\left[\mathrm{Tr}\left(\partial_iA_j\,A_k\right) - \frac{2i}{3}\,g\ \mathrm{Tr}\left(A_iA_jA_k\right)\right] \\ &= \frac{g^2}{16\pi^2}\omega_3(A_\mu).\end{aligned} \tag{4.89}$$

The notation ω_3 refers to the Chern-Simons three-form which appeared already in eq. (2.10). n can be rewritten as integral between a reference time far in the past to the present time t,

$$n(A_\mu) = \frac{g^2}{16\pi^2}\int_0^t \mathrm{d}\widetilde{t}\int \mathrm{d}^3x\ \mathrm{Tr}\left(F_{\mu\nu}\widetilde{F}^{\mu\nu}\right). \tag{4.90}$$

This quantity is exactly the winding number of the gauge field identified in eq. (2.13), and counts the number of instantons between the two time boundaries of the integral. The last term on the right-hand side of (4.87) is a surface term, and vanishes provided that the fields are in the vacuum at

the spatial boundaries.[4] The gauge-invariant charge $\overline{B}$ splits therefore into a term involving only the scalar field Φ, which turns out to be the topological index $B(\Phi)$, and a term involving only gauge fields and counting the number of instantons in the theory. In the absence of gauge fields, the charge $\overline{B}$ reduces to the winding number of the field Σ. It is therefore the correct definition of the baryon number — or skyrmion number — of the theory. $\overline{B}$ is moreover conserved over time when "simple", topologically trivial gauge field configurations are taken into account. Only when instantons appear in the theory can $\overline{B}$ be modified over time. The way $\overline{B}$ is affected by instantons is better understood in terms of vector and axial gauge fields, defined as

$$g_V V_\mu(x) = g_L L_\mu(x) + g_R R_\mu(x), \tag{4.91}$$
$$g_A A_\mu(x) = g_L L_\mu(x) - g_R R_\mu(x), \tag{4.92}$$

and for which the covariant derivative becomes

$$D_\mu \Phi = \partial_\mu \Phi - i\, g_V\, [V_\mu, \Phi] - i\, g_A\, \{A_\mu, \Phi\}\,. \tag{4.93}$$

In this case, computing explicitly the value of the charge $\overline{B}$, one finds

$$\overline{B} = B(\Phi) - n(A_\mu). \tag{4.94}$$

$\overline{B}$ is therefore conserved in time if only vector fields are present in the theory, and the existence of such a quantity ensures the presence of stable skyrmions. On the contrary, gauge fields associated with an axial symmetry lead to the non-conservation of the charge $\overline{B}$, hence modifying the topological structure of the theory and leading to skyrmion decay, via an instanton [279]. Note that axial gauge symmetries are broken by the vacuum expectation value $\langle \Phi \rangle = \mathbb{1}$, so that they do not provide light gauge bosons in the spectrum of the theory and might remain hidden at low energies, but still play a very important role regarding the stability of skyrmions.

Skyrmion decay occur nevertheless only through instanton effects, which are strongly suppressed at low temperature [279, 23, 280]: A field configuration given at some time by the hedgehog solution presented above an vanishing gauge fields is actually equivalent upon a non-trivial gauge transformation to another configuration with vanishing winding number $B(\Phi)$, but with non-zero gauge fields. The latter can then tunnel via an instanton into a new state in which the gauge fields are again vanishing, but for which the winding number $B(\Phi)$ is now zero as well. In other words, the skyrmion can unwind with the help of an instanton, but the tunnelling probability for such a process to occur is found in the semiclassical approximation is found to be

$$\exp(-8\pi^2/g^2), \tag{4.95}$$

[4] This is only valid as long as no singularities are present; topological defects such as monopoles can induce a non-vanishing surface term, hence breaking the topological invariance of the charge $\overline{B}$ and leading to skyrmion decay [278].

hence a very tiny number. The lifetime of the skyrmion can therefore be estimated using this result as

$$\tau = \frac{1}{\Gamma} \sim \frac{e^{16\pi^2/g^2}}{M_0} \gg \tau_{\text{universe}}, \tag{4.96}$$

such that the skyrmion can be considered as stable on cosmological timescales even in the presence of axial gauge fields. Note that the estimate performed here can be dramatically enhanced if the skyrmion mass is as large as the energy required by the tunnelling process [281, 282]. We do not consider those effects here, since in the concerned region of small e, the skyrmion mass is largely reduced due to the presence of gauge fields as will be seen in the following sections.

Before moving to the explicit construction of a skyrmion solution in the presence of gauge fields, there is a last issue that need to be addressed regarding, namely the gauging of the Wess-Zumino-Witten term (3.54) present in the Skyrme model. The difficulty resides in the non-local, five-dimensional nature of this operator: While the field $\Phi(x)$ can obviously be extended to a fifth dimension — which once again has no effects on its equations of motion — since it is a Lorentz scalar, defining a gauge field in five dimensions requires the introduction of additional degrees of freedom, and is not desirable here. The latter is however actually unnecessary, since although the Wess-Zumino-Witten term (3.54) is not gauge invariant, its variation under gauge transformations is local and can be written as a four-dimensional quantity, which can then be compensated by local operators written in terms of gauge fields and of the Goldstone field $\Phi(x)$ [283]. We give here the example of a vector gauge transformation

$$\Phi \to U\Phi U^\dagger, \qquad U \in SU(N), \tag{4.97}$$

under which the variation of the five-dimensional action Γ_{WZW} can be written as a total derivative:

$$\begin{aligned}
\delta\Gamma_5 = \frac{iN_c}{48\pi^2}\int_{\mathcal{M}_5} \mathrm{d}\Big[&\mathrm{Tr}\left(U^\dagger \mathrm{d}U\,\Phi\,\mathrm{d}\Phi^\dagger \mathrm{d}\Phi\,\mathrm{d}\Phi^\dagger\right) \\
&+\frac{1}{2}\,\mathrm{Tr}\left(U^\dagger \mathrm{d}U\,\Phi\,\mathrm{d}\Phi^\dagger U^\dagger \mathrm{d}U\,\Phi\,\mathrm{d}\Phi^\dagger\right) \\
&+\mathrm{Tr}\left(U^\dagger \mathrm{d}U\,\Phi\,U^\dagger \mathrm{d}U\,\Phi^\dagger \mathrm{d}\Phi\,\mathrm{d}\Phi^\dagger\right) + \mathrm{Tr}\left(U^\dagger \mathrm{d}U\,\mathrm{d}U^\dagger \mathrm{d}U\,\Phi\,\mathrm{d}\Phi^\dagger\right) \\
&+\mathrm{Tr}\left(\mathrm{d}U^\dagger \mathrm{d}U\,\Phi\,U^\dagger \mathrm{d}U\,\mathrm{d}\Phi^\dagger\right) + \mathrm{Tr}\left(U^\dagger \mathrm{d}U\,\mathrm{d}U^\dagger \mathrm{d}U\,\Phi\,U^\dagger \mathrm{d}U\,\Phi^\dagger\right) \\
&+\mathrm{Tr}\left(U^\dagger \mathrm{d}U\,\Phi\,U^\dagger \mathrm{d}U\,\Phi^\dagger U^\dagger \mathrm{d}U\,\Phi\,\mathrm{d}\Phi^\dagger\right) \\
&+\frac{1}{4}\,\mathrm{Tr}\left(U^\dagger \mathrm{d}U\,\Phi\,U^\dagger \mathrm{d}U\,\Phi^\dagger U^\dagger \mathrm{d}U\,\Phi\,U^\dagger \mathrm{d}U\,\Phi^\dagger\right) - \left(\Phi \leftrightarrow \Phi^\dagger\right)\Big].
\end{aligned} \tag{4.98}$$

We have used here the language of differential forms, i.e. $\mathrm{d}\Phi = \partial_\mu \Phi \, \mathrm{d}x^\mu$, $\mathrm{d}U = \partial_\mu U \, \mathrm{d}x^\mu$, and the antisymmetrisation of indices is implicitly understood. Using Stokes' theorem, and since the boundary of $\mathcal{M}_5$ is the usual Minkowski space $\mathcal{M}_4$, $\delta\Gamma_5$ can be expressed as a four-dimensional integral. A gauge invariant form of the Wess-Zumino-Witten can thus be obtained by adding a four dimensional action written in terms of the scalar field Φ and of the gauge field $A = A_\mu \, \mathrm{d}x^\mu$, transforming under the $SU(N)$ vector gauge transformation as

$$A \to U A U^\dagger + \frac{i}{g} U \mathrm{d}U^\dagger. \tag{4.99}$$

The strategy to determine this gauge counterterm is to write all possible 4-forms in terms of Φ and A, and to choose the coefficients of each of them so that the total variation exactly cancels $\delta\Gamma_5$. We find in this way

$$\begin{aligned}
\Gamma_4 = \frac{iN_c}{48\pi^2} \int_{\mathcal{M}_4} \Big[& ig \,\mathrm{Tr}\left(A\,\Phi^\dagger \mathrm{d}\Phi \, d\Phi^\dagger \mathrm{d}\Phi\right) + g^2 \,\mathrm{Tr}\left((\mathrm{d}A\,A + A\,\mathrm{d}A)\Phi^\dagger \mathrm{d}\Phi\right) \\
& + g^2 \,\mathrm{Tr}\left(\mathrm{d}A\,\mathrm{d}\Phi^\dagger A\,\Phi\right) + g^2 \,\mathrm{Tr}\left(A\,\Phi^\dagger A \Phi\,\mathrm{d}\Phi^\dagger \mathrm{d}\Phi\right) \\
& + \frac{1}{2} g^2 \,\mathrm{Tr}\left(A\,\Phi^\dagger \mathrm{d}\Phi\, A \Phi^\dagger \mathrm{d}\Phi\right) + ig^3 \,\mathrm{Tr}\left(A^3 \Phi\,\mathrm{d}\Phi^\dagger\right) \\
& + ig^3 \,\mathrm{Tr}\left((\mathrm{d}A\,A + A\,\mathrm{d}A)\Phi\,A\,\Phi^\dagger\right) + ig^3 \,\mathrm{Tr}\left(A\,\Phi\,A\,\Phi^\dagger A\,\Phi\,\mathrm{d}\Phi^\dagger\right) \\
& + g^4 \,\mathrm{Tr}\left(A^3 \Phi\,A\,\Phi^\dagger\right) + \frac{1}{4} g^4 \,\mathrm{Tr}\left(A\,\Phi^\dagger A\,\Phi\,A\,\Phi^\dagger A\,\Phi\right) - \left(\Phi \leftrightarrow \Phi^\dagger\right) \\
& + c_1\, g^2 \,\mathrm{Tr}\,\mathrm{d}\left(A^2 \Phi^\dagger \mathrm{d}\Phi\right) + c_2\, g^2 \,\mathrm{Tr}\,\mathrm{d}\left(A^2 \Phi\,\mathrm{d}\Phi^\dagger\right) \\
& + c_3\, g^2 \,\mathrm{Tr}\,\mathrm{d}\left(\mathrm{d}A\,\Phi^\dagger A\,\Phi\right) + c_4\, g^2 \,\mathrm{Tr}\,\mathrm{d}\left(\mathrm{d}A\,\Phi\,A\,\Phi^\dagger\right) \\
& + c_5\, g^3 \,\mathrm{Tr}\,\mathrm{d}\left(A^2 \Phi^\dagger A\,\Phi\right) + c_6\, g^3 \,\mathrm{Tr}\,\mathrm{d}\left(A^2 \Phi\,A\,\Phi^\dagger\right) \\
& + c_7\, g^2 \,\mathrm{Tr}\,\mathrm{d}\left(A\,\Phi^\dagger A\,\mathrm{d}\Phi + A\,\Phi\,A\,\mathrm{d}\Phi^\dagger\right) + c_0\, g^2 \,\mathrm{Tr}\left(F\,\Phi\,F\,\Phi^\dagger\right) \Big],
\end{aligned} \tag{4.100}$$

where $F = \mathrm{d}A - igA^2$ is the field strength tensor. The eight coefficients c_i can in principle be chosen freely, since the variation of the corresponding operators is zero (for the c_0 term) or vanish upon integration (c_1 to c_7 terms). The total Wess-Zumino-Witten action

$$\Gamma_{\mathrm{WZW}} + \Gamma_4 \tag{4.101}$$

is then gauge-invariant. The Noether currents associated with a global $SU(N)_V$ infinitesimal transformation defined as

$$\delta\Phi = i\,[T, \Phi] \qquad \text{and} \qquad \delta A_\mu = i\,[T, A_\mu]\,, \tag{4.102}$$

where T is some generator of $SU(N)$, is then

$$\begin{aligned}
J^{\mu}_{WZW} = \frac{N_c}{48\pi^2}\varepsilon^{\mu\nu\rho\sigma}\Big[& \operatorname{Tr}\Big(T\,\Phi^\dagger\partial_\nu\Phi\,\partial_\rho\Phi^\dagger\partial_\sigma\Phi\Big) + ig\operatorname{Tr}\Big(T\,A_\nu\partial_\rho\Phi\,\partial_\sigma\Phi^\dagger\Big) \\
& + ig\operatorname{Tr}\Big(T\,\partial_\nu\Phi^\dagger A_\rho\partial_\sigma\Phi\Big) + ig\operatorname{Tr}\Big(T\,\partial_\nu\Phi\,\partial_\rho\Phi^\dagger A_\sigma\Big) \\
& + ig\operatorname{Tr}\Big(T\,\Phi\,A_\nu\Phi^\dagger\partial_\rho\Phi\,\partial_\sigma\Phi^\dagger\Big) + ig\operatorname{Tr}\Big(T\,\Phi\,\partial_\nu\Phi^\dagger A_\rho\Phi\,\partial_\sigma\Phi^\dagger\Big) \\
& + ig\operatorname{Tr}\Big(T\,\Phi\,\partial_\nu\Phi^\dagger\partial_\rho\Phi\,A_\sigma\Phi^\dagger\Big) + g^2\operatorname{Tr}\Big(T\,A_\nu A_\rho\Phi\,\partial_\sigma\Phi^\dagger\Big) \\
& + g^2\operatorname{Tr}\Big(T\,A_\nu\Phi^\dagger\partial_\rho\Phi\,A_\sigma\Big) + g^2\operatorname{Tr}\Big(T\,\Phi\,\partial_\nu\Phi^\dagger A_\rho A_\sigma\Big) \\
& + g^2\operatorname{Tr}\Big(T\,A_\nu\Phi^\dagger A_\rho\partial_\sigma\Phi\Big) + g^2\operatorname{Tr}\Big(T\,A_\nu\partial_\rho\Phi\,A_\sigma\Phi^\dagger\Big) \\
& + g^2\operatorname{Tr}\Big(T\,\Phi\,\partial_\nu\Phi^\dagger A_\rho\Phi\,A_\sigma\Phi^\dagger\Big) + g^2\operatorname{Tr}\Big(T\,\Phi\,A_\nu\Phi^\dagger\partial_\rho\Phi\,A_\sigma\Phi^\dagger\Big) \\
& + g^2\operatorname{Tr}\Big(T\,\Phi\,A_\nu\Phi^\dagger A_\rho\Phi\,\partial_\sigma\Phi^\dagger\Big) + g^2\operatorname{Tr}\Big(T\,A_\nu\Phi\,\partial_\rho A_\sigma\Phi^\dagger\Big) \\
& + g^2\operatorname{Tr}\Big(T\,\Phi\,A_\nu\Phi^\dagger\partial_\rho A_\sigma\Big) + g^2\operatorname{Tr}\Big(T\,\Phi\,A_\nu\partial_\rho A_\sigma\Phi^\dagger\Big) \\
& + g^2\operatorname{Tr}\Big(T\,\Phi\,\partial_\nu A_\rho A_\sigma\Phi^\dagger\Big) + ig^3\operatorname{Tr}\Big(T\,A_\nu A_\rho\Phi^\dagger A_\sigma\Phi\Big) \\
& + ig^3\operatorname{Tr}\Big(T\,A_\nu\Phi\,A_\rho\Phi^\dagger A_\sigma\Big) + ig^3\operatorname{Tr}\Big(T\,\Phi^\dagger A_\nu\Phi\,A_\rho A_\sigma\Big) \\
& + ig^3\operatorname{Tr}\Big(T\,\Phi^\dagger A_\nu A_\rho A_\sigma\Phi\Big) + ig^3\operatorname{Tr}\Big(T\,\Phi^\dagger A_\nu\Phi\,A_\rho\Phi^\dagger A_\sigma\Phi\Big) \\
& - \Big(\Phi\leftrightarrow\Phi^\dagger\Big)\Big]. \qquad (4.103)
\end{aligned}$$

We recover in the first term of the integrand the expression of eq. (4.56) coming from the five-dimensional part of the action. All remaining terms arise directly from Γ_4. Note that for a field configuration Φ_0 which is not charged under the generator T, i.e. satisfying $[T, \Phi_0]$, the variation $\delta\Phi_0$ vanishes, and so do all the terms in the current coming from the local part of the Wess-Zumino-Witten action. However, the five-dimensional terms can still give a contribution. Similarly, taking $T = \mathbb{1}$ generates a transformation under which the field $\Phi(x)$ is invariant, but still the Noether current (4.103) does not vanish due to the non-local part of the action, and yield the current of eq. (4.57), which corresponds to a charge proportional to the winding number of the field $\Phi(x)$.

4.2.3 The $U(1)$ gauged skyrmion

Our treatment of gauge interactions in the Skyrme model followed so far the historical developments, but doing so was missing an important point. We presented explicitly the construction of a solution of unit winding number in the absence of gauge fields in section 4.1.3, then quantised it, and finally derived the interactions of this skyrmion with gauge fields from its quantum

numbers only. It was shown however in the previous section that gauge fields can play a more fundamental role in the Skyrme model. They can affect the stability of the skyrmion, and we will now see that they should also be taken into account in the construction of the skyrmion itself.

We start the discussion by considering only an abelian gauge field $\mathcal{A}_\mu$, since in the low-energy theory of QCD only electromagnetism is present as a gauge group. Our conventions are taken from section 3.1.4. Since electromagnetism is embedded in the model as a subgroup of the conserved vector symmetry, it preserves the topological properties of the skyrmion. The fact that it is an abelian $U(1)$ group prevents anyway from the presence of instantons. Interestingly, an inequality similar to the Bogomolny bound (4.15) can be derived in the presence of gauge fields, following the procedure outlined in section 4.1.2. In this case, one can define three gauge-independent and Hermitian quantities,

$$K_i^{(1)} = i\left[c_1\,\Phi^\dagger D_i\Phi + c_2\varepsilon_{ijk}\,D_j\Phi^\dagger D_k\Phi\right], \tag{4.104}$$

$$K_{ij}^{(2)} = \left[c_3\,F_{ij} + c_4\varepsilon_{ijk}\,\Phi^\dagger D_k\Phi\right], \tag{4.105}$$

$$K_{ij}^{(3)} = \left[c_5\,F_{ij} + c_6\varepsilon_{ijk}\,\Phi^\dagger D_k\Phi\right], \tag{4.106}$$

where the coefficients c_i are real numbers. The sum of these quantities squared is therefore positive definite, and adjusting the coefficients properly, can be written as the energy density of the model and a term proportional to the gauge-invariant topological charge (4.87), yielding finally a lower bound on the energy [284]

$$E(\Phi) \geq 6\pi^2\frac{f}{e}\,|B|\left[1+\left(\frac{3g}{2e}\right)^2\right]^{-\frac{1}{2}}, \tag{4.107}$$

where g denotes here the electric charge and B is the topological charge for the field Φ. In the limit $g \to 0$, the usual Bogomolny bound (4.15) for an ungauged skyrmion is recovered. Note that this bound is weaker than eq. (4.15), which seems to indicate that the classical skyrmion mass can be lowered in the presence of gauge fields. This is indeed the case, as presented now.

We are interested in finding a field configuration with unit winding number for the scalar field $\Phi(x)$, i.e. $B(\Phi) = 1$, but with topologically trivial gauge fields, $n(\mathcal{A}_\mu) = 0$. Note that the latter condition implies that one can always perform a gauge transformation $A_0 \to UA_0U^\dagger + iU\partial_0U^\dagger = 0$ where U is time-dependent and topologically trivial, so that the winding number of the gauge field is unchanged. In other words, we can always work in the temporal gauge $A_0 = 0$. Note that skyrmions build with non-vanishing field $A_0 \neq 0$ can be constructed and correspond to electrically charged states,

but they are not the lightest states in the skyrmions' spectrum [284]. The presence of an electromagnetic field associated with a generator $Q \in SU(2)$ implies that a given direction in the $SU(2)$ target space is treated differently than the other two. It is therefore natural to make an ansatz preserving an axial symmetry along the ungauged directions, but which does not preserve the full spherical symmetry of the original hedgehog ansatz [284]. The ansatz for the field $\Phi(x)$ can be made as

$$\Phi(x) = \exp\left[i\, F_a(x)\frac{\sigma^a}{2}\right], \tag{4.108}$$

where

$$\begin{cases} F_1(x) \;=\; F(r,\theta)\sin G(r,\theta)\cos\varphi, \\ F_2(x) \;=\; F(r,\theta)\sin G(r,\theta)\sin\varphi, \\ F_3(x) \;=\; F(r,\theta)\cos G(r,\theta), \end{cases} \tag{4.109}$$

and F and G are two unknown functions. This ansatz is equivalent to the one of eq. (4.70) with $m = 1$, which was used to construct the solution of winding number two. Note also that one recovers the hedgehog ansatz (4.17) if F is only dependent on the radial coordinate r and G is fixed to $G = \theta$. The three non-zero components of the gauge fields can be parametrised in an axially symmetric way as

$$\mathcal{A}_1 \;=\; -\frac{a(r,\theta)}{g\, r\sin\theta}\sin\varphi + \frac{b_1(r,\theta)}{g\, r\sin\theta}\cos\varphi, \tag{4.110}$$

$$\mathcal{A}_2 \;=\; \frac{a(r,\theta)}{g\, r\sin\theta}\cos\varphi + \frac{b_1(r,\theta)}{g\, r\sin\theta}\sin\varphi, \tag{4.111}$$

$$\mathcal{A}_3 \;=\; \frac{b_2(r,\theta)}{g\, r}. \tag{4.112}$$

This ansatz can now be plugged into the Lagrangian, and the energy density can be written down as a functional of the unknown functions F, G, a, b_1 and b_2. Computing the Euler-Lagrange equations for the latter two indicates that the energy is minimised if they are identically set to zero, $b_1(r,\theta) = b_2(r,\theta) = 0$. The energy functional in terms of the remaining three functions can then be written as

$$E[F,G,a] = 2\pi \int_0^\infty \mathrm{d}r\, r^2 \sin\theta\, [\mathcal{H}_2 + \mathcal{H}_4 + \mathcal{H}_{YM}]\,, \tag{4.113}$$

where $\mathcal{H}_2$, $\mathcal{H}_4$ and $\mathcal{H}_{YM}$ denote respectively the Hamiltonian density obtained from the kinetic term for the field Φ, from the Skyrme term and from

the kinetic term for the gauge fields, and read

$$\mathcal{H}_2 = \frac{1}{2}\left[\left((\partial_r F)^2 + \frac{1}{r^2}(\partial_\theta F)^2\right) + \sin^2 F\left((\partial_r G)^2 + \frac{1}{r^2}(\partial_\theta G)^2\right)\right] + \frac{(1+a)^2 \sin^2 F \sin^2 G}{2r^2 \sin^2\theta}, \tag{4.114}$$

$$\mathcal{H}_4 = \frac{(1+a)^2 \sin^2 F \sin^2 G}{2r^2 \sin^2\theta} \cdot \left[\left((\partial_r F)^2 + \frac{1}{r^2}(\partial_\theta F)^2\right) + \sin^2 F\left((\partial_r G)^2 + \frac{1}{r^2}(\partial_\theta G)^2\right)\right] + \frac{\sin^2 F}{2r^2}\left(\partial_r F \partial_\theta G - \partial_r G \partial_\theta F\right)^2, \tag{4.115}$$

$$\mathcal{H}_{YM} = \frac{1}{8g^2 r^2 \sin^2\theta}\left((\partial_r a)^2 + \frac{1}{r^2}(\partial_\theta a)^2\right). \tag{4.116}$$

A solution with winding number one is obtained by imposing same boundary conditions on F and G as for the deuteron solution in section 4.1.6. The requirement $n(\mathcal{A}_\mu) = 0$ is automatically satisfied by the ansatz made above. Having a well-defined gauge field everywhere requires nevertheless to impose boundary conditions on the function $a(r,\theta)$ as

$$a(0,\theta) = a(r,0) = a(r,\pi) = 0, \qquad \partial_r a(\infty,\theta) = 0. \tag{4.117}$$

From the explicit form of the energy density defined above, it can be seen that the constant value value $a(r,\theta) = -1$ would minimise the energy density, but is not however consistent with the boundary condition. There is therefore a tension, which is materialised in the observation that a solution with non-vanishing gauge field is favoured, independently of the strength of the gauge coupling. The energy density obtained after the numerical resolution of the problem can be expressed as a function of the dimensionless quantity (g/e), and will be later shown in fig. 4.20. The deviations with respect to the ungauged hedgehog solution are nevertheless very small, and using the latter in the computation of the skyrmion's static properties was shown to be a valid approximation [284].

4.2.4 The $SU(2)$ gauged skyrmion

There is however a different gauging of the Skyrme model which has more dramatic effects on the classical solution, namely when gauging a diagonal $SU(2)$ subgroup of the global symmetry, i.e. when promoting the space-time derivative to a covariant one,

$$D_\mu \Phi = \partial_\mu \Phi - i\, g\, [W_\mu, \Phi], \tag{4.118}$$

where an $SU(2)$-valued gauge field $W_\mu = W_\mu^a \frac{\sigma^a}{2}$ was introduced. The same arguments as in the previous section can be used to derive a lower bound on

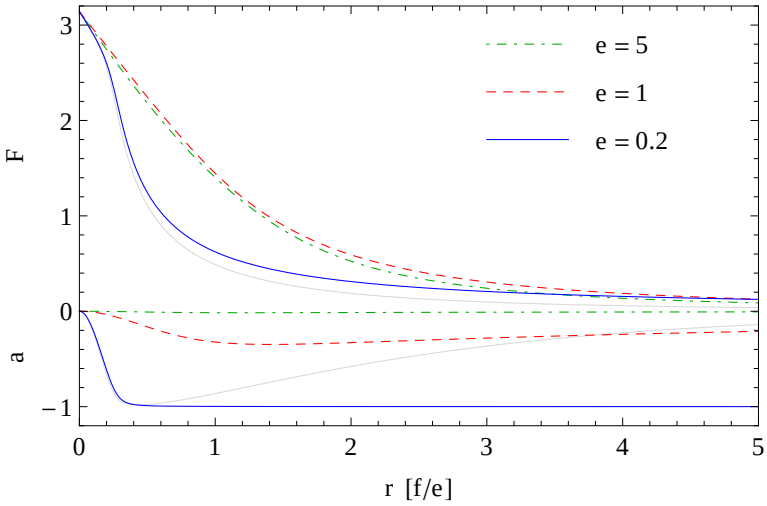

Figure 4.12: The functions F and a minimising the energy functional (4.120) for different values of the Skyrme coupling e, while $g = 0.653$ is fixed. The grey solid line corresponds to $e = 0.2$ when the $SU(2)$ breaking term (4.167) is turned on (with $\varepsilon = 0.1$).

the energy, and turns out to be exactly the quantity defined in eq. (4.107), where the gauge coupling g refers now to the $SU(2)$ gauge group [285, 286]. The main difference with respect to the $U(1)$ gauged skyrmion is that an ansatz can be made including non-vanishing gauge fields while preserving the spherical symmetry of the field configuration. This is the so-called *Skyrme-Wu-Yang ansatz*, which takes for the field Φ the form of the hedgehog ansatz (4.17) and for the $SU(2)$ gauge field [285, 286],

$$W_i^a = \frac{a(r)}{2gr}\varepsilon_{iak}\,\hat{x}_k, \qquad W_0^a = 0, \tag{4.119}$$

where $a(r)$ is a function playing the same role as $F(r)$. The boundary conditions for $a(r)$ have to be fixed to $a(0) = 0$ for definiteness at the origin, while at spatial infinity $a(r)$ is only required to take a constant value, i.e. $a'(\infty) = 0$. Using the Skyrme-Wu-Yang ansatz, the energy of the skyrmion configuration can be written as a functional of $F(r)$ and $a(r)$, independent of the angular variables, as

$$\begin{aligned} E[F,a] = 2\pi\frac{f}{e}\int_0^\infty \mathrm{d}r \Bigg[& \frac{e^2}{g^2}\left(2\left(a'\right)^2 + \frac{a^2(a+2)^2}{r^2}\right) \\ & + \left(r^2 + 2(1+a)^2\sin^2 F\right)\left(F'\right)^2 \\ & + (1+a)^2\sin^2 F\left(2 + (1+a)^2\frac{\sin^2 F}{r^2}\right)\Bigg]. \end{aligned} \tag{4.120}$$

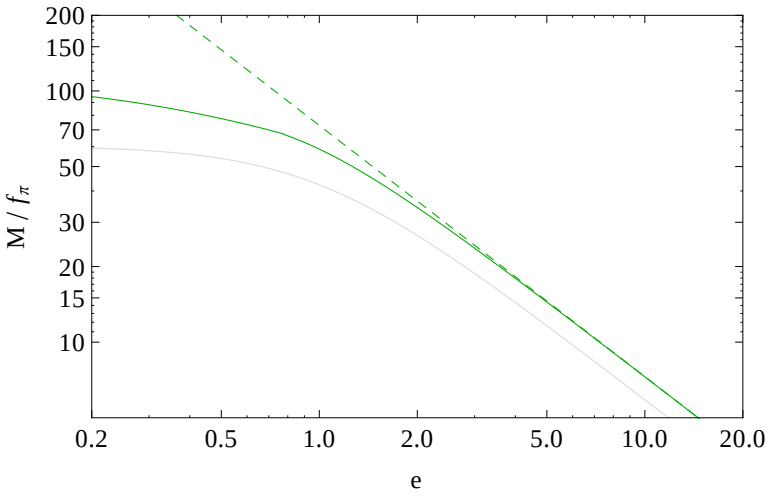

Figure 4.13: Energy of the skyrmion configuration given by eq. (4.120) as a function of the Skyrme parameter e, compared to the ungauged solution of eq. (4.27) (dashed line). The light grey line corresponds to the Bogomolny bound given in eq. (4.107).

The functions F and a minimising this integral for different values of the Skyrme coupling e are shown on figure 4.12. In the limit of vanishing gauge coupling, or equivalently for a large e/g ratio, F tends towards the ungauged solution, while a remains small. On the contrary, for values of $e/g \lesssim 1$, the gauge potential decreases as $\frac{1}{r}$, as the function a goes asymptotically to the constant value -1. In the latter case the $SU(2)$ gauge field mimics at large distances the field induced by a magnetic monopole. The energy of the skyrmion configuration is shown on figure 4.13, where g was fixed to the value of the electroweak $SU(2)_W$ gauge coupling at the Z-pole mass. Note that the gauged skyrmion solution found here does not have a direct application in models of low-energy QCD, since there is no such gauge group there, but will be very useful when applying the Skyrme model to composite Higgs and little Higgs models.

4.2.5 Other group structures

Our goal in this chapter is to study extensively the presence of skyrmions in composite Higgs and little Higgs models. As it was discussed in chapter 3, most existing models are not QCD-like, but rely on a very different symmetry breaking pattern. The presence of skyrmions in the low-energy description of QCD is due to the fact that the vacuum manifold — the space in which the Goldstone bosons live, in this case $SU(N_f)$ — has a non trivial topology. We want to consider now different theories, also described at low-

		π_2	π_3	π_4
$SU(N)$	$N = 2$	0	$\mathbb{Z}$	$\mathbb{Z}_2$
	$N \geq 3$	0	$\mathbb{Z}$	0
$SO(N)$	$N = 3, 5$	0	$\mathbb{Z}$	$\mathbb{Z}_2$
	$N = 4$	0	$\mathbb{Z} \oplus \mathbb{Z}$	$\mathbb{Z}_2 \oplus \mathbb{Z}_2$
	$N \geq 6$	0	$\mathbb{Z}$	0
$Sp(2N)$		0	$\mathbb{Z}$	0
G_2		0	$\mathbb{Z}$	0

Table 4.1: Homotopy of different simple Lie groups [12].

energy by a non-linear σ-model, but with arising from a different symmetry breaking pattern. The presence of skyrmions and their stability in a given theory depends of course on many details of the theory, but a necessary condition is that the third homotopy of the vacuum manifold is non-trivial, which can be studied purely on the mathematical side.

In general, the vacuum manifold can be a simple Lie group, for example $SU(N)$ or $SO(N)$. This is the case in little Higgs models based on product groups, in which a vector subgroup G_V of the product $G \times G$ is preserved by the vacuum, while the axial subgroup G_A is broken and corresponds to the vacuum manifold. Homotopy classes of simple groups can be found in the literature, and are summarised here in table 4.1. The third homotopy group π_3 is the one playing the deciding role about the presence of skyrmion: any non-trivial structure corresponds to the conservation of a topological quantity, hence guaranteeing the presence of skyrmion provided that they are properly stabilised in the physical theory. Also important is the fourth homotopy π_4, which if it contains a $\mathbb{Z}_2$ subgroup permits to quantise the skyrmion freely as a fermion or a boson, following the Finkelstein-Rubinstein rule [267]. It is actually a general rule that all simple, compact Lie group have $\mathbb{Z}$ as a third homotopy classes, and models based on product groups generically contain skyrmions [12].

A large class of models of electroweak symmetry breaking does not however rely on product groups, but rather on cosets of simple groups, a number of them being referenced in table 3.2. In this case, the third and fourth homotopy groups can be calculated from the *exact homotopy sequence* relating the homotopy of simple groups and quotient of them in the following way:

$$\ldots \to \pi_k(H) \to \pi_k(G) \to \pi_k(G/H) \to \pi_{k-1}(G) \to \pi_{k-1}(H) \to \ldots \quad (4.121)$$

The sequence of maps is exact in the mathematical sense that the image of each map is precisely equal to the kernel of the map following it. As an

example, we proceed in calculating π_3 and π_4 for the coset $SU(N)/SO(N)$, on which e.g. the littlest Higgs model was based. We denote the maps belonging to the exact homotopy sequence by α_i, and one has then

$$\begin{aligned} \ldots \;\to\; \pi_4\big(SU(N)\big) \xrightarrow{\alpha_1} \pi_4\big(SU(N)/SO(N)\big) \xrightarrow{\alpha_2} \pi_3\big(SO(N)\big) \\ \xrightarrow{\alpha_3} \pi_3\big(SU(N)\big) \xrightarrow{\alpha_4} \pi_3\big(SU(N)/SO(N)\big) \xrightarrow{\alpha_5} \pi_2\big(SO(N)\big) \to \ldots \end{aligned} \tag{4.122}$$

The exactness of the sequence means explicitly that $\operatorname{im}\alpha_1 = \ker\alpha_2$, and so on. Using this important piece of information together with the homotopy classes of simple groups given in table 4.1, one can derive the unknown $\pi_3(SU(N)/SO(N))$ and $\pi_4(SU(N)/SO(N))$. First we use the fact that both $SU(N)$ and $SO(N)$ have non-trivial third homotopy groups, $\pi_3(SU(N)) = \pi_3(SO(N)) = \mathbb{Z}$. Since we know already an expression for the winding number of a field $\Phi(x) \in SU(N)$ as an integral over space, one can use this tool and evaluate the same integral on $SO(N)$-valued fields. The $SO(N)$ configurations of lowest-possible winding number turns out to have winding number two in $SU(N)$ for $N \geq 4$ and winding number four for $N = 3$ [265]. All possible non-trivial field configurations can then be generated by multiplying copies of the configurations of lowest winding number. The mapping denoted α_3 in the sequence (4.122) is therefore simply a multiplication in the form

$$\begin{aligned} \alpha_3 : \mathbb{Z} &\to \mathbb{Z} \\ k &\mapsto p\,k \end{aligned} \qquad \text{with } p = \begin{cases} 4 & \text{for } N = 3, \\ 2 & \text{for } N \geq 4, \end{cases} \tag{4.123}$$

the image of which can be used to gain information about the following mapping α_4 as

$$\ker\alpha_4 = \operatorname{im}\alpha_3 = p \cdot \mathbb{Z}. \tag{4.124}$$

α_4 maps therefore every p-th integer to zero, and must be identified with the modulo operation as

$$\begin{aligned} \alpha_4 : \mathbb{Z} &\to \pi_3\big(SU(N)/SO(N)\big) \\ k &\mapsto \quad k \mod p \end{aligned} \tag{4.125}$$

On the far right-hand side of the homotopy sequence (4.122), $\pi_2(SO(N)) = 0$ is trivial — as for the second homotopy group any simple Lie group. From the exactness of the homotopy sequence, the kernel of the mapping α_5 must be all of the group $\pi_3(SU(N)/SO(N))$, and thus

$$\operatorname{im}\alpha_4 = \ker\alpha_5 = \pi_3\big(SU(N)/SO(N)\big). \tag{4.126}$$

The latter can then be read directly from the definition of α_3 above to be the cyclic group

$$\pi_3\big(SU(N)/SO(N)\big) = \mathbb{Z}_p. \tag{4.127}$$

		π_3	π_4
$SU(N)/SO(N)$	$N=3$	$\mathbb{Z}_4$	0
	$N\geq 4$	$\mathbb{Z}_2$	0
$SU(N)/SU(N-1)$		0	0
$SO(N)/SO(N-1)$		0	0
$SU(2N)/Sp(2N)$		0	0

Table 4.2: Third and fourth group of homotopy of different quotient groups G/H [265].

The same procedure can be used to determine the fourth homotopy group of this coset. The mapping α_3 as defined above as a trivial kernel, hence

$$\operatorname{im}\alpha_2 = \ker\alpha_3 = 0. \tag{4.128}$$

Since α_2 maps every element to zero, $\pi_4(SU(N)/SO(N))$ is exactly the kernel of α_2

$$\pi_4\big(SU(N)/SO(N)\big) = \ker\alpha_2 = \operatorname{im}\alpha_1. \tag{4.129}$$

On the other hand, since $\pi_4(SU(N))$ is trivial for any $N \geq 3$, the image of the mapping α_1 has to be trivial as well, and one obtains finally $\pi_4(SU(N)/SO(N)) = 0$. This results are reported in table 4.2, together with the third and fourth homotopy groups of various cosets. Among all cosets under consideration, only $SU(N)/SO(N)$ is found to have a non-trivial topology. Constructing the skyrmion solution in this case will be the subject of section 4.3.

4.2.6 The holographic skyrmion

Before moving to the explicit study of skyrmions in non-QCD-like models, it is worth mentioning recent results obtained in the holographic description of QCD already discussed in section 3.2.4. An important drawback of the Skyrme model in four dimensions is that the skyrmion mass and size are affected by all higher-order operator in the non-linear σ-model, and there is no guarantee that the quantities computed in section 4.1.3 properly describe the skyrmion's properties. The issue can actually be seen from the fact that the skyrmion size is similar as the cutoff length $1/(4\pi f_\pi)$, so that short-distance operators involving more derivatives will play an important role as well. In a five-dimensional theory, the validity of the σ-model description extends beyond the four-dimensional cutoff $\Lambda_4 \approx 4\pi f_\pi$, and a skyrmion configuration can be build which has a size much larger than the typical range of interactions arising from higher-order terms.

A holographic skyrmion is present in a model with a gauge symmetry $SU(2)_L \times SU(2)_R$ in the bulk, broken down by boundary conditions to the diagonal subgroup $SU(2)_V$ on the IR brane [287]. The low-energy physics of such a theory is described by a $SU(2)$ non-linear σ-model in five dimensions, which possesses stable skyrmion solutions like its four-dimensional counterpart. Analogously to the original four-dimensional Skyrme model, the presence of just the kinetic term for the gauge fields in the bulk is actually not sufficient to stabilise the size of the skyrmion. One needs to add an additional term localised on the IR brane. In the absence of such a term, the five-dimensional skyrmion take the form of a four-dimensional instanton of arbitrarily small size. A brane-localised term stabilises the size of the skyrmion. If the latter is small, the shape of the skyrmion is close to that of an instanton, while in the opposite limit, when the boundary term dominates, the holographic skyrmion tends to the solution obtained in a variation of the Skyrme model not discussed in this thesis, in which the skyrmion's size is stabilised by the presence of vector mesons only [288].

The holographic skyrmion obtained in this way is providing a valid description of the baryon in the AdS/QCD formalism [289, 290], and permits for example a perturbative computation of nucleon form factors [291]. The model can also be easily extended to include pion masses [292], and the global agreement with experimental data is good in both meson and baryon sectors. In the effective field theory spirit of this thesis, we will restrict ourselves to the four-dimensional description of skyrmions in composite Higgs model. Extending this study to the extra-dimensional picture is nevertheless a interesting subject which deserves to be investigated in the future.

4.3 SU(N)/SO(N) skyrmions

The coset $SU(N)/SO(N)$ was shown in section 4.2.5 to have a non-trivial topology,

$$\pi_3(SU(N)/SO(N)) = \mathbb{Z}_p, \qquad p = \begin{cases} 4 & \text{for } N = 3, \\ 2 & \text{for } N \geq 4. \end{cases} \tag{4.130}$$

leading to the possible presence of skyrmion in models based on this symmetry breaking pattern. Composite Higgs models can be built in this form, but require $N \geq 5$ in order to permit the embedding of a Higgs doublet [130]. The littlest Higgs model [216] is precisely such a realisation with $N = 5$, for which skyrmions are present [244] and can even act as dark matter [293, 294, 5].[5] Before studying the latter in detail in

[5]The non-trivial topology of the $SU(5)/SO(5)$ coset also induces the presence of other topological defects in the littlest Higgs model, such as cosmic strings and $\mathbb{Z}_2$ monopoles [295].

section 4.5, we discuss here the classical properties of skyrmion arising in $SU(N)/SO(N)$ cosets for both cases $N = 3$ and $N \geq 4$. In general, the $SU(N)/SO(N)$ symmetry breaking pattern can be obtained from a strongly interacting theory with Weyl fermions in the adjoint representation of the gauge group [296, 297, 298, 299].

4.3.1 The SU(N)/SO(N) σ-model

We consider a σ-model defined by the Lagrangian density

$$\begin{aligned}\mathcal{L}_{\text{Skyrme}} = \frac{f^2}{4}\,\mathrm{Tr}\left(\partial_\mu \Sigma^\dagger \partial^\mu \Sigma\right) \\ + \frac{1}{32e^2}\,\mathrm{Tr}\left[\Sigma^\dagger\partial_\mu\Sigma, \Sigma^\dagger\partial_\nu\Sigma\right]\left[\Sigma^\dagger\partial^\mu\Sigma, \Sigma^\dagger\partial^\nu\Sigma\right],\end{aligned} \tag{4.131}$$

where $\Sigma(x)$ is a $SU(N)$ *symmetric* matrix. The model has a global $SU(N)$ symmetry under which $\Sigma(x)$ transforms in the two-indices symmetric representation as

$$\Sigma \mapsto U\Sigma U^T, \qquad U \in SU(N). \tag{4.132}$$

The vacuum state is obtained by taking a constant value for the field $\Sigma(x)$. Here we choose it to be the identity matrix

$$\langle\Sigma\rangle = \mathbb{1}_{N\times N}. \tag{4.133}$$

This vacuum expectation value spontaneously breaks the global $SU(N)$ symmetry down to $SO(N)$, since only the $SO(N)$ subgroup of $SU(N)$ leaves the vacuum unchanged under the transformation rule (4.132). As a consequence the Goldstone field $\Sigma(x)$ takes its values in the coset $SU(N)/SO(N)$.

The Lagrangian (4.131) is identical to the one of the Skyrme model (4.10) describing the low-energy chiral limit of QCD, in which f is identified with the pion decay constant and e is a parameter depending on the high-energy behaviour of the theory, found empirically to be $e \cong 5$ [263]. The notable difference is that in the original Skyrme model the field transforms in the adjoint representation of $SU(N_f)_L \times SU(N_f)_R$, where N_f is the number of light flavours, and a global diagonal $SU(N_f)_V$ symmetry is preserved after spontaneous symmetry breaking.

The presence of skyrmions in the model (4.131) is due to the fact that the third homotopy group π_3 of the target space is non-trivial and from the presence of a four-derivative term $\mathcal{L}_4$ stabilising the skyrmion's size. For simplicity, we will always consider static solutions — moving skyrmions can be obtained by applying a Lorentz boost — and work in dimensionless units $\widetilde{x} = (fe)\,x$, hence having an energy density in the form of eq. (4.12).

The elements $\Sigma(x)$ of the coset $SU(N)/SO(N)$ can be parametrised by

the Cartan embedding [265,296], starting from a matrix $\Phi(x)$ in $SU(N)$, as

$$\begin{aligned} SU(N) &\to \quad SU(N)/SO(N), \\ \Phi(x) &\mapsto \Sigma(x) = \Phi(x)\Phi(x)^T. \end{aligned} \tag{4.134}$$

The matrix $\Phi(x)$ is only defined up to right-multiplication with an $SO(N)$ matrix. The advantage of this embedding is that the winding number of a field configuration $\Phi(x)$ in $SU(N)$ is then simply given in terms of an integral over space by eq. (4.4).

The winding number of $\Sigma(x)$ can then be straightforwardly identified with the winding number of the field $\Phi(x)$ used to construct it. However, this mapping is not unique: the multiplication of $\Phi(x)$ from the right with an $SO(N)$ matrix $R(x)$ leaves $\Sigma(x)$ unchanged, but not the winding number (4.4), which is raised or lowered as $B(\Phi R) = B(\Phi) + B(R)$. The crucial point here is that $B(R)$ cannot take an arbitrary integer value, since the winding number integral (4.4) evaluated on an element of $SO(N)$ gives an integer multiple of 4 for $N = 3$ and of 2 for $N \geq 4$ [265]. Therefore the winding number of an element in the coset $SU(N)/SO(N)$ is only defined modulo a factor of 4 or 2, for $N = 3$ and $N \geq 4$ respectively. Moreover, two field configuration $\Sigma_1(x)$ and $\Sigma_2(x)$ built respectively from $SU(N)$ fields $\Phi_1(x)$ and $\Phi_2(x)$ differing by one unit of winding number cannot be continuously transformed into another and thus belong to different homotopy classes. This is an immediate consequence of the statement made above that $\pi_3(SU(3)/SO(3)) = \mathbb{Z}_4$ and $\pi_3(SU(N)/SO(N)) = \mathbb{Z}_2$ for $N \geq 4$. The winding number for the field $\Sigma(x) = \Phi(x)\Phi(x)^T$ can thus be expressed unambiguously as

$$B(\Sigma) = B(\Phi) \bmod p, \tag{4.135}$$

where p is defined as in eq. (4.130).

With the help of the Cartan embedding (4.134), the challenge of constructing a field configuration in each of the homotopy classes of the coset space reduces to finding an appropriate configuration $\Phi(x)$ in $SU(N)$ with the desired winding number. A naive choice consists in taking the lightest $SU(N)$ skyrmion solution of a given winding number and building the corresponding $SU(N)/SO(N)$-valued field directly out of it. For $B = 1$ the lightest solution is known to be the hedgehog configuration (4.17) with spherical symmetry and mass $M_0 = 72.9\ \frac{f}{e}$ given in eq. (4.27). The Cartan embedding of this solution yields a skyrmion of mass $4M_0 = 291.7\ \frac{f}{e}$ whose symmetry is however only axial. This is a hint that the hedgehog ansatz might not yield the lightest field configuration, as we shall see. For $B = 2$, the $SU(N)$ skyrmion has a toroidal shape, and its mass of $139.6\ \frac{f}{e}$ was obtained in eq. (4.76). The naive Cartan embedding of this $B = 2$ configuration gives a mass of $599.0\ \frac{f}{e}$ for the corresponding $SU(N)/SO(N)$

field. We can therefore infer the following upper bounds on the skyrmion masses:

$$M_{B=\pm1} \leq 291.7\ \frac{f}{e}, \qquad M_{B=2} \leq 599.0\ \frac{f}{e}. \tag{4.136}$$

We are actually going to show in the next sections that the true skyrmion solutions have masses much below these naive bounds.

Note that in this case one cannot use the alternative term (4.77) to stabilise the skyrmion size: the equivalent of the topological current (4.78) with the field $\Sigma(x)$ replacing $\Phi(x)$ vanishes identically due to the structure of the coset, so that the Lagrangian term (4.77) is automatically absent of the theory. For the same reason, the usual Bogomolny bound [258] for the mass of a $SU(N)$ skyrmion of winding number B, $M_B \geq 6\pi^2|B|\frac{f}{e}$, does not apply since the component B_0 of the topological current (4.78) is zero. A crucial consequence is that the mass of the skyrmion is not necessarily increasing with increasing winding number. Indeed, we shall see in the following that for $N = 3$ the $B = 2$ skyrmion is lighter than the $B = \pm1$ ones.

4.3.2 The skyrmion for N > 3

As shown in section 4.1.3, the construction of the lightest skyrmion solution makes use only of a subgroup of $SU(N)$ satisfying a $\mathfrak{su}(2)$ algebra. We postulate here that this rule can also be applied to the construction of the $SU(N)/SO(N)$ skyrmion, so that in general the field $\Phi(x)$ can be written as $\Phi(x) = \exp[i\, f_i(x)T_i]$, where the T_i are generators of a $SU(2)$ subgroup of $SU(N)$. However, while in the original Skyrme model the relevant subgroup could be trivially chosen to live in the upper-left 2×2 block of the matrix Φ, this is not the case in the coset, where not every choice of $SU(2)$ subgroup is equivalent: among the diagonal $SU(N)$ transformations $\Phi \to U\Phi U^\dagger$, only the ones satisfying $U^\dagger\langle\Sigma\rangle = \langle\Sigma\rangle U^T$ are symmetries of the model. The form of the ansatz (4.20) is nevertheless very useful to ensure a correct winding number by construction, so instead of considering a different ansatz for Φ we keep this form and work in a different basis where the vacuum expectation value is not necessarily diagonal. The most general form of the Cartan embedding (4.134) is $\Sigma(x) = \Phi(x)\Sigma_0\Phi(x)^T$, where $\Sigma_0 = \langle\Sigma\rangle$ denotes the vacuum state.

A second crucial point which can be learnt from the construction of the $SU(N)$ skyrmion is the requirement of a spherical symmetry. We have seen that this is possible if the transformation $\Phi_0 \to U_0\Phi_0U_0^\dagger$ is a symmetry of the Lagrangian. This $SU(2)$ transformation of Φ_0 can be promoted to a $SU(N)$ transformation by considering $\Phi \to U\Phi U^\dagger$, with

$$U = \begin{pmatrix} U_0 & \\ & V \end{pmatrix}, \qquad U_0 \in SU(2), \quad V \in SU(N-2). \tag{4.137}$$

As discussed above, this transformation is a symmetry of the Lagrangian only if it satisfies

$$U^\dagger \Sigma_0 = \Sigma_0 U^T. \tag{4.138}$$

Since $U_0^\dagger$ and U_0^T live respectively on the left- and right-hand side of eq. (4.138) and cannot be related by multiplication with a matrix Σ_0 for arbitrary values of U_0, the equation can only be fulfilled if the $(N-2)$-dimensional matrix V is proportional to U_0^*. From this point, we have to consider two separated cases: for $N = 3$, the one-dimensional matrix V is fixed to $V = 1$, hence eq. (4.138) cannot be satisfied and the $SU(2)$ transformation rule of Φ_0 cannot be promoted to a symmetry of the Lagrangian, independently of the basis. Thus we conclude that there exist no spherically symmetric ansatz of unit winding number in the coset $SU(3)/SO(3)$. On the contrary, for $N \geq 4$, choosing

$$\Sigma_0 = \begin{pmatrix} & \mathbb{1}_2 & \\ \mathbb{1}_2 & & \\ & & \mathbb{1}_{N-4} \end{pmatrix}, \qquad U = \begin{pmatrix} U_0 & & \\ & U_0^* & \\ & & \mathbb{1}_{N-4} \end{pmatrix}, \tag{4.139}$$

the transformation $\Phi \to U\Phi U^\dagger$ acts on Φ_0 as a diagonal $SU(2)$ transformation $\Phi_0 \to U_0 \Phi_0 U_0^\dagger$ and simultaneously preserves the vacuum, so that the Lagrangian can be made spherically symmetric. This is the most general choice of basis, up to global $SU(N)$ transformations, and we expect therefore to build the lightest skyrmion configuration with the help of this ansatz.

With the choice of basis (4.139), we have just proved that the skyrmion can be made spherically symmetric. Indeed, an important property of the Skyrme Lagrangian (4.131) is that it can be expressed in terms of the currents $\Sigma^\dagger \partial_\mu \Sigma$, which take in this case a block diagonal form,

$$\Sigma = \begin{pmatrix} & \Phi_0 & \\ \Phi_0^T & & \\ & & \mathbb{1}_{N-4} \end{pmatrix}, \tag{4.140}$$

hence

$$\Sigma^\dagger \partial_\mu \Sigma = \begin{pmatrix} -\left(\Phi_0 \partial_\mu \Phi_0^\dagger\right)^T & & \\ & \Phi_0^\dagger \partial_\mu \Phi_0 & \\ & & 0_{N-4} \end{pmatrix}, \tag{4.141}$$

so that each of the two 2×2 blocks contributes equally to the energy density, which becomes twice the functional (4.12) expressed in terms of the $SU(2)$-valued field $\Phi_0(x)$,

$$E[\Sigma] = 2\, E[\Phi_0]. \tag{4.142}$$

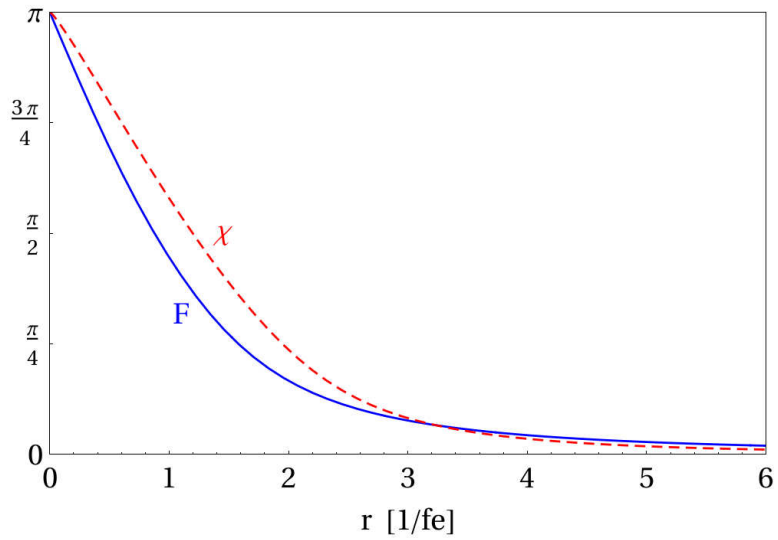

Figure 4.14: The profile functions F and χ for the $N = 4$, $B = 1$ and $N = 3$, $B = 2$ skyrmions respectively.

Hence the mass of the $SU(N)/SO(N)$ skyrmion with $N \geq 4$ is exactly twice the mass of the original $SU(2)$ skyrmion. The solution minimising the energy $E[\Phi_0]$ is obtained using the hedgehog ansatz (4.17), and was found in eq. (4.27) to corresponds to an energy $E[\Phi_0] = 72.9\ f/e$. We find therefore for the $SU(N)/SO(N)$ skyrmion

$$M_{N=4,B=1} = 145.8\ \frac{f}{e}. \tag{4.143}$$

This mass is exactly twice the mass of the $SU(N)$ skyrmion, and only half the value of the upper bound (4.136) found from the naive Cartan embedding of the original solution. We do not have a proof that it is indeed the lightest topologically non-trivial field configuration, but it is the only simple embedding preserving the spherical symmetry of the Lagrangian, and it is much lighter than other constructions based on different choices of ansatz, as for example the $N = 3$ case discussed below.

4.3.3 The skyrmion of unit winding number for N = 3

The solution of unit winding number in $SU(3)/SO(3)$ was not computed so far in the literature, and requires a more involved ansatz. The reason for this is that the spherical symmetry cannot be preserved, as argued before.

In the original basis $\langle \Sigma \rangle = \mathbb{1}_3$, the ansatz (4.20) nevertheless allows to preserve an axial symmetry in the Lagrangian, and we expect therefore that it yields the lowest-energy skyrmion solution. The most general form of

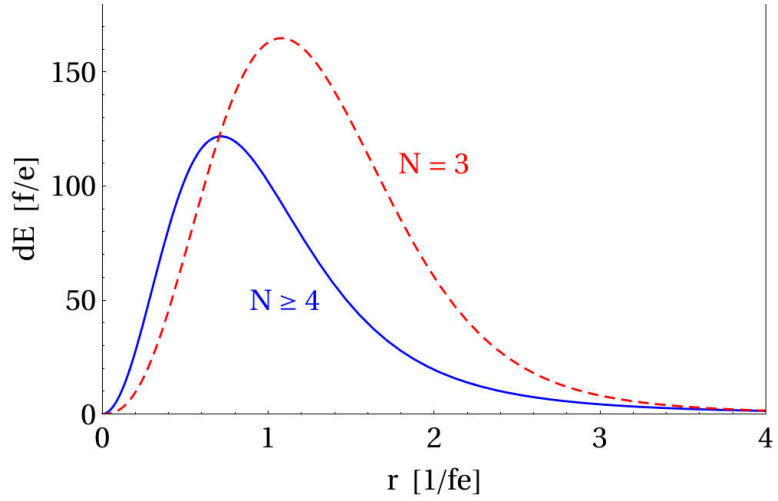

Figure 4.15: The radial energy distributions $dE = -4\pi\mathcal{L}$ (right) as functions of the radius r in dimensionful units of $1/fe$.

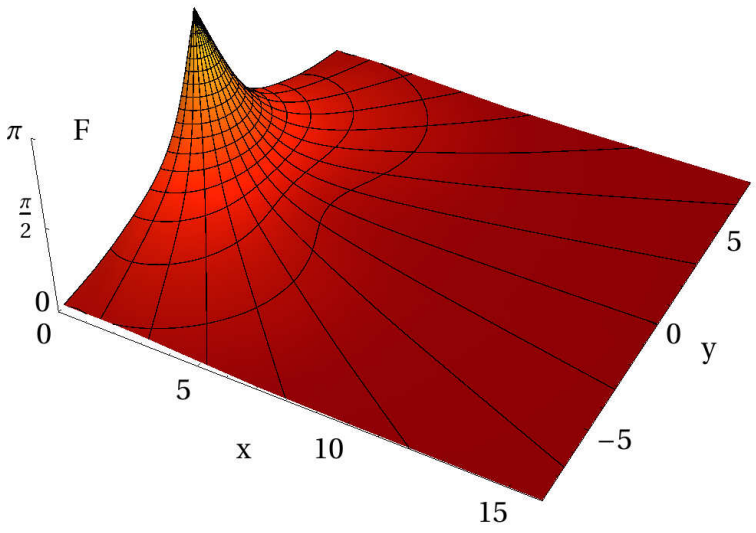

Figure 4.16: The numerical solution in the case $N = 3$, $B = 1$ for F, in the plane $(x, y) = (\widetilde{r}\sin\theta, \widetilde{r}\cos\theta)$.

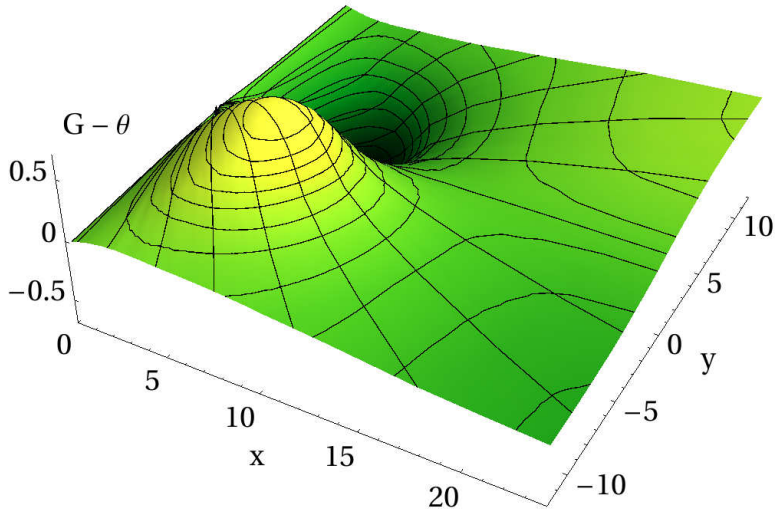

Figure 4.17: The numerical solution in the case $N = 3$, $B = 1$ for the difference $G - \theta$ (right), in the plane $(x, y) = (\widetilde{r}\sin\theta, \widetilde{r}\cos\theta)$.

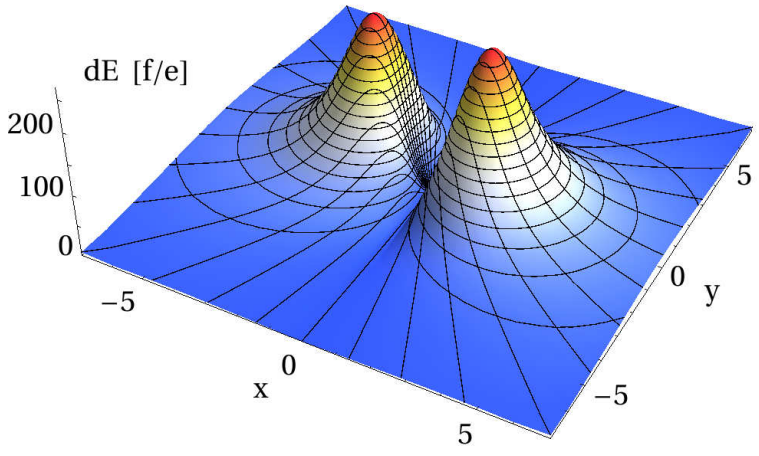

Figure 4.18: The energy density of the $N = 3$, $B = 1$ solution in a plane containing the axis of symmetry of the skyrmion (located along $x = 0$).

Φ_0 preserving this axial symmetry can then be written in analogy to the construction of the deuteron solution [270] as

$$\Phi_0(x) = \exp\left[i\, F(r,\theta)\, n_i(r,\theta,\varphi)\, \sigma_i\right], \tag{4.144}$$

where n is a vector of unit length, given in spherical coordinates by

$$(n_1, n_2, n_3) = (\sin G(r,\theta)\sin\varphi,\, \cos G(r,\theta),\, \sin G(r,\theta)\cos\varphi)\,. \tag{4.145}$$

Instead of a single profile function F of the radial variable r as in the hedgehog ansatz (4.17), we are now left with two functions F and G of two variables r and θ. The boundary conditions are fixed to $F(0,\theta) = \pi$, $F(\infty,\theta) = 0$, $G(r,0) = 0$ and $G(r,\pi) = \pi$, so that the field $\Phi(x)$ is well defined everywhere. With this ansatz, the winding number integral (4.4) becomes

$$B(\Phi) = \frac{1}{\pi}\int_0^\infty \mathrm{d}r \int_0^\pi d\theta\ \sin^2 F \sin G\,(\partial_r F \partial_\theta G - \partial_\theta F \partial_r G) \tag{4.146}$$

and gives the expected value of one upon integration by parts. Similarly, a solution of winding number $B = -1$ (or equivalently $B = 3$) is obtained by inverting the boundary condition for F at the origin to $F(0,\theta) = -\pi$; the energy of this solution is identical to the $B = 1$ case, and we will therefore not discuss it further. Plugging the ansatz (4.144) into the energy functional (4.12), one obtains

$$\begin{aligned} E[F,G] = 4\pi \int_0^\infty \mathrm{d}r \int_0^\pi d\theta \sin\theta \\ \Bigg\{ &\sin^2 G \left(1 + \frac{\sin^2 2F \sin^2 G}{r^2 \sin^2\theta}\right)\left[r^2 (\partial_r F)^2 + (\partial_\theta F)^2\right] \\ &+ \sin^2 F \left(1 - \cos^2 F \sin^2 G + \frac{\sin^2 F \sin^2 2G}{r^2 \sin^2\theta}\right) \\ &\qquad \cdot \left[r^2 (\partial_r G)^2 + (\partial_\theta G)^2\right] \\ &+ \frac{1}{2}\sin 2F \sin 2G \left(1 + 4\frac{\sin^2 F \sin^2 G}{r^2 \sin^2\theta}\right) \\ &\qquad \cdot \left[r^2 \partial_r F \partial_r G + \partial_\theta F \partial_\theta G\right] \\ &+ 4 \sin^4 F \sin^2 G \left[\partial_r F \partial_\theta G - \partial_\theta F \partial_r G\right]^2 \\ &+ \frac{\sin^2 F \sin^2 G (1 - \sin^2 F \sin^2 G)}{\sin^2\theta} \Bigg\}. \end{aligned} \tag{4.147}$$

The corresponding Euler-Lagrange equations for F and G are too long to be displayed here, but can be solved numerically using relaxation methods.

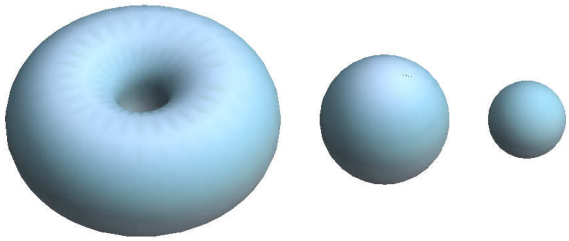

$N = 3$	$N = 3$	$N \geq 4$
$B = \pm 1$	$B = 2$	$B = 1$

Figure 4.19: Isosurfaces of energy density $dE = 100\,\frac{f}{e}$ showing the relative size of the three solutions.

The solution of these equations are shown in fig. 4.16 and 4.17, and the corresponding energy density on fig. 4.18. As one can see, unlike the spherical energy distribution of the previous two sections, the energy density is in this case located along a torus.[6] The mass of the skyrmion, obtained by integrating this energy density, is found to be

$$M_{N=3,B=\pm 1} = 273.5\ \frac{f}{e}. \tag{4.148}$$

The relative size of the different skyrmion solutions is shown for comparison in fig. 4.19.

4.3.4 The skyrmion of winding number two for N = 3

The general rule stating that solutions with the highest symmetries tend to have the lowest mass also apply to the $N = 3$ case, where the spherically symmetric solution of winding number two found by Balachandran et al. [301, 302] is the lightest known skyrmion configuration. It is constructed from the $SO(3)$ generators $T_i \in \{\lambda_2, \lambda_5, \lambda_7\}$, where the λ_i denote Gell-Mann matrices. The ansatz is built as follows:

$$\Phi(x) = \exp\left[i\,\alpha(r)\,\hat{x}_i\,T_i\right] \exp\left[i\,\chi(r)\left(\frac{2}{3}\mathbb{1} - (\hat{x}_i T_i)^2\right)\right]. \tag{4.149}$$

[6] Note that our solution resembles the numerical skyrmion solution of the $O(3)$ σ-model of ref. [300].

	$B = \pm 1$	$B = 2$
$N = 3$	$273.5\ \frac{f}{e}$	$228.7\ \frac{f}{e}$
$N \geq 4$	$145.8\ \frac{f}{e}$	

Table 4.3: Classical masses of the $SU(N)/SO(N)$ skyrmions.

The two exponentials commute; the first of them belongs to $SO(3)$ and is therefore irrelevant in the coset space, as can be seen from the Cartan embedding (4.134), yielding

$$\Sigma(x) = \exp\left[2i\,\chi(r)\left(\frac{2}{3}\,\mathbb{1} - (\hat{x}_i\,T_i)^2\right)\right]. \tag{4.150}$$

However, it is the first exponential which fixes the winding number (4.4):

$$\begin{aligned} B(\Phi) &= \frac{2}{\pi}\int_0^\infty \mathrm{d}r\,\left[\alpha'\,(\cos\alpha\cos\chi - 1) - \chi'\,\sin\alpha\sin\chi\right] \\ &= \frac{2}{\pi}\,(\sin\alpha\cos\chi - \alpha)\Big|_{r=0}^{r\to\infty}, \end{aligned} \tag{4.151}$$

since the expected value $B = 2$ of the winding number is achieved by choosing the boundary conditions $\alpha(\infty) = 0$ and $\alpha(0) = \pi$. Nevertheless, with this choice the first exponential in (4.149) is ill-defined around the origin, and the introduction of the second exponential with boundary conditions $\chi(\infty) = 0$ and $\chi(0) = \pi$ is required to cancel the angular dependence at the boundary point $r = 0$. Plugging this ansatz into the energy density (4.12), one obtains the following functional, also independent of the angular variables,

$$E[\chi] = 8\pi\,\frac{f}{e}\int_0^\infty \mathrm{d}r\,\left[\left(\frac{1}{3}r^2 + 2\sin^2\chi\right)\chi'^2 + \left(2r^2 + \sin^2\chi\right)\frac{\sin^2\chi}{r^2}\right], \tag{4.152}$$

which is minimised when χ satisfies the Euler-Lagrange equation

$$\left(\frac{1}{3}r^2 + 2\sin^2\chi\right)\chi'' + \frac{2}{3}r\chi' + \sin 2\chi\left(\chi'^2 - 1 - \frac{\sin^2\chi}{r^2}\right) = 0. \tag{4.153}$$

The numerical solution for $\chi(r)$ is shown in fig 4.14, and the energy distribution along the radial direction in fig 4.15. The mass of the $B = 2$ skyrmion is hence

$$M_{N=3,B=2} = 228.7\ \frac{f}{e}. \tag{4.154}$$

The masses of the three different $SU(N)/SO(N)$ skyrmion solutions are summarised in Table 4.3. For $N = 3$, the skyrmions of winding number plus and minus one are heavier than the one of winding number two, so that the mass hierarchy is inverted compared to $SU(N)$ models. Although this result can be surprising, it could be expected from the symmetry of the solutions. Notice that the two masses are nevertheless close to each other — only about 20% difference — whereas in the $SU(N)$ case the Bogomolny bound [258] implies that the mass of the second heaviest skyrmion — which has a toroidal shape as in the $SU(3)/SO(3)$ case — is nearly twice the mass of the lightest, spherically symmetric skyrmion. The $N \geq 4$ solution with spherical symmetry is significantly lighter than both $N = 3$ skyrmions. It is actually a rather surprising fact that for any values of $N > 2$, there always exists a spherically symmetric solution, and that this solution is the lightest even when its winding number is not unity.

The finiteness of the third homotopy groups for $N = 3$ and $N \geq 4$ ensure special annihilation properties for the skyrmions: in the latter case, the skyrmion is its own antiskyrmion, so that any two skyrmions can annihilate into a final state with trivial topology. For $N = 3$, the skyrmion of winding number two has the same properties as the $N \geq 4$ one; on the other hand, two toroidal skyrmions can annihilate into a state containing a spherical symmetric skyrmion or not, depending if they have the same or opposite winding number. Notice also that although multiple skyrmion solutions are not favoured by energy considerations, no important attractive force between them is expected at large distances (see section 4.1.5), so that the skyrmions appearing in theories described at intermediate energies by a $SU(N)/SO(N)$ σ-model can be long-lived. The $N = 3$ case is especially interesting since the two different kinds of skyrmions are both stable and have a mass hierarchy prohibiting the heaviest state to decay into a pair of light ones. Note also that the masses computed here are only obtained at the classical level. The quantisation of the model typically makes the physical masses increase depending on the spin of the skyrmion, as shown in sec. 4.1.4. Notice moreover that the inclusion of higher-dimensional terms in the Lagrangian (4.131) would also modify the skyrmion masses, but not their symmetry properties nor the way they are embedded in the coset.

4.4 Skyrmions in composite Higgs models

We are now ready to study the skyrmions appearing in the composite models which were the main topic of chapter 3. The homotopy groups of the various symmetry breaking patterns appearing in the numerous composite Higgs and little Higgs models were all determined in section 4.2.5, and the results were summarised in tables 4.1 and 4.2. For the cosets potentially leading to the presence of skyrmions, the classical solutions were all constructed

above. The quantum properties of the skyrmions in composite and little Higgs models remain however to be determined, and this is the task of this section. Note that skyrmions can appear as well in technicolor models, where due to their stability, they can naturally be dark matter candidates [303]. The discussion presented here is however based on the assumption that an electroweak doublet with the quantum numbers of a Higgs belongs to the Goldstone sector of the model. Many of our conclusions rely on this crucial point.

We consider a theory containing a new, strongly-interacting sector in which a global symmetry G is broken down to a subgroup H of it, yielding a certain number of Goldstone bosons, among which the Higgs doublet. At energies below the symmetry breaking scale f, the Higgs sector is described by a non-linear sigma-model in the form

$$\mathcal{L} = \frac{f^2}{4} \mathrm{Tr}\left(D_\mu \Phi D^\mu \Phi^\dagger\right) + \text{higher order terms}, \tag{4.155}$$

where $\Phi(x)$ is the Goldstone field and f parametrises the scale of new physics, typically of the order of a few TeV. This description of the Higgs field is common to both little Higgs and holographic Higgs models. The global symmetry group G of the strong sector is furthermore explicitly broken by gauging at least a $SU(2)_W \times U(1)_Y$ subgroup of it; realistic models often require to gauge a larger subgroup. The gauged electroweak subgroup of G has to be chosen carefully so that the Goldstone field Φ contains an $SU(2)_W$ doublet with hypercharge $\frac{1}{2}$ to be identified with the Higgs boson. The gauge bosons couple to the Goldstone sector through the covariant derivative. In the absence of electroweak couplings g_2, g_1 and of Yukawa couplings to the Standard Model fermions, the Higgs would be massless, as an exact Goldstone boson. Only radiative corrections trigger the electroweak symmetry breaking and give a mass to the W and Z bosons as well as to the Higgs.

4.4.1 A minimal model

For simplicity, we will first restrict our discussion to a minimal model, then show that the lessons we learn from it can be extended to more general cases. The simplest realisation of the Higgs as a pseudo-Goldstone boson consists in taking $\Phi \in SU(3)$. This can be achieved by adding a new strongly interacting sector to the Standard Model, composed of 3 families of fermions, each of them coming in N_c colours. The Standard Model gauge group is therefore enlarged with a new $SU(N_c)$, under which the new fermions transform in the fundamental representation. In the absence of fermion masses, there is a global $SU(3)_L \times SU(3)_R$ symmetry rotating the left- and right-handed fermions of the 3 families. This symmetry is spontaneously broken down to the diagonal subgroup $SU(3)_V$ by fermion

condensates. Note that realistic models based on the symmetry breaking pattern $SU(3)_L \times SU(3)_R \to SU(3)_V$ actually require the introduction of several copies of the global symmetry group, as in the "minimal moose" model [219].

To correctly describe the anomalies induced by loops of fermions of the strongly interacting sector, the Wess-Zumino-Witten (WZW) term (3.54) has to be added to the Lagrangian (4.155), and takes here the form

$$\Gamma_{WZW} = -\frac{iN_c}{240\pi^2}\int_{\mathcal{M}_5} \mathrm{d}^5x\,\varepsilon^{\mu\nu\rho\sigma\tau}\,\mathrm{Tr}\left(\Phi^\dagger\partial_\mu\Phi\,\partial_\nu\Phi^\dagger\partial_\rho\Phi\,\partial_\sigma\Phi^\dagger\partial_\tau\Phi\right) + \text{local terms required by gauge invariance,} \tag{4.156}$$

where N_c is the number of colours of the underlying strongly-interacting theory. The exact form of this term depends on the choice of the gauge group; it was demonstrated in section 4.2.2 for a vector gauge group. The number of colours N_c can in principle be taken to zero, in which case the underlying theory is not anymore a theory of strongly-interacting fermions and the scalars described by the sigma-model (4.155) are fundamental scalars. Note, however, that such a weakly-coupled UV completion might reintroduce the hierarchy problem.

In our minimal model the field $\Phi(x)$ transforms in the adjoint representation of $SU(3)_V$. The covariant derivative used in the Lagrangian (4.155) is given by

$$D_\mu\Phi = \partial_\mu\Phi - igW^a_\mu\left[Q^a,\Phi\right] - ig'B_\mu\left[Y,\Phi\right]. \tag{4.157}$$

The commutators ensure that the electroweak gauge group belongs to the unbroken diagonal subgroup $SU(3)_V$. This description in terms of the low-energy effective theory does not fix the charge of the technifermions under the electroweak gauge group: the diagonal $SU(2)_W \times U(1)$ subgroup of the global $SU(3)_L \times SU(3)_R$ symmetry can be gauged as such, but can also arise as the unbroken combination of a larger gauge group, for example in the form $SU(2)_L \times SU(2)_R \times U(1)_L \times U(1)_R$. A remarkable result of our analysis is indeed that the skyrmion charge does not directly depend on the technifermion content of the theory, as explained in the following. The generators of the electroweak $SU(2)_W$ gauge subgroup can be taken without loss of generality to live in the upper-left 2×2 block of the 3×3 matrix, as

$$Q^a = \frac{1}{2}\begin{pmatrix}\sigma^a & & \\ & & \\ & & \end{pmatrix}, \tag{4.158}$$

where the σ_a are the usual Pauli matrices. The hypercharge generator has to commute with the Q^a and be traceless, it is therefore fixed up to an overall factor to

$$Y = \frac{1}{6}\begin{pmatrix}\mathbb{1} & & \\ & & \\ & & -2\end{pmatrix}. \tag{4.159}$$

The $\frac{1}{6}$ factor is chosen to obtain among the Goldstone bosons a $SU(2)_W$ doublet with the quantum numbers of the Higgs.[7] The Goldstone field Π, given in the nonlinear realisation of the sigma-model by

$$\Phi = \exp\left[2i\Pi/f\right], \tag{4.160}$$

can then be decomposed as

$$\Pi = \begin{pmatrix} \boldsymbol{\omega} + \frac{1}{2\sqrt{3}}\,\eta & h \\ h^\dagger & -\frac{1}{\sqrt{3}}\,\eta \end{pmatrix}, \tag{4.161}$$

where $\boldsymbol{\omega}$ is a real triplet, h a complex doublet and η a real singlet of $SU(2)_W$, denoted by

$$\boldsymbol{\omega} = \begin{pmatrix} \frac{1}{2}\,\omega^0 & \frac{1}{\sqrt{2}}\,\omega^+ \\ \frac{1}{\sqrt{2}}\,\omega^- & -\frac{1}{2}\,\omega^0 \end{pmatrix}, \qquad h = \frac{1}{\sqrt{2}} \begin{pmatrix} h^+ \\ h^0 \end{pmatrix}, \qquad \eta = \eta^0. \tag{4.162}$$

Note that $\boldsymbol{\omega}$ and η have automatically zero hypercharge, independently of the choice of the normalisation of the generator Y, while this is not the case for h. The generator of the electric charge is then given by

$$Q_{em} = Q^3 + Y = \begin{pmatrix} \frac{2}{3} & & \\ & -\frac{1}{3} & \\ & & -\frac{1}{3} \end{pmatrix}, \tag{4.163}$$

and turns out to be the same as in the low-energy chiral description of QCD, with the u, d and s quarks taken as massless. For this reason, this model is also a plausible composite Higgs candidate, since the charges of the new technifermions match the ones of the Standard Model quarks, and one could choose not to couple the latter directly to the Higgs sector, but still obtain a mass by mixing with the heavy fermions resonances.[8]

4.4.2 Skyrmions and the electroweak gauge group

The presence of skyrmions in this model is due to the fact that the third homotopy group of the coset space $SU(N)$ is non-trivial, $\pi_3(SU(N)) =$

[7] Note that unlike for the $SU(2)_W$ generators Q_a, we do not require the hypercharge generator Y to satisfy the normalisation condition $\mathrm{Tr}\, YY = \frac{1}{2}$. This permits to write the covariant derivative in the form of eq. (4.157), i.e. without an extra factor in front of the term $B_\mu\,[Y, \Phi]$. In other words, the hypercharge of the Goldstone field Φ is directly encoded into the generator Y.

[8] This would however require the strong sector to be the usual colour $SU(3)_c$, hence fixing N_c to be a multiple of three in the WZW term (4.156).

$\mathbb{Z}$. If only the unbroken $SU(2)_W \times U(1)_Y$ gauge group is present in the model, then the topological charge (4.4) is a gauge-independent, conserved quantity and the skyrmion is stable. If there are on the contrary additional gauge fields in the model, which belong to the broken subgroup of $SU(N)$, then the skyrmion might decay. This is the case in all models of little Higgs involving two copies of the electroweak gauge group, among others the models including a T-parity. The tunnelling probability for the skyrmion to decay is nevertheless exponentially suppressed, so that the skyrmions remain stable anyway on cosmological timescales, as discussed in section 4.2.2

The different sectors of the space of field configurations are labelled by the integer-valued winding number (4.4). The vacuum configuration $\Phi = \mathbb{1}$ and any continuous transformation of it correspond to the topologically trivial sector of the theory with $B = 0$. Field configuration of non-zero winding number can be obtained from the hedgehog ansatz of section 4.1.3. In order to stabilise the skyrmion size, at least one term of higher order in powers of the derivative must be added to the Lagrangian (4.155). In general, we can assume that these higher-order term are present in our models, but one cannot know their precise form from the point of view of the low-energy theory. The mass of the skyrmion may depend dramatically on the coefficients of higher-order term and cannot be computed without fixing them.

For now, the relevant properties of the skyrmion are its symmetries (both global and local), but not its mass, size, or other static properties. We will therefore get around the problem of higher-order operators by first discussing a simpler model where only the Skyrme term of eq. (4.10) is present, and then show that our conclusions are actually independent of the exact form of the sigma-model Lagrangian. With this choice, all the skyrmion's properties will depend only on the two unknown parameters f and e.[9] With this choice of higher order terms, the mass of the skyrmions are bounded from below by the Bogomolny bound (4.107). This bound cannot be saturated but gives already a good estimation of the skyrmion mass. It shows also that the presence of gauge fields allows to lower the mass of the skyrmion, as we will see in the next section.

In the absence of gauge fields, the hedgehog ansatz (4.17) is known to yield the lowest energy configuration of unit winding number in the Skyrme model [263]. Any embedding of the hedgehog into the $SU(3)$ field Φ is equivalent, i.e. any choice of $\mathfrak{su}(2)$ generators T^a is allowed. Turning on the $SU(2)_W \times U(1)_Y$ electroweak gauge group removes this degeneracy. The crucial point is now to find the form of the lightest field configuration of unit winding number. Non-vanishing gauge fields give a positive contribution to the energy of a skyrmion configuration through their kinetic term, but they

[9] The other two parameters of the model, the gauge coupling g and g', are here implicitly fixed to the Standard Model values.

can still lower the overall energy by their interplay with the scalar field $\Phi(x)$.

The effect of a $U(1)$ gauge field on the skyrmion mass has been discussed in section 4.2.3. The field configuration in this case is not spherically symmetric anymore, but still preserves an axial symmetry. Such a field configuration can be achieved in our model by choosing the T^a to be the generators of a $SU(2)$ subgroup living in the upper-left block of the $SU(3)$ matrix Φ and considering the gauge field of electromagnetism only. The resulting decrease in the energy of the classical skyrmion configuration with respect to the ungauged hedgehog is shown on figure 4.20 as a function of the Skyrme parameter e. In general, any of the three components of the $SU(2)_W$ gauge field can play the same role and lower the mass of the skyrmion while spoiling its spherical symmetry. The lightest field configuration is however obtained using all three components of W^a_μ, as the Skyrme-Wu-Yang ansatz of section 4.2.4. It is realised when taking the hedgehog ansatz (4.17) to live along the $SU(2)_W$ gauged subgroup, i.e. choose the hedgehog generators to match the gauge ones

$$T^a = Q^a. \tag{4.164}$$

With this choice, the spherical symmetry of the skyrmion can be preserved, since $SU(2)_W$ gauge transformations acts then in a similar fashion as spatial rotations on the hedgehog configuration. The so-constructed hedgehog lives exclusively in the upper-left 2×2 block of the matrix $\Phi(x)$, and commutes with the hypercharge generator. Thus the $U(1)_Y$ gauge field cannot help lowering the energy and is set to zero, $B_\mu = 0$. The ansatz for the gauge field is then given in eq. (4.119), and the corresponding mass of the skyrmion is computed from the energy density (4.120), and shown in fig. 4.20 (corresponding to $\varepsilon = 0$). The property of the Skyrme-Wu-Yang ansatz to yield always the classical field configuration of lowest energy is expected to be valid independently of the exact form of the higher order terms in the sigma-model, and therefore to be universal.[10] It is another example of the fact that the lowest energy soliton configurations are generally the ones with the highest symmetry properties. The spherical symmetry of the Skyrme-Wu-Yang ansatz is naturally preserved by all terms in the derivative expansion due to the gauge invariance of the model, as long as the alignment of the gauge and hedgehog generators is chosen, as in eq. (4.164). The two limiting cases $e \to 0$ and $e \to \infty$ are somewhat special. In the former limit, the gauge fields play a very important role, up to the point where the lightest energy solution takes the asymptotic form of a magnetic monopole; the transition to this regime is visible on figure 4.20 around $e \approx 0.75$ where the energy density shows a knee. Conversely, in the limit of large e (vanishing Skyrme

[10] In principle a $U(1)$-gauged skyrmion might be lighter than a $SU(2)$-gauged one, provided that the coupling constant associated with the $U(1)$ gauge field is much larger that the one associated with $SU(2)$. This situation does not happen when considering the electroweak gauge group of the Standard Model.

term), the gauge field becomes very weak, and the various skyrmion configurations are nearly degenerate in energy. We want to emphasise however that both limits seem unphysical once all terms in the derivative expansion are taken into account. The optimal value of e in the original chiral Lagrangian of QCD is indeed precisely in the intermediate range, namely $e \approx 4$, in order to predict the correct baryon properties.

The discussion so far was based onto the assumption that the vacuum expectation value of the field $\Phi(x)$ is strictly equal to the identity matrix, $\langle \Phi \rangle = \mathbb{1}$. In this case however the Goldstone bosons would be exactly massless and the electroweak symmetry group would remain unbroken. In realistic models a mass for the Higgs boson is actually obtained by radiative corrections. The details of this mechanism depend on the exact realisation of the composite Higgs model, and we do not want to discuss them here. In our formalism, the breaking of the electroweak symmetry manifest itself as a vacuum misalignment conveniently expressed in terms of the Goldstone field (4.161) as

$$\langle \Pi \rangle = \begin{pmatrix} & & \\ & & v \\ & v & \end{pmatrix}, \tag{4.165}$$

where $v \approx 246$ GeV is the electroweak symmetry breaking scale. This vacuum expectation value yields through the kinetic term for the field Φ a mass term for the W and Z bosons, of the form

$$m_W = \sin\left(\frac{v}{2f}\right) gf \approx \frac{gv}{2}, \qquad m_Z = \frac{1}{2}\sin\left(\frac{v}{f}\right)\frac{gf}{\cos\theta_W} \approx \frac{gv}{2\cos\theta_W}, \tag{4.166}$$

where θ_W denotes the Weinberg angle. In the right-hand side equalities we have taken the limit $v \ll f$, recovering the Standard Model values. It is evident that the breaking of the electroweak symmetry also automatically breaks the spherical symmetry of the Skyrme-Wu-Yang ansatz. The correction to the energy of the skyrmion induced by the vacuum expectation value v can be expressed as a correction to the energy density (4.120) in the form

$$E[F,a] = 2\pi\frac{f}{e}\int_0^\infty \mathrm{d}r \left[\ldots + \frac{\varepsilon}{2}a^2 + \mathcal{O}\left(\varepsilon^2\right)\right], \tag{4.167}$$

where $\varepsilon = v^2/f^2$, and the dots denote the ε-independent terms of eq. (4.120). Note that the leading order contribution in ε preserves the spherical symmetry of the skyrmion; higher order terms do not. The true gauge group of the Standard Model being $U(1)_{em}$, no spherically symmetric skyrmion configuration including gauge fields can actually be constructed. However, the very small size of the correction introduced in eq. (4.167) implies that the

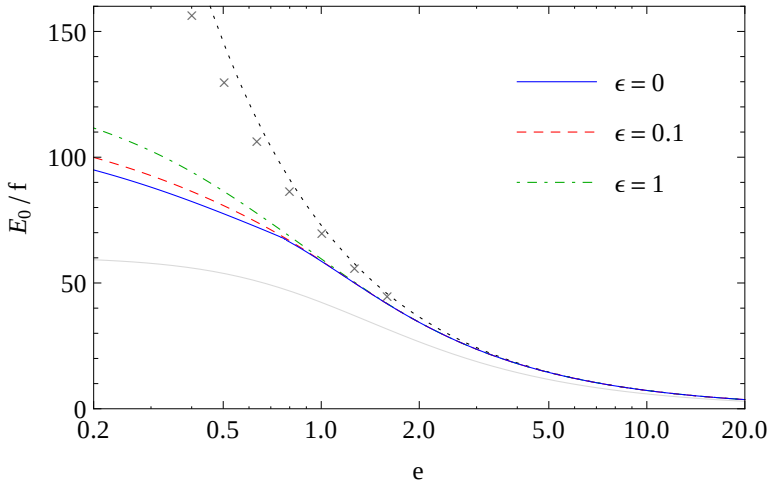

Figure 4.20: Energy of the skyrmion configuration given by eq. (4.120) and (4.167) as a function of the Skyrme parameter e, for different values of $\varepsilon = v^2/f^2$. The dotted black line corresponds to the ungauged case, the solid grey one to the Bogomolny bound given in eq. (4.107). The crosses show for comparison the mass of the $U(1)_{em}$ gauged solution of section 4.2.3.

lowest energy configuration is still provided by the Skyrme-Wu-Yang ansatz. The contribution to the energy density coming from the zeroth order in v/f are of order 10–100 f/e. Leading order corrections in v/f have already very little effect, since the correction term is bounded by $|a(r)| \leq 1$; the difference is only significant in the regime of small e, but remains small even in the unrealistic limit $\varepsilon \to 1$, as shown in figure 4.20. The next-to-leading order terms breaking the spherical symmetry have therefore a negligible effect on the mass of the skyrmion. The ε-term plays nevertheless a important role in the sense that it forbids monopole-like solutions, for which the asymptotic value of the function $a(r)$ is different from zero at spatial infinity; its effects on the profile functions F and a are visible on figure 4.12 for $e = 0.2$ and $\varepsilon = 0.1$.

The physical skyrmion states are obtained, following the discussion of section 4.1.4, by performing a zero-mode quantisation around the classical solution. The zero-modes are transformations that leave invariant the energy of the skyrmion solution found in the previous section. This comprises the Lorentz transformations and the internal symmetries of the skyrmion. The latter reduce after electroweak symmetry breaking to the $U(1)_{em}$ global transformations. However, the correction to the spherical symmetric skyrmion are in our case so negligible compared to the overall skyrmion energy that all $SU(2)_W$ and $U(1)_Y$ global transformations are approximate symmetries of the classical skyrmion, and will be considered as

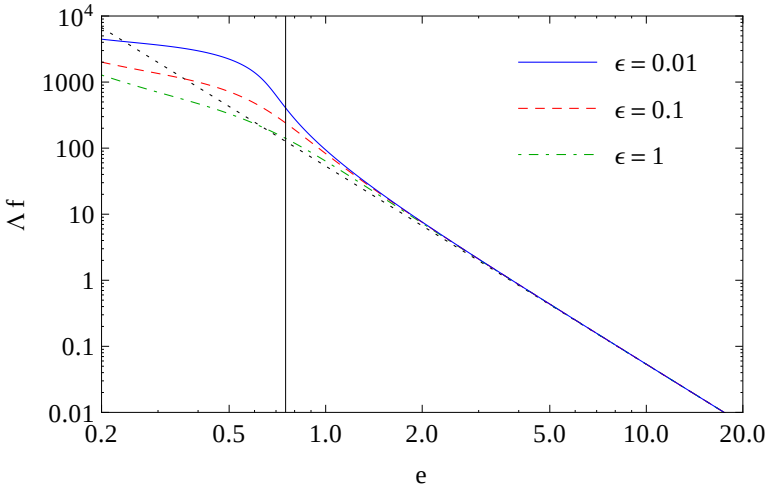

Figure 4.21: Value of Λ given by equation (4.168) as a function of the Skyrme parameter e, for different values of $\varepsilon = v^2/f^2$. The straight dotted line corresponds to the ungauged case. The vertical bar at $e \cong 0.75$ is the value below which the integral diverges in the absence of the electroweak symmetry breaking term (4.167).

exact in the following. Note that, as mentioned before, the total spin-isospin equivalence found in section 4.1.4 is actually broken by the Higgs vacuum expectation value.

Like the energy density, the moment of inertia of the skyrmion Λ gets modified with respect to eq. (4.36) by the presence of the gauge fields, expressed here as the dependence on the function $a(r)$ and on the electroweak symmetry breaking parameter ε, as

$$\Lambda = \frac{8\pi}{3}\frac{1}{fe^3}\int_0^\infty \mathrm{d}r \left[r^2 \sin^2 F \left(\left(F'\right)^2 + 1 + (1+a)^2 \frac{\sin^2 F}{r^2}\right) + 2\frac{e^2}{g^2}a^2\right]. \tag{4.168}$$

The numerical value of Λ is displayed in figure 4.21. Note that the dependence on ε comes at the lowest order only implicitly through the functions F and a. In the limit of large e, Λ tends to the value $53.4/\left(fe^3\right)$ of eq. (4.37). For $SU(3)$ as for all relevant choices of cosets leading to a pseudo-Goldstone Higgs boson (see tables 4.1 and 4.2), $\pi_4(G/H)$ is trivial. This means that the spin statistics of the skyrmion is unambiguously fixed by the coefficient of the Wess-Zumino-Witten term: if N_c is even, the skyrmion is a boson; if N_c is odd, it is a fermion. If the skyrmion is a boson, the mass of the lowest state is given by E_0, displayed on figure 4.20 for the simplest case where only the Skyrme term is taken into account. On the contrary, if it is

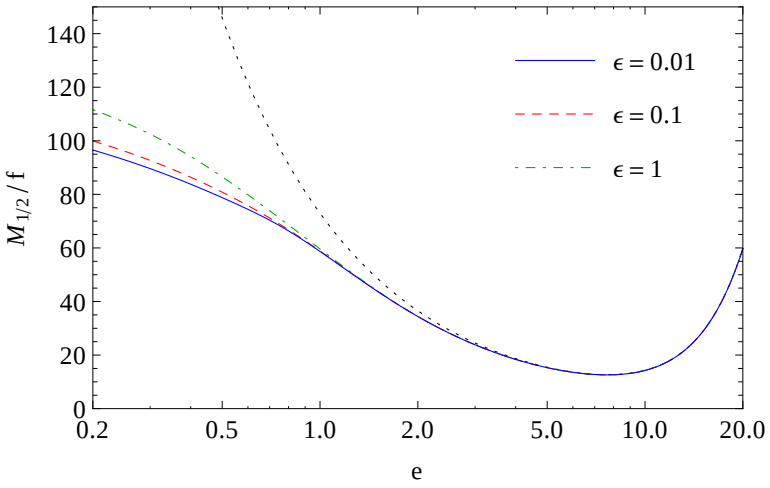

Figure 4.22: Mass of the lightest skyrmion state if it is a fermion as a function of the Skyrme parameter e, for different values of $\varepsilon = v^2/f^2$. The grey dotted line is the corresponding mass in the absence of gauge fields.

a fermion, its mass becomes

$$M_{\frac{1}{2}} = E_0 + \frac{3}{8\Lambda}, \tag{4.169}$$

and is shown on figure 4.22. The different scalings of E_0 and Λ^{-1} relative to the Skyrme parameter e imply that a minimum occurs around $e_{min} \approx 7.7$, with $M_{\frac{1}{2},min} \approx 12.7\ f$. The two lowest energy skyrmion states are then part of an isospin doublet, like the proton and the neutron in the Standard Model. Although the skyrmion mass is strongly dependent on the higher order terms in the sigma-model, its quantum numbers do not depend on the precise form of these terms, since the results rely only on the assumption that the solution is approximately spherically symmetric, which is always true when the skyrmion lives along the gauged $SU(2)_W$ subgroup of the global symmetry group.

The hypercharge of the skyrmion can similarly be extracted from the Noether current associated with $U(1)_Y$ transformations. There is neither a contribution from the local Lagrangian given by the kinetic term and the Skyrme term in eq. (4.10), nor from higher order operators, since the hypercharge generator commutes with the generators T^a used to construct the hedgehog configuration. A non-zero contribution comes nevertheless from the non-local part of the Wess-Zumino-Witten term (4.156), as discussed above. Regarding the skyrmion configuration living in the upper-left block of the matrix Φ, the hypercharge generator appears as a multiple of the identity matrix, and therefore the contribution from the Wess-Zumino-Witten

term is in the form of eq. (4.58), i.e. proportional to the number of colours N_c of the underlying theory. In our toy model, the generator Y given in (4.159) comes with a factor $\frac{1}{6}$, so that the hypercharge of the skyrmion is fixed to be

$$Y_{\text{skyrmion}} = \frac{N_c}{6}. \tag{4.170}$$

The electric charge of the lightest skyrmion state, given by $Y + Q^3$, is then

$$q = \begin{cases} \frac{1}{6}\, N_c & \text{if } N_c \text{ is even (boson),} \\ \\ \frac{1}{6}\,(N_c \pm 3) & \text{if } N_c \text{ is odd (fermion).} \end{cases} \tag{4.171}$$

There are subsequently only two cases in which the skyrmion can be electrically neutral: $N_c = 0$, for which the underlying theory is not strongly-coupled, and $N_c = 3$, as in QCD.

The skyrmion electric charge may also be understood in terms of the technifermions of the strongly-coupled theory. The form of the generator of electromagnetism (4.163) indicates that the technifermions have electric charges $\frac{2}{3}$ and $-\frac{1}{3}$. The skyrmion appears then as a bound state of N_c technifermions. Either left-handed, right-handed, or both left- and right-handed technifermions form doublets of $SU(2)_W$, and the lightest skyrmion state is then made of $N_c/2$ "up-type" fermions and $N_c/2$ "down-type" ones if N_c is even, yielding the overall electric charge $q = N_c/6$. If N_c is odd, the two lightest states are made respectively of $(N_c \pm 1)/2$ "up-type" and $(N_c \mp 1)/2$ "down-type" technifermions, hence the result obtained in eq. (4.171).

4.4.3 A next-to-minimal model

There is of course a simple possibility to relax the strong constraint (4.171) on the electric charge by enlarging the model to a global $SU(N)_L \times SU(N)_R$ symmetry with $N \geq 4$. Keeping the $SU(2)_W$ subgroup to live in the upper-left corner, we can now take the hypercharge generator to be of the more general form

$$Y = \begin{pmatrix} \mu & & & \\ & \mu & & \\ & & \mu - \frac{1}{2} & \\ & & & \ddots \end{pmatrix}, \tag{4.172}$$

where factors denoted by the dots have to be chosen so that Y remains traceless. This is the most general choice that produces a doublet with the correct hypercharge to play the role of a Higgs boson. A similar form

can also be obtained within the simplest $N = 3$ model if one allows the hypercharge generator not to be traceless. This happens quite generically when the $U(1)_Y$ gauge group contains a part coming from the unbroken $U(1)_V$ symmetry. In both cases, all the analysis made above remains valid, up to the skyrmion hypercharge, which gets replaced by

$$Y_{\text{skyrmion}} = \mu\, N_c. \tag{4.173}$$

In terms of the electric charge, this means

$$q = \begin{cases} \mu\, N_c & \text{if } N_c \text{ is even (boson),} \\ \\ \mu\, N_c \pm \frac{1}{2} & \text{if } N_c \text{ is odd (fermion).} \end{cases} \tag{4.174}$$

If N_c is even, the hypercharge of the skyrmion — or equivalently its electric charge — can always be made zero by choosing $\mu = 0$. The generator of electromagnetism is then

$$Q = \begin{pmatrix} \frac{1}{2} & & & \\ & -\frac{1}{2} & & \\ & & -\frac{1}{2} & \\ & & & \ddots \end{pmatrix}, \tag{4.175}$$

which reflects the electric charge of the technifermions. If N_c is odd, a neutral skyrmion is achieved by taking $\mu = \pm 1/(2N_c)$. There must thus be a weak doublet with charges $(1 + N_c)/(2N_c)$ and $(1 - N_c)/(2N_c)$ (or opposite) among the technifermions of the underlying theory. In both cases, we see that the electric charges of the strongly-interacting technifermions have to be fractional in order to account for a neutral state among the lightest skyrmions.

4.4.4 Other realisations of a composite Higgs

There are many possible symmetry breaking patterns which enter the construction of a composite Higgs model. Some of them were presented in table 3.2 or consists in products of simple groups, and the most used ones will be now discussed separately. The presence of skyrmions depends on the third homotopy group of the vacuum manifold G/H. Note that in all examples presented here, the fourth homotopy group of the coset space is trivial, implying that the spin statistics of the skyrmion is entirely determined by the coefficient of the Wess-Zumino-Witten term, as for the model discussed above.

SU(N)×SU(N)/SU(N)

This is the symmetry breaking pattern of the chiral theory of mesons in QCD, which was used to construct the original technicolor models [85, 86], as well as the "minimal moose" class of little Higgs models [219]. In the latter, many copies of the global symmetry need to be implemented, and there might also be many independent skyrmions, living in different sectors of the model. Their characteristic features follow directly from the toy model presented in section 4.4.1.

SO(N)×SO(N)/SO(N)

The $SO(N) \times SO(N)/SO(N)$ symmetry breaking pattern is similar to the precedent, with the field $\Phi(x)$ being represented by a real-valued matrix in $SO(N)$. The representation of the $SU(2)_W$ gauge group has to be real and the Higgs field is not represented by a complex doublet, but rather by a real quadruplet. Little Higgs models based on this symmetry breaking pattern have the advantage of preserving a $SO(4)$ symmetry in the Goldstone sector, which acts as a custodial symmetry for the Higgs boson [231, 220]. Note that the simplest real representation of $SU(2)$ based on the generators of $SO(3)$ does not allow the existence of such a quadruplet. We can take without loss of generality the gauge generators to be in the four-dimensional representation

$$Q^1 = \frac{1}{2}\begin{pmatrix} & & i & \\ & i & & \\ & -i & & \\ -i & & & \\ & & & \ddots \end{pmatrix}, \qquad Q^2 = \frac{1}{2}\begin{pmatrix} & -i & & \\ i & & & \\ & & -i & \\ & & i & \\ & & & \ddots \end{pmatrix},$$

$$Q^3 = \frac{1}{2}\begin{pmatrix} & i & & \\ & & -i & \\ -i & & & \\ & i & & \\ & & & \ddots \end{pmatrix}. \tag{4.176}$$

The construction of the lightest skyrmion follows similar principles as in the previous section, with a hedgehog ansatz living within the $SU(2)_W$ subgroup, i.e. choosing $T^a = Q^a$. The generators above obey the normalisation $\mathrm{Tr}\left(Q^a Q^b\right) = \delta_{ab}$, which is twice the value required in (4.18) to construct a skyrmion of unit winding number, but on the other hand the topological

index in $SO(N)$ is defined as half the winding number integral (4.4), so that the skyrmion can indeed be built out of gauge generators as in the toy model. This peculiar normalisation is irrelevant to the computation of the skyrmion's quantum numbers. The fundamental difference with respect to the toy model of section 4.4.1 is that the Wess-Zumino-Witten term vanishes when the field $\Phi(x)$ takes its values in $SO(N)$ as a consequence of the fact that the underlying theory is free of anomalies. Since there is no term in the action contributing a negative sign upon spatial rotation of the skyrmion, it must necessarily be quantised as a boson. Its hypercharge also vanishes independently of the implementation of the hypercharge generator and the skyrmion is automatically neutral, i.e.

$$q = 0. \tag{4.177}$$

SU(N)/SO(N)

The symmetry breaking pattern $SU(N) \to SO(N)$ is realised with $N = 5$ in the "littlest Higgs" model [216]. The field Φ has to be taken in the two-indices symmetric representation of $SU(N)$, i.e. transforming as

$$\Phi \to U\Phi U^T, \qquad U \in SU(5), \tag{4.178}$$

and a vacuum expectation value proportional to the identity breaks the global symmetry down to $SO(N)$. In this representation the definition of the covariant derivative must also be changed to

$$D_\mu\Phi = \partial_\mu\Phi - igA_\mu \left(Q\,\Phi + \Phi\,Q^T\right), \tag{4.179}$$

where A_μ denotes generically any gauge field. Such a symmetry breaking pattern can be achieved by considering technifermions transforming in the fundamental representation of $SU(N)$. The mechanism guaranteeing the quantum stability of the skyrmion in $SU(N)/SO(N)$ cosets is also completely different from the previous two cases, since there is no equivalent of a topological charge here [296, 297, 298, 299].

The generators of the weak gauge group can be taken as in (4.176) as a subgroup of $SO(4)$, but there is a unique implementation of the hypercharge — up to global transformations — yielding a quadruplet of $SO(4)$ which can be identified with the Higgs, namely

$$Y = \frac{1}{2}\begin{pmatrix} & & i & \\ & & & i \\ -i & & & \\ & -i & & \\ & & & \ddots \end{pmatrix}. \tag{4.180}$$

The Higgs appears then in the Goldstone field as

$$\Pi = \begin{pmatrix} & & h & \\ & & -i\,h & \\ h^\dagger & i\,h^\dagger & & \\ & & & \ddots \end{pmatrix}, \tag{4.181}$$

where h is the complex doublet defined in eq. (4.162).

The major difference with respect to our $SU(3)$-based example hides in the way the classical skyrmion solution is constructed. The embedding of the $SU(2)_W$ gauge generators in the unbroken $SO(N)$ subgroup of $SU(N)$ implies already that the skyrmion cannot be aligned with the gauge subgroup: due to the normalisation $\mathrm{Tr}\left(Q^a Q^b\right) = \delta^{ab}$, the topological index of a hedgehog configuration built out of the generators Q^a — now measured again in $SU(N)$ by the winding number integral (4.4) — is always a multiple of two, and the configuration is therefore topologically trivial due to the $\mathbb{Z}_2$ homotopy structure of the vacuum manifold. As shown in section 4.3, a skyrmion of unit winding number is actually obtained by the Cartan embedding of a $SU(N)$ hedgehog Φ_h,

$$\Phi = \Phi_h \Phi_h^T, \qquad \text{where} \quad \Phi_h = \exp\left[2i\,F(r)\,\hat{x}_i\,T^i\right], \tag{4.182}$$

with a special choice of generators allowing to preserve the spherical symmetry

$$T^a = \frac{1}{4}\begin{pmatrix} \sigma^a & i\sigma^a & & \\ -i\sigma^a & \sigma^a & & \\ & & & \ddots \end{pmatrix}. \tag{4.183}$$

Note that these generators have the property that they commute with their transpose, i.e. $\left[T^a, (T^b)^T\right] = 0$, and are related to the $SU(2)_W$ gauge generators through

$$Q^a = T^a - (T^a)^T. \tag{4.184}$$

The skyrmion field Φ constructed using the Cartan embedding (4.182) lives actually in the broken subgroup of $SU(N)$. In the presence of the standard electroweak gauge field, the skyrmion configuration minimising the energy is obtained using the Skyrme-Wu-Yang ansatz (4.119) for the gauge field, although the misalignment of the generators implies that the energy functional takes a form different from our toy model (4.120). In the littlest Higgs model, however, the presence of an extra $SU(2)$ gauge group living in the broken part of the global $SU(N)$ symmetry affects the properties of the classical skyrmion solution. We present in the next section an explicit

construction of the lowest-energy skyrmion configuration within this particular model. The lightest skyrmion configuration is found to be a spherically symmetric configuration in which the electroweak gauge field vanishes. In general, the presence or absence of this extra spontaneously broken gauge field does not modify the way the skyrmion is embedded into $SU(N)$, so that the charge under the electroweak gauge group can be derived independently of the details of the model considered. The quantisation procedure follows a path similar to the discussion above. The relevant zero-modes in this case are spatial rotations only, which do not coincide with isospin transformations. The Hamiltonian and energy levels of the theory appear as in eq. (4.40) and (4.41) respectively, with the slight difference that both the energy E_0 and kinetic momentum Λ differ from the purely $SU(N)$ skyrmion. While j and m still correspond to the spin quantum numbers, taking (half-)integer values when the skyrmion is a boson (fermion), the isospin gets actually multiplied by a factor of two compared to eq. (4.43), so that the relation between spin and isospin becomes

$$I_k = -2\Omega_{kl} J_l, \qquad \text{hence} \quad I^2 = 4J^2. \tag{4.185}$$

The third component of isospin of the skyrmion state is then given by $2m'$, where m' takes integer steps from $-j$ to $+j$. The lightest skyrmion state has thus zero isospin as before if it is a boson. If it is quantised as a fermion, the skyrmion has however an isospin number $I_3 = \pm 1$ and its electric charge is equal to its hypercharge plus or minus one unit. The hypercharge itself is uniquely fixed: it is computed similarly as above using the Noether currents associated with the $U(1)_Y$ transformation. Due to the commutation relations $[Y, T^a] = \left[Y, (T^a)^T\right] = 0$, the skyrmion is again invariant under hypercharge transformations, and none of the local terms in the Lagrangian contribute to the Noether current. Still, the five-dimensional part of the Wess-Zumino-Witten term gives the usual non-zero contribution, fixing

$$Y_{\text{skyrmion}} = \pm N_c. \tag{4.186}$$

The plus or minus sign here refers to the fact that there are two distinct possibilities to construct the skyrmion field, namely using either the generators T^a as above or the transpose thereof, $(T^a)^T$, or equivalently choosing the $SU(N)$ hedgehog configuration Φ_h in eq. (4.182) to have plus or minus one unit of winding number. Note that apart from their hypercharge, both field configurations are absolutely identical at the classical level. The skyrmion charge associated with the solution of hypercharge $+N_c$ is then

$$q = \begin{cases} N_c & \text{if } N_c \text{ is even (boson),} \\ \\ N_c \pm 1 & \text{if } N_c \text{ is odd (fermion).} \end{cases} \tag{4.187}$$

As a direct consequence, there are only two possibilities to have a neutral skyrmion: the first consists in taking $N_c = 0$, i.e. considering a weakly-coupled UV completion and quantising the skyrmion as a boson, and the second to $N_c = 1$, which does not correspond to a satisfactory strongly-coupled UV completion either. Note that a weakly-coupled UV completion exists for the littlest Higgs [250], but the quantum nature of the skyrmion with both $N_c = 0, 1$ is still not understood at all. On the other hand, any strongly-coupled UV completion with $N_c \geq 2$ possesses a charged skyrmion in its spectrum.

The integer value of the charge can be found surprising at first. However, it can be understood in terms of the (techni-)fermions of a strongly-coupled underlying theory. To see this, it is convenient to rotate the vacuum expectation value $\langle \Phi \rangle = \mathbb{1}$ into a basis where the generators Q^3 and Y are diagonal. This can be done as in the original little Higgs model of ref. [216], where we have

$$\left.\begin{aligned} Q^3 &= \mathrm{diag}\left(\tfrac{1}{2}, -\tfrac{1}{2}, \tfrac{1}{2}, -\tfrac{1}{2}, 0, \ldots\right) \\ Y &= \mathrm{diag}\left(-\tfrac{1}{2}, -\tfrac{1}{2}, \tfrac{1}{2}, \tfrac{1}{2}, 0, \ldots\right) \end{aligned}\right\} \Longrightarrow \quad Q_{em} = \mathrm{diag}\left(0, -1, 1, 0, \ldots\right). \tag{4.188}$$

The (techni-)fermions have therefore all integer electric charge in this model, which is consistent with the integer charge of the skyrmion. Note that in contrary to the previous cases, the skyrmion in the $SU(N)/SO(N)$ coset is not made of an antisymmetric bound state of N_c technifermions, but appears as a bound state of $N_c\left(N_c+1\right)/2$ of them [296,297,298,299]. A skyrmion of charge N_c can for example be constructed with N_c positively charged technifermions and $N_c\left(N_c-1\right)/2$ neutral ones, although other combinations are possible. The quantum nature of the skyrmion in this case remains to be elucidated.

Cosets with trivial homotopy

The remaining symmetry patterns presented in table 4.2 all have a trivial third homotopy group, and therefore do not contain skyrmions and are not concerned by our study. The simplest little Higgs model [217] and its variations [218,221], based on the coset $SU(N)/SU(N-1)$, are examples of models free of skyrmions. The field Φ is taken there to be a N-component vector of unit length, transforming under $SU(N)$ and spontaneously breaking the symmetry by choosing any definite value in the vacuum. The same concept applies when the field Φ is real-valued, hence providing a $SO(N)/SO(N-1)$ vacuum manifold, as in the minimal composite Higgs model [131] discussed in section 3.3 and its extension [124], with $N = 5$ and 6 respectively. The last coset mentioned in the table, namely $SU(2N)/Sp(2N)$, is realised in

the "antisymmetric condensate" little Higgs [224]. Note that the list given by tables 4.1 and 4.2 is not exhaustive. Other cosets may be considered, in particular when H is not a simple group.

Our findings about the skyrmions in composite Higgs models can finally be summarised into three main points:

(i) Skyrmions can generally use gauge fields to reduce their mass. The lightest field configuration of unit winding number is obtained at the classical level by combining the Goldstone fields with a $SU(2)$ gauge field, independently of the coefficients of the higher-order terms in the sigma-model. This configuration also preserves generically the spherical symmetry of the ungauged skyrmion. Notice that this statement is universal, and that it does not matter if the $SU(2)$ subgroup is fundamental to the theory, or if it arises as the unbroken remnant of a larger gauge group.

(ii) In the real world, there is no such exact $SU(2)$ symmetry, since the electroweak gauge group is broken down to $U(1)_{em}$. However, at the scale 10–100 TeV where the skyrmion lives, the $SU(2)_W \times U(1)_Y$ gauge symmetry is approximately preserved, up to corrections of order v^4/f^4, where f is the TeV-order symmetry breaking scale. As a consequence, the skyrmion in composite Higgs models prefers to live in a subspace of the global symmetry where it can use this $SU(2)_W$ symmetry.

(iii) The isospin of the skyrmion depends on its fermionic/bosonic nature, which is fixed via the Wess-Zumino-Witten term by the number of colours of the underlying strongly-coupled theory (if any). It is also the non-local part of this Wess-Zumino-Witten term which contributes to the hypercharge of the skyrmion, so that the electric charge of the lightest state(s) is completely fixed by the embedding of the hypercharge generator relatively to the $SU(2)_W$ subgroup.

Of the various cosets obtained from product groups or simple groups listed in table 4.2, we found that two of them contain in general electrically charged skyrmions. Unfortunately, these two are also the most used symmetry breaking patterns. In the various littlest Higgs models, where the vacuum manifold is $SU(5)/SO(5)$, the skyrmion takes an integer electric charge, necessarily different from zero for $N_c \geq 2$. For $SU(N) \times SU(N)/SU(N)$ cosets which mimic the chiral theory of QCD, neutral skyrmions can be obtained, provided certain rules are respected concerning the embedding of the hypercharge in the global symmetry group. In terms of degrees of freedom of the underlying theory, a neutral skyrmion requires that the technifermions have fractional electric charges. As a general result, weakly coupled UV completions may always admit neutral skyrmions, since non-zero charges are induced via the anomalous Wess-Zumino-Witten term present

in strongly-coupled theories only; in that case however it is not clear what the skyrmion really represents at the quantum level of the theory. Also if the underlying theory is strongly-coupled but still anomaly free, as for the $SO(N) \times SO(N)/SO(N)$ cosets realised in models with a custodial symmetry, the skyrmion has to be quantised as a boson and is automatically neutral. Other models based on the remaining symmetry breaking patterns don't contain skyrmions at all.

An estimate of the relic density for a neutral skyrmion will be discussed in the next section. The key point of this discussion is that skyrmion are always expected to be thermally produced in the early universe, while their pair-annihilation cross-section is naturally very low — scaling with the inverse of the symmetry breaking scale f — which ensure relatively large relic densities. This relic density at present time can be of the order of the observed dark matter density, although much smaller or larger densities can also be obtained depending on the exact value of the skyrmion mass. The latter cannot be computed without knowing the full underlying theory.

In the presence of an electrically charged skyrmion, the situation is very different. Due to electromagnetic interactions, the skyrmion can form bound states with ordinary matter. If the skyrmion charge is an integer, neutral bound states are formed and can be very difficult to detect. The strongest experimental bounds come from the concentration of such superheavy "atoms" on earth, as studied for example in ref. [304, 305]. Although the relevant properties of these skyrmions are simply their mass and electric charge, it is not straightforward to extract experimental bounds on these parameters, due to the fact that the whole early universe cosmology would be affected by the presence of new stable charged objects (see for example the effects of a stable particle of charge -2 in ref. [306]). Note also that the skyrmions described in this work always come in pairs with an antiskyrmion of opposite charge: in the scenario where the topological index takes any integer value, the antiskyrmion is a field configuration with opposite winding number; for $SU(N)/SO(N)$ with $\pi_3 = \mathbb{Z}_2$, the partner of the skyrmion comes actually from a different embedding into the coset. In any case, if no asymmetry is generated, the relic density of skyrmions might be largely reduced compared to a naive estimate.

In contrast to little Higgs models, the minimal composite Higgs models have a very simple group structure and do not admit skyrmions. One crucial difference with respect to little Higgs models is that the technifermions have to share the same quantum number as the Standard Model quarks and leptons so that they can generate masses with the latter via the partial compositeness mechanism. Neutral skyrmions could subsequently be easier to obtain in composite Higgs models, and would appear as heavy objects bounded by strong interactions in a similar fashion as the proton in QCD.

Our analysis also contains a few caveats, since the description of non-perturbative objects such as skyrmions in quantum field theories is not well

understood yet. The conclusions of this work might be relaxed under special conditions. First of all, we actually only understand the quantum nature of the skyrmion in the background of a strongly-coupled underlying theory. In the cases $N_c = 0$ or $N_c = 1$ discussed above, the role of the skyrmion in the spectrum of the quantum theory is not known: the skyrmion might actually be unstable despite its topological nature, or might even not correspond to a particle state. The second unknown concerns the regime in which the level splitting between the various skyrmion states is very small. Quantum corrections to the skyrmion masses could possibly reverse the hierarchy of the states, making practically impossible any predictions in terms of the low-energy effective theory. Loop corrections to the skyrmion mass in the chiral theory of QCD happen indeed to be important [268], but one can expect them to act in an universal way on all states so that such a hierarchy-reversing phenomenon is rather unlikely to occur.

Note finally that for composite models based on the holographic principle, where an extra-dimensional description of the strongly-coupled underlying theory exists, the properties of the skyrmion might be better understood by directly computing them within the five-dimensional framework, as discussed in section 4.2.6. This subject remains open for future analysis.

4.5 The skyrmion in the littlest Higgs model

As a final part of this thesis, we present here the study of skyrmion in a particular realisation of the little Higgs idea. The special form of the topological index and the presence of additional gauge fields in the model studied here make this study of particular interest.

4.5.1 The littlest Higgs

We consider the littlest Higgs model of ref. [216]. The model is based on a global $SU(5)$ symmetry, spontaneously broken down to $SO(5)$ by a vacuum expectation value. The Goldstone bosons are therefore described by a $SU(5)/SO(5)$ non-linear sigma model

$$\mathcal{L}_\Sigma = \frac{f^2}{4} \operatorname{Tr} \partial_\mu \Sigma \partial^\mu \Sigma^\dagger, \tag{4.189}$$

where $\Sigma(x)$ is a 5×5 symmetric matrix. Under a global $SU(5)$ transformation, Σ transforms as

$$\Sigma \to V \Sigma V^T, \qquad V \in SU(5). \tag{4.190}$$

The vacuum expectation value is taken to be the identity matrix, $\langle \Sigma \rangle = \mathbb{1}_5$, so that the 10 unbroken generators obey $(T^a)^T = -T^a$, and the 14 broken

ones $(X^a)^T = X^a$. The Goldstone bosons π^a can therefore be parametrised as

$$\Sigma = (e^{i\pi^a X^a/f})\,\mathbb{1}\,(e^{i\pi^a X^a/f})^T = e^{2i\pi^a X^a/f}. \tag{4.191}$$

The global $SU(5)$ symmetry is then explicitly broken by gauging an $[SU(2)\times U(1)]^2$ subgroup. The generators of this gauge group are chosen as[11]

$$Q_i^{(1)} = \frac{1}{4}\begin{pmatrix} \sigma_i & 0 & i\sigma_i \\ 0 & 0 & 0 \\ -i\sigma_i & 0 & \sigma_i \end{pmatrix}, \qquad Q_i^{(2)} = -Q_i^{(1)T}, \tag{4.192}$$

$$Y^{(1)} = \frac{1}{20}\begin{pmatrix} \mathbb{1}_2 & 0 & 5i\mathbb{1}_2 \\ 0 & -4 & 0 \\ -5i\mathbb{1}_2 & 0 & \mathbb{1}_2 \end{pmatrix}, \qquad Y^{(2)} = -Y^{(1)T}, \tag{4.193}$$

and they obey

$$[Q_i^{(\alpha)}, Q_j^{(\beta)}] = i\delta^{\alpha\beta}\varepsilon_{ijk}Q_k^{(\alpha)}, \qquad [Q_i^{(\alpha)}, Y^{(\beta)}] = [Y^{(\alpha)}, Y^{(\beta)}] = 0. \tag{4.194}$$

The commutation relations of the $SU(2)$ and $U(1)$ subgroups is easier to see in the original parametrisation of ref. [216], in which the vacuum expectation value $\langle\Sigma\rangle$ is not diagonal. In our case however, it will be more convenient to work in a basis where $\langle\Sigma\rangle = \mathbb{1}_5$. The Lagrangian is made gauge invariant by promoting the spacetime derivatives to covariant derivatives:

$$D_\mu\Sigma = \partial_\mu\Sigma - i\left(A_\mu\Sigma + \Sigma A_\mu^T\right), \tag{4.195}$$

where

$$A_\mu = \sum_{\alpha=1,2}\left(g_\alpha W_\mu^{(\alpha),a}Q_a^{(\alpha)} + g'_\alpha B_\mu^{(\alpha)}Y^{(\alpha)}\right). \tag{4.196}$$

Only the linear combinations $Q_a = Q_a^{(1)} + Q_a^{(2)}$, $Y = Y^{(1)} + Y^{(2)}$ of the gauge generators are symmetric and thus preserve the vacuum. The orthogonal combinations $\overline{Q}_a = Q_a^{(1)} - Q_a^{(2)}$, $\overline{Y} = Y^{(1)} - Y^{(2)}$ do not. The

[11] With respect to the generators as defined in ref. [216], our generators are rotated according to the rule $Q_i^{(\alpha)} \to \Omega Q_i^{(\alpha)}\Omega^\dagger$ (and similarly for the $Y^{(\alpha)}$, where our definition differs by an additional overall minus sign). Here, Ω is a $SU(5)$ matrix taking the vacuum expectation value Σ_0 of ref. [216] to the identity, $\Sigma_0 \to \Omega\Sigma_0\Omega^T = \mathbb{1}_5$, and is defined as

$$\Omega = \frac{1}{\sqrt{2}}\begin{pmatrix} \mathbb{1}_2 & 0 & \mathbb{1}_2 \\ 0 & -\sqrt{2} & 0 \\ -i\mathbb{1}_2 & 0 & i\mathbb{1}_2 \end{pmatrix}.$$

$[SU(2) \times U(1)]^2$ gauge group is therefore spontaneously broken down to a diagonal $SU(2) \times U(1)$ subgroup. The latter is identified with the Standard Model electroweak gauge group.

To simplify the structure of the gauge sector of the model we work in the T-parity symmetric limit [233] which is obtained by setting $g_1 = g_2 = \sqrt{2}g$ and $g_1' = g_2' = \sqrt{2}g'$. This also allows us to consider values of the breaking scale $f \lesssim 1$ TeV. The Standard Model gauge bosons are identified with the parity even linear combinations

$$W_\mu^a = \frac{1}{\sqrt{2}}\left(W_\mu^{(1),a} + W_\mu^{(2),a}\right), \qquad B_\mu = \frac{1}{\sqrt{2}}\left(B_\mu^{(1)} + B_\mu^{(2)}\right). \tag{4.197}$$

The parity odd linear combinations

$$\overline{W}_\mu^a = \frac{1}{\sqrt{2}}\left(W_\mu^{(1),a} - W_\mu^{(2),a}\right), \qquad \overline{B}_\mu = \frac{1}{\sqrt{2}}\left(B_\mu^{(1)} - B_\mu^{(2)}\right). \tag{4.198}$$

are responsible for cutting off the quadratically divergent contribution to the Higgs mass in the gauge sector. They obtain tree-level masses

$$m_{\overline{W}}^2 = 2g^2 f^2, \qquad\qquad m_{\overline{B}}^2 = \frac{2}{5}g'^2 f^2. \tag{4.199}$$

The 14 Goldstone bosons can be parametrised as $\Sigma = e^{2i\Pi/f}$. They decompose under the electroweak gauge group as $\mathbf{1}_0 \oplus \mathbf{3}_0 \oplus \mathbf{2}_{\pm 1/2} \oplus \mathbf{3}_{\pm 1}$. Explicitly, we have

$$\Pi = \frac{1}{2\sqrt{2}} \begin{pmatrix} -i\phi - \omega - \frac{1}{2\sqrt{5}}\eta & -h & -\phi - i\omega \\ -h^T & \frac{2}{\sqrt{5}}\eta & ih^T \\ -\phi + i\omega & ih & i\phi - \omega - \frac{1}{2\sqrt{5}}\eta \end{pmatrix} + \text{c.c.}, \tag{4.200}$$

$$h = \begin{pmatrix} h^+ \\ h^0 \end{pmatrix}, \quad \phi = \begin{pmatrix} \phi^{++} & \frac{1}{\sqrt{2}}\phi^+ \\ \frac{1}{\sqrt{2}}\phi^+ & \phi^0 \end{pmatrix}, \quad \omega = \begin{pmatrix} \frac{1}{2}\omega^0 & \frac{1}{\sqrt{2}}\omega^+ \\ \frac{1}{\sqrt{2}}\omega^- & -\frac{1}{2}\omega^0 \end{pmatrix}.$$

The real triplet ω and the singlet η are eaten by the Higgsing of the broken $SU(2) \times U(1)$. The complex doublet h is identified with the standard Higgs boson, while the complex triplet ϕ is a new field of the model, which receives a large $\mathcal{O}(gf)$ mass at the one loop level. The degeneracy between the triplet states is lifted after electroweak symmetry breaking by a vacuum expectation value for the Higgs doublet $\langle h \rangle = (0, v/\sqrt{2})^T$, also giving the Standard Model $W^\pm$ and Z bosons their mass. More details can be found in ref. [239].

We are interested in finding skyrmions as solutions of the classical equations of motion for the field Σ with nontrivial topological charge. As mentioned above, there is no universal quantity describing the winding number

of a field configuration in the coset $SU(N)/SO(N)$ similar to the winding number integral (4.4) for the group $SU(N)$. We can nevertheless construct a field with non-trivial topology by using the Cartan embedding $\Sigma(x) = \Phi(x)\Phi(x)^T$, based on a field $\Phi(x) \in SU(5)$ with winding number one. The winding number of the field $\Sigma(x)$ is then assessed by the quantity

$$B(\Sigma) = B(\Phi) \text{ mod } 2. \tag{4.201}$$

The stability of the skyrmion in the presence of gauge fields is however not guaranteed, since the expression above is not invariant under the local $[SU(2) \times U(1)]^2$ gauge symmetry of the littlest Higgs model. Compared to our construction of a gauge-invariant topological charge of section 4.2.2, an additional complication arises because the representation of Σ in terms of Φ is not unique. In particular, the matrix ΦR where R belongs to $SO(5)$ yields the same Σ. So the topological charge $B(\Sigma)$ in the coset has to be an integral containing Φ, A_μ and derivatives thereof, and must satisfy the following conditions:

(i) invariance under the global $SU(5)$ symmetry $\Phi \to L\Phi$, such that $\Sigma \to L\Sigma L^T$ transforms as required,

(ii) invariance under gauge transformations

$$\Phi \to V(x)\Phi\,, \qquad A_\mu \to V(x)A_\mu V^\dagger(x) + \frac{i}{g}V(x)\partial_\mu V^\dagger(x)\,,$$

where $V(x)$ belongs to the $[SU(2) \times U(1)]^2$ gauge group,

(iii) invariance under a local $SO(5)$ symmetry $\Phi \to \Phi R(x)$, with $R(x)R^T(x) = \mathbb{1}$,

(iv) in the limit of vanishing gauge fields, one recovers the winding number (4.4),

(v) time-conservation $\partial_0 B = 0$.

With the exception of point (iii), all properties above are recovered by using the gauge-invariant definition of the topological charge $\overline{B}(\Phi)$ of eq. (4.87), identifying the gauge fields of the littlest Higgs model as a subgroup of the matrix L_μ used in eq. (4.87). Due to the additivity of the topological charge and to the property that $SO(N)$ fields have an even integer topological index in $SU(N)$, the condition (iii) is actually automatically satisfied by the definition (4.201): under a local $SO(5)$ transformation $\Phi \to \Phi R(x)$, one finds then

$$\overline{B}(\Sigma) \to \overline{B}(\Phi R) \text{ mod } 2 = \left[\overline{B}(\Phi) + B(R)\right] \text{ mod } 2 = \overline{B}(\Sigma) \tag{4.202}$$

As in the discussion of section (4.2.2), this quantity is actually not conserved in time but might be shifted by integer values corresponding to instantons.

The two $U(1)$ gauge fields do not have such instantons, but the $SU(2)$ fields do. One finds in particular

$$\overline{B}(\Phi) = B(\Phi) - n(W_\mu^{(1)}) - n(W_\mu^{(2)}). \tag{4.203}$$

A consequence of this is that the skyrmion is not stable but may decay through an electroweak instanton. However, as illustrated by its lifetime (4.96), the skyrmion can be considered stable on cosmological timescales, and thus if its mass and couplings are appropriated, it can serve as a potential dark matter candidate.

In order to stabilise the energy and size of the skyrmion obtained in this way, one need to complete the Lagrangian with terms with higher number of derivatives. We consider here only the simplest case, adding the Skyrme term

$$\mathcal{L} \supset \frac{1}{32e^2} \operatorname{Tr}\left[\Sigma^\dagger D_\mu \Sigma, \Sigma^\dagger D_\nu \Sigma\right]\left[\Sigma^\dagger D^\mu \Sigma, \Sigma^\dagger D^\nu \Sigma\right]. \tag{4.204}$$

The Skyrme term does not modify the mass of the gauge bosons at tree-level, but it induces new couplings between gauge and Goldstone bosons. The gauge-boson four vertices are of particular interest since they might contribute at one loop to the electroweak precision measurements. In practice, the contributions to the Peskin-Takeuchi S and T parameter [99, 103] are suppressed by the loop factor and by powers of $(v/f)^2$ and are thus negligible as long as $(1/e^2) \lesssim 32$. The other important place where the Skyrme term might play a role is in the potential for the scalars. Since the Skyrme term involves four derivatives, these contributions only start at the two loop level. The protection of the Higgs mass through the collective symmetry breaking mechanism is therefore not affected by the addition of the Skyrme term.

The spherically symmetric solution for a skyrmion in the coset $SU(5)/SO(5)$ was presented in section 4.3 in the absence of gauge fields. It relies on the existence of a $SU(2)$ subgroup of $SU(5)$ whose generators are satisfy the property that they commute with their transpose. This is the case of the $SU(2)$ gauge generators $Q_i^{(1,2)}$ defined above in eq. (4.192): they are related through $Q_i^{(1)T} = -Q_i^{(2)}$, and satisfy $[Q_i^{(1)}, Q_j^{(2)}] = 0$ and $\operatorname{Tr} Q_i^{(1)} Q_j^{(2)} = 0$. The ansatz

$$\Phi(x) = \exp\left[2iF(r)\hat{x}_i Q_i^{(1)}\right] \tag{4.205}$$

realises therefore the lightest skyrmion configuration. Note that taking $Q_i^{(2)}$ for the generators yields exactly the same results. The Lagrangian obtained with this ansatz is exactly twice the Lagrangian one would obtain starting from a sigma model with the $SU(5)$-valued field $\Phi(x)$ instead of $\Sigma(x)$. Therefore, the mass of the $SU(5)/SO(5)$ coset skyrmion is twice the mass of a corresponding $SU(5)$ skyrmion of winding number one. In terms of the

profile function $F(r)$, the energy $E = -\int d^3x\ \mathcal{L}$ of this static field configuration becomes

$$E[F] = 4\pi \frac{f}{e} \int_0^\infty d\widetilde{r} \left[\left(\widetilde{r}^2 + 2\sin^2 F\right) F'^2 + \left(2\widetilde{r}^2 + \sin^2 F\right) \frac{\sin^2 F}{\widetilde{r}^2} \right], \quad (4.206)$$

where we have performed the rescaling $r = \widetilde{r}/(fe)$. The profile function F solving the Euler-Lagrange equation (4.26) was shown on fig. 4.1, and the corresponding energy density in fig. 4.2. The mass of the ungauged skyrmion was found to be

$$M_0 = 145.8\ \frac{f}{e}, \quad (4.207)$$

The scaling of the skyrmion mass with the coefficient of the Skyrme term is particularly interesting. There is actually no upper bound on the constant e from phenomenological arguments, so the mass of the skyrmion is, in principle, a free parameter of the theory. It would require knowledge of the UV completion of the littlest Higgs model to obtain an estimate of its value. Assuming a QCD like UV completion it might be reasonable to use $e \sim 5$, which is obtained from a fit to nucleon properties, as seen in section 4.1.4. With a symmetry breaking scale f around 1 TeV, this gives a mass of the order of 30 TeV for the skyrmion. Naive dimensional analysis (NDA) gives a pre-factor of $c_S/(4\pi)^2$ for the Skyrme term, where c_S is a coefficient of order one. This also seems to motivate $1 \lesssim e \lesssim 10$. We will see in the next section that the inclusion of gauge interactions modifies the dependence of the skyrmion mass on the parameter e.

4.5.2 Skyrmion solution with gauge fields

Turning on the gauge fields can only reduce the mass of the skyrmion. We are actually looking for field configurations which have $B(\Phi) = 1$ and are topologically equivalent to a configuration with zero gauge fields, so that they satisfy $n(W_\mu^{(1)}) = n(W_\mu^{(2)}) = 0$. This choice will ensure a non-trivial topological charge for the field $\Sigma(x)$. Such a configuration can be gauge-equivalent to another configuration with $B(\Phi) = 0$ and $n = 1$, but it would take a huge amount of time for the first configuration to evolve into the second, so that we can consider the first case to be quasi-stable.

The ansatz (4.205) used for the ungauged solution above spans only a 4×4 block of the whole $SU(5)$. While the embedding has no influence when the gauge fields are set to zero, it does have an importance for non-vanishing gauge fields. If the generators of the $SU(2)$ subgroup used in the ansatz (4.205) do not match the gauge generators (4.192), the spherical symmetry would be broken by the gauge fields. We therefore assume that the lowest energy configuration is indeed correctly described by the ansatz (4.205) made above. Since the $U(1)$ gauge generators $Y^{(1,2)}$ commute with the $SU(2)$ gauge generators, the contribution of the B_μ and $\overline{B}_\mu$

fields to the field energy is simply given by their mass term. In order to reach the lowest energy configuration, $\overline{B}_\mu$ has then to be zero everywhere, while B_μ being massless is free and does not contribute to the mass of the skyrmion. An ansatz for the fields W^a_μ and $\overline{W}^a_\mu$ preserving the spherical symmetry can be made by writing the most general tensor decomposition in terms of the angular variables $\hat{x}_i$:

$$\begin{aligned} W^a_i &= \frac{1}{gr}\left[(\delta_{ia} - \hat{x}_i\hat{x}_a)\, a_1(r) + \hat{x}_i\hat{x}_a a_2(r) + \varepsilon_{iak}\hat{x}_k a_3(r)\right], \\ \overline{W}^a_i &= \frac{1}{gr}\left[(\delta_{ia} - \hat{x}_i\hat{x}_a)\, b_1(r) + \hat{x}_i\hat{x}_a b_2(r) + \varepsilon_{iak}\hat{x}_k b_3(r)\right]. \end{aligned} \tag{4.208}$$

Note that the factor $1/gr$ is purely conventional, and that we work in the temporal gauge, so $W^a_0 = \overline{W}^a_0 = 0$. Plugging this ansatz into the Lagrangian, we obtain

$$\mathcal{L}_{\text{Skyrme}} = -\frac{1}{r^2}\left[f^2\,(2A+B) - \frac{1}{e^2}\frac{A}{r^2}\,(A+2B)\right], \tag{4.209}$$

where we have defined

$$A = \left[(1+a_3)\sin F - b_1\cos F\right]^2 + \left[a_1\sin F + b_3\cos F\right]^2, \tag{4.210}$$

$$B = \left[rF' - b_2\right]^2. \tag{4.211}$$

The spherical symmetry is here completely explicit, since the Lagrangian density depends only on r. The Lagrangian also contains the usual kinetic term for the gauge fields,

$$\mathcal{L}_{YM} = -\frac{1}{4}F^a_{ij}F^a_{ij} - \frac{1}{4}\overline{F}^a_{ij}\overline{F}^a_{ij} \tag{4.212}$$

where

$$F^a_{ij} = \partial_i W^a_j - \partial_j W^a_i + g\varepsilon^{abc}(W^b_i W^c_j + \overline{W}^b_i\overline{W}^c_j), \tag{4.213}$$

$$\overline{F}^a_{ij} = \partial_i \overline{W}^a_j - \partial_j \overline{W}^a_i + g\varepsilon^{abc}(W^b_i \overline{W}^c_j + \overline{W}^b_i W^c_j). \tag{4.214}$$

With our ansatz, this is

$$\begin{aligned} \mathcal{L}_{YM} = -\frac{1}{g^2r^4}\Big[&\left(ra_1' - a_2(1+a_3) - b_2b_3\right)^2 + \left(ra_3' + a_1a_2 + b_1b_2\right)^2 \\ &+ \left(rb_1' - b_2(1+a_3) - a_2b_3\right)^2 + \left(rb_3' + a_1b_2 + b_1a_2\right)^2 \\ &+ \frac{1}{2}\left(a_1^2 + (1+a_3)^2 + b_1^2 + b_3^2 - 1\right)^2 \\ &+ + 2\left(a_1b_1 + (1+a_3)b_3\right)^2\Big]. \end{aligned} \tag{4.215}$$

The lowest energy configuration is then obtained by solving the corresponding Euler-Lagrange equations. One should not forget however that the winding numbers n for the gauge fields as defined in eq. (4.90) have to remain zero. This translates into the following constraints on the profile functions:

$$\int_0^\infty dr \left[a_1 a_3' - a_1' a_3 + \frac{a_2}{r}\left(a_1^2 + (1+a_3)^2 + b_1^2 + b_3^2 - 1\right) \right. \tag{4.216}$$
$$\left. + b_1 b_3' - b_1' b_3 + 2\frac{b_2}{r}\left(a_1 b_1 + (1+a_3) b_3\right) \right] = 0,$$

$$\int_0^\infty dr \left[a_1 b_3' - a_1' b_3 + \frac{b_2}{r}\left(a_1^2 + (1+a_3)^2 + b_1^2 + b_3^2 - 1\right) \right. \tag{4.217}$$
$$\left. + b_1 a_3' - b_1' a_3 + 2\frac{a_2}{r}\left(a_1 b_1 + (1+a_3) b_3\right) \right] = 0.$$

The profile functions $a_i(r), b_i(r)$ are moreover constrained by the form of the ansatz (4.208). To obtain a finite energy solution, $a_i(r), b_i(r)$ must approach a constant value as $r \to \infty$. Definiteness at the origin furthermore implies $a_3(0) = 0$ and $a_1(0) = a_2(0)$, and similarly for the $b_i(r)$.

The Euler-Lagrange equations for a_1, a_2 and b_3 are satisfied by setting these three fields to zero. With this choice, the constraint (4.216) is automatically fulfilled. There is then a non-trivial solution with zero-energy corresponding to $a_3 = -(1+\cos F)$, $b_1 = -\sin F$ and $b_2 = rF'$, but this solution does not satisfy eq. (4.217), the left-hand side being non-zero. There are actually two obvious ways to satisfy the constraint (4.217):

(I) The first possibility it to set $a_3 = b_1 = 0$, and turn on only b_2. In this case the energy functional becomes

$$E_I[F, b_2] = 4\pi \frac{f}{e} \int_0^\infty d\widetilde{r} \left[\sin^2 F \left(2 + \frac{\sin^2 F}{\widetilde{r}^2} + \frac{2(\widetilde{r}F' - b_2)^2}{\widetilde{r}^2} \right) \right.$$
$$\left. + (\widetilde{r}F' - b_2)^2 + \frac{e^2}{g^2}\frac{b_2^2}{\widetilde{r}^2} \right], \tag{4.218}$$

where we have used again the rescaled variable $\widetilde{r} = (fe)r$. Since the energy functional does not depend on the derivative of b_2, the Euler-Lagrange equation for b_2 yields directly

$$b_2(r) = \widetilde{r}F' \left(1 - \frac{1}{1 + (g/e)^2(\widetilde{r}^2 + 2\sin^2 F)} \right). \tag{4.219}$$

b_2 automatically satisfies its boundary conditions. Substituting into

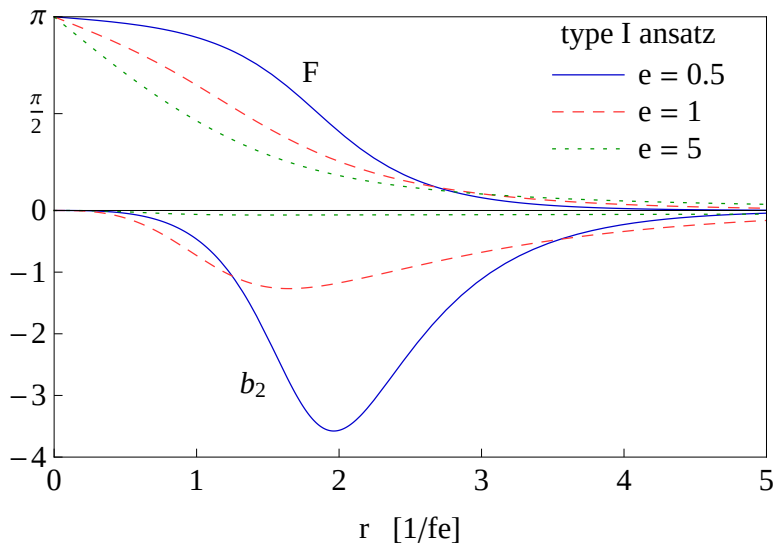

Figure 4.23: The profile functions $F(r)$, $b_2(r)$ and $a(r)$ for different values of the parameter e with the ansatz I.

eq. (4.218), we get

$$E_I[F] = 4\pi \frac{f}{e} \int_0^\infty d\widetilde{r} \left[\sin^2 F \left(2 + \frac{\sin^2 F}{\widetilde{r}^2} \right) + F'^2 \frac{(\widetilde{r}^2 + 2\sin^2 F)}{1 + (g/e)^2(\widetilde{r}^2 + 2\sin^2 F)} \right], \quad (4.220)$$

and the Euler-Lagrange equation for F becomes

$$\left(1 + (g/e)^2(\widetilde{r}^2 + 2\sin^2 F)\right)\left(\widetilde{r}^2 + 2\sin^2 F\right) F'' + 2\widetilde{r}F' + \sin 2F \left[F'^2 - \left(1 + (g/e)^2(\widetilde{r}^2 + 2\sin^2 F)\right)^2 \left(1 + \frac{\sin^2 F}{\widetilde{r}^2}\right) \right] = 0. \quad (4.221)$$

As one can see, the mass of the skyrmion scales with f and $1/e$, but depends also in a non-trivial way on the ratio g/e. The gauge coupling g is fixed by its Standard Model value. For the numerical studies we use $g = 0.653$.[12] The solution of the Euler-Lagrange equation for $F(r)$ with $F(0) = \pi$ and $F(r \to \infty) = 0$ is shown on Fig. 4.23 for different values of e. Notice in this case that at large values of r, F is now vanishing exponentially as $F(r) \propto \exp(-\sqrt{2}fgr)$, in strong contrast with the ungauged solution where F decreases as $1/r^2$.

[12] We use the value of g at the scale $\mu = m_Z$. Our results do not depend significantly on this choice of scale, in particular in the region of interest corresponding to $e \gtrsim 1$.

(II) The alternative possibility to impose the constraint (4.217) consists in setting $b_2 = 0$ and fixing a_3 and b_1 to be proportional to each other:

$$a_3(r) = a(r)\cos\omega, \qquad b_1(r) = a(r)\sin\omega \tag{4.222}$$

where ω is an arbitrary constant parameter. The energy functional is then

$$E_{II}[F,a] = 4\pi\frac{f}{e}\int_0^\infty d\widetilde{r}\left[\left(\widetilde{r}^2+2C^2\right)F'^2 + 2C^2 + \frac{C^4}{\widetilde{r}^2}\right. \tag{4.223}$$
$$\left. + \frac{e^2}{g^2}\left(a'^2 + \frac{a^2(a+2\cos\omega)^2}{2\widetilde{r}^2}\right)\right],$$

where we denoted $C = \sin F + a\sin(F-\omega)$. The corresponding Euler-Lagrange equations for $F(r)$ and $a(r)$ are

$$\left(\widetilde{r}^2+2C^2\right)F'' + 2\widetilde{r}F' + 4\sin(F-\omega)CF'a' \tag{4.224}$$
$$+2C(\cos F + a\cos(F-\omega))\left(F'^2 - 1 - \frac{C^2}{\widetilde{r}^2}\right) = 0,$$

$$a'' - \frac{a(a+\cos\omega)(a+2\cos\omega)}{\widetilde{r}^2} \tag{4.225}$$
$$-\left(\frac{g}{e}\right)^2 2C\sin(F-\omega)\left(F'^2 + 1 + \frac{C^2}{\widetilde{r}^2}\right) = 0.$$

The numerical solutions for $F(r)$ and $a(r)$ with $F(0) = \pi$, $F(r\to\infty) = 0$, $a(0) = 0$ and $a'(r\to\infty) = 0$ are shown in fig. 4.24. In general, the dependence on ω is completely non-trivial. Nevertheless, for small e, the lowest mass is obtained for $\omega \cong 0$ and the profile function $a(r)$ goes to -1 as r goes to infinity. Note that if one chooses $\omega = 0$, only a_3 is turned on and our ansatz resembles the so-called Skyrme-Wu-Yang ansatz used for a $SU(2)$ gauged skyrmion in ref. [286].

Although looking very different, the two ansätze yield very similar masses, as can be seen on Fig. 4.26. For $e \lesssim 10$, the lowest energy solution is obtained using the type I ansatz, while for $e \gtrsim 10$ the two choices give approximately equal masses, both very close to the ungauged case. For $e \gtrsim 5$, the mass of the gauged solution is at least 97% of the mass of the ungauged one, the profile function F is very close to the ungauged case value, and the gauge field is extremely small. In this regime, the ungauged solution can be considered a reasonable approximation. The mass of the gauged skyrmion can however be significantly reduced compared to the ungauged solution at small e. In particular, the mass of the skyrmion within the ansatz of type I has a well defined limit at $e \to 0$. The latter is not easy to determine numerically: the shooting method which can be used for $e \gtrsim 1$, where the profile

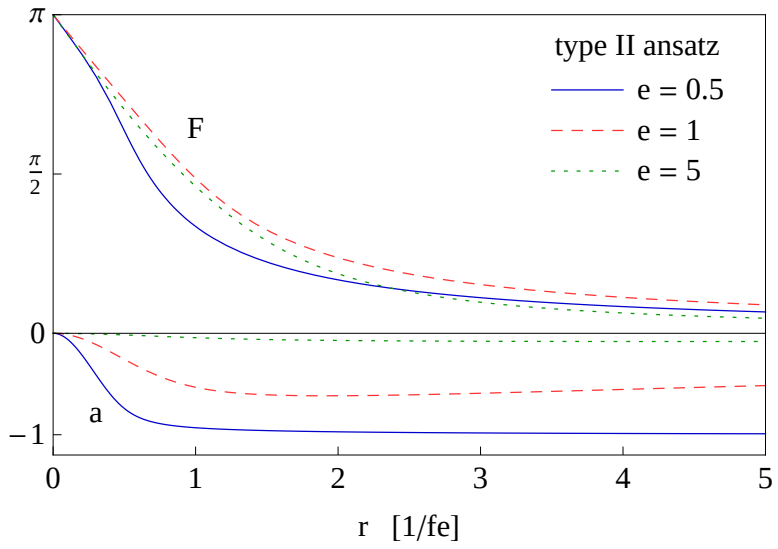

Figure 4.24: The profile functions $F(r)$, $b_2(r)$ and $a(r)$ for different values of the parameter e with the ansatz II. On the right-hand side, the parameter ω is chosen to yield the lowest possible mass, namely $\omega = 0$ for $e = 0.5$, $\omega = -0.27$ for $e = 1$ and $\omega = -1.13$ for $e = 5$.

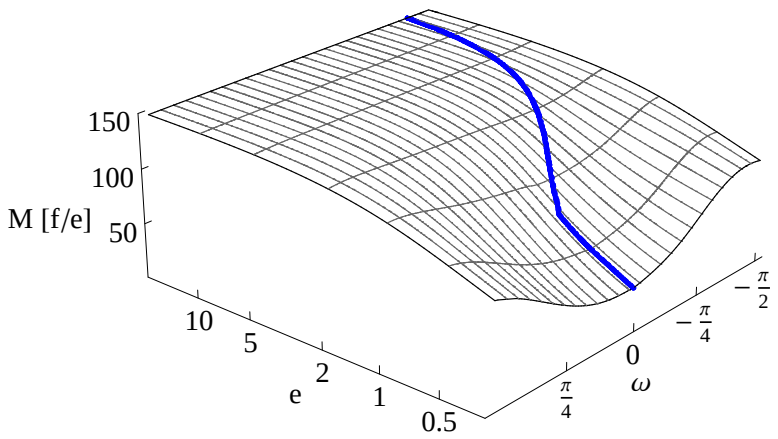

Figure 4.25: The mass of the type II solution as a function of e and ω (the thick blue line corresponds to the lowest mass for each value of e).

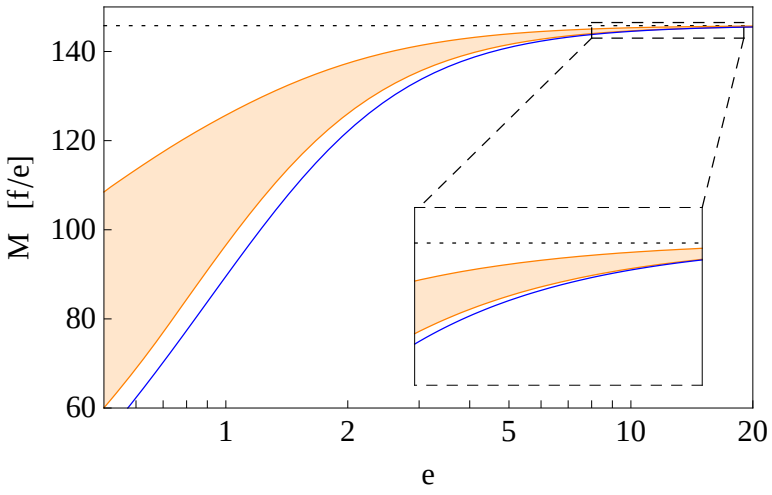

Figure 4.26: Comparison of the ungauged solution $M_0 = 145.8 f/e$ (dotted line), the type I ansatz (blue solid line) and the type II ansatz (orange band, with ω free to vary) as functions of e.

function F has a finite negative slope at $r = 0$, cannot be used to solve the Euler-Lagrange equation (4.222). At small e, the profile function F tends to be very flat around the boundary $r = 0$, and our shooting implementation becomes increasingly unstable. Instead, we resort to a relaxation algorithm, which produces reliable results for the profile functions down to values of e not much smaller than 0.4. For even smaller values of e it becomes increasingly difficult to obtain precise results, also with the relaxation method. Nevertheless, the limit in which e goes to zero can be taken analytically by making the following observations:

(a) The fraction in the last term of eq. (4.220) tends towards e^2/g^2 as $e \to 0$. The resulting term $e^2/g^2(F')^2$ can however still be large, since F tends to become a step function, and hence F' is large around the step.

(b) The term $\sin^4 F/r^2$ becomes subdominant in comparison with $2\sin^2 F$, since the sine is small everywhere except around the step of F, and the factor $1/r^2$ makes the contribution around the step small, due to the large value of r there.

With those two observations, the energy functional (4.220) can be approximated as

$$E_{I,e\to 0}[F] = 4\pi \frac{f}{e} \int_0^\infty \mathrm{d}r \left[2\sin^2 F + \frac{e^2}{g^2} F'^2 \right], \tag{4.226}$$

yielding the Euler-Lagrange equation for F

$$\frac{e^2}{g^2} F'' = \sin 2F. \tag{4.227}$$

Since this equation is independent of r, it can be integrated directly, giving

$$\frac{e^2}{g^2}F'^2 = 2\sin^2 F + C, \tag{4.228}$$

where C is a constant. Requiring $F'(r \to \infty) = 0$ fixes the constant to $C = 0$. This value of C also implies that at $r = 0$, where $F(0) = \pi$, the derivative of F vanishes, as observed numerically. Since F has to be decreasing between π and 0, the equation for F becomes

$$F' = -\sqrt{2}\frac{g}{e}\sin F, \tag{4.229}$$

which is solved by the function

$$F(r) = 2\arctan\left[\exp\left(-\sqrt{2}\frac{g}{e}(r - r_*)\right)\right]. \tag{4.230}$$

r_* is a constant fixing the position of the step, which is supposedly going to infinity at small values of e. However, the energy obtained with this F is independent of r_*: using eq. (4.229), one can rewrite the energy functional (4.226) as

$$E_{I,e\to 0}[F] = 8\sqrt{2}\pi\frac{f}{g}\int_0^\infty \mathrm{d}r(-\sin F)F' = 8\sqrt{2}\pi\frac{f}{g}\int_\pi^0 dF\cos F = 16\sqrt{2}\pi\frac{f}{g}. \tag{4.231}$$

With our numerical value for the gauge coupling, this gives

$$M_{e\to 0} = 16\sqrt{2}\pi\frac{f}{g} \cong 108.9\ f, \tag{4.232}$$

Both the step function (4.230) mass given by eq. (4.232) are in good agreement with the full numerical solution for $e \cong 0.4$ already, as shown on fig. (4.27) and (4.28) respectively. Note that while the skyrmion mass is bounded at large still large compared to the symmetry breaking scale f, so that the small e limit can not provide a physically interesting dark matter candidate.

The mass of the skyrmion so far is obtained following a classical procedure. In order to compute other physical properties of the skyrmion, like its coupling to the gauge fields, one should quantise the model. As shown in section 4.4, the bosonic or fermionic nature of the skyrmion does not only depend on the low-energy effective model described here, but also on the UV completion of the littlest Higgs model. Its charge was also determined in eq. (4.187). The skyrmion mass is affected by the quantisation procedure. While the mass of the lowest skyrmion state should remain close to the classical mass computed here — at least if the skyrmion is a scalar — excited states of higher mass are also expected.

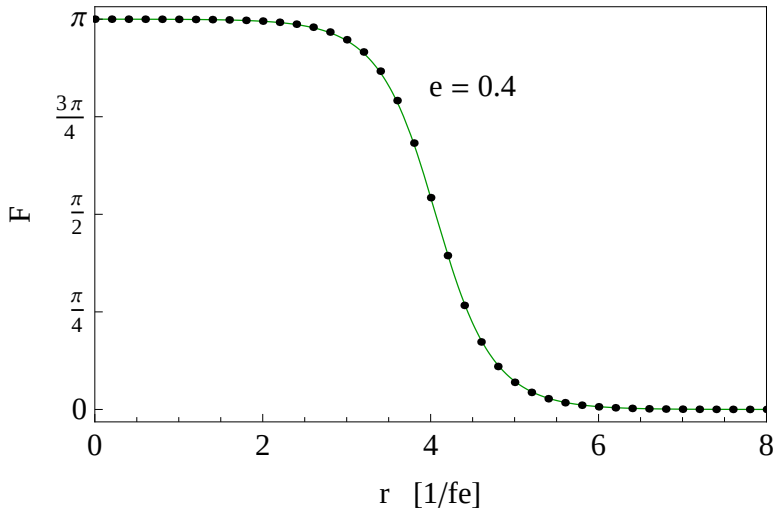

Figure 4.27: The profile function F as computed numerically (black points) in the type I ansatz for $e = 0.4$, compared with the analytical result of eq. (4.230) with $r_* = 4.06$ (green line).

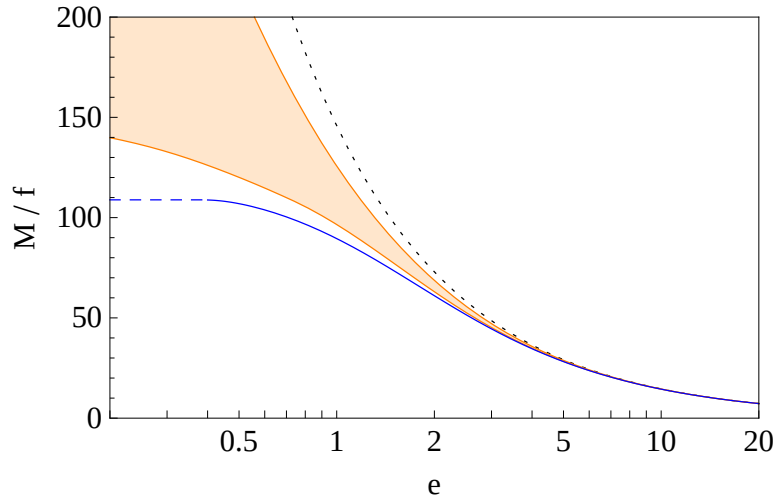

Figure 4.28: The skyrmion mass corresponding to the ansätze of type I (blue solid line) and II (orange band) compared to the ungauged mass (dotted line) diverging as $1/e$; for $e \lesssim 0.5$, the convergence of the numerical method is poor, but it agrees with the analytical limit of eq. (4.232).

4.5.3 Skyrmion interactions and constraints from cosmology

The skyrmion is a massive stable particle with at most weak couplings to Standard Model particles, and thus a potential dark matter candidate. Apart from its electric charge, which was discussed in section 4.4, most of the constraints relevant for cosmology can be derived using the classical properties of the skyrmion only. In the early universe the skyrmions in the littlest Higgs model will be thermally produced just like any other state in the particle spectrum. In contrast to protons, they may annihilate in pairs due to their topological $\mathbb{Z}_2$ quantum number. Therefore, the relic abundance of skyrmions is directly determined by their annihilation cross section.

Let us first not that long range forces between widely separated skyrmions are negligible at the classical level. A computation of the strength of such forces was performed in section 4.1.5. At distances much larger than the skyrmion radius, the potential energy between the two skyrmions can be computed employing the multiplicative ansatz (4.62), and its form is actually only determined by the large distance behaviour of the two single skyrmion solutions. In the absence of gauge interactions, the asymptotic behaviour of the profile function $F(r)$ as $1/r^2$, so that the potential vanishes as $1/d^3$, where d is the distance between the two skyrmions. For the gauged solutions, an analogous multiplicative ansatz for the two-skyrmion state cannot be employed directly, since the gauge field also contributes to the energy. However, we expect as for the ungauged solution that the potential only depends on the asymptotic behaviour of the profile functions F, a_i and b_i. For the gauged type I solution, which is always lighter than the ungauged and type II solutions, the profile functions vanish exponentially at large r:

$$\begin{aligned} F(r) &\xrightarrow{r\to\infty} c\, e^{-\sqrt{2}fgr}, \\ b_2(r) &\xrightarrow{r\to\infty} -\sqrt{2}\, f\, g\, c\, r\, e^{-\sqrt{2}fgr}, \end{aligned} \tag{4.233}$$

where c is a numerical factor depending of the value of the Skyrme coupling e. We can hence safely expect the strength of the interaction to be exponentially suppressed with the distance, and therefore no large attractive or repulsive force is present at large distances, despite the fact that any two skyrmions can annihilate into light particles. Note finally that the skyrmion might be charged under the electroweak gauge group, and that a potential falling off as $\exp(-m_W d)$ due to the exchange of gauge bosons can be present and of equal importance.

In the early universe, at temperatures $T \gtrsim M_0$, it is safe to assume that the skyrmions are in thermal equilibrium. The relic density then depends crucially on the pair annihilation cross section. A reasonable first estimate for this quantity is the geometric cross section

$$\sigma_A = \pi \langle r^2 \rangle \cong \frac{\pi}{(fe)^2}. \tag{4.234}$$

A comparison with proton anti-proton annihilation in the original Skyrme model shows that the geometric cross section yields at least the correct order of magnitude for this process at intermediate energies [44]. To parametrise the remaining uncertainty, we let the cross section vary by an order of magnitude, i.e. we take $\sigma = 10^{\pm 1}\sigma_A$ for the numerical analyses.

In addition to the cross section also the dominant final states of the annihilation process are unknown. To circumvent this problem, and to make a numerical analysis feasible, we introduce effective couplings of the skyrmion, which we assume to be a scalar, to the degrees of freedom of the littlest Higgs. To estimate the uncertainty introduced by this procedure we consider two distinct possibilities:

(a) The first possibility we consider is to couple the skyrmion directly to the Goldstone sector using the gauge invariant effective operator

$$\mathcal{L}_{\text{int}} = -\frac{1}{8} G_\Sigma \; S^2 \,\text{Tr}(D_\mu \Sigma D^\mu \Sigma^\dagger)\,, \tag{4.235}$$

where S describes the skyrmion. This terms yields an infinite number of interactions with an arbitrary number of external legs. For simplicity we only consider the four particle operators that mediate the annihilation of skyrmion pairs into heavy and light gauge bosons, heavy triplets ϕ and into little Higgses h. All of these annihilation channels give approximately the same contribution to the cross-section, as long as the mass of the final states is small compared to the skyrmion mass M_0:

$$\sigma_{SS\to hh} = \frac{G_\Sigma^2 M_0^2}{128\pi f^4} \frac{\beta_h (1+\beta_h^2)^2}{\beta_S (1-\beta_S^2)} \cong \frac{G_\Sigma^2 M_0^2}{32\pi f^4} \frac{1}{\beta_S (1-\beta_S^2)}\,, \tag{4.236}$$

and similarly for the other scalars and vector bosons. Here, β_S and β_h are the relativistic velocities of the annihilating skyrmions and the produced Higgses, respectively, in the centre-of-mass frame. The cross-section diverges at small and large energies, in a similar fashion as the proton-antiproton annihilation cross-section. To make connection with the estimate (4.234) for the total cross section, we determine the parameter G_Σ such that the annihilation cross section for momenta $|\mathbf{p}| \sim \frac{1}{\sqrt{2}} M_0$, i.e. $\beta_S = \frac{1}{\sqrt{3}}$, agrees with (4.234). This translates into

$$G_\Sigma^2 = \frac{64\pi^2 \langle r^2 \rangle}{3\sqrt{3} N_b} \frac{f^4}{M_0^2}\,, \tag{4.237}$$

where $N_b = 14$ is the number of bosons entering eq. (4.235). G_Σ is independent of f and e, due to the scaling properties of M_0 and $\langle r^2 \rangle$, and hence takes the constant value $G_\Sigma \cong 0.024$. Figure 4.29 shows the region in the $f - e$ plane where the skyrmion relic density agrees with the observed value. The correct dark matter abundance is obtained

for relatively large values of e, due to the $1/e$ scaling of the geometric cross section. For small values of f this corresponds to a skyrmion mass in the low TeV range, which raises some hope that these particles can be observed at the LHC. The freeze-out temperature and relic density were obtained using the littlest Higgs implementation of ref. [307] in the cosmology code micrOMEGAs [308].

(b) To reduce the uncertainty from the unknown final states of the annihilation, we consider a second, purely phenomenological interaction of the form

$$\mathcal{L}_{\text{int}} = -\frac{1}{2} G_\psi \; S^2 \overline{\psi}\psi \,, \tag{4.238}$$

where again S denotes the skyrmion and ψ any of the Standard Model quarks or leptons. The coupling G_ψ is taken to be

$$G_\psi^2 = \frac{8\pi^2 \langle r^2 \rangle}{N_f}, \tag{4.239}$$

where $N_f = 24$ is the number of Standard Model fermions. The partial cross-section into any quark or lepton pair decreases with increasing energy as

$$\sigma_{SS\to\overline{\psi}\psi} = \frac{G_\psi^2}{8\pi} \frac{\beta_\psi^3}{\beta_S} \cong \frac{G_\psi^2}{8\pi} \frac{1}{\beta_S} \,, \tag{4.240}$$

where β_ψ is the relativistic velocity of the produced fermions in the centre-of-mass frame. The second equality holds when the mass M_0 of the skyrmion is much larger than the mass m_ψ of the quarks and leptons. With this choice, the sum over all Standard Model fermions again yields the geometric cross section. The resulting constraints on f and e are shown in fig. 4.30.

Both models lead to similar constraints on the parameter space, the main difference being due to the different energy behaviour of the annihilation cross sections. Another check can be performed using the famous formula of ref. [52] that relates the relic density to the annihilation cross-section of the dark matter particles,

$$\Omega h^2 \cong \frac{3 \cdot 10^{-27} \text{cm}^3/\text{s}}{\langle \sigma v \rangle} \cong 0.1. \tag{4.241}$$

Using the naive estimate $\sigma \sim \sigma_A$, and taking the average velocity of the skyrmions to be $v \sim \frac{1}{2}c$, this yields the constraint

$$fe \sim 35 \text{ TeV}, \tag{4.242}$$

which is in complete agreement with the favoured regions of fig. 4.29 and 4.30.

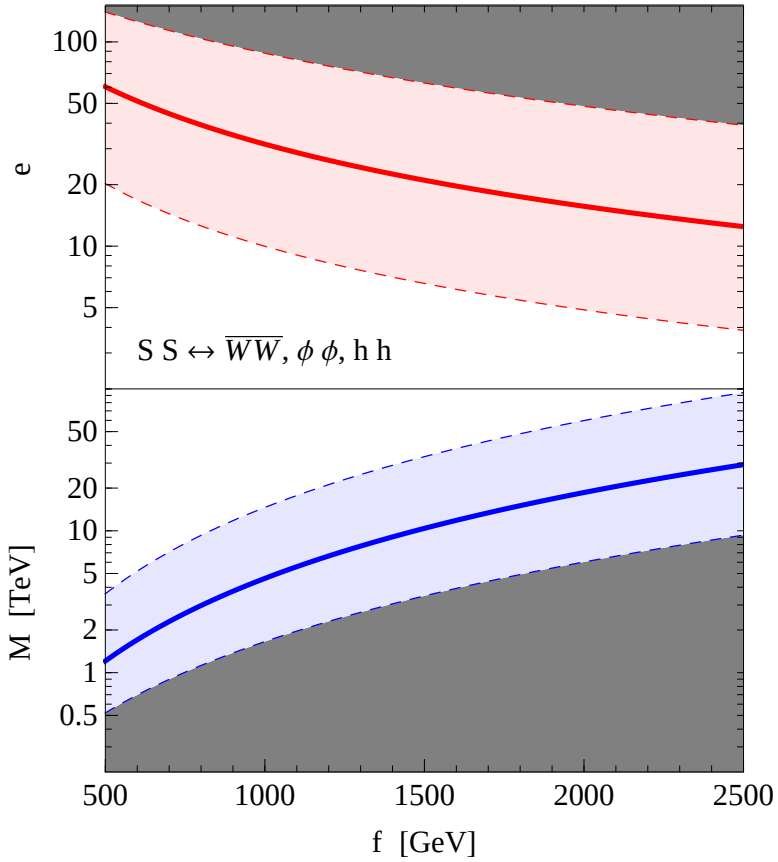

Figure 4.29: The value of the Skyrme coupling e (upper plots) and of the corresponding skyrmion mass M_0 (lower plots) matching the observed dark matter relic density as a function of the symmetry breaking scale f. The skyrmion is coupled to the Goldstone sector as in eq. (4.235). The coloured band corresponds to fixing the coupling constant G so that the skyrmion annihilation cross-section σ is in the range $\frac{1}{10}\sigma_A < \sigma < 10\sigma_A$, with the thick line corresponding to the middle value $\sigma = \sigma_A$. The dark grey regions are excluded since they predict a too large dark matter relic density.

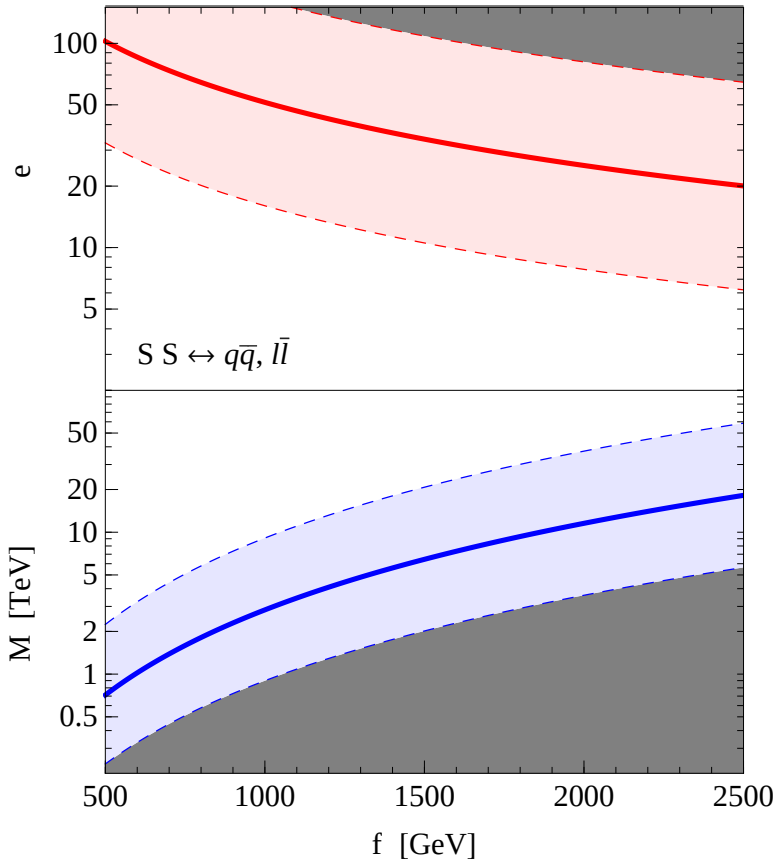

Figure 4.30: Same as fig. 4.29, with the implementation (4.238) of interactions between the skyrmion and Standard Model quarks and leptons.

An important consequence of the preceding results is that the parameter e is bounded from above, which implies a lower bound on the skyrmion mass. For small values of the symmetry breaking scale f the bound is rather weak, but it leads to the constraint $M_0 > f$ for $f \gtrsim 1$ TeV. If the skyrmions were lighter than these bounds, they would be massively produced in the early universe and their annihilation cross-section would be small, so that their relic abundance at present day would exceed the observed dark matter density. Conversely, for moderate values of the Skyrme parameter, $10 \lesssim e \lesssim 100$, the skyrmion can account for the observed dark matter relic density.

There is however no lower bound on e to be read from cosmological considerations. In other words, the skyrmion is allowed to be really heavy, since in this case its large mass and important annihilation cross-section makes it completely absent from our present universe. In this case, the dark matter has to be of different origin.

5 Conclusions

This thesis has been devoted to the study of composite Higgs models, to their phenomenology at collider experiments, and to their possible further implications in domains as far as cosmology. It was emphasised that a natural alternative to supersymmetry exists, and can similarly reproduce to a certain level of accuracy the phenomenology of the Standard Model with a Higgs boson at low energy. The discovery of the Higgs made by ATLAS and CMS experiments at CERN does not yet provide insight about its true nature. Although no significant deviations from the Standard Model have been observed so far, the possibility that the electroweak symmetry breaking arises from a strongly-interacting sector is well alive. As advocated in chapter 3, the postulated existence of a strong sector together with the precision electroweak data gathered at LEP were already pointing in the direction of a light Higgs boson similar to the one discovered.

If by chance the model presented of section 3.3 turns out to be realised in nature, new effects should soon be observed at the LHC. In general, the first experimental signature of composite Higgs models would probably be the presence of fermionic resonances, corresponding to the light top partners required by the partial compositeness mechanism. Deviations from the standard Higgs couplings should also appear once the luminosity of the LHC machine is increased. Identifying the nature of electroweak symmetry breaking as being of strong origin may however be more complicated. The discovery of vector resonances would be an important step in this direction. Alternatively, measuring the Higgs self-couplings and indirect effects of composite fermions on the single- and pair-production of a Higgs boson could provide an essential insight in the theory.

An alternative possibility, often described as the “nightmare scenario”

by particle physicists, is that absolutely no significant deviations from the Standard Model will be observed, even after the LHC upgrade to its design energy. The models described above, where the compositeness scale f is located around the TeV scale, would then be indubitably excluded. In this case, both supersymmetric and strong dynamics models would need a considerable amount of fine-tuning to evade all experimental constraints. Composite Higgs models provide naturally a decoupling limit when $v \ll f$. Explaining this highly-unnatural hierarchy requires however new mechanisms, which could in principle arise from little-Higgs-like models. It was nevertheless argued in this thesis that none of the existing models suitably realises the mechanism of collective symmetry breaking, at least in the presence of a unique Higgs doublet.

The current situation of composite Higgs models regarding experimental data is therefore suffering a certain tension. The theoretical effort to improve the situation can follow two different ways. In a "top-down" approach, one can try to get a better understanding of strongly-interacting theories. Many concepts used to build the present composite and little Higgs models still come from analogies with large-N_c considerations of QCD. The development of new methods to study (nearly-)conformal field theories is of crucial importance, as is the further study of holographic descriptions of four-dimensional theories. At the same time, numerical studies on the lattice can provide a help towards a better theoretical understanding of strongly-coupled models. The second approach which can be envisaged is of the "bottom-up" type. Effective models matching the (absence of) experimental observations should be built and their validity range pushed to higher and higher energy, while still matching the successful results of the Standard Model at low energy. The success of this approach relies on the theorists' capability to invent models in which the divergences in the Higgs potential vanish from symmetry arguments. Both of the ways described here must certainly be explored simultaneously. The hope is that the two approaches will overlap at some point, and provide a fully consistent description of nature.

Acknowledgements

I would like to thank all the people who contributed in a way or another to the accomplishment of this thesis. This includes of course my advisor Daniel Wyler, my direct collaborators Pedro Schwaller, Andreas von Manteuffel, Ennio Salvioni, Christophe Grojean, Ramona Gröber and Margarethe Mühlleitner. Special thanks go to Thomas Gehrmann and Riccardo Rattazzi who supported my application for a postdoc position, Andreas Papaefstathiou and Erich Weihs who spent time proofreading this (somewhat lengthy) thesis, as well as José Zurita, Florian Goertz, Rikkert Frederix, Timo Schmidt, Gizem Öztürk, Tobias Hurth, Babis Anastasiou, Elisabetta Furlan and José Santiago for many stimulating discussion at the blackboard. Many thanks goes as well to all the PhD students, postdoc and staff at the University of Zurich and at the ETH, whose contributions spread from late-night discussion on the meaning of quantum mechanics, daily coffee breaks and Töggele games, football games in the park, Doppelkopf nights, separta parties and much more, namely in alphabetical order Donnino Anderhalden, Raymond Angélil, Tobias Baldauf, Simone Balmelli, Jonathan Blazek, Andreas Bleuler, Radja Boughezal, Stefan Bühler, Mathias Brucherseifer, Simone Callegari, Julián Cancino, Fabio Cascioli, Jonathan Coles, Claude Duhr, Sebastian Elser, Andreu Font, Marina Galvagni, Lea Giordano, Massimiliano Grazzini, Nico Greiner, Nico Hamaus, Franz Herzog, Volker Hoffmann, Lucia Hosekova, Cedric Huwyler, Matthieu Jaquier, Stefan Kallweit, Antoine Klein, Christian Kurz, Achilleas Lazopoulos, Lucas Lombriser, Thomas Lübbert, Mario Lubini, Gionata Luisoni, Philipp Maierhöfer, Davide Martizzi, Esther Meier, Pier Francesco Monni, Ben Moore, Christine Moran, Tobias Motz, Romain Müller, Giuliano Panico, Doug Potter, Stefano Pozzorini, Darren Reed, Rok Roskar, Prasenjit Saha, Regina Schmid, Aurel Schneider, Joachim Stadel, Cedric Studerus, Nurhana Tajuddin, Lorenzo Tancredi, Romain Teyssier, Alessandro Torre, Crescenzo Tortora, Zvonimir Vlah, Tina Wentz, Suzanne Wilde, Lilin Yang, Jaiyul Yoo, and all the amazing people I met at various schools and conferences, and others who I may have forgotten. Last but not least, all my gratitude goes to my family and to Daniela for the uninterrupted support. You all made my time in Zürich an unforgettable experience!

A

Solving Differential Equations with Boundary Value Problems

In this appendix, we describe how to solve numerically differential equations subject to boundary conditions imposed at different points in space. This is the kind of problems we have to solve in order to determine the lightest skyrmion solution in the different models appearing in this thesis. The methods presented here are adapted from the textbook "Numerical Recipes" [309].

A.1 Shooting method in one dimension

The first type of differential equation we were confronted to is eq. (4.26), associated with the energy density (4.24). The unknown function $F(r)$ describes the profile of the hedgehog ansatz,

$$\left(r^2 + 2\sin^2 F\right) F'' + 2rF' + \sin 2F \left(F'^2 - 1 - \frac{\sin^2 F}{r^2}\right) = 0, \qquad \text{(A.1)}$$

with boundary conditions $F(0) = \pi$ and $F(\infty) = 0$. This equation can be solved locally using infinitesimal steps, starting from a given point r_* in the interval $[0, \infty)$, provided that the value of F and F' at this point are known. This is *a priori* not the case, since the boundary conditions only specify the value of F, not of its first derivative. A simple solution to this problem, called the shooting method, consists in solving the equation starting at the boundary point $r_* = 0$ for any value of $F'(r_*)$, and find among the continuum of solution which of them also satisfy the boundary

at $F(\infty) = 0$. The subtle point in this case is to evaluate the value of F at $r \to \infty$, since the non-linear form of the equation (A.1) yields solutions oscillating at large r, whose asymptotic value is not well defined.

Alternatively, we can use the shooting method starting from the other boundary, at $r \to \infty$ and run back to $r = 0$. In order to do so, we first evaluate the asymptotic behaviour of the profile function F. At large r, F and its first derivative have to be small in order to satisfy the boundary condition, and therefore eq. (A.1) reduces to

$$r^2 F''_\infty + 2rF'_\infty - 2F_\infty = 0, \tag{A.2}$$

whose most general solution is

$$F_\infty(r) = c_1 r + c_2 \frac{1}{r^2}. \tag{A.3}$$

The boundary condition $F_\infty(\infty) = 0$ can only be respected if the constant c_1 is adjusted to zero, while c_2 is left unspecified. Therefore, the asymptotic behaviour of F can be described as

$$F_\infty(r) = \frac{\alpha}{r^2}, \tag{A.4}$$

where α is a constant to be determined. Similarly, at small values of r, the solution to the differential equation (A.1) is simply linear:

$$F_0(r) = \pi + c\, r. \tag{A.5}$$

The complete numerical solution can therefore be built, for an arbitrary value of α, by gluing the solutions in the three region, namely

$$F(r) = \begin{cases} F_\infty(r) \text{ for } r \in [r_b, \infty), \\ F_{ab}(r) \text{ for } r \in [r_a, r_b], \\ F_0(r) \quad \text{for } r \in [0, r_a], \end{cases} \tag{A.6}$$

where r_a and r_b are limiting values to be taken sufficiently small, respectively large, and $F_{ab}(r)$ is the numerical solution obtained by running from the point r_b with initial values $F(r_b) = F_\infty(r_b) = \alpha/r_b^2$ and $F'(r_b) = F'_\infty(r_b) = -2\alpha/r_b^3$. The radii r_a and r_b are chosen empirically to be

$$r_a = 0.05, \qquad r_b = 20. \tag{A.7}$$

With this setup, the differential equation can be solved for any value of α. The correct solution is then the one yielding the correct boundary condition at $F(0) = \pi$. The value of F which is obtained at $r = 0$ as a function of α is shown on Figure A.1. The correct value for α is found to be

$$\alpha = 2.160. \tag{A.8}$$

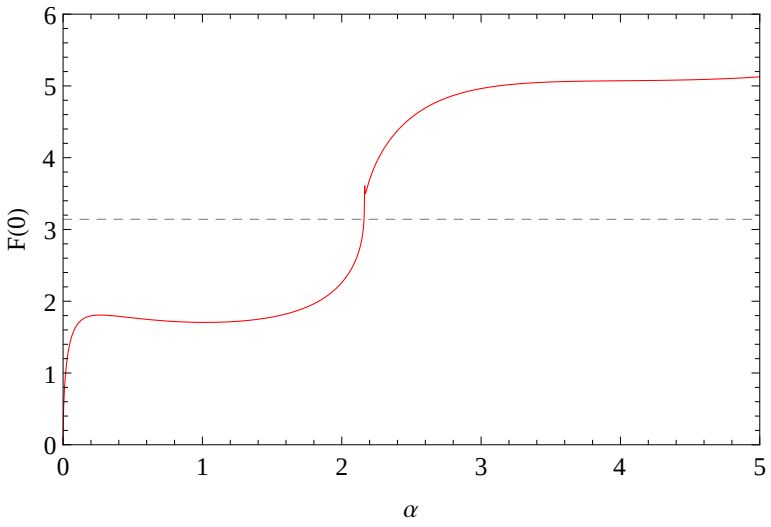

Figure A.1: Value of F at the boundary point $r = 0$ obtained by running from the opposite boundary $r \to \infty$ depending on the coefficient α of the asymptotic form $F_\infty(r) = \alpha/r^2$.

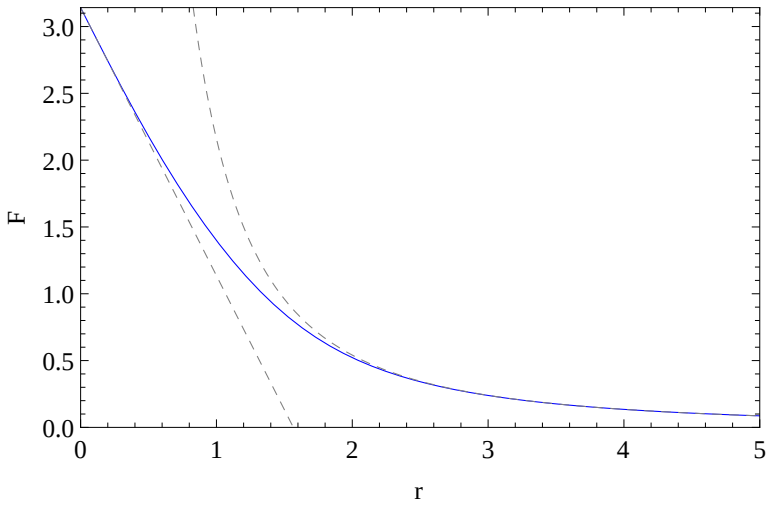

Figure A.2: Numerical solution for $F(r)$ (solid blue line) compared to the analytical power-law limits F_0 and F_∞ (dashed lines).

For this value, the profile function F is displayed on Figure A.2, together with the asymptotic cases F_0 and F_∞. As one can see, the agreement is very good even for values of r much larger than r_a and much smaller than r_b.

The same method can be used to solve numerically eq. (4.152) and (4.222). However, we will see in the next section that a alternative method yields even faster results.

A.2 Relaxation method in one dimension

We will now present an alternative method to solve eq. (A.1). Although the method presented in the previous section is fast and reliable, this alternative method was proved to be useful in certain special cases where the convergence of the shooting algorithm is bad. This is the case in particular in the regime of small e in eq. (4.222), where the first derivative of the function F tends to zero at both boundary points. Moreover, the relaxation method presented here can then be extended to two dimensional differential equations, as shall be seen in the next section.

The use of relaxation techniques imply a discretisation of the interval between the two boundaries, which in turn requires this interval to be finite. We will therefore first compactify the radial coordinate $r \in [0, \infty]$ to a finite interval $y \in [0, \pi/2]$ by applying the following transformation,

$$r \to \tan(y), \quad F(r) \to F(y), \quad F'(r) \to \cos^2 y\, F'(y),$$
$$F''(r) \to \cos^2 y \left(\cos^2 y\, F''(y) - \sin 2y\, F'(y)\right). \tag{A.9}$$

The differential equation (A.1) takes then the compactified form

$$\left(\sin y^2 + 2\cos^2 y \sin^2 F\right) F'' + \sin 2y \cos 2F\, F' + \sin 2F \left(\cos^2 y\, F'^2 - \frac{1}{\cos^2 y} - \frac{\sin^2 F}{\sin y^2}\right) = 0, \tag{A.10}$$

The relaxation method consists in discretising the interval $y \in [0, \pi/2]$, choose an initial shape for the profile function F, try to adjust locally the value of F in order to minimise the left-hand size of eq. (A.10), and iterate the last step until a given precision is reached. This is achieved at each point y_k on a N-site lattice by adding to $F_k \equiv F(y_k)$ a small quantity chosen to reduce locally the left-hand side of eq. (A.10), in small steps, until this left-hand side is considered close enough to zero. The convergence of the method can be largely improved by splitting the second order equation (A.10) into two first order equations, written as $E_F = 0$ and $E_P = 0$, where

$$E_F = F' - P, \tag{A.11}$$

$$E_P = P' + \frac{\sin 2y \cos 2F\, P + \sin 2F \left(\cos^2 y\, P^2 - \frac{1}{\cos^2 y} - \frac{\sin^2 F}{\sin y^2}\right)}{\sin y^2 + 2\cos^2 y \sin^2 F}. \tag{A.12}$$

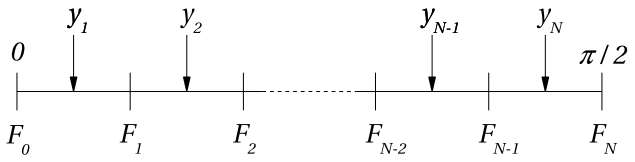

Figure A.3: Discretisation of the interval $y \in [0, \pi/2]$, indicating the position of the lattice points y_k and of the variables F_k (and similarly of P_k).

The first of those two equation just forces P to be equal to the first derivative of F, while the second is then equivalent to eq. (A.10). These quantities E_F and E_P can be computed locally at each lattice site in terms of F, F', P and P'. For simplicity, we split the interval $y \in [0, \pi/2]$ into N segments of same length d as in Figure A.3, and define

$$y_k = \left(k - \frac{1}{2}\right) d, \qquad d = \frac{\pi}{2N} \tag{A.13}$$

The value of F, G and of their derivatives at a given point y_k are then described by

$$\begin{aligned} F(y_k) &= \frac{F_k + F_{k-1}}{2}, \qquad & F'(y_k) &= \frac{F_k - F_{k-1}}{d}, \\ P(y_k) &= \frac{P_k + P_{k-1}}{2}, \qquad & P'(y_k) &= \frac{P_k - P_{k-1}}{d}. \end{aligned} \tag{A.14}$$

The boundary conditions impose $F_0 = \pi$, $F_N = 0$, while P_0 and P_N remain free. The values of E_F and E_P at the sites y_k are then simply functions of F and P at the two nearest-neighbour points:

$$\begin{aligned} E_F(y_k) &= E_F\left(F_k, F_{k-1}, P_k, P_{k-1}\right), \\ E_P(y_k) &= E_P\left(F_k, F_{k-1}, P_k, P_{k-1}\right). \end{aligned} \tag{A.15}$$

The dependence of these functions on the lattice points y_k is implicit, since the lattice is fixed once for all at the beginning of the computation. Now at each step of the iterative process, we modify the values F_k and P_k by adding to them small corrections ΔF_k and ΔP_k respectively, so that

$$\begin{aligned} E_F^{(t+1)}(y_k) &= E_F^{(t)}\left(F_k + \Delta F_k, F_{k-1} + \Delta F_{k-1}, P_k + \Delta P_k, P_{k-1} + \Delta P_{k-1}\right) \\ &\cong E_F^{(t)}(y_k) + \left(\frac{\partial E_F^{(t)}(y_k)}{\partial F_k}\right) \Delta F_k + \left(\frac{\partial E_F^{(t)}(y_k)}{\partial P_k}\right) \Delta P_k \\ &\quad + \left(\frac{\partial E_F^{(t)}(y_{k-1})}{\partial F_{k-1}}\right) \Delta F_{k-1} + \left(\frac{\partial E_F^{(t)}(y_{k-1})}{\partial P_{k-1}}\right) \Delta P_{k-1}, \end{aligned} \tag{A.16}$$

where the index t denotes the iteration number. The same is valid for E_P. The second equality is a Taylor expansion of E_F to the first order in the corrections ΔF_k, ΔP_k. The challenge now is to find appropriate values for ΔF_k and ΔP_k in order to make the left-hand side of (A.16) as small as possible. While it is not possible to invert the function E_F and E_P directly since they are highly non-linear, one can use the first-order Taylor expansion in (A.16) to estimate the value of ΔF_k and ΔP_k. There are actually $2(N+1)$ unknowns ΔF_k and ΔP_k with $k \in \{0, \ldots, N\}$, $2N$ linear equations in the form of eq. (A.16), and two additional equations for ΔF_0 and ΔF_N imposed by the boundary conditions for F_0 and F_N, so that the whole problem can be expressed as a $2N + 2$-dimensional linear system of equations

$$S\,\vec{x} = \vec{b}. \tag{A.17}$$

Here $\vec{x}$ describes all the unknowns

$$\vec{x} = (\Delta F_0, \Delta P_0, \Delta F_1, \Delta P_1, \ldots, \Delta F_N, \Delta P_N)^T, \tag{A.18}$$

the right-hand side is given by

$$\vec{b} = (\pi - F_0, -E_F(y_1), -E_P(y_1), \ldots, -E_F(y_N), -E_P(y_N), -F_N)^T, \tag{A.19}$$

and S is a $(N+2)\times(N+2)$ matrix with the peculiar quasi-diagonal structure

$$S = \begin{pmatrix} \boxed{S_0} & & & & \\ & \boxed{S_1} & & & \\ & & \boxed{S_2} & & \\ & & & \ddots & \\ & & & & \boxed{S_{N-1}} \\ & & & & & \boxed{S_N} \\ & & & & & & \boxed{S_{N+1}} \end{pmatrix}, \tag{A.20}$$

where the S_k for $k \in \{1, \ldots, N\}$ are 2×4 blocks given by

$$S_k = \begin{pmatrix} \frac{\partial E_F(y_k)}{\partial F_{k-1}} & \frac{\partial E_F(y_k)}{\partial P_{k-1}} & \frac{\partial E_F(y_k)}{\partial F_k} & \frac{\partial E_F(y_k)}{\partial P_k} \\ \frac{\partial E_P(y_k)}{\partial F_{k-1}} & \frac{\partial E_P(y_k)}{\partial P_{k-1}} & \frac{\partial E_P(y_k)}{\partial F_k} & \frac{\partial E_P(y_k)}{\partial P_k} \end{pmatrix}, \tag{A.21}$$

and the 1×2 blocks S_0 and S_{N+1} fix the boundary conditions, in our case

$$S_0 = S_{N+1} = \begin{pmatrix} 1 & 0 \end{pmatrix}. \tag{A.22}$$

Iteration	Estimated error	Energy $[f/e]$
0		177.653
1	$6.88 \cdot 10^{-1}$	77.764
2	$3.05 \cdot 10^{-1}$	73.020
3	$5.65 \cdot 10^{-2}$	72.924
4	$5.56 \cdot 10^{-3}$	72.924
5	$1.82 \cdot 10^{-6}$	72.924
6	$2.13 \cdot 10^{-12}$	72.924

Table A.1: The energy (4.26) of the field after a given number of iterations, on a lattice with $N = 1000$ sites. The error estimate is computed from eq. (A.23).

The special form of S permits the use of an improved version of the Gauss algorithm to solve the linear system of equation. The authors of the textbook "Numerical Recipes" [309] provide for this a very powerful C++ routine [310]. As input, this routine only needs the values of the matrix S and of the vector $\vec{b}$ as functions of the F_k and G_k, and an initial guess for those values. We choose here initially $F(y) = \pi - 2y$ and $G(y) = -2$ so that the boundary conditions are satisfied.[1] With this choice, the initial energy is given by $18\pi^2 \cong 177.7$, and is expected to reach a minimum after a few iterations. The error at each step of the process can be estimated by the size of the quantities $E_{F,P}$. A natural choice made in the routine [310] consists in taking

$$\xi = \frac{1}{2N} \sum_k \left(|E_F(y_k)| + |E_P(y_k)| \right) . \tag{A.23}$$

The procedure is iterated until this error estimate is small enough. In our analysis, we end the iterative process once $\xi < 10^{-8}$.

Running the whole algorithm on a lattice of size $N = 1000$ takes only six iterations until the error becomes negligible, and the total CPU time is only about 15 ms. The energy (4.26) and estimated error after each iteration is given in Table A.1. The result is perfectly in agreement with the one obtained in the last section using the shooting method. Notice that the convergence of the algorithm is remarkable, since after only three iterations, the energy is already extremely close to its final value.

The main disadvantage of this method is that it is relatively complicated

[1] Note however that this implementation of the relaxation algorithm does not explicitly require the initial guess to respect the boundary conditions: the iterative process enforces them progressively anyway.

to implement compared to the shooting method described above. However, once the implementation is done, the solving procedure is extremely fast and reliable. It is actually a huge advantage when one has to repeat the computation a large number of times, for example when the differential equation depends on an external parameter to be taken in a large range of values. This is for example the case for the energy functional (4.220), associated with the Euler-Lagrange equation (4.222):

$$\left(1+\left(\frac{g}{e}\right)^2\left(r^2+2\sin^2 F\right)\right)\left(r^2+2\sin^2 F\right)F''+2rF' \qquad (A.24)$$
$$+\sin 2F\left[F'^2-\left(1+\left(\frac{g}{e}\right)^2\left(r^2+2\sin^2 F\right)\right)^2\left(1+\frac{\sin^2 F}{r^2}\right)\right]=0.$$

Here e and g are parameters of the model, the latter being fixed to $g = 0.653$. We want to solve this equation for any value of e. Again, we first need to compactify the interval, using the substitution (A.2), split the second order equation into a system of two first order equations (defining $P \equiv F'$), and apply the iterative algorithm as above. We use the same initial guess as before for F. The results of the iterative process are shown in Table A.2 for two typical values of e. It can be seen that the number of iterations required is significantly larger than before. The reason for this is that our relaxation method sometimes "overshoots", i.e. provides too large corrections ΔF_k and ΔP_k, so that the field configuration obtained at the step $(t+1)$ might have a larger energy than the initial configuration at step (t). This kind of issues results in oscillations around the true minimum, reducing the convergence of the algorithm; in some cases, the convergence can even be lost. For this reason, one introduces a "slowing factor" $\zeta \in [0,1]$, and at each step the values F_k and P_k are incremented by $\zeta\Delta F_k$ and $\zeta\Delta P_k$ respectively, i.e. only a fraction of the correction is applied. Choosing a small factor ζ ensures the convergence of the algorithm, but increases the required number of iterations. The results shown in Table A.2 are obtained with a "slowing factor" $\zeta = 0.9$.

The whole relaxation procedure can be extended to larger systems of differential equations. This is actually the method chosen to solve equations (4.224) and (4.225),

$$\left(r^2+2C^2\right)F''+2rF'+4\sin(F-\omega)CF'a'$$
$$+2C(\cos F+a\cos(F-\omega))\left(F'^2-1-\frac{C^2}{r^2}\right)=0, \qquad (A.25)$$
$$a''-\frac{a(a+\cos\omega)(a+2\cos\omega)}{r^2}$$
$$-\left(\frac{g}{e}\right)^2 2C\sin(F-\omega)\left(F'^2+1+\frac{C^2}{r^2}\right)=0. \qquad (A.26)$$

	$e = 0.5$		$e = 5$	
Iteration	Est. error	Energy $[f/e]$	Est. error	Energy $[f/e]$
1	1.63	126.922	1.70	89.738
2	$7.32 \cdot 10^{-1}$	113.554	2.41	103.704
3	$3.03 \cdot 10^{-1}$	109.239	$6.26 \cdot 10^{-1}$	87.890
4	$3.74 \cdot 10^{-1}$	108.026	4.25	77.237
5	$1.78 \cdot 10^{-1}$	107.376	10.74	57.536
6	$2.37 \cdot 10^{-1}$	107.137	7.75	39.065
7	$1.03 \cdot 10^{-1}$	107.014	1.19	29.097
8	$1.37 \cdot 10^{-1}$	106.975	$1.67 \cdot 10^{-1}$	28.181
9	$4.74 \cdot 10^{-2}$	106.961	$3.12 \cdot 10^{-3}$	28.181
10	$4.25 \cdot 10^{-2}$	106.959	$1.03 \cdot 10^{-5}$	28.181
11	$7.11 \cdot 10^{-3}$	106.959	$9.07 \cdot 10^{-11}$	28.181
12	$8.38 \cdot 10^{-4}$	106.959		
13	$3.48 \cdot 10^{-6}$	106.959		
14	$1.67 \cdot 10^{-10}$	106.959		

Table A.2: The energy (4.220) of the field after a given number of iterations, on a lattice with $N = 1000$ sites, for the cases $e = 0.5$ and $e = 5$.

	$e = 0.5$, $\omega = 0$		$e = 5$, $\omega = -1.13$	
Iteration	Est. error	Energy $[f/e]$	Est. error	Energy $[f/e]$
1	4.82	317.909	1.45	181.531
5	2.11	221.847	1.88	159.066
10	$8.85 \cdot 10^{-1}$	144.886	1.38	36.136
15	$4.11 \cdot 10^{-1}$	120.519	$8.09 \cdot 10^{-13}$	28.316
20	$1.38 \cdot 10^{-1}$	120.234		
25	$2.37 \cdot 10^{-2}$	120.130		
30	$7.71 \cdot 10^{-2}$	120.126		
35	$1.19 \cdot 10^{-1}$	120.046		
40	$4.50 \cdot 10^{-6}$	120.055		
41	$2.97 \cdot 10^{-9}$	120.055		

Table A.3: The energy (4.224) of the field after a given number of iterations, on a lattice with $N = 1000$ sites, for the cases $e = 0.5$ and $e = 5$, with ω adjusted to minimise the energy.

where $C = \sin F + a \sin(F - \omega)$, and e, g and ω are parameters of the model. Once again, these two second order equations for $F(r)$ and $a(r)$ can be compactified using the substitution (A.2) and similarly for $a(r)$, and then split into four first order equations, defining $P \equiv F'$ and $q \equiv a'$. The iterative algorithm is not very different from the previous case: one defines four quantities E_F, E_P, E_a and E_q which have to be equally zero for the differential equation to be solved. Each of these four quantities can be computed locally on a one-dimensional lattice in terms of F, P, a and q evaluated at the nearest-neighbours sites only. The transformation rules of E_F, E_P, E_a and E_q under small corrections ΔF_k, ΔP_k, Δa_k and Δq_k determines a linear system of $4N + 4$ equations, which can be written in a similar form as before. The main difference is that the blocks S_k of the matrix S as defined in (A.20) are now 4×8 dimensional. The initial guess for F is taken as above, while for a we choose the constant value $a = 0$. A slowing factor $\zeta = 0.3$ is found empirically to improve the convergence of the method. The result of the algorithm after every fifth iteration in given in Table A.3. Although the required number of iterations might be larger than for a single differential equation, the whole process is still very efficient: the two cases $e = 0.5$, $\omega = 0$ and $e = 5$, $\omega = -1.13$ require respectively around 250 ms and 100 ms of CPU time and yield very precise results.

A.3 Relaxation method in two dimensions

The last numerical issue that we have to face is to solve system of differential equations of two variables, as required to minimise eq. (4.147). In principle, the relaxation method defined above could be use: the only difference is that the lattice has to be two dimensional, since the functions depends now on two variables. The compactification to a finite interval does not require a different treatment than above. They are however two issues associated with the relaxation method in two dimensions: first, the second-order equations contain both second order derivatives with respect to one variable and partial derivatives with respect to two different variables, so they cannot be simply split into a certain number of first-order equations; second, the local definition of partial derivatives requires using nearest-neighbours sites in two directions on the lattice, so that if a linearised version of the differential equation can be written as in eq. (A.17), the matrix S would not be quasi-diagonal, but would include "fringes", i.e. be of the form

$$S \sim \left(\begin{array}{cc|cc} \bullet & \bullet & \bullet & \\ \bullet & \bullet\ \bullet & & \bullet & \\ & \bullet\ \bullet\ \bullet & & & \bullet \\ & \bullet\ \bullet\ \bullet & & & \ddots \\ & \bullet\ \bullet & & & \\ \hline \bullet & & \bullet & \bullet & \\ & \bullet & \bullet & \bullet\ \bullet & \\ & \bullet & & \bullet\ \bullet\ \bullet & \\ & \bullet & & \bullet\ \bullet & \ddots \\ & \ddots & & \ddots & \ddots \end{array}\right), \qquad \text{(A.27)}$$

where the dots represent non-zero entries. Efficient algorithms to solve linear systems of this kind exist, so the relaxation method described in the previous section could in principle be applied to solve two-dimensional systems of differential equations. However, in practice this would be very complicated, due to the very high complexity of the entries of this matrix S. Already the Euler-Lagrange equations derived from (4.147) are difficult to treat: they can be written

$$
\begin{aligned}
&2\sin^2 G\left(r^2\sin\theta+\frac{\sin^2 2F\sin^2 G}{\sin\theta}\right)\nabla^2 F+\frac{1}{2}\sin 2F\sin 2G\left(r^2\sin\theta+4\frac{\sin^2 F\sin^2 G}{\sin\theta}\right)\nabla^2 G\\
&+8\sin\theta\sin^4 F\sin^2 G\left[\partial_r^2 F(\partial_\theta G)^2+\partial_\theta^2 F(\partial_r G)^2+(\partial_r F\partial_\theta G+\partial_\theta F\partial_r G)\partial_r\partial_\theta G-\partial_r F\partial_\theta^2 G\partial_r G-\partial_\theta F\partial_r^2 G\partial_\theta G-2\partial_r\partial_\theta F\partial_r G\partial_\theta G\right]\\
&+2\frac{\sin 4F\sin^4 G}{\sin\theta}(\nabla F)^2+\sin 2F\sin^2 G\left(-r^2\sin\theta(1+2\sin^2 F)+4\frac{\sin^2 F\cos 2G}{\sin\theta}\right)(\nabla G)^2\\
&+2\sin 2G\left(r^2\sin\theta+2\frac{\sin^2 2F\sin^2 G}{\sin\theta}\right)\nabla F\cdot\nabla G+4r\sin\theta\sin^2 G\,\partial_r F+r\sin\theta\sin 2F\sin 2G\,\partial_r G\\
&+2\cos\theta\sin^2 G\left(1-\frac{\sin^2 2F\sin^2 G}{r^2\sin^2\theta}\right)\partial_\theta F+\frac{1}{2}\cos\theta\sin 2F\sin 2G\left(1-4\frac{\sin^2 F\sin^2 G}{r^2\sin\theta}\right)\partial_\theta G-\sin 2F\sin^2 G\frac{1-2\sin^2 F\sin^2 G}{\sin\theta}\\
&-8r\cos\theta\sin^4 F\sin^2 G\,(\nabla F\times\nabla G)\,\partial_r G+8r^2\sin\theta\sin 2F\sin^2 F\sin^2 G\,(\nabla F\times\nabla G)^2=0,
\end{aligned}
\tag{A.28}
$$

$$
\begin{aligned}
&2\sin^2 F\left(r^2\sin\theta(1-\cos^2 F\sin^2 G)+\frac{\sin^2 F\sin^2 2G}{\sin\theta}\right)\nabla^2 G+\frac{1}{2}\sin 2F\sin 2G\left(r^2\sin\theta+4\frac{\sin^2 F\sin^2 G}{\sin\theta}\right)\nabla^2 F\\
&+8\sin\theta\sin^4 F\sin^2 G\left[\partial_r^2 G(\partial_\theta F)^2+\partial_\theta^2 G(\partial_r F)^2+(\partial_r G\partial_\theta F+\partial_\theta G\partial_r F)\partial_r\partial_\theta F-\partial_r G\partial_\theta^2 F\partial_r F-\partial_\theta G\partial_r^2 F\partial_\theta F-2\partial_r\partial_\theta G\partial_r F\partial_\theta F\right]\\
&+\sin^2 F\sin 2G\left(-r^2\sin\theta\cos^2 F+4\frac{\sin^2 F\cos 2G}{\sin\theta}\right)(\nabla G)^2+2\sin^2 F\sin 2G\left(-r^2\sin\theta+2\frac{\cos 2F\sin^2 G}{\sin\theta}\right)(\nabla F)^2\\
&+2\sin 2F\left(r^2\sin\theta(1-\cos 2F\sin^2 G)+2\frac{\sin^2 F\sin^2 2G}{\sin\theta}\right)\nabla G\cdot\nabla F+\frac{1}{2}\cos\theta\sin 2F\sin 2G\left(1-4\frac{\sin^2 F\sin^2 G}{r^2\sin\theta}\right)\partial_\theta F\\
&+4r\sin\theta\sin^2 F\left(1-\cos^2 F\sin^2 G\right)\partial_r G+r\sin\theta\sin 2F\sin 2G\,\partial_r F+2\cos\theta\sin^2 F\left(1-\cos^2 F\sin^2 G-\frac{\sin^2 F\sin^2 2G}{r^2\sin^2\theta}\right)\partial_\theta G\\
&+8r\cos\theta\sin^4 F\sin^2 G\,(\nabla F\times\nabla G)\,\partial_r F+4r^2\sin\theta\sin^4 F\sin 2G\,(\nabla F\times\nabla G)^2-\sin^2 F\sin 2G\frac{1-2\sin^2 F\sin^2 G}{\sin\theta}=0,
\end{aligned}
\tag{A.29}
$$

where $\nabla = \left(\partial_r, \frac{1}{r}\partial_\theta\right)$ denotes the gradient in cylindrical coordinates, i.e.

$$\nabla^2 F = \partial_r^2 F + \frac{1}{r^2}\partial_\theta^2 F, \tag{A.30}$$

$$\nabla F \cdot \nabla G = \partial_r F \partial_r G + \frac{1}{r^2}\partial_\theta F \partial_\theta G, \tag{A.31}$$

and the cross-product is defined so that

$$\nabla F \times \nabla G = \frac{1}{r}\left(\partial_r F \partial_\theta G - \partial_\theta F \partial_r G\right). \tag{A.32}$$

Due to the complexity of the two equations to solve, we choose to use a much simpler version of the relaxation algorithm, for which we do not need to compute the coefficient of the S matrix: at each iteration, the values of F_k and G_k at each lattice point are corrected proportionally to the quantities $E_{F,G}(y_k, \theta_k)$ defined as the left-hand side of equations (A.28) and (A.29), as

$$F_k^{(t+1)} = F_k^{(t)} + \varepsilon\, E_F^{(t)}(y_l, \theta_l)_k, \tag{A.33}$$

$$G_k^{(t+1)} = G_k^{(t)} + \varepsilon\, E_F^{(t)}(y_l, \theta_l)_k, \tag{A.34}$$

where ε is a tiny quantity fixing the size of the step. The profile functions F and G are expected to reach a stable point after a large number of iterations, which means in turn that the corrections $E_{F,G}(y_k, \theta_k)$ are zero, i.e. the equation is solved. The difficulty of this method is to choose the coefficient ε appropriately: if it is too large, the method does not converge; conversely, if it is taken too small, the convergence is very slow. In a similar fashion to the one-dimensional relaxation method, we can expand the value of $E_{F,G}$ after $(t+1)$ iterations as a Taylor series in ε, as long as this ε is small enough:

$$E_F^{(t+1)}(y_l, \theta_l) \cong E_F^{(t)}(y_l, \theta_l) + \varepsilon\, b_F(y_l, \theta_l), \tag{A.35}$$

$$E_G^{(t+1)}(y_l, \theta_l) \cong E_G^{(t)}(y_l, \theta_l) + \varepsilon\, b_G(y_l, \theta_l), \tag{A.36}$$

where

$$b_{F,k} = \sum_l \left[\frac{\partial E_{F,k}}{\partial F_l} E_{F,l} + \frac{\partial E_{F,k}}{\partial G_l} E_{G,l}\right], \tag{A.37}$$

$$b_{G,k} = \sum_l \left[\frac{\partial E_{G,k}}{\partial F_l} E_{F,l} + \frac{\partial E_{G,k}}{\partial G_l} E_{G,l}\right]. \tag{A.38}$$

The sum over all lattice sites can be avoided, since only nearest-neighbours

give a non-zero contribution. Writing it explicitly, we obtain

$$\begin{aligned} b_{F,k} = & \left(\frac{\partial E_F}{\partial F}\right)_k E_{F,k} + \left(\frac{\partial E_F}{\partial(\partial_r F)}\right)_k \partial_r E_{F,k} + \left(\frac{\partial E_F}{\partial(\partial_\theta F)}\right)_k \partial_\theta E_{F,k} \\ & + \left(\frac{\partial E_F}{\partial(\partial_r^2 F)}\right)_k \partial_r^2 E_{F,k} + \left(\frac{\partial E_F}{\partial(\partial_\theta^2 F)}\right)_k \partial_\theta^2 E_{F,k} \\ & + \left(\frac{\partial E_F}{\partial(\partial_r \partial_\theta F)}\right)_k \partial_r \partial_\theta E_{F,k} \\ & + \left(\frac{\partial E_F}{\partial G}\right)_k E_{G,k} + \left(\frac{\partial E_F}{\partial(\partial_r G)}\right)_k \partial_r E_{G,k} + \left(\frac{\partial E_F}{\partial(\partial_\theta G)}\right)_k \partial_\theta E_{G,k} \\ & + \left(\frac{\partial E_F}{\partial(\partial_r^2 G)}\right)_k \partial_r^2 E_{G,k} + \left(\frac{\partial E_F}{\partial(\partial_\theta^2 G)}\right)_k \partial_\theta^2 E_{G,k} \\ & + \left(\frac{\partial E_F}{\partial(\partial_r \partial_\theta G)}\right)_k \partial_r \partial_\theta E_{G,k}, \end{aligned} \tag{A.39}$$

and similarly for b_G, with the partial derivatives of E_F being replaced by partial derivatives of E_G. For simplicity, we use an different error estimate than the one of eq. (A.23), namely at step t,

$$\xi^{(t)} = \frac{1}{N_r N_\theta} \left[\sum_k \left(E_F^{(t)}(y_k, \theta_k)^2 + E_G^{(t)}(y_k, \theta_k)^2 \right) \right]^{1/2}. \tag{A.40}$$

Given a certain configuration at the step t, the error at step $t+1$ is then minimised when ε satisfies the condition

$$\varepsilon^{(t)} = - \left[\sum_k \left(E_{F,k} b_{F,k} + E_{G,k} b_{G,k} \right) \right] / \left[\sum_l \left(b_{F,l}^2 + b_{G,l}^2 \right) \right]. \tag{A.41}$$

The evaluation of $E_{F,G}$ and specially of $b_{F,G}$ at each step requires a large number of operations, but is however much easier to implement than the method of the last section, which required solving a linear system of equations. The solving process requires here a very large number of iterations, and the convergence is really slow and not guaranteed. We therefore proceed with the following strategy. First, an initial guess is made, namely $F(y, \theta) = \pi - 2y$ and $G(y, \theta) = \theta$, and the solving algorithm is then applied on a small lattice of size 20×20, until the error estimate (A.40) is sufficiently small and does not significantly decrease after more iterations. In our case, this required about 3 million of iterations, performed in about 15 minutes on a single CPU, until the error estimate was about $\xi \cong 8 \cdot 10^{-6}$. As a second step, the approximate solution obtained with this 20×20 was used to generate an initial guess on a larger lattice of size 50×50, where the solving procedure was then applied. The run took 28 hours of CPU time until a good precision is achieved. We then increased the lattice size

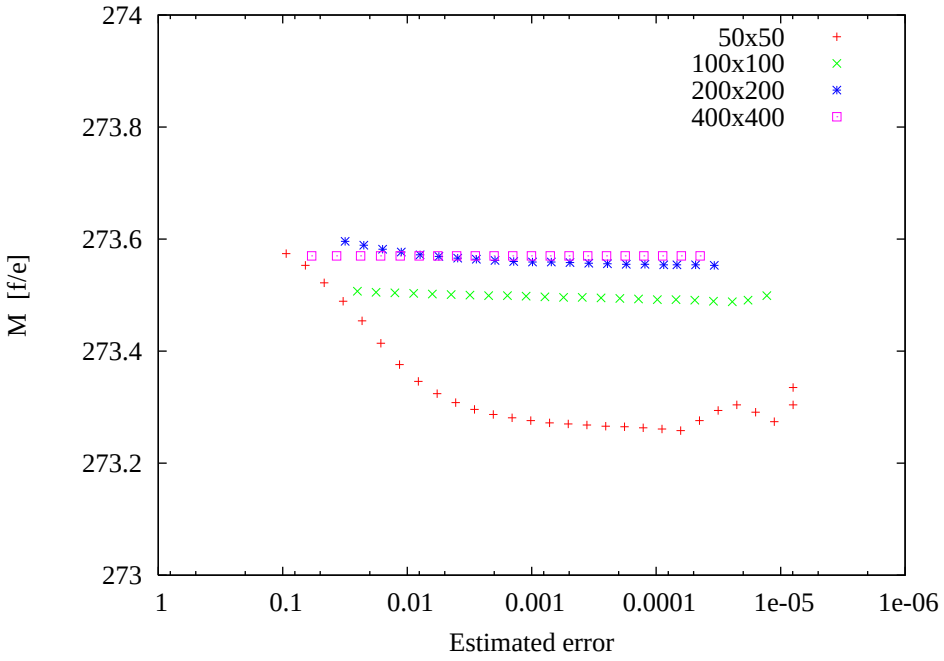

Figure A.4: The energy defined by eq. (4.147) as a function of the error estimate (A.40) for different lattice sizes.

recursively to 100×100, 200×200 and finally 400×400. The results are shown on Figure A.4. As one can see, the numerical solutions converge to a point located around 273.55 ± 0.1 with increasing lattice size.

Bibliography

[1] M. Gillioz, "A Light composite Higgs boson facing electroweak precision tests," *Phys.Rev.* D80 (2009) 055003, arXiv:0806.3450.

[2] M. Gillioz, R. Grober, C. Grojean, M. Muhlleitner, and E. Salvioni, "Higgs Low-Energy Theorem (and its corrections) in Composite Models," arXiv:1206.7120.

[3] M. Gillioz, "Classical skyrmions in SU(N)/SO(N) cosets," *JHEP* 1109 (2011) 014, arXiv:1103.5990.

[4] M. Gillioz, "Dangerous Skyrmions in Little Higgs Models," *JHEP* 1202 (2012) 121, arXiv:1111.2047.

[5] M. Gillioz, A. von Manteuffel, P. Schwaller, and D. Wyler, "The Little Skyrmion: New Dark Matter for Little Higgs Models," *JHEP* 1103 (2011) 048, arXiv:1012.5288.

[6] S. Glashow, "Partial Symmetries of Weak Interactions," *Nucl.Phys.* 22 (1961) 579–588.

[7] S. Weinberg, "A Model of Leptons," *Phys.Rev.Lett.* 19 (1967) 1264–1266.

[8] A. Salam, "Weak and Electromagnetic Interactions," *Conf.Proc.* C680519 (1968) 367–377.

[9] M. E. Peskin and D. V. Schroeder, "An Introduction to quantum field theory," *Addison-Wesley Advanced Book Program* (1995).

[10] L. H. Ryder, "Quantum Field Theory," *Cambridge Univ. Pr.* (1985).

[11] S. Weinberg, "The Quantum theory of fields. Vol. 1: Foundations," *Cambridge Univ. Pr.* (1995).

[12] S. Weinberg, "The quantum theory of fields. Vol. 2: Modern applications," *Cambridge Univ. Pr.* (1996).

[13] H. Georgi, "Lie Algebras in Particle Physics. From Isospin to Unified Theories," *Front.Phys.* 54 (1982).

[14] H. Weigel, "Chiral Soliton Models for Baryons," *Lect. Notes Phys.* 743 (2008) 1–274.

[15] J. Santiago, "The Physics of Electroweak Symmetry Breaking," lectures given at the ETH Zurich, `www.ugr.es/~jsantiago/PoEWSBLectures.pdf`.

[16] R. Contino, "Composite Higgs Models," School on Strongly Coupled Physics Beyond the Standard Model, ICTP Trieste, `http://cdsagenda5.ictp.it/full_display.php?ida=a11150`.

[17] S. Willenbrock, "Symmetries of the standard model," `arXiv:hep-ph/0410370`, lectures presented at TASI 2004.

[18] T. Schwetz, "Neutrino physics: A theoretical review," *PoS* FPCP2010 (2010) 051.

[19] S. Davidson, E. Nardi, and Y. Nir, "Leptogenesis," *Phys.Rept.* 466 (2008) 105–177, `arXiv:0802.2962`.

[20] M. Dine, "TASI lectures on the strong CP problem," `arXiv:hep-ph/0011376`.

[21] C.-N. Yang and R. L. Mills, "Conservation of Isotopic Spin and Isotopic Gauge Invariance," *Phys.Rev.* 96 (1954) 191–195.

[22] A. Belavin, A. M. Polyakov, A. Schwartz, and Y. Tyupkin, "Pseudoparticle Solutions of the Yang-Mills Equations," *Phys.Lett.* B59 (1975) 85–87.

[23] G. 't Hooft, "Symmetry breaking through Bell-Jackiw anomalies," *Phys. Rev. Lett.* 37 (1976) 8–11.

[24] S. L. Adler, "Axial vector vertex in spinor electrodynamics," *Phys.Rev.* 177 (1969) 2426–2438.

[25] J. Bell and R. Jackiw, "A PCAC puzzle: $\pi^0 \to \gamma\gamma$ in the σ model," *Nuovo Cim.* A60 (1969) 47–61.

[26] S. R. Coleman and E. J. Weinberg, "Radiative Corrections as the Origin of Spontaneous Symmetry Breaking," *Phys.Rev.* D7 (1973) 1888–1910.

[27] N. Cabibbo, "Unitary Symmetry and Leptonic Decays," *Phys.Rev.Lett.* 10 (1963) 531–533.

[28] M. Kobayashi and T. Maskawa, "CP Violation in the Renormalizable Theory of Weak Interaction," *Prog.Theor.Phys.* 49 (1973) 652–657.

[29] B. W. Lee, C. Quigg, and H. Thacker, "The Strength of Weak Interactions at Very High-Energies and the Higgs Boson Mass," *Phys.Rev.Lett.* 38 (1977) 883–885.

[30] B. W. Lee, C. Quigg, and H. Thacker, "Weak Interactions at Very High-Energies: The Role of the Higgs Boson Mass," *Phys.Rev.* D16 (1977) 1519.

[31] J. M. Cornwall, D. N. Levin, and G. Tiktopoulos, "Derivation of Gauge Invariance from High-Energy Unitarity Bounds on the s Matrix," *Phys.Rev.* D10 (1974) 1145.

[32] R. Contino, C. Grojean, M. Moretti, F. Piccinini, and R. Rattazzi, "Strong Double Higgs Production at the LHC," *JHEP* 1005 (2010) 089, `arXiv:1002.1011`.

[33] A. Falkowski, S. Rychkov, and A. Urbano, "What if the Higgs couplings to W and Z bosons are larger than in the Standard Model?," `arXiv:1202.1532`.

[34] A. Azatov, R. Contino, and J. Galloway, "Model-Independent Bounds on a Light Higgs," `arXiv:1202.3415`.

[35] J. Espinosa, C. Grojean, M. Muhlleitner, and M. Trott, "Fingerprinting Higgs Suspects at the LHC," `arXiv:1202.3697`.

[36] G. 't Hooft, "Renormalizable Lagrangians for Massive Yang-Mills Fields," *Nucl.Phys.* B35 (1971) 167–188.

[37] P. W. Anderson, "Plasmons, Gauge Invariance, and Mass," *Phys.Rev.* 130 (1963) 439–442.

[38] F. Englert and R. Brout, "Broken Symmetry and the Mass of Gauge Vector Mesons," *Phys.Rev.Lett.* 13 (1964) 321–322.

[39] P. W. Higgs, "Broken Symmetries and the Masses of Gauge Bosons," *Phys.Rev.Lett.* 13 (1964) 508–509.

[40] G. Guralnik, C. Hagen, and T. Kibble, "Global Conservation Laws and Massless Particles," *Phys.Rev.Lett.* 13 (1964) 585–587.

[41] P. W. Higgs, "Spontaneous Symmetry Breakdown without Massless Bosons," *Phys.Rev.* 145 (1966) 1156–1163.

[42] J. Davis, Raymond, D. S. Harmer, and K. C. Hoffman, "Search for neutrinos from the sun," *Phys.Rev.Lett.* 20 (1968) 1205–1209.

[43] V. Gribov and B. Pontecorvo, "Neutrino astronomy and lepton charge," *Phys.Lett.* B28 (1969) 493.

[44] Particle Data Group, K. Nakamura *et al.*, "Review of particle physics," *J.Phys.G* G37 (2010) 075021.

[45] P. Minkowski, "$\mu \to e\gamma$ at a Rate of One Out of 1-Billion Muon Decays?," *Phys.Lett.* B67 (1977) 421.

[46] S. Weinberg, "Baryon and Lepton Nonconserving Processes," *Phys.Rev.Lett.* 43 (1979) 1566–1570.

[47] M. Magg and C. Wetterich, "Neutrino Mass Problem and Gauge Hierarchy," *Phys.Lett.* B94 (1980) 61.

[48] R. Foot, H. Lew, X. He, and G. C. Joshi, "Seesaw Neutrino Masses Induced by a Triplet of Leptons," *Z.Phys.* C44 (1989) 441.

[49] T. Asaka, S. Blanchet, and M. Shaposhnikov, "The nuMSM, dark matter and neutrino masses," *Phys.Lett.* B631 (2005) 151–156, `arXiv:hep-ph/0503065`.

[50] S. Dodelson and L. M. Widrow, "Sterile-neutrinos as dark matter," *Phys.Rev.Lett.* 72 (1994) 17–20, `arXiv:hep-ph/9303287`.

[51] F. Bezrukov and M. Shaposhnikov, "The Standard Model Higgs boson as the inflaton," *Phys.Lett.* B659 (2008) 703–706, `arXiv:0710.3755`.

[52] K. Griest and M. Kamionkowski, "Unitarity Limits on the Mass and Radius of Dark Matter Particles," *Phys.Rev.Lett.* 64 (1990) 615.

[53] A. Sakharov, "Violation of CP Invariance, c Asymmetry, and Baryon Asymmetry of the Universe," *Pisma Zh.Eksp.Teor.Fiz.* 5 (1967) 32–35.

[54] M. Fukugita and T. Yanagida, "Baryogenesis Without Grand Unification," *Phys.Lett.* B174 (1986) 45.

[55] R. Crewther, P. Di Vecchia, G. Veneziano, and E. Witten, "Chiral Estimate of the Electric Dipole Moment of the Neutron in Quantum Chromodynamics," *Phys.Lett.* B88 (1979) 123.

[56] R. Peccei and H. R. Quinn, "CP Conservation in the Presence of Instantons," *Phys.Rev.Lett.* 38 (1977) 1440–1443.

[57] H. Georgi and S. Glashow, "Unity of All Elementary Particle Forces," *Phys.Rev.Lett.* 32 (1974) 438–441.

[58] G. 't Hooft, "Magnetic monopoles in unified gauge theories," *Nucl. Phys.* B79 (1974) 276–284.

[59] A. M. Polyakov, "Particle spectrum in quantum field theory," *JETP Lett.* 20 (1974) 194–195.

[60] J. C. Pati and A. Salam, "Lepton Number as the Fourth Color," *Phys.Rev.* D10 (1974) 275–289.

[61] H. Fritzsch and P. Minkowski, "Unified Interactions of Leptons and Hadrons," *Annals Phys.* 93 (1975) 193–266.

[62] S. Rychkov, "Higgs boson and compositeness," lectures on BSM Physics, Pauli Center for Theoretical Studies, ETH Zurich, `http://www.phys.ethz.ch/~banfi/bsmphysics/program.html`.

[63] E. Farhi and L. Susskind, "Technicolor," *Phys.Rept.* 74 (1981) 277.

[64] R. Contino, "The Higgs as a Composite Nambu-Goldstone Boson," `arXiv:1005.4269`, lectures presented at TASI 2009.

[65] R. Barbieri, "Electroweak precision tests: what do we learn?," *Lectures given at the Cargèse Summer School* (1992) CERN–TH–6659–92.

[66] R. Barbieri, "Ten Lectures on the ElectroWeak Interactions," `arXiv:0706.0684`.

[67] R. Sundrum, "Tasi 2004 lectures: To the fifth dimension and back," `arXiv:hep-th/0508134`.

[68] D. Gross and F. Wilczek, "Ultraviolet Behavior of Nonabelian Gauge Theories," *Phys.Rev.Lett.* 30 (1973) 1343–1346.

[69] H. Politzer, "Reliable Perturbative Results for Strong Interactions?," *Phys.Rev.Lett.* 30 (1973) 1346–1349.

[70] M. Gell-Mann, "A Schematic Model of Baryons and Mesons," *Phys.Lett.* 8 (1964) 214–215.

[71] G. Zweig, "An SU(3) model for strong interaction symmetry and its breaking 2," Published in 'Developments in the Quark Theory of Hadrons'. Volume 1. Edited by D. Lichtenberg and S. Rosen. Nonantum, Mass., Hadronic Press, 1980. pp. 22-101.

[72] G. 't Hooft, "A Planar Diagram Theory for Strong Interactions," *Nucl.Phys.* B72 (1974) 461.

[73] E. Witten, "Baryons in the 1/n Expansion," *Nucl.Phys.* B160 (1979) 57.

[74] Y. Nambu and G. Jona-Lasinio, "Dynamical Model of Elementary Particles Based on an Analogy with Superconductivity. I.," *Phys.Rev.* 122 (1961) 345–358.

[75] E. Witten, "Instantons, the Quark Model, and the 1/n Expansion," *Nucl.Phys.* B149 (1979) 285.

[76] S. R. Coleman, J. Wess, and B. Zumino, "Structure of phenomenological Lagrangians. 1.," *Phys.Rev.* 177 (1969) 2239–2247.

[77] J. Callan, Curtis G., S. R. Coleman, J. Wess, and B. Zumino, "Structure of phenomenological Lagrangians. 2.," *Phys.Rev.* 177 (1969) 2247–2250.

[78] M. A. Shifman, A. Vainshtein, and V. I. Zakharov, "QCD and Resonance Physics. Sum Rules," *Nucl.Phys.* B147 (1979) 385–447.

[79] S. Weinberg, "Precise relations between the spectra of vector and axial vector mesons," *Phys.Rev.Lett.* 18 (1967) 507–509.

[80] E. Witten, "Some Inequalities Among Hadron Masses," *Phys.Rev.Lett.* 51 (1983) 2351.

[81] T. Das, G. Guralnik, V. Mathur, F. Low, and J. Young, "Electromagnetic mass difference of pions," *Phys.Rev.Lett.* 18 (1967) 759–761.

[82] J. Wess and B. Zumino, "Consequences of anomalous Ward identities," *Phys. Lett.* B37 (1971) 95.

[83] E. Witten, "Global Aspects of Current Algebra," *Nucl. Phys.* B223 (1983) 422–432.

[84] Y. Nambu and G. Jona-Lasinio, "Dynamical Model of Elementary Particles Based on an Analogy with Superconductivity. II," *Phys.Rev.* 124 (1961) 246–254.

[85] S. Weinberg, "Implications of Dynamical Symmetry Breaking," *Phys.Rev.* D13 (1976) 974–996.

[86] L. Susskind, "Dynamics of Spontaneous Symmetry Breaking in the Weinberg-Salam Theory," *Phys.Rev.* D20 (1979) 2619–2625.

[87] S. Dimopoulos and L. Susskind, "Mass Without Scalars," *Nucl.Phys.* B155 (1979) 237–252.

[88] E. Eichten and K. D. Lane, "Dynamical Breaking of Weak Interaction Symmetries," *Phys.Lett.* B90 (1980) 125–130.

[89] B. Holdom, "Raising the Sideways Scale," *Phys.Rev.* D24 (1981) 1441.

[90] T. Banks and A. Zaks, "On the Phase Structure of Vector-Like Gauge Theories with Massless Fermions," *Nucl.Phys.* B196 (1982) 189.

[91] R. Rattazzi, V. S. Rychkov, E. Tonni, and A. Vichi, "Bounding scalar operator dimensions in 4D CFT," *JHEP* 0812 (2008) 031, arXiv:0807.0004.

[92] V. S. Rychkov and A. Vichi, "Universal Constraints on Conformal Operator Dimensions," *Phys.Rev.* D80 (2009) 045006, arXiv:0905.2211.

[93] D. Poland, D. Simmons-Duffin, and A. Vichi, "Carving Out the Space of 4D CFTs," arXiv:1109.5176.

[94] C. T. Hill, "Topcolor: Top quark condensation in a gauge extension of the standard model," *Phys.Lett.* B266 (1991) 419–424.

[95] C. T. Hill, "Topcolor assisted technicolor," *Phys.Lett.* B345 (1995) 483–489, arXiv:hep-ph/9411426.

[96] V. Miransky, M. Tanabashi, and K. Yamawaki, "Is the t Quark Responsible for the Mass of W and Z Bosons?," *Mod.Phys.Lett.* A4 (1989) 1043.

[97] V. Miransky, M. Tanabashi, and K. Yamawaki, "Dynamical Electroweak Symmetry Breaking with Large Anomalous Dimension and t Quark Condensate," *Phys.Lett.* B221 (1989) 177.

[98] W. A. Bardeen, C. T. Hill, and M. Lindner, "Minimal Dynamical Symmetry Breaking of the Standard Model," *Phys.Rev.* D41 (1990) 1647.

[99] M. E. Peskin and T. Takeuchi, "A New constraint on a strongly interacting Higgs sector," *Phys. Rev. Lett.* 65 (1990) 964–967.

[100] R. Barbieri, A. Pomarol, R. Rattazzi, and A. Strumia, "Electroweak symmetry breaking after LEP-1 and LEP-2," *Nucl.Phys.* B703 (2004) 127–146, arXiv:hep-ph/0405040.

[101] R. Barbieri, M. Beccaria, P. Ciafaloni, G. Curci, and A. Vicere, "Two loop heavy top effects in the Standard Model," *Nucl.Phys.* B409 (1993) 105–127.

[102] M. Veltman, "Limit on Mass Differences in the Weinberg Model," *Nucl.Phys.* B123 (1977) 89.

[103] M. E. Peskin and T. Takeuchi, "Estimation of oblique electroweak corrections," *Phys. Rev.* D46 (1992) 381–409.

[104] G. D. Kribs, T. Plehn, M. Spannowsky, and T. M. Tait, "Four generations and Higgs physics," *Phys.Rev.* D76 (2007) 075016, arXiv:0706.3718.

[105] H. Georgi, "Effective field theory and electroweak radiative corrections," *Nucl.Phys.* B363 (1991) 301–325.

[106] M. Veltman, "Second Threshold in Weak Interactions," *Acta Phys.Polon.* B8 (1977) 475.

[107] G. Altarelli and R. Barbieri, "Vacuum polarization effects of new physics on electroweak processes," *Phys.Lett.* B253 (1991) 161–167.

[108] G. Altarelli, R. Barbieri, and S. Jadach, "Toward a model independent analysis of electroweak data," *Nucl.Phys.* B369 (1992) 3–32.

[109] ALEPH Collaboration, DELPHI Collaboration, L3 Collaboration, OPAL Collaboration, SLD Collaboration, LEP Electroweak Working Group, SLD Electroweak Group, SLD Heavy Flavour Group, "Precision electroweak measurements on the Z resonance," *Phys.Rept.* 427 (2006) 257–454, arXiv:hep-ex/0509008.

[110] K. Agashe and R. Contino, "The Minimal composite Higgs model and electroweak precision tests," *Nucl.Phys.* B742 (2006) 59–85, arXiv:hep-ph/0510164.

[111] G. Montagna, O. Nicrosini, F. Piccinini, and G. Passarino, "TOPAZ0 4.0: A New version of a computer program for evaluation of deconvoluted and realistic observables at LEP-1 and LEP-2," *Comput.Phys.Commun.* 117 (1999) 278–289, arXiv:hep-ph/9804211.

[112] G. Altarelli, R. Barbieri, and F. Caravaglios, "Nonstandard analysis of electroweak precision data," *Nucl.Phys.* B405 (1993) 3–23.

[113] CDF Collaboration, T. Aaltonen *et al.*, "Precise measurement of the W-boson mass with the CDF II detector," *Phys.Rev.Lett.* 108 (2012) 151803, arXiv:1203.0275.

[114] D0 Collaboration, V. M. Abazov *et al.*, "Measurement of the W Boson Mass with the D0 Detector," *Phys.Rev.Lett.* 108 (2012) 151804, arXiv:1203.0293.

[115] Tevatron Electroweak Working Group, "2012 Update of the Combination of CDF and D0 Results for the Mass of the W Boson," arXiv:1204.0042.

[116] P. Sikivie, L. Susskind, M. B. Voloshin, and V. I. Zakharov, "Isospin Breaking in Technicolor Models," *Nucl.Phys.* B173 (1980) 189.

[117] M. A. Luty and T. Okui, "Conformal technicolor," *JHEP* 0609 (2006) 070, arXiv:hep-ph/0409274.

[118] F. Sannino and K. Tuominen, "Orientifold theory dynamics and symmetry breaking," *Phys.Rev.* D71 (2005) 051901, arXiv:hep-ph/0405209.

[119] T. A. Ryttov and F. Sannino, "Ultra Minimal Technicolor and its Dark Matter TIMP," *Phys.Rev.* D78 (2008) 115010, arXiv:0809.0713.

[120] D. B. Kaplan and H. Georgi, "SU(2) x U(1) Breaking by Vacuum Misalignment," *Phys.Lett.* B136 (1984) 183.

[121] D. B. Kaplan, H. Georgi, and S. Dimopoulos, "Composite Higgs Scalars," *Phys. Lett.* B136 (1984) 187.

[122] H. Georgi and D. B. Kaplan, "Composite Higgs and Custodial SU(2)," *Phys. Lett.* B145 (1984) 216.

[123] J. Mrazek, A. Pomarol, R. Rattazzi, M. Redi, J. Serra, *et al.*, "The Other Natural Two Higgs Doublet Model," *Nucl.Phys.* B853 (2011) 1–48, arXiv:1105.5403.

[124] B. Gripaios, A. Pomarol, F. Riva, and J. Serra, "Beyond the Minimal Composite Higgs Model," *JHEP* 0904 (2009) 070, arXiv:0902.1483.

[125] B. Bellazzini, C. Csaki, A. Falkowski, and A. Weiler, "Buried Higgs," *Phys.Rev.* D80 (2009) 075008, arXiv:0906.3026.

[126] B. Bellazzini, C. Csaki, A. Falkowski, and A. Weiler, "Charming Higgs," *Phys.Rev.* D81 (2010) 075017, arXiv:0910.3210.

[127] M. E. Peskin, "The Alignment of the Vacuum in Theories of Technicolor," *Nucl.Phys.* B175 (1980) 197–233.

[128] J. Preskill, "Subgroup Alignment in Hypercolor Theories," *Nucl.Phys.* B177 (1981) 21–59.

[129] T. Banks, "Constraints on SU(2) x U(1) Breaking by Vacuum Misalignment," *Nucl. Phys.* B243 (1984) 125.

[130] M. J. Dugan, H. Georgi, and D. B. Kaplan, "Anatomy of a Composite Higgs Model," *Nucl.Phys.* B254 (1985) 299.

[131] K. Agashe, R. Contino, and A. Pomarol, "The Minimal composite Higgs model," *Nucl.Phys.* B719 (2005) 165–187, arXiv:hep-ph/0412089.

[132] T. Kaluza, "On the Problem of Unity in Physics," *Sitzungsber.Preuss.Akad.Wiss.Berlin (Math.Phys.)* (1921) 966–972.

[133] O. Klein, "Quantum Theory and Five-Dimensional Theory of Relativity. (In German and English)," *Z.Phys.* 37 (1926) 895–906.

[134] J. M. Maldacena, "The Large N limit of superconformal field theories and supergravity," *Adv.Theor.Math.Phys.* 2 (1998) 231–252, arXiv:hep-th/9711200.

[135] S. Gubser, I. R. Klebanov, and A. M. Polyakov, "Gauge theory correlators from noncritical string theory," *Phys.Lett.* B428 (1998) 105–114, arXiv:hep-th/9802109.

[136] E. Witten, "Anti-de Sitter space and holography," *Adv.Theor.Math.Phys.* 2 (1998) 253–291, arXiv:hep-th/9802150.

[137] D. Son and M. Stephanov, "QCD and dimensional deconstruction," *Phys.Rev.* D69 (2004) 065020, arXiv:hep-ph/0304182.

[138] J. Erlich, E. Katz, D. T. Son, and M. A. Stephanov, "QCD and a holographic model of hadrons," *Phys.Rev.Lett.* 95 (2005) 261602, arXiv:hep-ph/0501128.

[139] L. Da Rold and A. Pomarol, "Chiral symmetry breaking from five dimensional spaces," *Nucl.Phys.* B721 (2005) 79–97, arXiv:hep-ph/0501218.

[140] H. R. Grigoryan and A. V. Radyushkin, "Form Factors and Wave Functions of Vector Mesons in Holographic QCD," *Phys.Lett.* B650 (2007) 421–427, arXiv:hep-ph/0703069.

[141] H. J. Kwee and R. F. Lebed, "Pion form-factors in holographic QCD," *JHEP* 0801 (2008) 027, arXiv:0708.4054.

[142] V. Rubakov and M. Shaposhnikov, "Do We Live Inside a Domain Wall?," *Phys.Lett.* B125 (1983) 136–138.

[143] N. Arkani-Hamed, S. Dimopoulos, and G. Dvali, "The Hierarchy problem and new dimensions at a millimeter," *Phys.Lett.* B429 (1998) 263–272, arXiv:hep-ph/9803315.

[144] I. Antoniadis, N. Arkani-Hamed, S. Dimopoulos, and G. Dvali, "New dimensions at a millimeter to a Fermi and superstrings at a TeV," *Phys.Lett.* B436 (1998) 257–263, arXiv:hep-ph/9804398.

[145] L. Randall and R. Sundrum, "A Large mass hierarchy from a small extra dimension," *Phys.Rev.Lett.* 83 (1999) 3370–3373, arXiv:hep-ph/9905221.

[146] L. Randall and R. Sundrum, "An Alternative to compactification," *Phys.Rev.Lett.* 83 (1999) 4690–4693, arXiv:hep-th/9906064.

[147] C. Csaki, C. Grojean, H. Murayama, L. Pilo, and J. Terning, "Gauge theories on an interval: Unitarity without a Higgs," *Phys.Rev.* D69 (2004) 055006, arXiv:hep-ph/0305237.

[148] Y. Hosotani, "Dynamical Mass Generation by Compact Extra Dimensions," *Phys.Lett.* B126 (1983) 309.

[149] K. Agashe, A. Delgado, M. J. May, and R. Sundrum, "RS1, custodial isospin and precision tests," *JHEP* 0308 (2003) 050, arXiv:hep-ph/0308036.

[150] R. Contino, Y. Nomura, and A. Pomarol, "Higgs as a holographic pseudoGoldstone boson," *Nucl.Phys.* B671 (2003) 148–174, arXiv:hep-ph/0306259.

[151] D. Becciolini, M. Redi, and A. Wulzer, "AdS/QCD: The Relevance of the Geometry," *JHEP* 1001 (2010) 074, arXiv:0906.4562.

[152] J. A. Cabrer, G. von Gersdorff, and M. Quiros, "Warped Electroweak Breaking Without Custodial Symmetry," *Phys.Lett.* B697 (2011) 208–214, arXiv:1011.2205.

[153] J. A. Cabrer, G. von Gersdorff, and M. Quiros, "Suppressing Electroweak Precision Observables in 5D Warped Models," *JHEP* 1105 (2011) 083, arXiv:1103.1388.

[154] J. A. Cabrer, G. von Gersdorff, and M. Quiros, "Improving Naturalness in Warped Models with a Heavy Bulk Higgs Boson," *Phys.Rev.* D84 (2011) 035024, arXiv:1104.3149.

[155] W. Buchmuller and D. Wyler, "Effective Lagrangian Analysis of New Interactions and Flavor Conservation," *Nucl.Phys.* B268 (1986) 621.

[156] A. Manohar and H. Georgi, "Chiral Quarks and the Nonrelativistic Quark Model," *Nucl.Phys.* B234 (1984) 189.

[157] G. Giudice, C. Grojean, A. Pomarol, and R. Rattazzi, "The Strongly-Interacting Light Higgs," *JHEP* 0706 (2007) 045, arXiv:hep-ph/0703164.

[158] I. Low and A. Vichi, "On the production of a composite Higgs boson," *Phys.Rev.* D84 (2011) 045019, arXiv:1010.2753.

[159] J. R. Ellis, M. K. Gaillard, and D. V. Nanopoulos, "A Phenomenological Profile of the Higgs Boson," *Nucl.Phys.* B106 (1976) 292.

[160] M. A. Shifman, A. Vainshtein, M. Voloshin, and V. I. Zakharov, "Low-Energy Theorems for Higgs Boson Couplings to Photons," *Sov.J.Nucl.Phys.* 30 (1979) 711–716.

[161] B. A. Kniehl and M. Spira, "Low-energy theorems in Higgs physics," *Z.Phys.* C69 (1995) 77–88, arXiv:hep-ph/9505225.

[162] A. Pierce, J. Thaler, and L.-T. Wang, "Disentangling Dimension Six Operators through Di-Higgs Boson Production," *JHEP* 0705 (2007) 070, arXiv:hep-ph/0609049.

[163] I. Low, R. Rattazzi, and A. Vichi, "Theoretical Constraints on the Higgs Effective Couplings," *JHEP* 1004 (2010) 126, arXiv:0907.5413.

[164] A. Falkowski, "Pseudo-goldstone Higgs production via gluon fusion," *Phys.Rev.* D77 (2008) 055018, arXiv:0711.0828.

[165] E. Furlan, "Gluon-fusion Higgs production at NNLO for a non-standard Higgs sector," *JHEP* 1110 (2011) 115, arXiv:1106.4024.

[166] A. Azatov and J. Galloway, "Light Custodians and Higgs Physics in Composite Models," *Phys.Rev.* D85 (2012) 055013, arXiv:1110.5646.

[167] A. Djouadi, W. Kilian, M. Muhlleitner, and P. Zerwas, "Production of neutral Higgs boson pairs at LHC," *Eur.Phys.J.* C10 (1999) 45–49, arXiv:hep-ph/9904287.

[168] A. Djouadi, W. Kilian, M. Muhlleitner, and P. Zerwas, "The Reconstruction of trilinear Higgs couplings," arXiv:hep-ph/0001169.

[169] M. M. Muhlleitner, "Higgs particles in the standard model and supersymmetric theories," arXiv:hep-ph/0008127.

[170] M. Muhlleitner, "Testing Higgs selfcouplings at high-energy linear colliders," arXiv:hep-ph/0101262.

[171] R. Grober and M. Muhlleitner, "Composite Higgs Boson Pair Production at the LHC," *JHEP* 1106 (2011) 020, arXiv:1012.1562.

[172] C. O. Dib, R. Rosenfeld, and A. Zerwekh, "Double Higgs production and quadratic divergence cancellation in little Higgs models with T parity," *JHEP* 0605 (2006) 074, arXiv:hep-ph/0509179.

[173] R. Contino, M. Ghezzi, M. Moretti, G. Panico, F. Piccinini, *et al.*, "Anomalous Couplings in Double Higgs Production," arXiv:1205.5444.

[174] O. Matsedonskyi, G. Panico, and A. Wulzer, "Light Top Partners for a Light Composite Higgs," arXiv:1204.6333.

[175] E. N. Glover and J. van der Bij, "Higgs boson pair production via gluon fusion," *Nucl.Phys.* B309 (1988) 282.

[176] T. Plehn, M. Spira, and P. Zerwas, "Pair production of neutral Higgs particles in gluon-gluon collisions," *Nucl.Phys.* B479 (1996) 46–64, arXiv:hep-ph/9603205.

[177] U. Baur, T. Plehn, and D. L. Rainwater, "Measuring the Higgs boson self coupling at the LHC and finite top mass matrix elements," *Phys.Rev.Lett.* 89 (2002) 151801, arXiv:hep-ph/0206024.

[178] R. Contino, T. Kramer, M. Son, and R. Sundrum, "Warped/composite phenomenology simplified," *JHEP* 0705 (2007) 074, arXiv:hep-ph/0612180.

[179] R. Contino, D. Marzocca, D. Pappadopulo, and R. Rattazzi, "On the effect of resonances in composite Higgs phenomenology," *JHEP* 1110 (2011) 081, arXiv:1109.1570.

[180] R. Contino, L. Da Rold, and A. Pomarol, "Light custodians in natural composite Higgs models," *Phys.Rev.* D75 (2007) 055014, arXiv:hep-ph/0612048.

[181] K. Agashe, R. Contino, L. Da Rold, and A. Pomarol, "A Custodial symmetry for Zb anti-b," *Phys.Lett.* B641 (2006) 62–66, arXiv:hep-ph/0605341.

[182] R. Barbieri, B. Bellazzini, V. S. Rychkov, and A. Varagnolo, "The Higgs boson from an extended symmetry," *Phys.Rev.* D76 (2007) 115008, arXiv:0706.0432.

[183] P. Lodone, "Vector-like quarks in a 'composite' Higgs model," *JHEP* 0812 (2008) 029, arXiv:0806.1472.

[184] C. Anastasiou, E. Furlan, and J. Santiago, "Realistic Composite Higgs Models," *Phys.Rev.* D79 (2009) 075003, arXiv:0901.2117.

[185] CDF and D0 Collaboration, T. E. W. Group, "Combination of CDF and D0 Measurements of the Single Top Production Cross Section," arXiv:0908.2171.

[186] C. Bini, R. Contino, and N. Vignaroli, "Heavy-light decay topologies as a new strategy to discover a heavy gluon," *JHEP* 1201 (2012) 157, arXiv:1110.6058.

[187] CMS Collaboration, "Search for t' pair production in lepton+jets channel," report number CMS-PAS-EXO-11-099.

[188] CMS Collaboration, S. Chatrchyan *et al.*, "Search for heavy, top-like quark pair production in the dilepton final state in *pp* collisions at $\sqrt{s} = 7$ TeV," arXiv:1203.5410.

[189] CMS Collaboration, "Search for a Heavy Bottom-like Quark in pp Collisions at sqrt(s) = 7 TeV," report number CMS-PAS-EXO-11-036.

[190] CMS Collaboration, S. Chatrchyan *et al.*, "Search for heavy bottom-like quarks in 4.9 inverse femtobarns of pp collisions at sqrt(s) = 7 TeV," *JHEP* 1205 (2012) 123, arXiv:1204.1088.

[191] CMS Collaboration, S. Chatrchyan *et al.*, "Search for a Vector-like Quark with Charge 2/3 in t + Z Events from pp Collisions at sqrt(s) = 7 TeV," *Phys.Rev.Lett.* 107 (2011) 271802, arXiv:1109.4985.

[192] ATLAS Collaboration, G. Aad *et al.*, "Search for pair production of a heavy quark decaying to a W boson and a b quark in the lepton+jets channel with the ATLAS detector," arXiv:1202.3076.

[193] ATLAS Collaboration, G. Aad *et al.*, "Search for pair-produced heavy quarks decaying to Wq in the two-lepton channel at sqrt(s) = 7 TeV with the ATLAS detector," arXiv:1202.3389.

[194] ATLAS Collaboration, G. Aad *et al.*, "Search for down-type fourth generation quarks with the ATLAS detector in events with one lepton and high transverse momentum hadronically decaying W bosons in sqrt(s) = 7 TeV pp collisions," arXiv:1202.6540.

[195] ATLAS Collaboration, G. Aad *et al.*, "Search for same-sign top-quark production and fourth-generation down-type quarks in pp

collisions at sqrt(s) = 7 TeV with the ATLAS detector," *JHEP* 1204 (2012) 069, arXiv:1202.5520.

[196] CDF Collaboration, T. Aaltonen *et al.*, "Search for a Heavy Top-Like Quark in $p\overline{p}$ Collisions at $\sqrt{s} = 1.96$ TeV," *Phys.Rev.Lett.* 107 (2011) 261801, arXiv:1107.3875.

[197] CDF Collaboration, T. Aaltonen *et al.*, "Search for heavy bottom-like quarks decaying to an electron or muon and jets in $p\overline{p}$ collisions at $\sqrt{s} = 1.96$ TeV," *Phys.Rev.Lett.* 106 (2011) 141803, arXiv:1101.5728.

[198] M. Aliev, H. Lacker, U. Langenfeld, S. Moch, P. Uwer, *et al.*, "HATHOR: HAdronic Top and Heavy quarks crOss section calculatoR," *Comput.Phys.Commun.* 182 (2011) 1034–1046, arXiv:1007.1327.

[199] A. Martin, W. Stirling, R. Thorne, and G. Watt, "Parton distributions for the LHC," *Eur.Phys.J.* C63 (2009) 189–285, arXiv:0901.0002.

[200] J. Alwall, M. Herquet, F. Maltoni, O. Mattelaer, and T. Stelzer, "MadGraph 5 : Going Beyond," *JHEP* 1106 (2011) 128, arXiv:1106.0522.

[201] G. Dissertori, E. Furlan, F. Moortgat, and P. Nef, "Discovery potential of top-partners in a realistic composite Higgs model with early LHC data," *JHEP* 1009 (2010) 019, arXiv:1005.4414.

[202] N. Vignaroli, "Discovering the composite Higgs through the decay of a heavy fermion," arXiv:1204.0468.

[203] R. Contino and G. Servant, "Discovering the top partners at the LHC using same-sign dilepton final states," *JHEP* 0806 (2008) 026, arXiv:0801.1679.

[204] K. Harigaya, S. Matsumoto, M. M. Nojiri, and K. Tobioka, "Search for the Top Partner at the LHC using Multi-b-Jet Channels," arXiv:1204.2317.

[205] A. Azatov, O. Bondu, A. Falkowski, M. Felcini, S. Gascon-Shotkin, *et al.*, "Higgs boson production via vector-like top-partner decays: Diphoton or multilepton plus multijets channels at the LHC," arXiv:1204.0455.

[206] M. Redi and A. Weiler, "Flavor and CP Invariant Composite Higgs Models," *JHEP* 1111 (2011) 108, arXiv:1106.6357.

[207] CMS Collaboration, S. Chatrchyan *et al.*, "Search for quark compositeness in dijet angular distributions from pp collisions at sqrt(s) = 7 TeV," *JHEP* 1205 (2012) 055, arXiv:1202.5535.

[208] O. Domenech, A. Pomarol, and J. Serra, "Probing the SM with Dijets at the LHC," *Phys.Rev.* D85 (2012) 074030, arXiv:1201.6510.

[209] U. Baur, T. Plehn, and D. L. Rainwater, "Determining the Higgs boson selfcoupling at hadron colliders," *Phys.Rev.* D67 (2003) 033003, arXiv:hep-ph/0211224.

[210] U. Baur, T. Plehn, and D. L. Rainwater, "Examining the Higgs boson potential at lepton and hadron colliders: A Comparative analysis," *Phys.Rev.* D68 (2003) 033001, arXiv:hep-ph/0304015.

[211] U. Baur, T. Plehn, and D. L. Rainwater, "Probing the Higgs selfcoupling at hadron colliders using rare decays," *Phys.Rev.* D69 (2004) 053004, arXiv:hep-ph/0310056.

[212] M. Perelstein, "Little Higgs models and their phenomenology," *Prog.Part.Nucl.Phys.* 58 (2007) 247–291, arXiv:hep-ph/0512128.

[213] M. Schmaltz and D. Tucker-Smith, "Little Higgs review," *Ann.Rev.Nucl.Part.Sci.* 55 (2005) 229–270, arXiv:hep-ph/0502182.

[214] N. Arkani-Hamed, A. G. Cohen, and H. Georgi, "Electroweak symmetry breaking from dimensional deconstruction," *Phys.Lett.* B513 (2001) 232–240, arXiv:hep-ph/0105239.

[215] N. Arkani-Hamed, A. G. Cohen, T. Gregoire, and J. G. Wacker, "Phenomenology of electroweak symmetry breaking from theory space," *JHEP* 0208 (2002) 020, arXiv:hep-ph/0202089.

[216] N. Arkani-Hamed, A. G. Cohen, E. Katz, and A. E. Nelson, "The littlest Higgs," *JHEP* 07 (2002) 034, arXiv:hep-ph/0206021.

[217] D. E. Kaplan and M. Schmaltz, "The Little Higgs from a simple group," *JHEP* 0310 (2003) 039, arXiv:hep-ph/0302049.

[218] M. Schmaltz, "The Simplest little Higgs," *JHEP* 0408 (2004) 056, arXiv:hep-ph/0407143.

[219] N. Arkani-Hamed *et al.*, "The Minimal Moose for a Little Higgs," *JHEP* 08 (2002) 021, arXiv:hep-ph/0206020.

[220] M. Schmaltz, D. Stolarski, and J. Thaler, "The Bestest Little Higgs," *JHEP* 1009 (2010) 018, arXiv:1006.1356.

[221] W. Skiba and J. Terning, "A Simple model of two little Higgses," *Phys.Rev.* D68 (2003) 075001, arXiv:hep-ph/0305302.

[222] M. Schmaltz and J. Thaler, "Collective Quartics and Dangerous Singlets in Little Higgs," *JHEP* 0903 (2009) 137, arXiv:0812.2477.

[223] S. Chang, "A 'Littlest Higgs' model with custodial SU(2) symmetry," *JHEP* 0312 (2003) 057, arXiv:hep-ph/0306034.

[224] I. Low, W. Skiba, and D. Tucker-Smith, "Little Higgses from an antisymmetric condensate," *Phys. Rev.* D66 (2002) 072001, arXiv:hep-ph/0207243.

[225] C. Csaki, J. Hubisz, G. D. Kribs, P. Meade, and J. Terning, "Big corrections from a little Higgs," *Phys.Rev.* D67 (2003) 115002, arXiv:hep-ph/0211124.

[226] J. L. Hewett, F. J. Petriello, and T. G. Rizzo, "Constraining the littlest Higgs," *JHEP* 0310 (2003) 062, arXiv:hep-ph/0211218.

[227] M. Perelstein, M. E. Peskin, and A. Pierce, "Top quarks and electroweak symmetry breaking in little Higgs models," *Phys.Rev.* D69 (2004) 075002, arXiv:hep-ph/0310039.

[228] C. Csaki, J. Hubisz, G. D. Kribs, P. Meade, and J. Terning, "Variations of little Higgs models and their electroweak constraints," *Phys.Rev.* D68 (2003) 035009, arXiv:hep-ph/0303236.

[229] W. Kilian and J. Reuter, "The Low-energy structure of little Higgs models," *Phys.Rev.* D70 (2004) 015004, arXiv:hep-ph/0311095.

[230] M. Farina, C. Grojean, and E. Salvioni, "(Dys)Zphilia or a custodial breaking Higgs at the LHC," arXiv:1205.0011.

[231] S. Chang and J. G. Wacker, "Little Higgs and custodial SU(2)," *Phys. Rev.* D69 (2004) 035002, arXiv:hep-ph/0303001.

[232] H.-C. Cheng and I. Low, "TeV symmetry and the little hierarchy problem," *JHEP* 0309 (2003) 051, arXiv:hep-ph/0308199.

[233] H.-C. Cheng and I. Low, "Little hierarchy, little Higgses, and a little symmetry," *JHEP* 08 (2004) 061, arXiv:hep-ph/0405243.

[234] I. Low, "T parity and the littlest Higgs," *JHEP* 0410 (2004) 067, arXiv:hep-ph/0409025.

[235] D. Pappadopulo and A. Vichi, "T-parity, its problems and their solution," *JHEP* 1103 (2011) 072, arXiv:1007.4807.

[236] J. Hubisz, P. Meade, A. Noble, and M. Perelstein, "Electroweak precision constraints on the littlest Higgs model with T parity," *JHEP* 0601 (2006) 135, arXiv:hep-ph/0506042.

[237] A. Freitas and D. Wyler, "Phenomenology of mirror fermions in the littlest Higgs model with T-parity," *JHEP* 0611 (2006) 061, arXiv:hep-ph/0609103.

[238] A. Birkedal-Hansen and J. G. Wacker, "Scalar dark matter from theory space," *Phys. Rev.* D69 (2004) 065022, arXiv:hep-ph/0306161.

[239] J. Hubisz and P. Meade, "Phenomenology of the littlest Higgs with T-parity," *Phys. Rev.* D71 (2005) 035016, arXiv:hep-ph/0411264.

[240] A. Birkedal, A. Noble, M. Perelstein, and A. Spray, "Little Higgs dark matter," *Phys.Rev.* D74 (2006) 035002, arXiv:hep-ph/0603077.

[241] M. Asano, S. Matsumoto, N. Okada, and Y. Okada, "Cosmic positron signature from dark matter in the littlest Higgs model with T-parity," *Phys.Rev.* D75 (2007) 063506, arXiv:hep-ph/0602157.

[242] M. Perelstein and A. Spray, "Indirect Detection of Little Higgs Dark Matter," *Phys.Rev.* D75 (2007) 083519, arXiv:hep-ph/0610357.

[243] C. T. Hill and R. J. Hill, "Topological Physics of Little Higgs Bosons," *Phys. Rev.* D75 (2007) 115009, arXiv:hep-ph/0701044.

[244] C. T. Hill and R. J. Hill, "T^- parity violation by anomalies," *Phys. Rev.* D76 (2007) 115014, arXiv:0705.0697.

[245] V. Barger, W.-Y. Keung, and Y. Gao, "T-Anomaly Induced LHC Signals," *Phys. Lett.* B655 (2007) 228–235, arXiv:0707.3648.

[246] A. Freitas, P. Schwaller, and D. Wyler, "Consequences of T-parity breaking in the Littlest Higgs model," *JHEP* 09 (2008) 013, arXiv:0806.3674.

[247] D. Krohn and I. Yavin, "Anomalies in Fermionic UV Completions of Little Higgs Models," *JHEP* 06 (2008) 092, arXiv:0803.4202.

[248] A. Freitas, P. Schwaller, and D. Wyler, "A Little Higgs Model with Exact Dark Matter Parity," *JHEP* 12 (2009) 027, arXiv:0906.1816.

[249] C. Kim and J. Park, "Little Higgs model with new X-parity and Dark matter," *Phys.Lett.* B688 (2010) 323–328, arXiv:0911.2389.

[250] C. Csaki, J. Heinonen, M. Perelstein, and C. Spethmann, "A Weakly Coupled Ultraviolet Completion of the Littlest Higgs with T-parity," *Phys. Rev.* D79 (2009) 035014, arXiv:0804.0622.

[251] E. Katz, J.-y. Lee, A. E. Nelson, and D. G. Walker, "A Composite little Higgs model," *JHEP* 0510 (2005) 088, arXiv:hep-ph/0312287.

[252] J. Thaler, "Little technicolor," *JHEP* 0507 (2005) 024, arXiv:hep-ph/0502175.

[253] J. Thaler and I. Yavin, "The Littlest Higgs in Anti-de Sitter space," *JHEP* 0508 (2005) 022, arXiv:hep-ph/0501036.

[254] R. Rajaraman, "Solitons and instantons. An introduction to solitons and instantons in Quantum Field Theory," *North-Holland Personal Library* (1982).

[255] N. S. Manton and P. Sutcliffe, "Topological solitons," *Cambridge Univ. Pr.* (2004).

[256] G. Derrick, "Comments on nonlinear wave equations as models for elementary particles," *J.Math.Phys.* 5 (1964) 1252–1254.

[257] T. H. R. Skyrme, "A Nonlinear field theory," *Proc. Roy. Soc. Lond.* A260 (1961) 127–138.

[258] E. Bogomolny, "Stability of Classical Solutions," *Sov.J.Nucl.Phys.* 24 (1976) 449.

[259] M. Prasad and C. M. Sommerfield, "An Exact Classical Solution for the 't Hooft Monopole and the Julia-Zee Dyon," *Phys.Rev.Lett.* 35 (1975) 760–762.

[260] E. Witten, "Current Algebra, Baryons, and Quark Confinement," *Nucl.Phys.* B223 (1983) 433–444.

[261] B. Julia and A. Zee, "Poles with Both Magnetic and Electric Charges in Nonabelian Gauge Theory," *Phys. Rev.* D11 (1975) 2227–2232.

[262] E. J. Weinberg and A. H. Guth, "Nonexistence of Spherically Symmetric Monopoles with Multiple Magnetic Charge," *Phys. Rev.* D14 (1976) 1660.

[263] G. S. Adkins, C. R. Nappi, and E. Witten, "Static Properties of Nucleons in the Skyrme Model," *Nucl. Phys.* B228 (1983) 552.

[264] R. Bott, "An Application of Morse theory to the topology of Lie groups," *Bull.Soc.Math.Fr.* 84 (1956) 251–281.

[265] J. A. Bryan, S. M. Carroll, and T. Pyne, "A Texture bestiary," *Phys. Rev.* D50 (1994) 2806–2818, arXiv:hep-ph/9312254.

[266] G. S. Adkins and C. R. Nappi, "The Skyrme Model with Pion Masses," *Nucl. Phys.* B233 (1984) 109.

[267] D. Finkelstein and J. Rubinstein, "Connection between spin, statistics, and kinks," *J. Math. Phys.* 9 (1968) 1762–1779.

[268] F. Meier and H. Walliser, "Quantum Corrections to Baryon Properties in Chiral Soliton Models," *Phys. Rept.* 289 (1997) 383–450, arXiv:hep-ph/9602359.

[269] A. Jackson, A. D. Jackson, and V. Pasquier, "The Skyrmion-Skyrmion Interaction," *Nucl. Phys.* A432 (1985) 567–609.

[270] E. Braaten and L. Carson, "The deuteron as a toroidal skyrmion," *Phys. Rev.* D38 (1988) 3525.

[271] C. J. Houghton, N. S. Manton, and P. M. Sutcliffe, "Rational maps, monopoles and Skyrmions," *Nucl.Phys.* B510 (1998) 507–537, arXiv:hep-th/9705151.

[272] R. A. Battye and P. M. Sutcliffe, "Skyrmions, fullerenes and rational maps," *Rev.Math.Phys.* 14 (2002) 29–86, arXiv:hep-th/0103026.

[273] N. Manton, "Classical Skyrmions: Static Solutions and Dynamics," arXiv:1106.1298.

[274] R. Battye and P. Sutcliffe, "Skyrmions and the pion mass," *Nucl.Phys.* B705 (2005) 384–400, arXiv:hep-ph/0410157.

[275] P. Batra and D. E. Kaplan, "Perturbative, non-supersymmetric completions of the little Higgs," *JHEP* 0503 (2005) 028, arXiv:hep-ph/0412267.

[276] G. S. Adkins and C. R. Nappi, "Stabilization of Chiral Solitons via Vector Mesons," *Phys. Lett.* B137 (1984) 251.

[277] A. Jackson, A. D. Jackson, A. S. Goldhaber, G. E. Brown, and L. C. Castillejo, "A modified skyrmion," *Phys. Lett.* B154 (1985) 101–106.

[278] J. Callan, Curtis G. and E. Witten, "Monopole catalysis of skyrmion decay," *Nucl.Phys.* B239 (1984) 161.

[279] E. D'Hoker and E. Farhi, "The decay of the skyrmion," *Phys. Lett.* B134 (1984) 86.

[280] G. 't Hooft, "Computation of the quantum effects due to a four-dimensional pseudoparticle," *Phys. Rev.* D14 (1976) 3432–3450.

[281] J. Ambjorn and V. Rubakov, "Classical Versus Semiclassical Electroweak Decay Of A Techniskyrmion," *Nucl.Phys.* B256 (1985) 434.

[282] V. A. Rubakov, B. E. Stern, and P. G. Tinyakov, "On the electroweak decay of a technibaryon in the soliton model," *Phys. Lett.* B160 (1985) 292–296.

[283] O. Kaymakcalan, S. Rajeev, and J. Schechter, "Nonabelian Anomaly and Vector Meson Decays," *Phys.Rev.* D30 (1984) 594.

[284] B. M. A. G. Piette and D. H. Tchrakian, "Topologically stable soliton in the U(1) gauged Skyrme model," *Phys. Rev.* D62 (2000) 025020, arXiv:hep-th/9709189.

[285] Y. Brihaye and D. Tchrakian, "Solitons/instantons in d-dimensional SO(d) gauged O(d+1) Skyrme models," *Nonlinearity* 11 (1998) 891–911.

[286] Y. Brihaye, C. T. Hill, and C. K. Zachos, "Bounding gauged skyrmion masses," *Phys. Rev.* D70 (2004) 111502, arXiv:hep-th/0409222.

[287] A. Pomarol and A. Wulzer, "Stable skyrmions from extra dimensions," *JHEP* 0803 (2008) 051–051, arXiv:0712.3276.

[288] Y. Igarashi, M. Johmura, A. Kobayashi, H. Otsu, T. Sato, *et al.*, "Stabilization of skyrmions via ρ mesons," *Nucl.Phys.* B259 (1985) 721–729.

[289] K. Nawa, H. Suganuma, and T. Kojo, "Baryons in holographic QCD," *Phys.Rev.* D75 (2007) 086003, arXiv:hep-th/0612187.

[290] A. Pomarol and A. Wulzer, "Baryon Physics in Holographic QCD," *Nucl.Phys.* B809 (2009) 347–361, arXiv:0807.0316.

[291] G. Panico and A. Wulzer, "Nucleon Form Factors from 5D Skyrmions," *Nucl.Phys.* A825 (2009) 91–114, arXiv:0811.2211.

[292] O. Domenech, G. Panico, and A. Wulzer, "Massive Pions, Anomalies and Baryons in Holographic QCD," *Nucl.Phys.* A853 (2011) 97–123, arXiv:1009.0711.

[293] H. Murayama and J. Shu, "Topological Dark Matter," *Phys. Lett.* B686 (2010) 162–165, arXiv:0905.1720.

[294] A. Joseph and S. G. Rajeev, "Topological Dark Matter in the Little Higgs Models," *Phys. Rev.* D80 (2009) 074009, arXiv:0905.2772.

[295] M. Trodden and T. Vachaspati, "Topology in the little Higgs models," *Phys. Rev.* D70 (2004) 065008, arXiv:hep-ph/0404105.

[296] R. Auzzi and M. Shifman, "Low-Energy Limit of Yang-Mills with Massless Adjoint Quarks: Chiral Lagrangian and Skyrmions," *J.Phys.A* A40 (2007) 6221–6238, arXiv:hep-th/0612211.

[297] S. Bolognesi and M. Shifman, "The Hopf Skyrmion in QCD with Adjoint Quarks," *Phys. Rev.* D75 (2007) 065020, arXiv:hep-th/0701065.

[298] R. Auzzi, S. Bolognesi, and M. Shifman, "Skyrmions in Yang–Mills Theories with Massless Adjoint Quarks," *Phys. Rev.* D77 (2008) 125029, arXiv:0804.0229.

[299] S. Bolognesi, "Skyrmions in Orientifold and Adjoint QCD," arXiv:0901.3796.

[300] L. Faddeev and A. J. Niemi, "Knots and particles," *Nature* 387 (1997) 58, arXiv:hep-th/9610193.

[301] A. P. Balachandran, V. P. Nair, N. Panchapakesan, and S. G. Rajeev, "Low Mass Solitons from Fractional Charges in QCD," *Phys. Rev.* D28 (1983) 2830.

[302] A. Balachandran, A. Barducci, F. Lizzi, V. Rodgers, and A. Stern, "A Doubly Strange Dibaryon in the Chiral Model," *Phys.Rev.Lett.* 52 (1984) 887.

[303] S. Nussinov, "Technocosmology: Could a technibaryon excess provide a 'natural' missing mass candidate ?," *Phys. Lett.* B165 (1985) 55.

[304] T. Hemmick, D. Elmore, T. Gentile, P. Kubik, S. Olsen, *et al.*, "A search for anomalously heavy isotopes of low Z nuclei," *Phys.Rev.* D41 (1990) 2074–2080.

[305] P. Smith, J. Bennett, G. Homer, J. Lewin, H. Walford, *et al.*, "A search for anomalous hydrogen in enriched D-2 O, using a time-of-flight spectrometer," *Nucl.Phys.* B206 (1982) 333–348.

[306] M. Y. Khlopov and C. Kouvaris, "Strong Interactive Massive Particles from a Strong Coupled Theory," *Phys.Rev.* D77 (2008) 065002, arXiv:0710.2189.

[307] A. Belyaev, C.-R. Chen, K. Tobe, and C. P. Yuan, "Phenomenology of littlest Higgs model with T^- parity: including effects of T^- odd fermions," *Phys. Rev.* D74 (2006) 115020, arXiv:hep-ph/0609179.

[308] G. Belanger *et al.*, "Indirect search for dark matter with micrOMEGAs2.4," arXiv:1004.1092.

[309] W. H. Press, S. A. Teukolsky, W. T. Vetterling, and B. P. Flannery, "Numerical Recipes in FORTRAN: The Art of Scientific Computing," *Cambridge Univ. Pr.* (1993).

[310] Numerical Recipes Software 2007, "Solvde Implementation," *Numerical Recipes Webnote No. 25,* http://www.nr.com/webnotes?25.